Ambiphilic C-H Activation Routes to Heterocycles

Thesis submitted for the degree of

Doctor of Philosophy

at the University of Leicester

by

Qudsia Khamker MChem

Department of Chemistry

University of Leicester

January 2014

Title: Ambiphilic C-H Activation Routes to Heterocycles

Author: Qudsia Khamker

Abstract

This thesis describes investigations of Cp*Rh- and (*p*-Cy)Ru-catalysed C-H functionalisation reactions of various substrates with alkynes and alkenes for the formation of several heterocycles and carbocycles. Mechanistic studies and DFT calculations are also presented.

Chapter One includes a discussion of different mechanisms of C-H activation namely oxidative addition, σ-bond metathesis, 1,2-addition, electrophilic activation and AMLA/CMD. The applications of these different mechanisms of C-H activation in catalysis are also discussed with a particular emphasis on the use of AMLA/CMD in direct arylation reactions.

Chapter Two gives an overview of stoichiometric and catalytic studies of AMLA C-H activation and subsequent reactivity with alkynes at Ir, Rh, and Ru. The results of Cp*Rh- and some (*p*-Cy)Ru-catalysed reactions of *C*-phenylpyrazoles with alkynes are presented. N-H and C-H activation occurs, leading to heterocycles. Mechanistic studies and DFT calculations show that C-H activation is reversible and rate limiting in the cases examined.

Chapter Three is similar to **Chapter Two** but focusses on reactions with alkenes. The Cp*Rh-catalysed reactions of *C*-phenylpyrazoles with alkenes lead to mono or divinyl products which may undergo further aza-Michael cyclisations if the alkene is a good Michael acceptor. Mechanistic studies and DFT calculations are also discussed.

Chapter Four deals with Cp*Rh-catalysed coupling reactions of other directing groups, including imidazole, imidazoline, pyrazolidinone, hydrazine, carboxylic acid and oxime with alkynes. Again, there is discussion on the different factors affecting product selectivity.

Chapter Five gives a summary of all the conclusions on the work presented in this thesis. Throughout the thesis, all new compounds are characterised spectroscopically and several compounds have been characterised by X-ray crystallography.

Acknowledgements

Firstly I would like to thank my supervisor Prof. Dai Davies for all his help, support, guidance and patience throughout this project. I would like to thank our collaborators at Heriot-Watt University Prof. Stuart Macgregor, Dr. Andrés Algarra and Dr. Claire McMullin for the computational work. I would also like to thank several other members of staff who gave me guidance including Dr. Warren Cross, Dr. Gregory Solan and Prof. Eric Hope.

I must thank the support staff who have been very helpful and friendly and who have contributed to the work presented in this thesis. This includes Dr. Gerry Griffith for the deuterium NMR studies, Mr. Kuldip Singh for all the X-ray crystallography and Mr. Mick Lee for the HRMS and for providing many preparative TLC plates. I would also like to thank Sai and Dave for the banter and the occasional kheema rice and cakes. Katy, Carla, Richard, Dawn and Emma have also been wonderful company during my demonstrating sessions.

I have worked with and made friends with many fantastic people at the University of Leicester. I must acknowledge Dr. Christopher Daly for helping me throughout most of my project and for sometimes providing me with rhodium dimer. I would like to thank Dr. Charles Ellul and Dr. Bárbara Villa-Marcos for all their guidance, doing some reactions for my project, proof-reading my thesis and for letting me make fun of them. Thanks to all my fellow postgraduates who I have had the pleasure to demonstrate with, sorry I cannot name you all, however I must thank Gemma and Luka for proof-reading my thesis. I have also had the pleasure of supervising and getting to know some great undergraduates. I would particularly like to thank Ashleigh, Beatrice, Lois and Nick for the funny banter and for amazing cakes. I would like to thank Kate, Kyle, Mark (Babyface), Mati, Matt, Olly, Rhiannon and Sunnah for the amazing parties, dancing and film discussions. I would also like to thank Aman, Anand, Andy and Raíssa for their great company.

I must of course thank my mother, Farida Khamker who I have seen very little over the past few years but who has given me much love and encouragement. Finally I want to thank my gorgeous boyfriend Philip Evans for supporting me through the times of enormous stress and helping me produce some of the illustrations in this thesis.

Statement

This thesis is based on work conducted by the author in the Department of Chemistry at the University of Leicester, during the period between September 2009 and September 2013. All X-ray crystallography was performed by Mr. Kuldip Singh.

Thanks to Dr. Charles Ellul for doing the ruthenium initial rates experiments and for some Cp*Rh-catalysed reactions of benzamide. Thanks to Dr. Bárbara Villa-Marcos for doing the ruthenium KIE experiments and to Kyle Toyne for the preliminary studies with 3-phenyl-1*H*-pyrazole (**2.43b**).

Thanks go to the group of Prof S. A. Macgregor who have performed DFT calculations to assess the mechanism of the coupling of alkynes and alkenes with *C*-phenylpyrazoles using {Cp*Rh} and {(*p*-Cy)Ru} catalysts.

All the work described in the thesis is original unless otherwise stated. This work is not being presented for any other degree.

Signed: _____ Date: _____

Qudsia Khamker

Abbreviations

General and Physical

°C	Degrees Centigrade
δ	Delta (NMR chemical shift)
ΔG	Gibbs Free Energy Change
Å	Angstroms
AMLA	Ambiphilic Metal Ligand Activation
APT	Attached Proton Test
br s	Broad singlet
br d	Broad doublet
ca.	Circa (around/about)
cal	Calories
CMD	Concerted Metalation-Deprotonation
COSY	Correlation Spectroscopy
d	Doublet
dd	Doublet of doublets
DEPT	Distortionless Enhancement by Polarization Transfer
DFT	Density Functional Theory
dt	Doublet of Triplets
EA	Electrophilic Activation
eq.	Equivalents
ESI	Electrospray Ionisation
et al.	and others
FAB	Fast Atom Bombardment
g	Gram
h	Hour
HMBC	Heteronuclear Multiple-bond Correlation Spectroscopy
HMQC	Heteronuclear Multiple Quantum Correlation Spectroscopy
HR	High Resolution
HSQC	Heteronuclear Single Quantum Correlation Spectroscopy
Hz	Hertz
i.e.	Id est (that is)

J	Joules
K	Kelvin
m	Multiplet
M	Molar (concentration)
mol	moles
MS	Mass Spectrometry
NMR	Nuclear Magnetic Resonance
NOE	Nuclear Overhauser Effect
NOESY	Nuclear Overhauser Effect Spectroscopy
OA	Oxidative Addition
ppm	Parts per million
q	Quartet
r. t.	Room temperature
s	Seconds
SBM	σ-Bond Metathesis
S_EAr	Electrophilic Aromatic Substitution
sex	Sextet
t	Triplet
td	Triplet of doublets
TLC	Thin Layer Chromatography
TS	Transition State
via	By means of

Chemical

acac	Acetylacetonate
Ar	Aryl
BAr_f	$B[3,5\text{-}C_6H_3(CF_3)_2]_4^-$
BQ	Benzoquinone
Bu	‘Normal’ butyl
Cp	Cyclopentadienyl anion
Cp*	Pentamethylcyclopentadienyl anion
cy	Cyclohexyl

Cy	Cymene
DCE	1,2-Dichloroethane
DDQ	2,3-Dichloro-5,6-dicyano-1,4-benzoquinone
DMBA	*N*,*N*′-Dimethylbenzylamine
DMA	Dimethyl Acetamide
DMAD	Dimethylacetylene Dicarboxylate
DMF	Dimethyl Formamide
dmpe	1,2-*bis*(dimethylphosphino)ethane
Et	Ethyl
Fe	Iron
^{i}Pr	Isopropyl
Ir	Iridium
Me	Methyl
Mes	Mesityl
NBA	3-Nitrobenzyl alcohol
NHC	N-Heterocyclic Carbene
NMP	N-Methyl-2-pyrrolidone
OAc	Acetate
OPiv	Pivalate
Os	Osmium
OTf	Trifluoromethanesulfonate
Pd	Palladium
Ph	Phenyl
PMe_3	Trimethylphosphine
$POMe_3$	Trimethoxyphosphine
PPh_3	Triphenylphosphine
Pt	Platinum
Rh	Rhodium
Ru	Ruthenium
t-AmOH	Tertiary amyl alcohol
^{t}Bu	Tertiary butyl
THF	Tetrahydrofuran
TMB	1,3,5-Trimethoxybenzene

TMS	Tetramethylsilane
Tp	Tris(pyrazolyl)borate
Ts	Tosyl

Table of Contents

Chapter One

Introduction

1 Chapter One – C-H Activation

1.1 Introduction

Methods for formation of C-C and C-Y (Y = O, N) bonds are crucial for the synthesis of new molecules. There have been huge advances in Pd-catalysed cross-coupling reactions but these generally rely on at least one starting material containing a C-X (X = Cl, Br, I) bond which itself is prepared from functionalising a C-H bond (**Scheme 1.1**). To improve the atom and step efficiency and hence sustainability, making C-C and C-Y (Y = O, N) bonds directly by catalytic C-H functionalisation is very desirable. The process would be more efficient if the C-H bond could be directly converted into the M-C bond in the catalytic cycle. There has been extensive progress in this field in the last few years.[1-3]

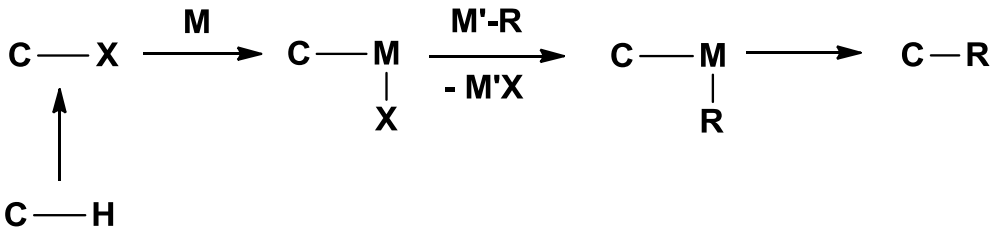

Scheme 1.1: Traditional cross-coupling reactions.

A key aim of research on C-H activation is to gain an understanding of the mechanisms involved in order to develop reagents that are able to selectively transform C-H bonds to more functionalised molecules. This chapter will start with an overview of the different mechanisms of C-H activation with examples of stoichiometric reactions and computational studies and finish with some of the applications of C-H activation in catalysis.

1.2 Mechanisms of C-H Activation

Experimental and computational studies have led to a greater understanding of the mechanisms of C-H activation. Four main mechanisms had been identified before 2000 namely (i) oxidative addition (OA), (ii) σ-bond metathesis (SBM), (iii) electrophilic activation (EA) and (iv) radical mechanisms, which will not be discussed here. Later came (v) 1,2-addition[4-7] and (vi) Ambiphilic Metal Ligand Activation (AMLA)[8, 9] also

known as Concerted Metalation-Deprotonation (CMD)[10] which shares similarities with 1,2-addition and electrophilic activation. This section will give a brief outline and discussion of mechanisms (i)-(iii) and (v)-(vi).

1.2.1 Oxidative Addition

Oxidative addition typically involves an electron-rich and coordinatively unsaturated metal reacting with a C-H bond. This is believed to occur via a 3-membered transition state and increases the oxidation state and coordination number by two to form an M-C and M-H bond (**Scheme 1.2**).[11]

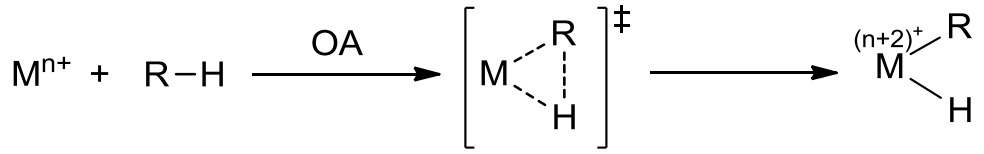

Scheme 1.2: Mechanism of OA showing the three-membered transition state.

Chatt and Davidson first reported oxidative addition of a C-H bond in 1964.[12] The Ru^0 complex, $Ru(dmpe)_2$ (**1.1**) activates either an sp^2 C-H bond of naphthalene or an sp^3 C-H bond of the dmpe ligand (**Scheme 1.3**).

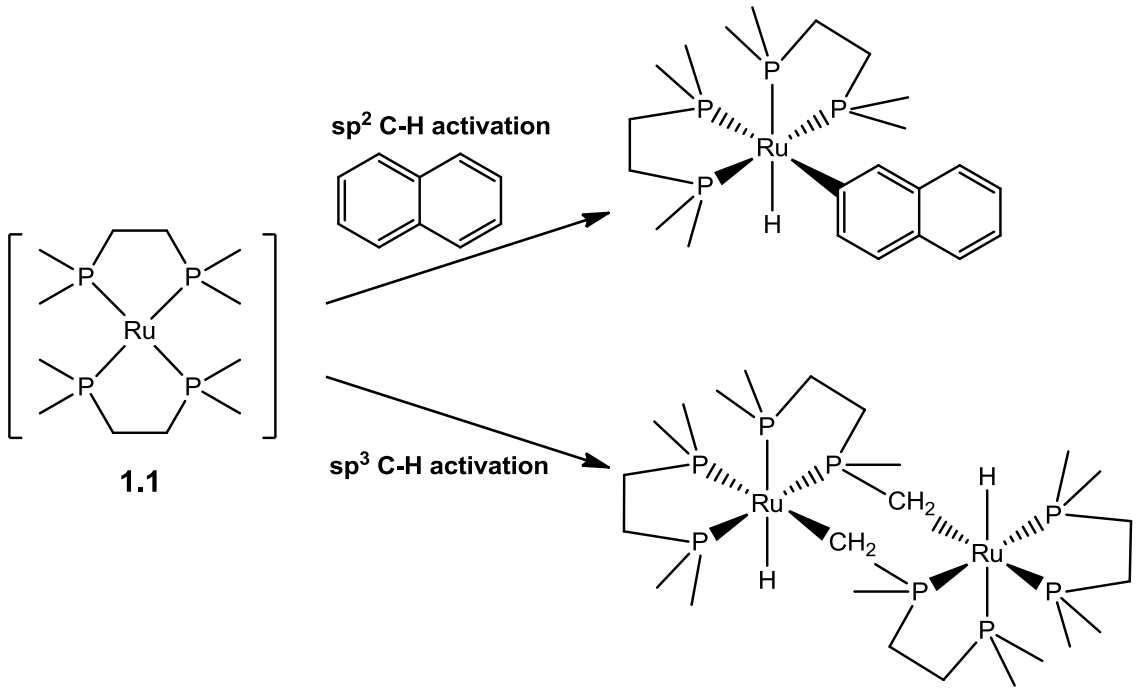

Scheme 1.3: First oxidative addition reported by Chatt and Davidson.[12]

An example of intramolecular oxidative addition was reported by Bennett and Milner in 1967.[13] This involved sp^2 C-H activation on an aryl group using Ir (**Scheme 1.4**). In 1978, Whitesides and Foley reported the intramolecular oxidative addition of an aliphatic sp^3 C-H bond using Pt.[14]

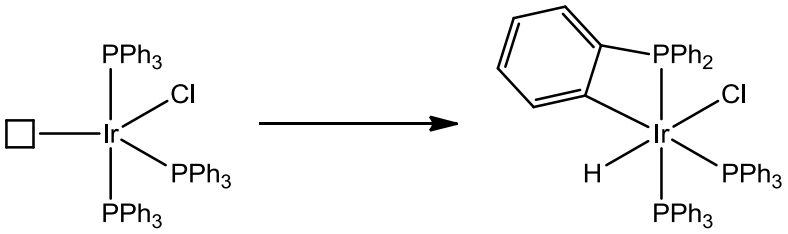

Scheme 1.4: Intramolecular oxidative addition using Ir.[13]

The groups of Bergman,[15] Graham[16] and Jones[17] carried out early studies on intermolecular oxidative addition using Cp*ML (M = Rh, Ir and L = CO, PMe_3) complexes. Further studies showed the formation of reactive 16-electron complexes before C-H activation.[18-20]

In the early 1980s, Bergman and Janowicz showed loss of H_2 occurs after photolysis of **1.2** to give an Ir^I complex (**1.3**) which undergoes oxidative addition of methane (**Scheme 1.5**).[15, 21] An Ir^{III} complex (**1.5**) is obtained via the proposed three-membered transition state (**1.4**).

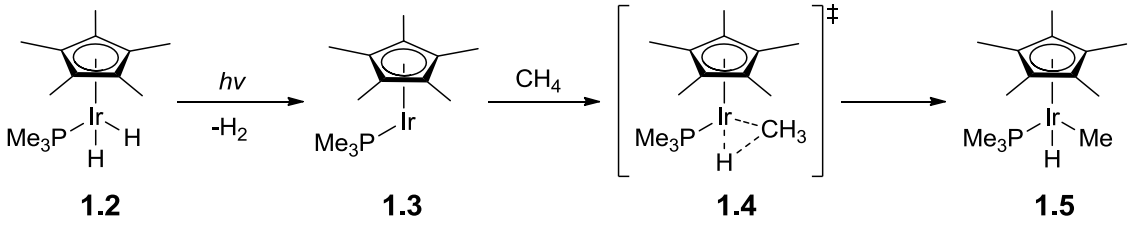

1.2 **1.3** **1.4** **1.5**

Scheme 1.5: Photolysis followed by oxidative addition of methane.

The electron-rich metal centre and the electron-donating Cp* are essential for the oxidative addition to occur. However, studies by Graham demonstrated that the less electron-rich Cp*Ir(CO) can also activate methane.[16]

The need for very electron-rich metal centres was challenged in 1993 by use of a cationic Ir complex. The group of Bergman confirmed C-H activation of alkanes using the Ir^{III} complex, [Cp*IrMe(OTf)(PMe_3)] (**1.6**) under mild conditions.[22, 23] Two mechanisms were proposed (**Scheme 1.6**). The first step is ionisation of **1.6** followed by

reaction of the C-H bond at the cationic Ir centre either by means of (a) oxidative addition via an Ir^{V} intermediate followed by reductive elimination of methane or (b) by a concerted σ-bond metathesis mechanism.

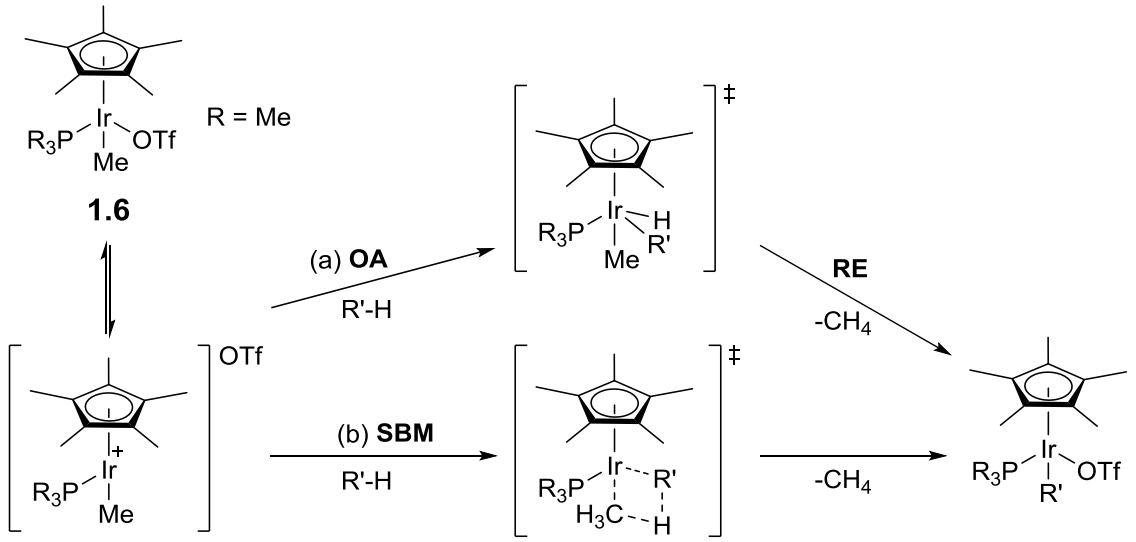

Scheme 1.6: C-H activation of alkanes using cationic Ir^{III}.[22]

The reaction depends on the ease of dissociation of OTf to form a 16-electron species. Bergman showed this to be the case since **1.7** reacts 3 times faster than **1.6**. Dichloromethane dissociates more easily than the triflate (**Scheme 1.7**) and the BAr_f anion is less coordinating than triflate.[23]

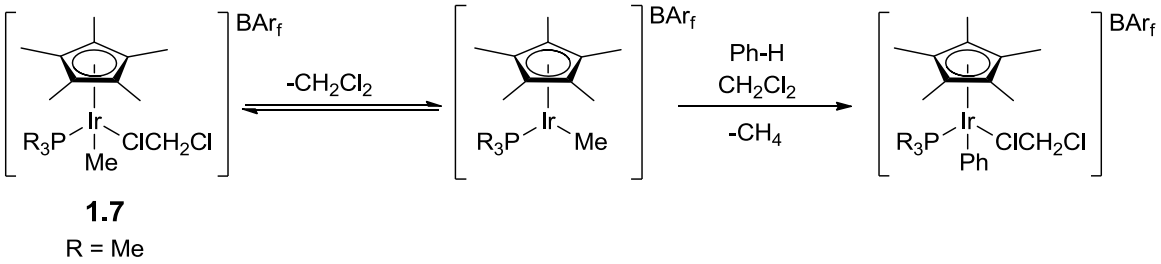

Scheme 1.7: OA using an Ir complex with a dissociating CH_2Cl_2 ligand and BAr_f anion.

In a later study, the rates of the reaction for the analogous Rh complexes (R = Me, OMe) were between 30 and 1000 times slower than for the Ir complexes (R = Me, OMe). According to the authors, this was due to triflate dissociation being easier in the case of Ir complexes.[24] This implied the rate-determining step is the dissociation. The rates for the PMe_3 and $P(OMe)_3$ complexes were about the same for Rh. However for Ir,

the rate for the more electron-donating PMe_3 complex was 30 times faster than for the $P(OMe)_3$ complex and it is thought that PMe_3 might favour the C-H activation step.

Computational studies by Hall and Niu of the reaction of $[CpIrMe(PMe_3)]^+$ with methane suggested that OA was a lower energy pathway than SBM.[25] No transition state for the SBM pathway could be determined and in this case computational chemistry helped distinguish the mechanism of the reaction, however it is worth noting the computational study used Cp instead of Cp* and steric factors may be important to consider.

C-H activation by oxidative addition causes an increase in the oxidation state and coordination number of a metal and has no intermediates. Initially it seemed that a very electron-rich transition metal is necessary for OA to occur however, later studies have shown this is not the case as shown in the examples with the cationic complexes.[22-24, 26]

1.2.2 σ-Bond Metathesis (SBM)

SBM is a concerted reaction where two σ-bonds are broken and two new σ-bonds are formed (**Scheme 1.8**). This overall process is the same as occurs for 1,2-addition (see later) so a distinction will be made based on the mechanism of the process. A SBM mechanism involves a four-centred, four-electron transition state and there is no change in the oxidation state of the metal. SBM is usually found for d^0 transition metal complexes which have no d-electrons to take part in redox reactions so cannot react via an OA mechanism.

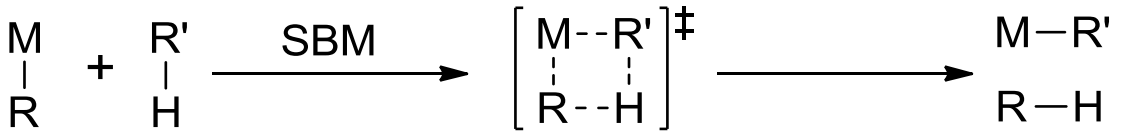

Scheme 1.8: σ-Bond Metathesis mechanism.

Watson first reported SBM of C-H bonds in 1983; the methyl group of $(Cp^*)_2LuMe$ exchanged with $^{13}CH_4$ which suggested a mechanism that involved a four-membered transition state (**Scheme 1.9**).[27] SBM with other sp^3 C-H bonds and with sp^2 C-H bonds using organolanthanides is also possible and has been reviewed.[28] In 1987, Bercaw *et al.* showed that Cp*ScR (R = alkyl, aryl) complexes exhibit similar reactivity with various substrates that include C-halogen (Cl, Br and I) and sp, sp^2 and sp^3 C-H bonds.[29]

He proposed the transition state may be quite non-polar and coined the term "σ-bond metathesis mechanism." However a more recent computational study by Eisenstein *et al.* suggested a more polar transition state.[30]

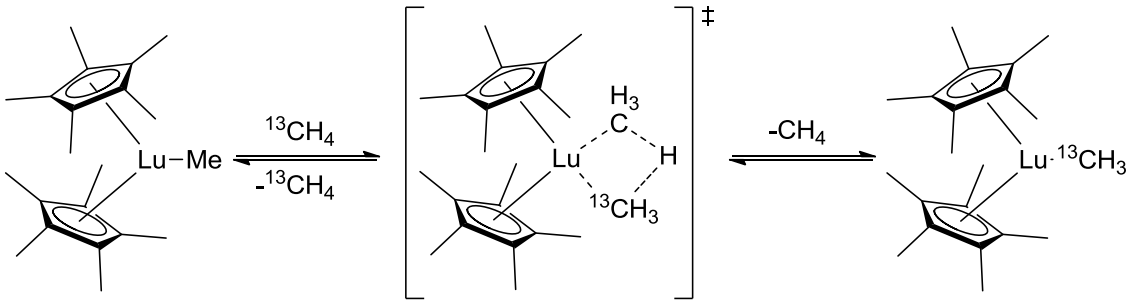

Scheme 1.9: SBM of $(Cp^*)_2LuMe$ with $^{13}CH_4$.[27]

In 2003, Lin, Eisenstein and co-workers carried out computational studies on methane activation with {$TpM(PH_3)Me$} (M = Fe, Ru, Os) complexes using four-membered ring transition states.[31, 32] It was found that the activation barrier was the highest for Fe and the lowest for Os. Four-membered transition states were computed for Fe and Ru complexes but a three-membered OA transition state was found for the Os analogue. C-H activation was shown to be a one-step process for M = Fe where the transition state highlighted a short Fe-H distance of 1.53 Å. This showed some Fe-H bonding which implied an oxidative character. Computed transition states for late transition metals often show an M-H bond and so Lin called these "oxidatively added transition states" (OATS) mechanisms.

Computational studies by Goddard *et al.* in 2003 showed that $[IrPh(acac)_2(pyridine)]$ undergoes C-H activation via SBM rather than OA.[33] The transition state showed a short Ir-H distance of 1.58 Å which implies oxidation at the metal centre. The authors called this an "oxidative hydrogen migration" (OHM) mechanism. They compared the difference in mechanism to Bergman's $[Cp^*IrMe(PMe_3)(OTf)]$ system[22] and stated that the presence of the more electron-donating ligands in Bergman's system favoured OA. They also speculated that the Cp* is less bulky than bis-acac which favours the Ir^V intermediate. In 2007, Gunnoe *et al.* reported an experimental and computational study on C-H activation with $[TpRu(L)(C_6H_5X)Me]$ (L = CO, PMe_3; X = H, OMe, F, Cl, Br, CN, NH_2, NO_2) and the results were in agreement with an OHM mechanism.[34-36]

Hall and Vastine summarised the various types of mechanisms for SBM reported in the literature (SBM, OATS (Lin), OHM (Goddard)) along with the OA/RE mechanism (**Fig 1.1**).[37] They illustrated these as a spectrum of metal-mediated hydrogen transfer. Various other groups have also suggested that OA/RE and SBM are two extremes of this continuum with OHM in the middle. The intermediate mechanisms depend on metal-substrate interaction in the transition state.[38, 39]

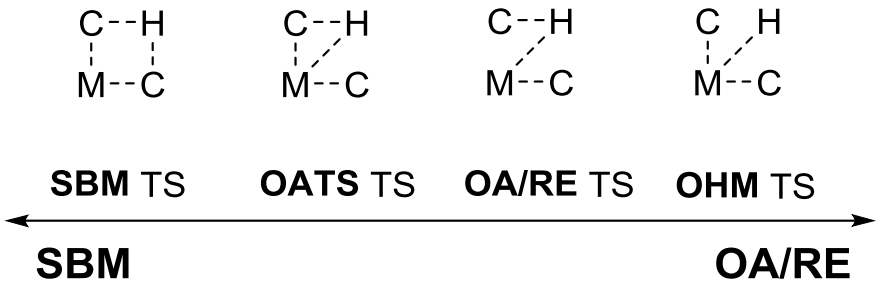

Fig 1.1: Hall's spectrum of mechanisms.[37]

On the whole, σ-bond metathesis is a C-H activation mechanism that usually involves exchanging organic groups between d^0 metal-alkyl complexes and organic substrates in a concerted manner through a four-membered transition state. One limitation is that this just results in a new metal-alkyl complex and another organic substrate. Computational studies have provided insight into different mechanisms such as OATS and OHM. The different SBM mechanisms cannot be distinguished experimentally, only computationally, and the differences between them are subtle, so therefore they will be considered the same for the purpose of this thesis.

1.2.3 1,2-Addition

1,2-addition of a C-H bond across a metal-ligand bond is a sigma bond metathesis type reaction which proceeds through a four-centred transition state, like SBM, but with involvement of π-electrons or lone pairs. This mechanism of C-H activation can occur with either a late transition metal amide/alkoxy bond or an early/middle transition metal-ligand multiple bond (**Scheme 1.10**).

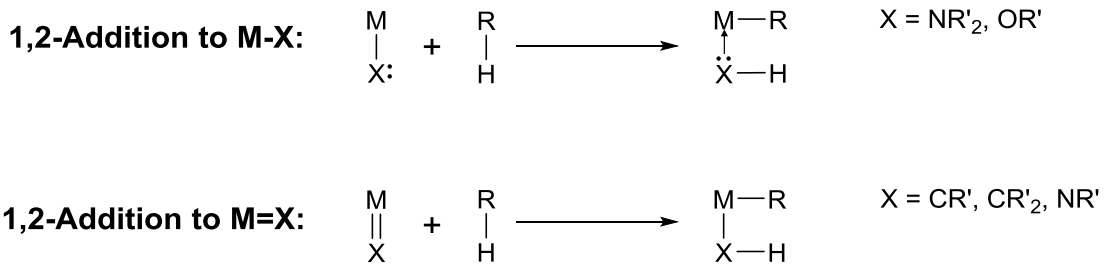

Scheme 1.10: The two types of 1,2-addition mechanism.

1,2-Addition to M-X

This type of 1,2-addition engages a late transition metal-heteroatom bond in a C-H activation and has significant involvement of the heteroatom lone pair in the reaction. In 2005, the groups of Periana[4] and Gunnoe[5] independently reported the first experimental results of 1,2-addition of a C-H bond across an M-X (X = O, N) single bond.

Periana's group reported the C-H activation of benzene using an Ir^{III} alkoxy complex (**Scheme 1.11**). Loss of MeOH from **1.8** creates a vacant coordination site and association of benzene follows. C-H activation subsequently takes place and goes via a four-membered transition state. Loss of methanol and coordination of pyridine then gives **1.9**. The reaction produced MeOD when it was carried out in the presence of C_6D_6.

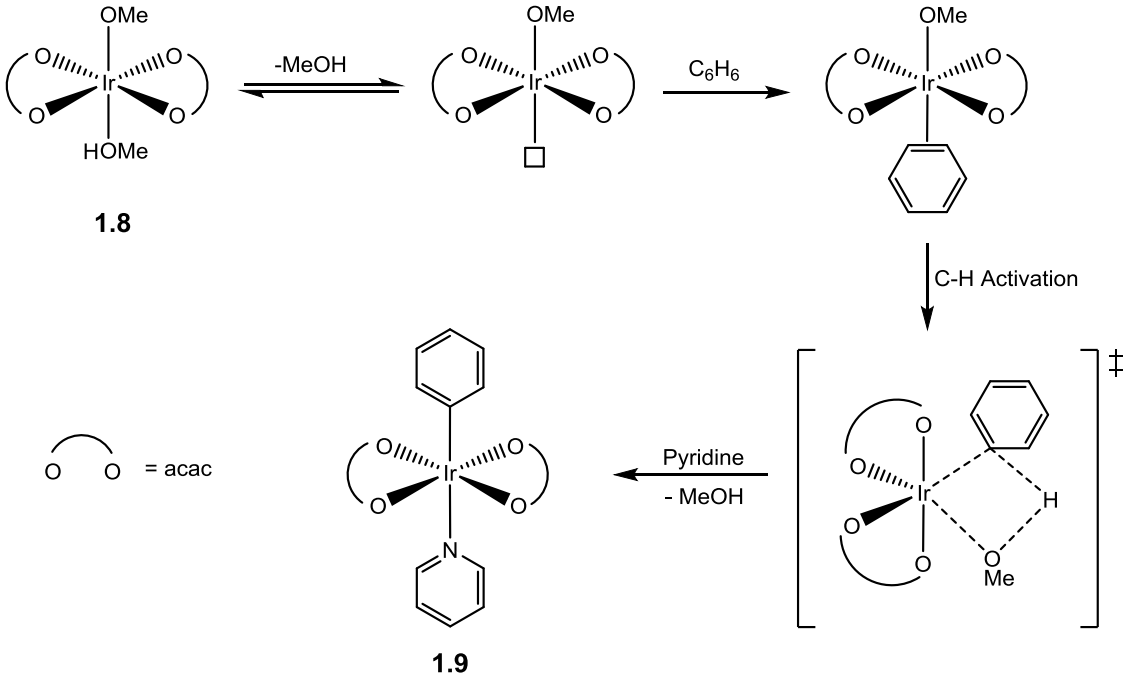

Scheme 1.11: C-H activation of benzene by a 1,2-addition mechanism.[4]

Initially this reaction was reported to be going via a SBM mechanism due to a computational study that showed a four-membered transition state rather than a three-membered OA transition state.[40] The computational study was carried out on an Ir^{III} hydroxy complex rather than the Ir^{III} alkoxy complex used in the experimental study. Further studies by Oxgaard, Goddard and co-workers computed the localised orbitals to analyse 1,2-addition across the Ir-OMe bond and revealed an electrophilic metal attacking the benzene and proton transfer to the coordinated alkoxide.[41] The authors proposed that the lone pair on the alkoxy ligand helped to remove a proton from benzene so a 1,2-addition mechanism was operating here. The authors termed this an Internal Electrophilic Substitution mechanism (IES) where the lone pair on an M-X (X = O, N) ligand forms an X-H bond while the M-X bond orbital forms a coordinating lone pair. The authors concluded that the 1,2-addition indeed occurs by a four-membered transition state and there is no M-H bonding interaction. The X-H bond formation and the M-X bond cleavage are not based on the same orbital therefore the process is essentially different to SBM.

Gunnoe *et al.* similarly reported H/D exchange of benzene with [TpRu(PMe_3)$_2$OH] (**1.10**) and D_2O.[5] Kinetic studies were carried out and it was proposed that PMe_3 dissociates before coordination of benzene. The same group later studied the effect of changing the hydroxyl group to OPh, NHPh, SH, Cl and OTf.[42] H/D exchange was only observed with NHPh as a substituent.

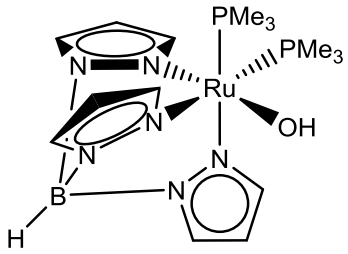

1.10

The authors proposed the C-H activation depends on the basicity of the group receiving the hydrogen. They suggested that non-dative heteroatom-based ligands on low oxidation late transition metals will have lower C-H activation barriers than similar metal-alkyl/aryl bonds. They remarked that the mechanism of C-H activation resembled SBM but later computational studies on benzene activation using 16-electron {Ru(PH_3)X} (X = Me, OH, NH_2) showed substantial differences in transition states.[43] X

= Me had a higher activation barrier and a shorter M-H bond distance (1.72 Å) (**Fig. 1.2**). X = OH, NH_2 have lower activation barriers and longer M-H bond distances (2.03 Å and 2.05 Å respectively). The authors concluded that when X = Me, the mechanism goes via OHM but when X = OH, NH_2, it goes via 1,2 addition as they found there is little M-H interaction. They describe the C-H activation as a metal-mediated proton transfer where the metal and ligand act as an electrophile and intramolecular base respectively.

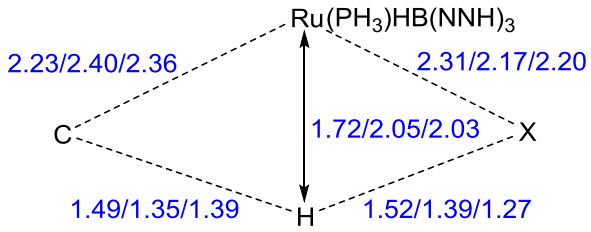

Fig. 1.2: Bond distance in transition state for X = Me, NH_2, OH.[43]

Intramolecular C-H activation by 1,2-addition is also known. Fryzuk *et al.* reported activation of an aromatic C-H bond across a Ru^{II} amide bond (**Scheme 1.12**).[44] In this case, the amide is part of a PNP pincer ligand. PEt_3 coordinates to the metal which forces the *trans* PPh_3 ligand into closer proximity to the nitrogen. C-H activation by 1,2-addition is then able to take place. Dissociation of PEt_3 and rearrangement give the final product. The rearrangement is thought to occur by dissociation of the nitrogen which then undergoes inversion and recoordinates with the chloride taking a *cis* position.

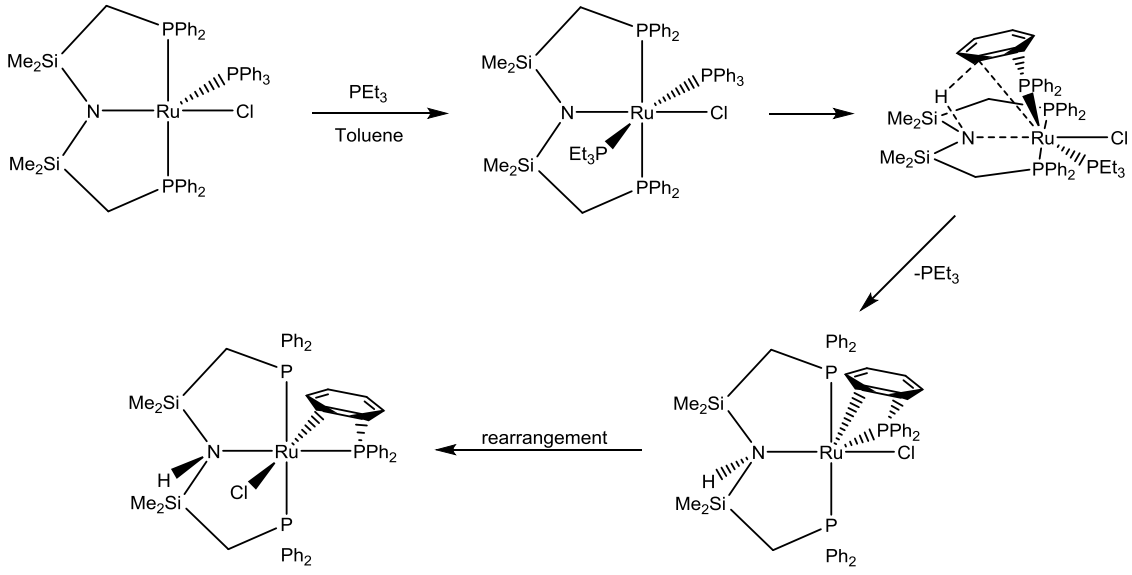

Scheme 1.12: Intramolecular C-H activation by 1,2-addition with Ru^{II}.[44]

1,2-Addition to M=X

This type of 1,2-addition involves an early/middle transition metal-ligand multiple bond with π-electrons helping the C-H activation process. In 1988, Bergman showed Zr^{IV} imido complexes activate a C-H bond via 1,2-addition (**Scheme 1.13**).[6] 1,2-elimination of methane from **1.11** leads to the formation of **1.12** which subsequently carries out C-H activation to give **1.13**. At the same time, Wolczanski independently reported similar chemistry using a transient zirconium imide with *t*-Bu_3SiNH ancillary ligands instead of Cp groups.[7] Later computational studies by Cundari and Wolczanski confirmed the 1,2-addition mechanism for the system using t-Bu_3SiNH ancillary ligands.[45, 46]

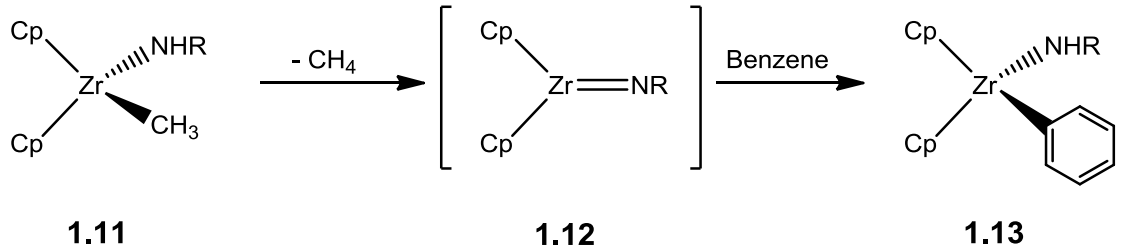

1.11 **1.12** **1.13**

Scheme 1.13: C-H activation via 1,2-addition using a Zr^{IV} imido complex.[6]

In 1997, Bennett and Wolczanski illustrated that an analogous titanium imidosiloxy complex could activate aryl and alkyl C-H bonds in a similar fashion (**Scheme 1.14**).[47] In an extensive computational study on this system, Sakaki *et al.* proposed that an unoccupied Ti d_{z^2} orbital accepts electrons from the C-H bonding orbital, while the occupied d_π-p_π M-N bonding picks up the proton.[48]

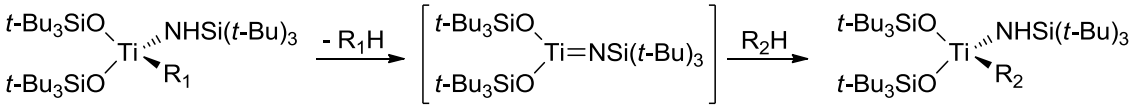

Scheme 1.14: C-H activation via 1,2-addition using a titanium imidosiloxy complex.[47]

In 2004, Bergman *et al.* reported the reactivity of a Zr imido complex with indenyl groups instead of Cp groups which was able to activate aryl, alkyl and alkenyl C-H bonds.[49] It was found that the complexes formed by sp^2 C-H bond activation were in general, more thermodynamically stable than those formed from sp^3 C-H bonds. Furthermore, complexes formed by primary C-H bond activation were favoured over complexes formed from secondary C-H bonds. The thermodynamic selectivity was

found to be heavily sterically influenced and substrate electronic effects only had a slight influence.

On the whole, 1,2-additions typically occur with late transition metal amide/alkoxy bonds or with early transition metal-ligand multiple bonds. The mechanisms go via a four-membered transition state like SBM but with involvement of heteroatom lone pairs or π-bonding orbitals. The 1,2–additions to M-X, including the IES mechanism, have all subsequently been classified as AMLA (Ambiphilic Metal Ligand Activation) C-H activations where an electron-deficient metal and a base work together to cause heterolytic scission of a C-H bond in a concerted process. This mechanism will be discussed in more detail in **Section 1.2.5**.

1.2.4 Electrophilic Activation

In electrophilic C-H activation, an electrophilic metal attacks an electron-rich carbon atom. A metal-carbon bond is created and a proton removed (**Scheme 1.15**).

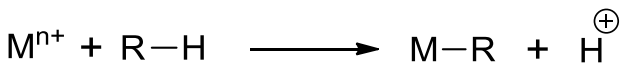

Scheme 1.15: Electrophilic activation.

In 1969, Shilov *et al.* reported H/D exchange of methane in a D_2O solution of K_2PtCl_4.[50] Subsequent studies led to the discovery of a selective methane oxidation reaction known as Shilov chemistry (**Scheme 1.16**)[51] which is believed to go via an electrophilic activation.[52] As robust as the method seems, the Shilov system requires stoichiometric amounts of expensive Pt^{IV} oxidant even though the reaction is catalytic in Pt^{II}.

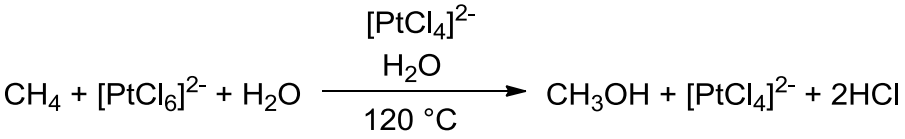

Scheme 1.16: Shilov chemistry used for the synthesis of methanol.[51]

The C-H activation proceeds via electrophilic displacement of a proton on methane by Pt^{II} but two different mechanisms have been proposed for this reaction (**Scheme 1.17**).[53-55] One pathway involves oxidative addition of a C-H bond at Pt^{II} (**1.14**) to yield a [Pt^{IV}(R)(H)] (R = Me) complex (**1.15**) which is followed by deprotonation to give **1.17**. The other pathway involves deprotonation of a Pt^{II}-alkane σ-adduct (**1.16**).

Substantial evidence has been obtained to support both species as intermediates.[56, 57] The reaction conditions for the C-H activation involve high temperatures (120 °C) so detection of reactive intermediates is extremely difficult. As a result, the majority of mechanistic information for the reaction has been gained by investigating the reverse of this reaction: protonolysis of alkylplatinum(II) complexes (**1.17**).

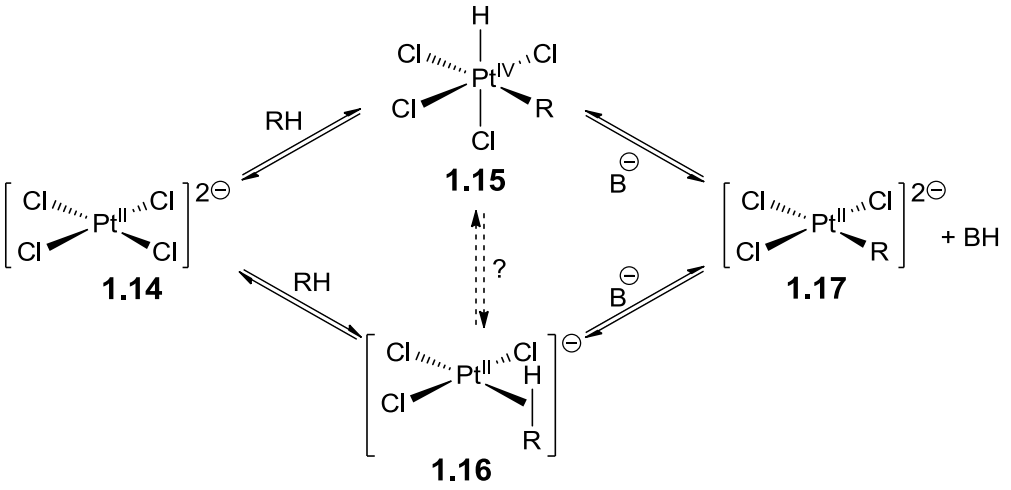

Scheme 1.17: Two proposed pathways for methane C-H activation by Pt^{II}.[53-55]

Alkyl(hydrido)platinum(IV) complexes have been prepared from alkylplatinum(II) complexes by addition of HX (X = halide, triflate).[52, 58] Results from various studies support the mechanism shown in **Scheme 1.18**.[56, 57, 59, 60] Protonation of **1.17** by an acid (or solvent) gives the alkyl(hydrido)platinum(IV) complex (**1.15**) which subsequently loses a halide (or solvent molecule) to give a cationic five-coordinate Pt^{IV} species (**1.18**). Reductive C-H formation gives the σ-adduct (**1.16**) and alkane elimination takes place through an irreversible associative or dissociative pathway. In deuterated acid, H/D exchange is observed into the alkyl positions before alkane elimination occurs.[59, 60] suggesting that equilibration of **1.15** and **1.16** must occur before elimination of alkane. These results can be extrapolated to the Shilov system to show that **1.15** and **1.16** are both intermediates in the C-H activation of methane by Pt^{II}.[52] This suggests that the C-H activation may be oxidative addition instead of electrophilic activation.

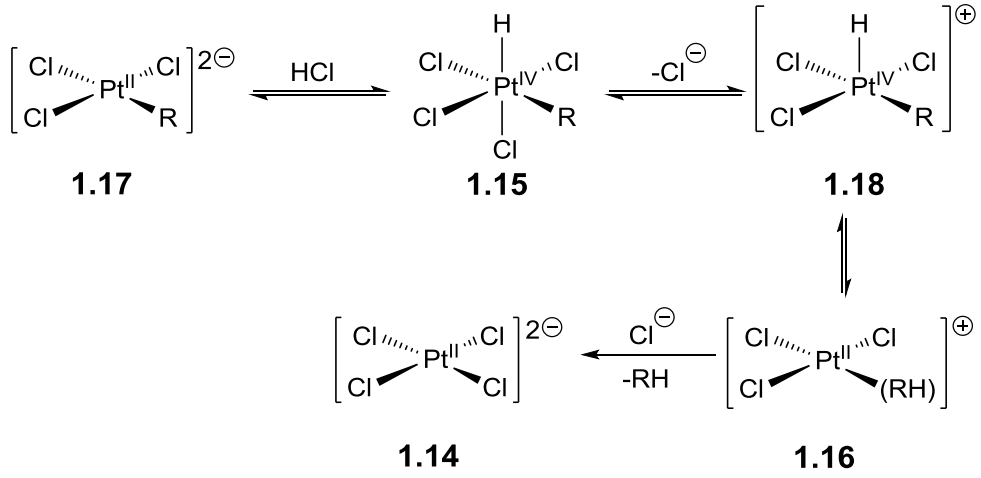

Scheme 1.18: Proposed mechanism for protonolysis of alkylplatinum(II) complexes.

In conclusion, electrophilic C-H activation takes place when an electrophilic metal activates a C-H bond, forming a complex with a metal-carbon bond and eliminating a proton. The Shilov methane oxidation system was believed to go by an electrophilic C-H activation mechanism, however the above studies on the system suggest an oxidative addition mechanism should be considered for the C-H activation step.[52-60]

1.2.5 AMLA/CMD

The term "Ambiphilic Metal-Ligand Activation" (AMLA) was coined by Davies and Macgregor[61] around the same time as Fagnou termed a similar process, "Concerted Metalation-Deprotonation" (CMD).[10] This is a bifunctional process which involves C-H activation by an electrophilic metal working synergistically with an intramolecular base. Four- or six-membered transition states may be formed during the C-H activation. These are called AMLA(4) and AMLA(6) processes respectively (**Scheme 1.19**).

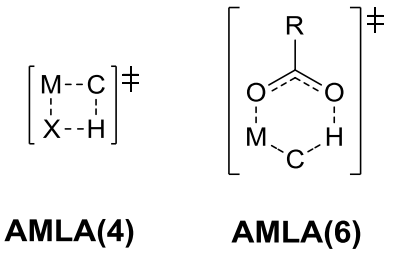

Scheme 1.19: AMLA(4) and AMLA(6) transition states.

In 1985, prior to the establishment of the AMLA mechanism, Ryabov *et al.* carried out the cyclometallation of N,N-dimethylbenzylamine (DMBA) with $Pd(OAc)_2$ and

investigated the mechanism.[62, 63] Kinetic studies with different substituents on the DMBA ring (H, Cl, Me and OMe) showed that the rate constant increased with donor strength of the substituent. The authors concluded an electrophilic C-H activation mechanism and suggested a Wheland intermediate. The activation enthalpy and entropy of the rate-limiting step (11 kJ mol^{-1} and -254 J K^{-1} mol^{-1} respectively) were in agreement with a highly ordered six-membered transition state (**Fig. 1.3**) where a proton is abstracted by an unbound oxygen of a monodentate acetate.

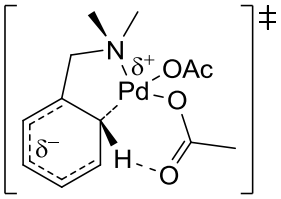

Fig. 1.3: Highly ordered six-membered transition state in cyclopalladation of DMBA.[62]

In 1997, Gomez, Martinez and co-workers carried out the cyclometallation of imines with $Pd(OAc)_2$[64] and proposed a highly ordered four-membered transition state (**Fig. 1.4**). As above, a bound acetate accepts the proton to produce acetic acid as a leaving group, however in this case it is a coordinated oxygen atom that acts as the proton acceptor via a four-membered transition state. The transition state proposed by Gomez and Martinez is very similar to the four-membered transition states of 1,2 addition put forward by the groups of Periana[4] and Gunnoe[5] discussed above (**Section 1.2.3**) where the heteroatom plays a significant role in the proton transfer.

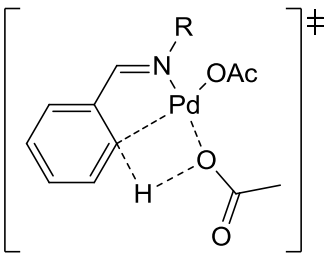

Fig. 1.4: Highly ordered four-membered transition state with monodentate acetate.[64]

In 2000 Sakaki *et al.* described a computational study of the C-H activation of benzene and methane by $M(O_2CH)_2$ and $M(PH_3)_2$ (M = Pd, Pt).[65] The authors concluded that C-H activation by OA using $M(PH_3)_2$ was disfavoured as it had a high activation energy and was considerably endothermic. However, C-H activation using $M(O_2CH)_2$ could be easily accomplished as it is assisted by formate through creating a strong O-H bond and

is exothermic. They suggested the mechanism involved $\eta^2 \rightarrow \eta^1$ displacement of one arm of the formate by the C-H bond and the C-H bond considerably lengthens in the transition state. Concerted electrophilic attack and proton abstraction subsequently occurs to give heterolytic fission of the C-H bond (**Fig. 1.5**).

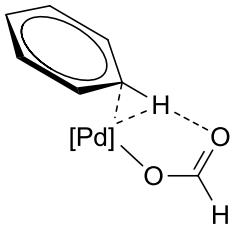

Fig. 1.5: Formate-assisted C-H activation of benzene by Pd.[65]

In a synthetic study in 2003, Davies showed acetate-assisted C-H activation of amines, imines and oxazolines with $[Cp^*MCl_2]_2$ (M = Ir, Rh) and $[(p\text{-}Cy)RuCl_2]_2$ could occur at room temperature (**Scheme 1.20**).[66] The authors concluded the role of the acetate was more than just that of a base. The reaction did not occur in the absence of acetate and in the case of imines, hydrolysis occurred instead to give primary amines. The reaction also did not occur when NaOAc was replaced with NEt_3. The Ir, Rh and Ru dimers all react with acetate to give $[Cp^*M(OAc)_2]$ and [(p-Cy)RuCl(OAc)] respectively. The authors suggested the acetate may help the breaking of the dimer and exchange of a chloride as well as acting as an intramolecular base as seen in previous literature. [66]

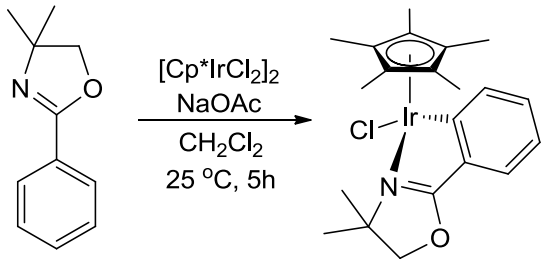

Scheme 1.20: Room temperature acetate-assisted C-H activation of an oxazoline.[66]

In 2005, Davies and Macgregor carried out a computational study on the cyclometallation of DMBA with $Pd(OAc)_2$.[8] Three mechanisms were investigated: oxidative addition, a four-membered mechanism and electrophilic (AMLA) activation via a six-membered transition state similar to that suggested by Ryabov.[62] A hydrogen-transfer process was found to be the most favoured pathway which occurred via a six-membered transition state. This involved an agostic C-H interaction with hydrogen

bonding to the acetate rather than the Wheland intermediate proposed by Ryabov (**Fig. 1.3**). The rate-determining step (13 kcal mol^{-1} activation barrier) was found to be displacement of one arm of acetate to form the agostic intermediate. The OA and four-membered pathways for hydrogen-transfer proved to be much less favoured with high activation barriers of 34.3 kcal mol^{-1} and 25.7 kcal mol^{-1} respectively. A small KIE of 1.2 was computed which was consistent with the small KIE observed by Ryabov. Davies and Macgregor later termed this mechanism AMLA.[61]

Following the study with $Pd(OAc)_2$, Davies and Macgregor performed a computational study on the acetate-assisted C-H activation of DMBA with $[Cp^*IrCl_2]_2$.[67] Once again, the six-membered AMLA transition state was the most favoured pathway (**Fig. 1.6**). This was the first C-H activation for a Cp*Ir species which did not proceed via an oxidative addition mechanism.

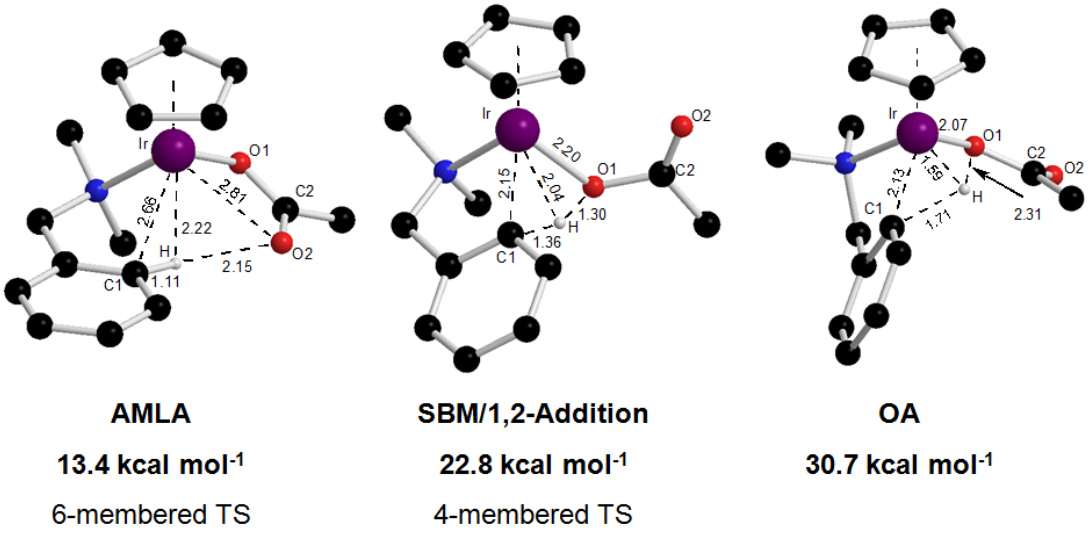

Fig. 1.6: Computed C-H activation transition states for DMBA cyclometallation with Ir.

In 2006 Fagnou described catalytic direct arylation with perfluorobenzenes using $Pd(OAc)_2$ (**Scheme 1.21**)[68] (direct arylation will be discussed in more detail in **Section 1.3.5**). The reaction worked better with electron-deficient arenes in contrast to an electrophilic aromatic substitution mechanism.

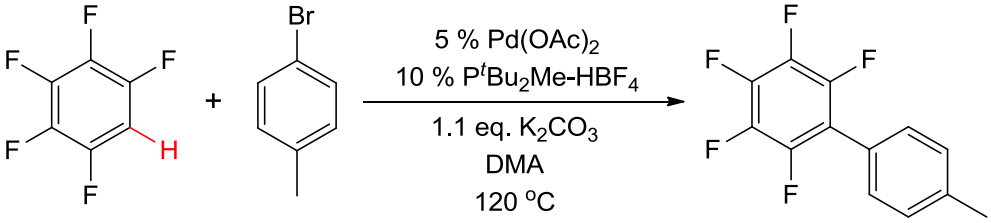

Scheme 1.21: Direct arylation of perfluorobenzenes.[68]

A computational study found a six-membered transition state and showed hydrogen-bonding to acetate plays an important part. The reaction proceeds through concerted arene metalation and C-H bond-cleavage which depends on the acidity of the C-H bond being broken. The lowest energy pathway was found to be hydrogen-transfer to the Pd-bound carbonate through a six-membered transition state (**Fig. 1.7**). H-transfer to the coordinated bromide was another possibility but was higher in energy and a pathway with intermolecular proton abstraction by external bicarbonate could not be found. Fagnou called the mechanism Concerted Metalation-Deprotonation (CMD) which emphasises that the proton is abstracted by base at the same time as M-C bond formation. Therefore, the easier reaction with electron-deficient arenes is due to the greater acidity of the proton being removed.

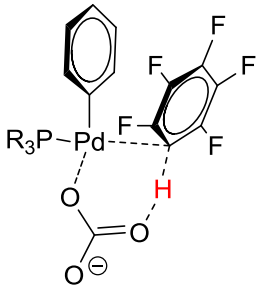

Fig. 1.7: Transition state for concerted metalation and H-transfer to carbonate.[68]

Fagnou later showed that addition of pivalic acid improved the reactivity and calculations showed that pivalate had a slightly lower transition state than carbonate (24.9 and 26.2 kcal mol^{-1} respectively).[69] Pivalate is thought to act as a catalytic proton shuttle from benzene to the stoichiometric carbonate. Davies and Macgregor later carried out a combined experimental and computational study on the effect of the intramolecular base in AMLA C-H activation of DMBA.[70] They tested a range of bases (acetate, trifluoroacetate, triflate, etc.) and found they all worked for the cyclometallation reaction but the pK_a only has a small effect on activation energy

barriers due to base strength reduction after coordination to the electrophilic metal. Also, they found that greater base strength means a stronger M-O bond.

In 2008, Ess *et al.* reported a DFT study on the C-H activation of benzene and methane by [Ir(acac)$_2$(OAc)] and [Ir(acac)$_2$(OH)].[71] They found the hydroxide can only act as an intramolecular base with a four-membered transition state but acetate can have four or six-membered transition states (**Scheme 1.22**). The six-membered transition state was found to be lower in energy than the two four-membered transition states for both benzene and methane. The authors concluded the energy difference between the two acetate-assisted transition states is due to energy required to deform the reacting species into their transition state geometries. The C-O bond lengths in the four-membered transition state are 1.21 and 1.36 Å which are rather different. However, in the six-membered transition state they are quite similar at 1.25 and 1.28 Å and this lowers the fragment distortion energy. These are essentially AMLA-4 and AMLA-6 mechanisms though the authors referred to them as acetate-assisted IES mechanism.

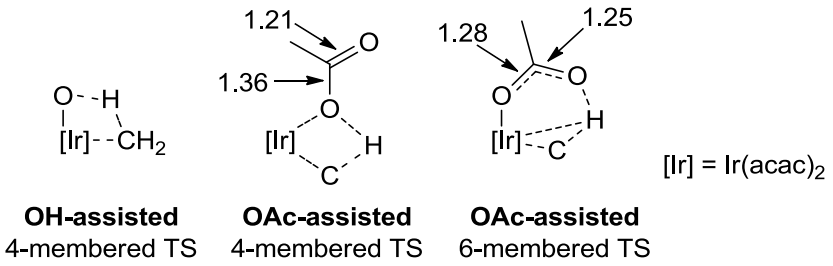

Scheme 1.22: Transition states for C-H activation of benzene and methane with Ir.[71]

The same group later carried out a combined experimental and computational study on the effects of carboxylic acids on benzene C-H activation.[72] Multideuteration was observed in the presence of CD_3CO_2D but only monodeuteration was observed in the presence of CF_3CO_2D. It was shown that the rate-determining step in acetic acid is displacement of one arm of acetate followed by benzene coordination which results in rapid deuterium exchange through a six-membered transition state. However in trifluoroacetic acid, C-H cleavage is the rate-determining step which is why only monodeuterated benzene is observed.

Overall, AMLA is a recently identified mechanism for C-H activation that involves activation by a Lewis acidic metal and an intramolecular base which work in synergy to provide a low energy pathway for C-H activation. AMLA can work with carbonate or

carboxylates as bases and cyclometallated complexes can be formed at room temperature. Calculations show the reaction proceeds via a six-membered agostic intermediate with significant hydrogen-bonding to the coordinated base. AMLA has been demonstrated by cyclometallation with various directing groups (see **Chapter 2**) and by numerous catalytic coupling reactions which continue to be a rapidly growing field (see **Section 1.3** and **Chapter 2**).

1.2.6 Conclusions on Mechanisms of C-H Activation

An overview of the different approaches to C-H activation has been given, describing the origins and details of the various mechanisms. It is clear that distinguishing between mechanisms can sometimes be difficult and this is where computation can help shed light in determining the mechanism of C-H activation. Goddard's computational study resulted in a spectrum of mechanisms showing that OA and SBM are different processes at opposite ends with OHM as a mechanism in between. Computation allows for fine distinctions between processes, however this has resulted in numerous different "sub-mechanisms" being reported for C-H activation by SBM, such as OHM and OATS. Both CMD and IES are electrophilic types of activation with an intramolecular base and therefore will be considered AMLA mechanisms as proposed by Davies and Macgregor. **Section 1.4** will give an overview of applications of C-H activation in catalysis.

1.3 Measurement of Kinetic Isotope Effect (KIE)

A key aspect in C-H functionalisation is whether the C-H activation step is rate-limiting. This is often assessed by measuring a deuterium kinetic isotope effect (KIE). The different types of experiment are illustrated in **Scheme 1.23**. **Type A** involves measuring the rate constants (k_H and k_D) for two reactions being carried out separately, one with a protio substrate and one with a deuterated substrate. The KIE is then calculated from the ratio of these rate constants (k_H/k_D). **Type B** involves carrying out a competition reaction with the protio and deutero substrates in the same flask. In this experiment, the two substrates compete for reaction with a limiting amount of a reaction partner. The KIE is calculated from the relative amount of products obtained by C-H vs C-D bond functionalisation (P_H/P_D). **Type C** is also a competition experiment but is intramolecular and involves competition between C-H and C-D bond functionalisation

on the same substrate. Again the KIE is calculated from the relative amounts of products formed from C-H vs C-D functionalisation (P_H/P_D). In all cases the observation of a KIE (different reactivity between deuterium and hydrogen) means that C-H bond is elongated in the transition state for the C-H activation step.

Type A: Comparing initial rates from intermolecular parallel reactions.

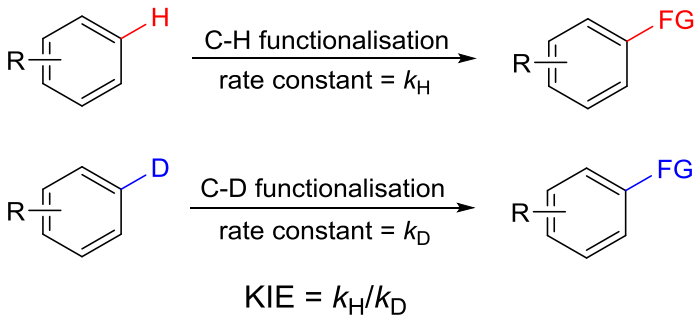

Type B: Comparing yields from intermolecular competition reactions.

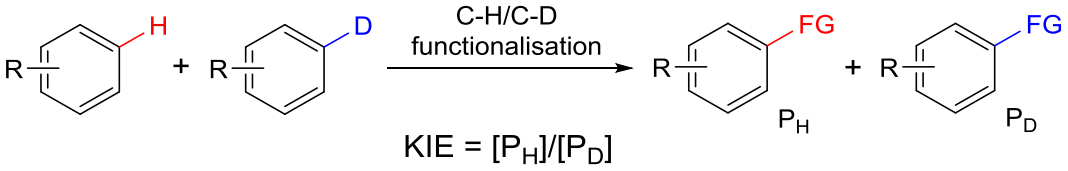

Type C: Comparing yields from intramolecular competition reaction.

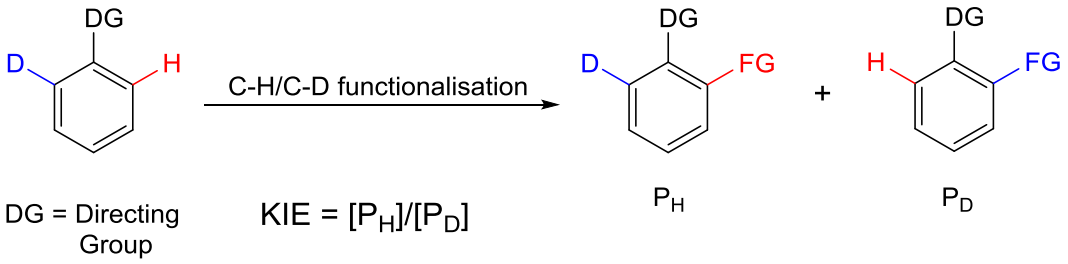

Scheme 1.23: Types of deuterium kinetic isotope effect (KIE) experiments.

In catalysis C-H functionalisation will only be one of possibly several steps and the correct interpretation of the different KIE experiments depends on the relative energy of C-H activation to the other steps. All three KIE experiments (**Types A-C**) only show a correct KIE for a reaction which has an irreversible rate-limiting C-H activation step (**Fig. 1.8**, Mechanism 1). This was discussed by Hartwig *et al.*[73] In mechanistic scenarios where a step not involving the substrate to be activated is rate-limiting and C-H activation is irreversible, **Type B** and **C** experiments may still show a KIE whereas

Type A does not (**Fig. 1.8**, Mechanism 2). If the rate-limiting step involves binding of the substrate that undergoes C-H activation, **Type C** may show a KIE whereas **Type A** and **B** experiments do not (**Fig. 1.8**, Mechanism 3). Where C-H activation is reversible and not rate-limiting but occurs before the rate-limiting step, all three experiments can still show a small KIE (**Fig. 1.8**, Mechanism 4). This can result from an equilibrium isotope effect depending on the rates of the forward and reverse reactions. Where C-H activation is reversible and not rate-limiting but occurs after the rate-limiting step (**Fig. 1.8**, Mechanism 5), the **Type A** experiment will not show a KIE as C-H activation occurs after the rate-limiting step. **Type B** and **C** experiments can still show a small KIE as substitution of a C-H for a C-D bond can change the equilibrium concentration of the species that reacts to form the product. It is clear from these scenarios that only **Type A** experiments provide conclusive evidence on whether C-H activation is rate-limiting. However, the absence of a KIE from a **Type B or Type C** experiment can be used to show C-H activation is not rate-limiting.[73]

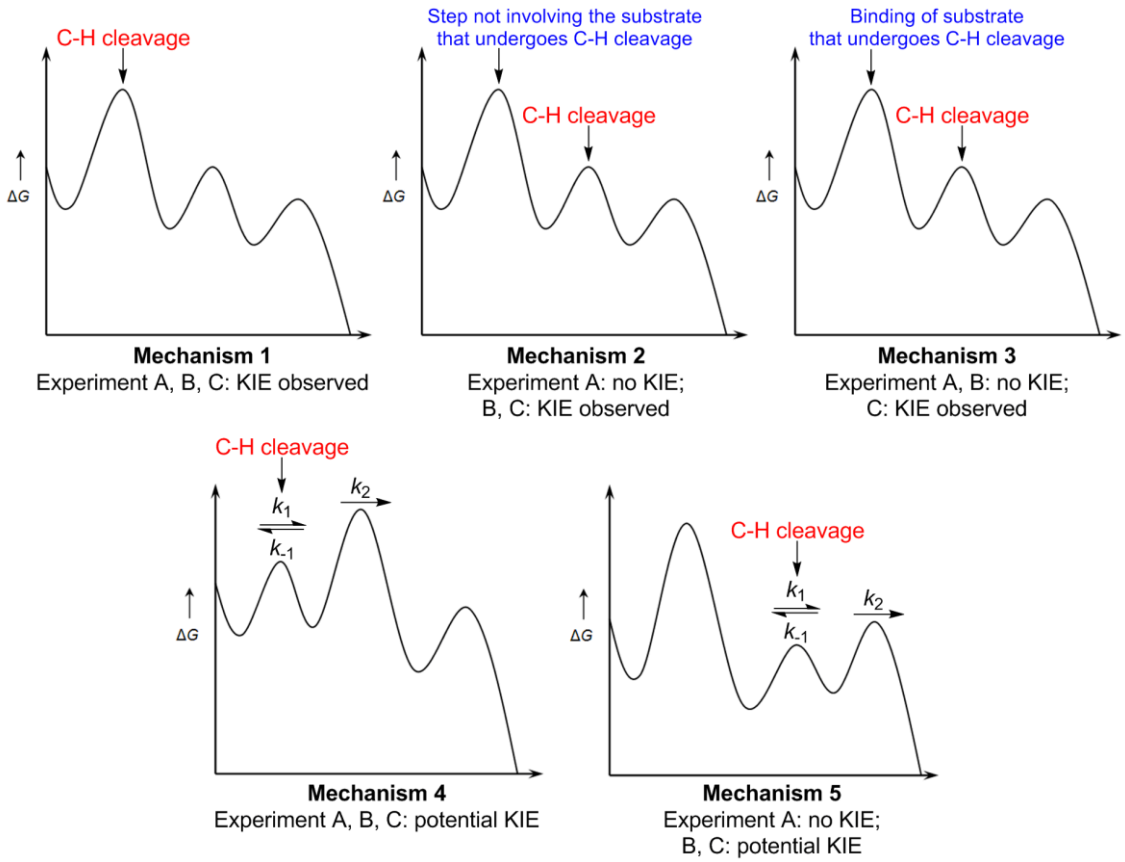

Fig. 1.8: Different catalytic mechanisms and expected KIE for Experiments A-C.[73]

1.4 Applications of C-H Activation in Catalysis

C-H activation is a very popular area of research in organometallic chemistry and very important in the area of green chemistry. C-H activation makes efficient use of cheap abundant hydrocarbons[11, 74] and is applicable in synthesis and catalysis.[75-78] Traditional approaches to direct C-H functionalisation require harsh conditions and suffer from issues concerning selectivity and functional group tolerance. They require use of strong bases or acids to remove H^- or H^+ and even radical reagents to abstract $H^{\bullet}$.[79] Activating a C-H bond using a transition metal is a more desirable route because (catalytic) functionalisation can occur with reduced waste and milder conditions. Most organic compounds have numerous C-H bonds; however transition metal complexes can be tuned to perform highly selective reactions.[80] This part of the chapter will give an overview of catalytic C-H functionalisation for each type of C-H activation mechanism.

1.4.1 Catalytic Oxidative Addition

In order for an oxidative addition/reductive elimination reaction to work in catalysis, the metal complex must initially favour C-H oxidative addition and then favour reductive elimination when in the higher oxidation state. The metal-ligand system can be tuned to accomplish this but it can be difficult. Tuning the system to favour OA can result in difficult reductive elimination and vice versa.

Intramolecular C-H activation followed by C-C bond formation is a very atom efficient process. An example of this is the catalytic reaction shown in **Scheme 1.24** which is a 100 % atom efficient reaction. The C-H activation step is oxidative addition and suitable catalysts for this reaction include $RuH_2(CO)(PPh_3)_3$[81] and $[Cp^*Rh(CH_2{=}CHSiMe_3)_2]$[82].

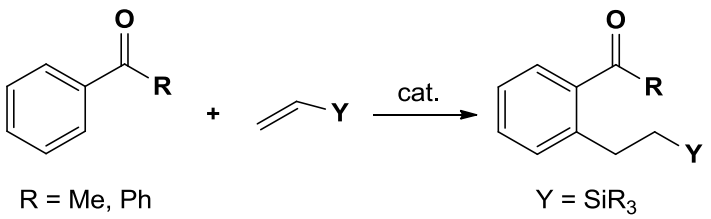

Scheme 1.24: A 100 % atom-efficient catalytic C-H activation reaction.

In 2006, Bergman and co-workers studied the scope of 100 % atom-efficient inter- and intramolecular couplings between dihydroquinazolines (**1.19**) and alkenes (**Scheme 1.25**).[83] A $Rh^{I}/P(cy)_3/HCl$ catalyst system gave high to excellent yields (60-90 %).

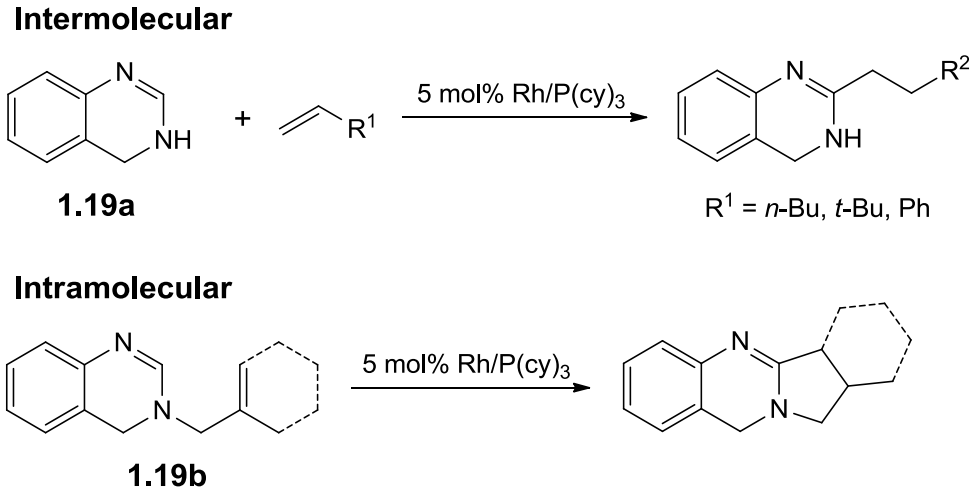

Scheme 1.25: Inter- and intramolecular couplings of alkenes to dihydroquinazolines.[83]

An experimental and DFT study was carried out to investigate the mechanism.[84] An OA mechanism was proposed (**Scheme 1.26**) whereby association of the heterocycle (**1.19**) to the metal takes place as a dative ligand through the sp^2 hybridised nitrogen (**1.20**). Intramolecular oxidative addition of the adjacent C-H bond occurs to give a rhodium hydride species (**1.21**). Finally rapid H-transfer gives **1.22** and restores Rh^{I}. Computation supported this mechanism and suggested OA is the rate-determining step. The final organic product is obtained after loss of one $P(cy)_3$ ligand, then alkene association is followed by C-C reductive elimination.

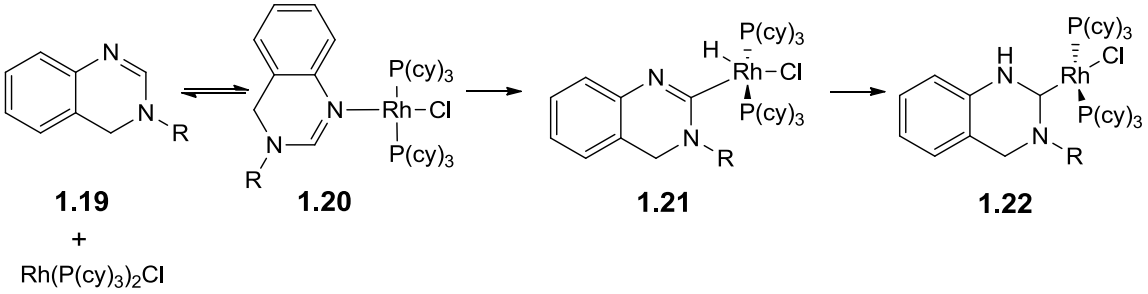

Scheme 1.26: Mechanism for C-H activation of dihydroquinazolines with Rh^{I}.[84]

1.4.2 Catalytic σ-Bond Metathesis

C-H activation by SBM in catalysis is rare. The group of Hartwig has shown catalytic C-H borylation of linear alkanes occurs using a Cp*Rh(η^4-C_6Me_6) catalyst to give linear alkylboranes in high yield up to 92 % (**Scheme 1.27**).[85, 86] A combined experimental and theoretical collaboration found that H-transfer to boron occurs by a SBM mechanism.[87] The unoccupied p orbital of boron accepts electron density from the metal and lowers the energy of the transition state.

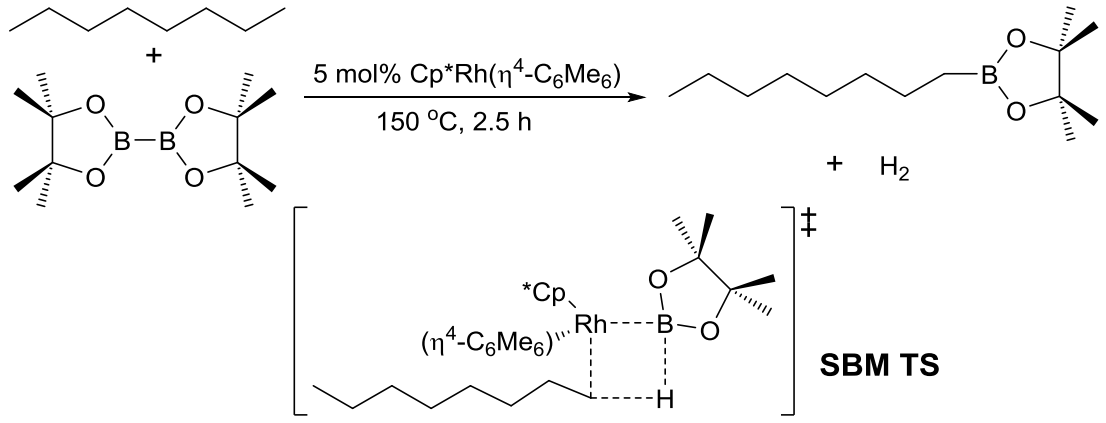

Scheme 1.27: Catalytic borylation of linear alkanes with SBM transition state.[86]

Sadow and Tilley observed catalytic SBM in a hydromethylation reaction using Cp^*_2ScMe.[88] Cp^*_2ScMe catalysed the addition of methane across the double bond of propene to form isobutane along with $Cp^*_2ScCH_2CHMe_2$ and $Cp^*_2ScCH{=}CMe_2$ (**Scheme 1.28**). $Cp^*_2ScCH{=}CMe$ and isobutane are formed via SBM of the insertion product $Cp^*_2ScCH_2CHMe_2$ and a second equivalent of propene (see scheme below). The rate determining step was deduced to be olefin insertion into the Sc-Me bond.

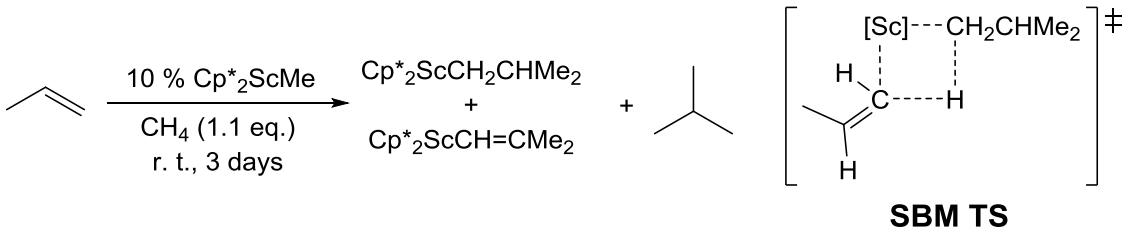

Scheme 1.28: Catalytic hydromethylation of propene with SBM transition state.[88]

1.4.3 Catalytic 1,2-Addition

Currently there are only a limited number of proven examples in the literature of C-H activation by 1,2-addition or AMLA(4), none with C-C bond formation. Catalysis by this mechanism is limited to H/D exchange. As mentioned above (**Section 1.2.3**), Gunnoe and co-workers observed catalytic H/D exchange of benzene and water catalysed by [TpRu(PMe_3)$_2$OH] (**1.10**).[5] A mixture of C_6D_6, [TpRu(PMe_3)$_2$OH] (1.6 mol %) and water at 100 °C produced $C_6D_xH_y$ ($x + y = 6$). Reaction without the Ru catalyst or replacing the hydroxyl group with OTf did not give H/D exchange.

The authors proposed the mechanism shown in **Scheme 1.29**. Ligand dissociation from **1.10** creates a vacant coordination site where d_6-benzene binds. Addition of the benzene C-D bond across the Ru-OH bond gives **1.23**. The reverse of these steps allows for H/D exchange between the OH and C_6D_6. ^{1}H NMR spectroscopy determined that rate of disappearance of hydrogen at OH is matched by rate of hydrogen incorporation into benzene. As discussed earlier, (see **Section 1.2.3**) a later computational study confirmed this as a 1,2-addition.[43]

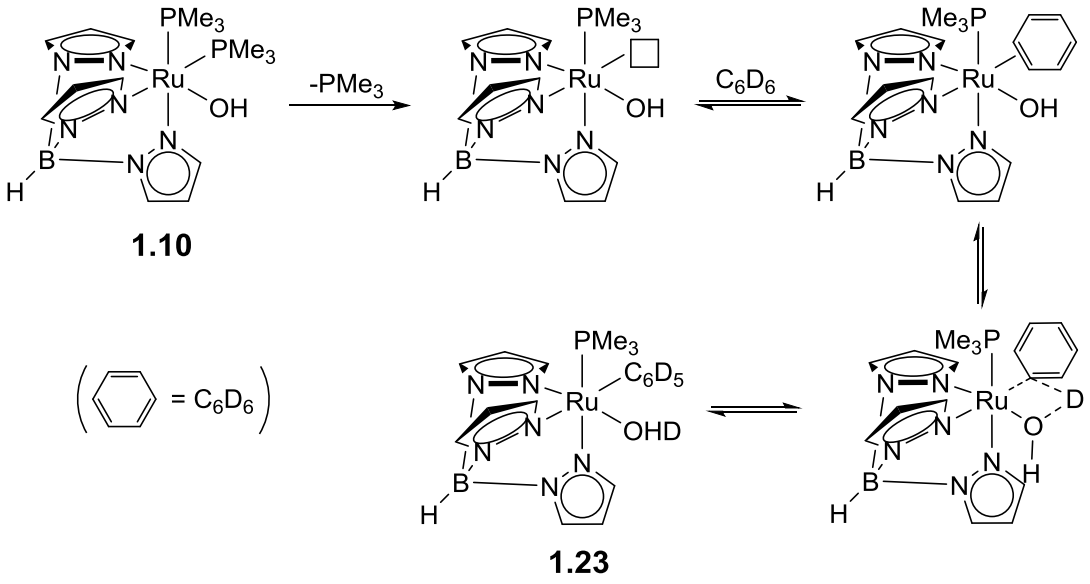

Scheme 1.29: Proposed mechanism for H/D exchange between C_6D_6 and water catalysed by **1.10**.[5]

1.4.4 Catalytic Electrophilic Activation

In 1998, Periana *et al.*, building on the Shilov system (see **Section 1.2.4**),[50, 51] reported the catalytic oxidation of methane to methyl bisulfate using a Pt^{II} bipyrimidine catalyst in concentrated sulfuric acid (**Scheme 1.30**).[89] The authors proposed a mechanism for the reaction with three key steps namely electrophilic C-H activation, oxidation and functionalisation.

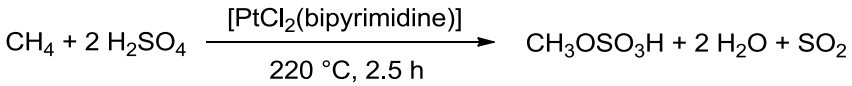

Scheme 1.30: Catalytic methane oxidation using Pt^{II}.[89]

In 2002, Strassner *et al.* reported oxidation of methane to CF_3CO_2Me using Pd bis-NHC complexes (**Fig. 1.9**) in trifluoroacetic acid/anhydride mixture with potassium peroxodisulphate oxidant.[90] The Pd catalysts are stable to the acidic conditions in contrast to the analogous Pt complexes which immediately decompose. The methyl ester product however, is of little commercial use and the system requires an expensive solvent system with 100 equivalents of oxidant.

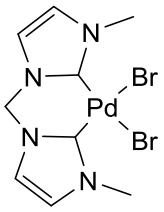

Fig. 1.9: Example of a Pd bis-NHC complex capable of oxidising methane.[90]

Many of the catalytic C-H oxidations based on the Shilov system use expensive oxidising agents in large excess and highly acidic conditions. As illustrated below, catalytic AMLA C-H activation which is based on electrophilic activation but with intramolecular base assistance, can overcome some of these problems.

1.4.5 Catalytic AMLA/CMD

AMLA C-H activation is an extension of electrophilic activation and in recent years has been exploited in many catalytic C-H functionalisation reactions including amidations,[91] aminations,[92] phosphorylations,[93] acylations[94-96] and oxygenations.[97] Since the discovery of AMLA/CMD its application in direct arylation has been reviewed.[2, 98-101] This section will focus on Pd, Ru, Rh and Ir-catalysed direct arylations and alkylations; other reactions will be dealt with in later chapters. Both intra- and intermolecular transformations have been studied with intermolecular transformations being more difficult and suffering from issues concerning selectivity. The reactions can be carried out using a directing group or can be non-directed.

In the AMLA C-H activation step there is no change in the oxidation state of the metal however, since the products are obtained after reductive elimination there is a need for an oxidative step somewhere within the catalytic cycle. To address this issue, reactions are either carried out by (i) using a halogenated substrate (Ar-X) which oxidatively adds (**Scheme 1.30 A**) or (ii) using an external oxidant (e.g. $Cu(OAc)_2$, $AgCO_3$) after the reductive elimination (**Scheme 1.31 B**). In the case of (i), many researchers have reported the C-H activation as non-directed however it could be argued that the AMLA C-H activation is C-directed as a carbon directing group has formed after OA of the C-X bond. In the case of (ii), the second aryl group can add via a second C-H activation, or transmetallation.

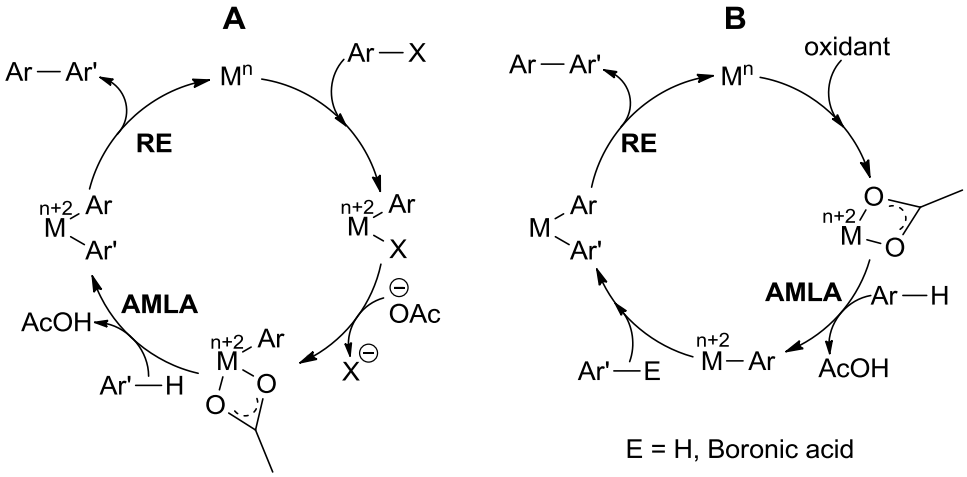

Scheme 1.31: Direct arylations with a substrate which oxidatively adds (**A**) and with an external oxidant (**B**).

Palladium Catalysis

As mentioned above (**Scheme 1.21)** in 2006 Fagnou demonstrated that palladium-catalysed direct arylation of perfluorobenzenes involves AMLA/CMD C-H activation.[68] At about the same time the groups of Echavarren and Maseras studied the intramolecular arylation of **1.24**, giving **1.25** and **1.26** depending on the substituent R **Scheme 1.32**).[102] The authors reported a high KIE ($K_{H/D}$ = 5) from a **Type A** experiment which suggested the rate-determining step is C-H activation.

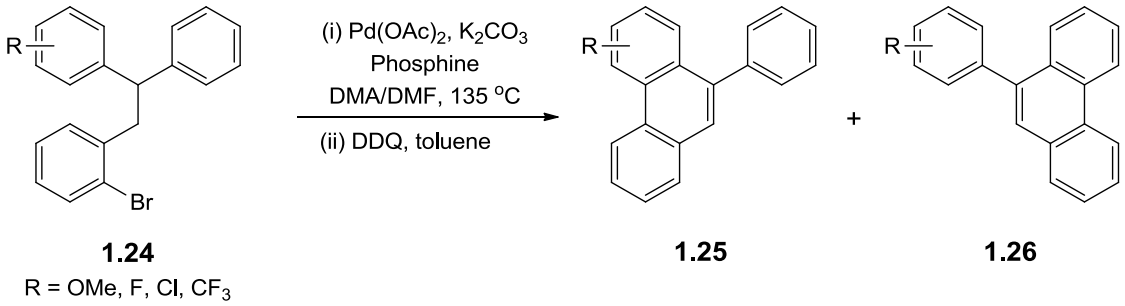

1.24
R = OMe, F, Cl, CF_3

1.25 **1.26**

Scheme 1.32: Palladium-catalysed bicarbonate-assisted arylation of arenes.[102]

Three different transition states were computed, TS1, a four-membered transition state with bromide as an acceptor, TS2 with external bicarbonate as base and TS3 with bound bicarbonate as base (**Fig. 1.10**). TS1 had the highest energy barrier (43.3 kcal mol^{-1}) and initially the authors favoured C-H activation through a six-membered transition state with strong hydrogen-bonding between the proton and bicarbonate (TS3, 23.5 kcal mol^{-1}). In a later publication, the authors reported that the energy difference between TS2 and TS3 was very small (6 kcal mol^{-1} at most) and that the favoured pathway depended on the ring substituents.[103] Calculations correctly modelled the experimental results in that electron-withdrawing substituents on the ring being activated favoured the formation of **1.25** whereas electron-donating substituents favoured **1.26**. In a later study, bidentate phosphines were tried and found to be very good ligands for this reaction.[104] In this case DFT studies suggested the reaction proceeds via an intermolecular base-assisted mechanism.

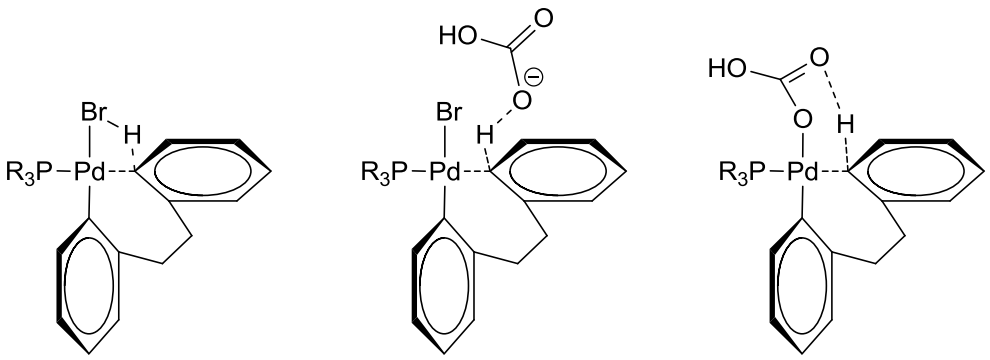

TS1 43.3 kcal mol^{-1} **TS2** 17.4 kcal mol^{-1} **TS3** 23.5 kcal mol^{-1}

Fig. 1.10: Transition states modelling intramolecular arylation of **1.25**.[103]

Fagnou's group also studied intramolecular direct arylation reactions using **1.27** and $Pd(OAc)_2$ (**Scheme 1.33**).[105] The cyclised product (**1.28**) was formed in high yield regardless of the X substituent being Cl, Br or I. Product **1.29** was only observed as a trace product in some cases.

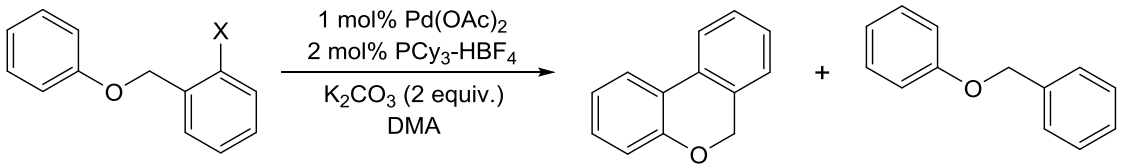

1.27 **1.28** **1.29**

Scheme 1.33: Palladium-catalysed direct arylation to form biaryls.[105]

The authors found the base and its counterion affected catalyst selectivity and reactivity.[106] A later experimental study found that using pivalate as the intramolecular base lowered the energy barrier.[107] The authors proposed the mechanism shown in **Scheme 1.34**. OA takes place into the C-X bond of **1.27** after which two pathways are possible. Anion exchange of pivalate for halide can occur and CMD can take place, alternatively, pivalate can act as an external base at the C-H bond being cleaved. In either case the biarylpalladium(II) intermediate then undergoes reductive elimination to the product.

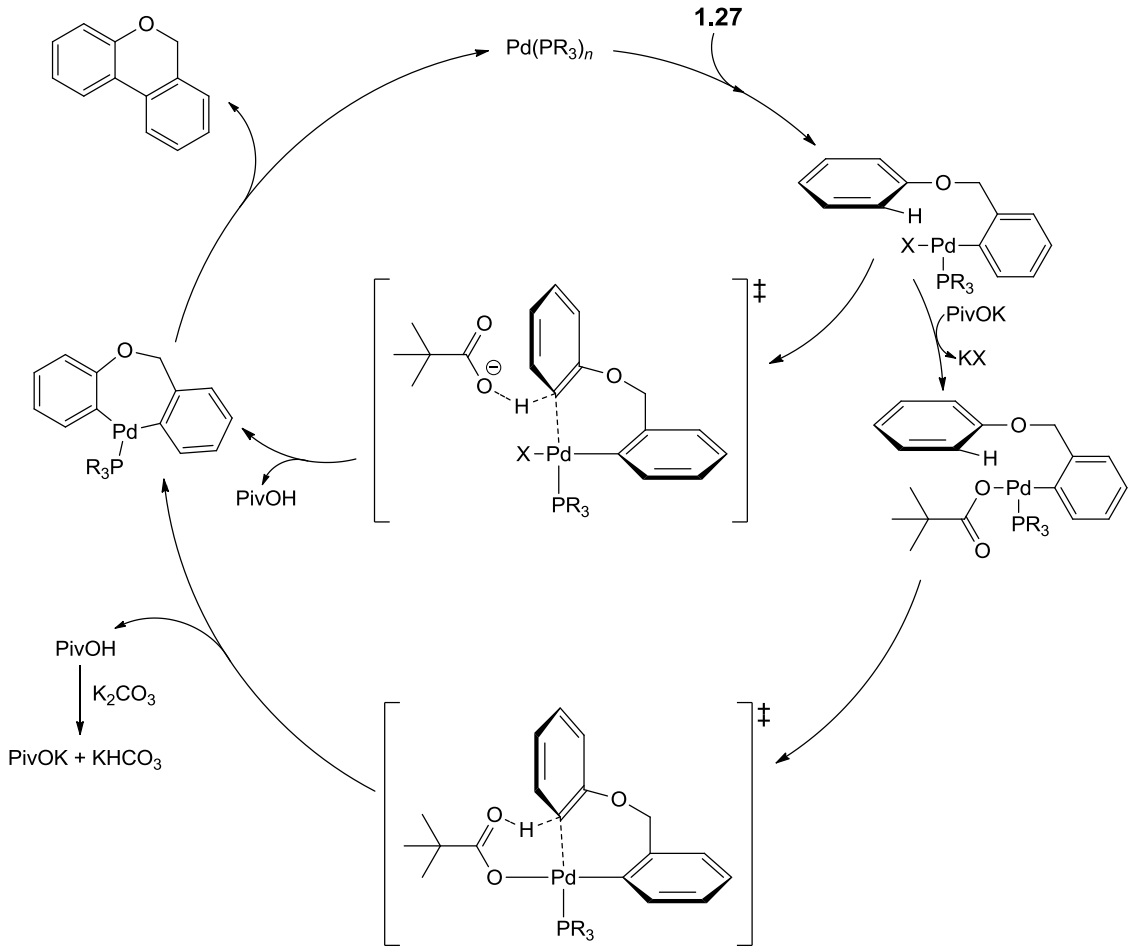

Scheme 1.34: Proposed catalytic cycle for intramolecular arylation.[107]

Fagnou's group investigated intramolecular sp^3 C-H bond activation in alkane arylation reactions (**Scheme 1.35**).[108] The products were formed in almost quantitative yield and were selective for the isomer produced, showing C-H activation on a methyl to be favoured over ethyl. Calculations showed a six-membered transition state with an agostic interaction between the C-H bond being activated and the palladium with hydrogen-bonding to the acetate (**Fig. 1.11**). Computation also agreed with the selectivity observed experimentally as primary C-H bond activation (**Fig. 1.11**) had a lower activation barrier than secondary C-H bond activation (27.0 kcal mol^{-1} vs 32.5 kcal mol^{-1}).

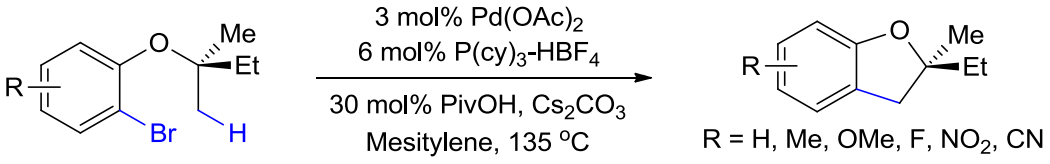

Scheme 1.35: Palladium-catalysed alkane arylation.[108]

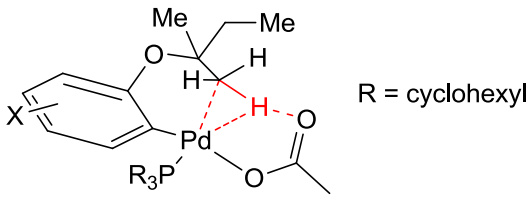

Fig. 1.11: Transition state for sp^3 C-H activation in intramolecular alkane arylations.[108]

Baudoin, Clot and co-workers studied the intramolecular sp^3 C-H activation of methyl groups using $Pd(OAc)_2$ to give benzocyclobutenes (**Scheme 1.36**).[109] C-H activation was suggested to be the rate-limiting step however, this is based on a **Type C** KIE experiment ($K_{H/D}$ = 5.8).

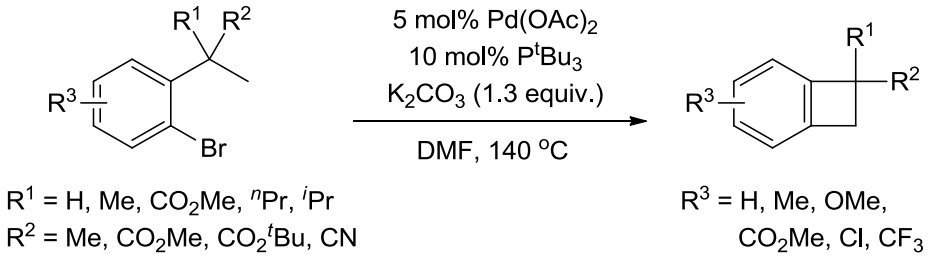

Scheme 1.36: Palladium-catalysed sp^3 C-H activation to give benzocyclobutenes.[109]

Two isomers (**1.30** and **1.31**) could be formed after the C-Br oxidative addition step (**Fig. 1.12**). A computational study showed **1.31** is more stable than **1.30** by 6.5 kcal mol^{-1}. Calculations of the substitution of Br in **1.31** by various bases (CO_2Me, CO_2^- and CO_2H) gave rise to transition states analogous to those found by Fagnou *et al.*[108] however, the transition states had higher activation energies (33-45 kcal mol^{-1} vs 27.0 kcal mol^{-1}). The TS from **1.30** shows an agostic interaction with a C-H bond on the ^{t}Bu group of the phenyl. Proton-transfer from the sp^3 carbon atom then occurs in a plane perpendicular to the P-Pd-Ph axis (**1.32**). This study showed the carbonate/carboxylate does not have to be *cis* to the site being activated in the square plane.

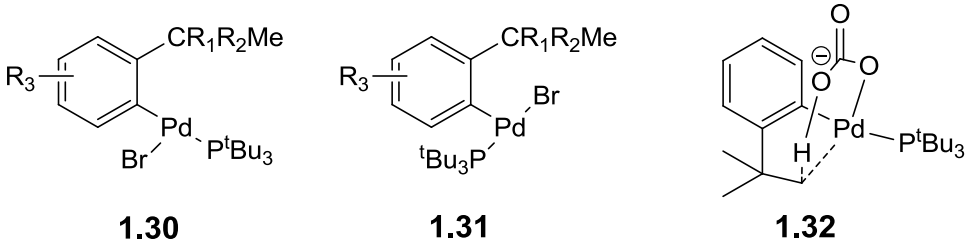

1.30 **1.31** **1.32**

Fig 1.12: Proposed isomers formed and the subsequent C-H activation transition state.

All reactions discussed so far describe intramolecular direct arylations, however intermolecular direct arylation using halogenated substrates is also known. Weak N-donor groups like oxazoles,[110] indoles,[111] pyrroles[112] and imidazoles[112] undergo Pd-catalysed direct arylation with aryl halides but an excess of one of the coupling partners is usually required. However Fagnou *et al.* showed that a 1:1 ratio of the aryl partners could be used for intermolecular arylation using a slight excess of K_2CO_3 and a sub-stoichiometric amount of pivalic acid but no phosphine (**Scheme 1.37**).[112] The benefits of these conditions were applied to a broad range of heterocycles.[113]

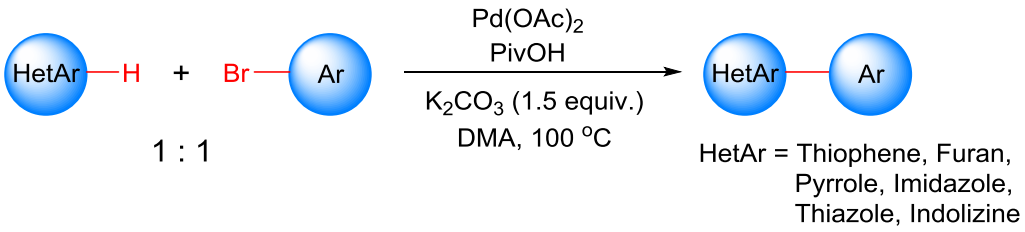

Scheme 1.37: Widely applicable palladium-catalysed direct arylation of heterocycles.[112]

The reactions described above all involve C-X bonds however, direct arylations involving non-halogenated substrates have been reported where an external oxidising agent is used for catalyst turnover **(Scheme 1.31 B)**. Unlike direct arylations with halogenated substrates, no phosphine is used in these reactions and cyclometallation occurs first rather than OA. Fagnou's group reported the intramolecular coupling of arenes using non-halogenated substrates (**Scheme 1.38**).[3, 114] The reaction worked well for both electron-rich and electron-deficient diarylamines and gave carbazoles or dibenzofurans as products (**1.34**). The group showed that air was a better oxidant than copper(II) acetate for these transformations. Pivalic acid produced optimum results when used as a solvent, giving high yields of **1.34.**

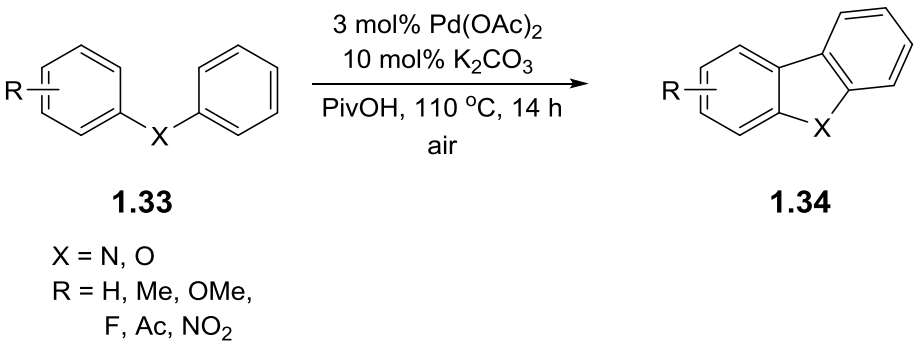

Scheme 1.38: Palladium-catalysed intramolecular coupling of diarylamines under air.[114]

Formation of carbazoles has also been reported by Fujii, Ohno and co-workers from the successful coupling of anilines and phenyl triflate (**Scheme 1.39**).[99, 115] This involves *N*-arylation followed by oxidative coupling of the two aryls with two intramolecular C-H activations taking place.

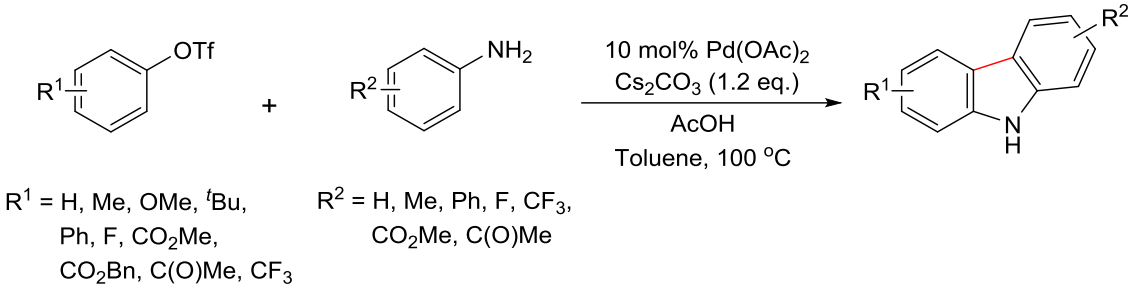

Scheme 1.39: Pd-catalysed coupling of phenyl triflates with anilines.[115]

Sanford's group reported an example of palladium-catalysed intermolecular direct arylation using non-halogenated substrates (**Scheme 1.40**).[76, 116] The cross-coupling of pyridines, quinolines, pyrimidines and pyrazoles with various arenes was carried out. Benzoquinone was used as a promoter in the reaction and C-H activation took place with high selectivity at the least hindered position for several 1,2-, 1,3- and 1,2,3-substituted arenes. Arenes with electron-donating and electron-withdrawing groups could be used. Mechanistic studies showed benzoquinone binds to the Pd^{II} centre making it more electrophilic but can then dissociate to facilitate reductive elimination.

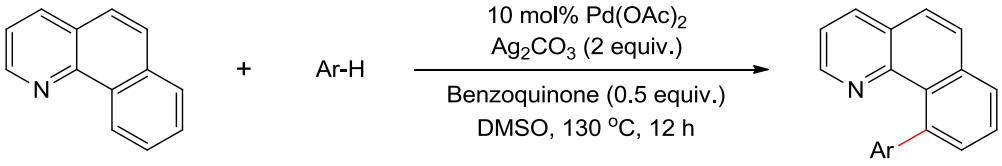

Scheme 1.40: Benzoquinone-promoted palladium-catalysed direct arylation.[116]

In 2011, Li, Zhang and co-workers reported the intermolecular Pd-catalysed coupling between pyridine *N*-oxides and indoles (**Scheme 1.41**).[117] Reactions proceeded with high selectivity and broad scope with C-H activation on both coupling partners even a bromine on the pyridine N-oxide is tolerated.

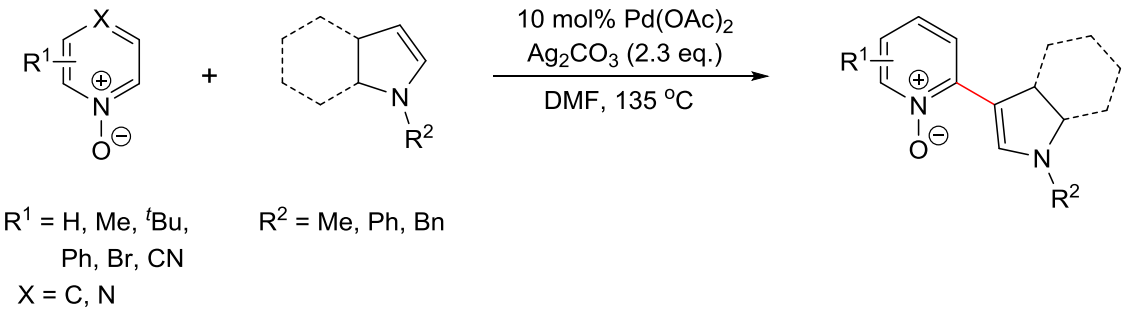

Scheme 1.41: Intermolecular coupling of pyridine *N*-oxides with indoles.[117]

All the examples discussed above involve Pd^{0}/Pd^{II} cycles. However Pd^{II}/Pd^{IV} is also possible. Sanford *et al.* reported the direct arylation of N-directing groups including phenylpyridine and quinoline using $[Ph_2I]BF_4$ or [Mes-I-Ar]BF_4 as the aryl reagents. It was proposed that N-directed AMLA C-H activation occurs to give a Pd^{II} cyclometallated complex followed by oxidation using the aryliodonium reagent to give an intermediate from which reductive elimination occurs to give the product.[118] Later studies showed that oxidation occurred at a Pd^{II} dimer giving a $Pd^{II/IV}$ or $Pd^{III/III}$ dimeric intermediate.[119]

Directing groups containing phosphorus have recently emerged as useful substrates for C-H functionalisation. In 2013, Kim *et al.* reported the Pd-catalysed direct arylation of *N*-aryl phosphoramidates using Ar_2IOTf as the aryl reagent.[120] The reaction proceeds at room temperature via AMLA C-H activation to give a six-membered palladacycle (**Fig 1.13**). This is followed by oxidative addition of the aryliodonium reagent and reductive elimination to give the product. The authors applied the same system to direct arylation of aryl phosphates as well.[121]

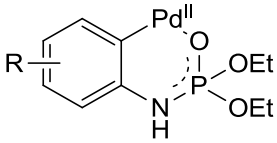

Fig 1.13: Six-membered palladacycle formed after AMLA C-H activation.[120]

In 2013, Sanford's group reported direct alkylation of phenylpyridines and anilides with potassium alkylfluoroborates using $Pd(OAc)_2$ (**Scheme 1.42**).[122] Methyl and primary alkyls were installed on the phenyl groups and reactions took place under weakly acidic conditions with no need for BQ. The authors showed that MnF_3 does not oxidise RBF_3K to give an alkyl radical (R•), rather it oxidises Pd^{II} by F^{+} transfer. Replacing MnF_3 with

an F^+ source (*N*-fluoro-2,4,6-trimethylpyridinium triflate) proceeded well, providing further evidence that the role of MnF_3 is to oxidise the Pd^{II} intermediate.

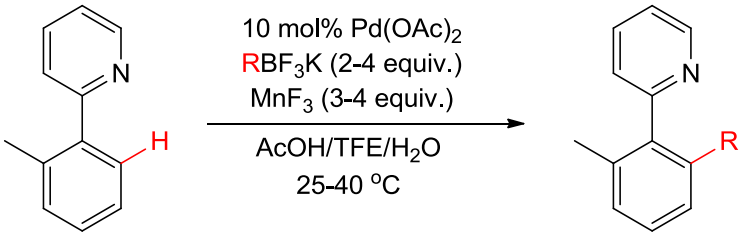

Scheme 1.42: Pd-catalysed alkylation of 2-(*o*-tolyl)pyridine.[122]

In conclusion, there are numerous reported examples of Pd-catalysed direct arylations. Both intra- and intermolecular reactions have been reported for direct arylations with halogenated substrates and with heteroatom directing groups. There are mostly examples of Pd^0/Pd^{II} cycles however Pd^{II}/Pd^{IV} cycles are also possible. In the case of Pd^{II}/Pd^{IV} cycles, directing groups are more likely as opposed to Pd^{II}/Pd^0 cycles where both directing groups and halogenated substrates are used.

Ruthenium Catalysis

The use of Ru catalysts for direct arylations and alkylations has been reviewed.[100] In 2008, Ackermann's group reported the first phosphine-free Ru-catalysed direct arylation of 1,2,3-triazoles (**Scheme 1.43**).[123] They studied the efficiency of cocatalyst additives and found acids to be the best with the sterically hindered carboxylic acid, $MesCO_2H$ giving optimal results. The excellent catalytic activity observed was explained by a base-assisted AMLA type mechanism, proceeding through a six-membered transition state. The system showed a broad scope and worked with arenes containing enolisable ketones, esters and heteroarenes. Competition experiments showed a preference for aryl bromides over aryl chlorides and so biaryls containing chlorides could be formed (**Scheme 1.43**).[100, 124] The group extended their studies to reactions with aryl chlorides and found reactions conditions could be tuned to selectively give monoarylated or diarylated products by changing the ratio of starting materials or by using phenyltriazoles with the R^2 substituent at different positions.[125] Recently, the group reported related direct arylation of 2-phenoxypyridines.[126]

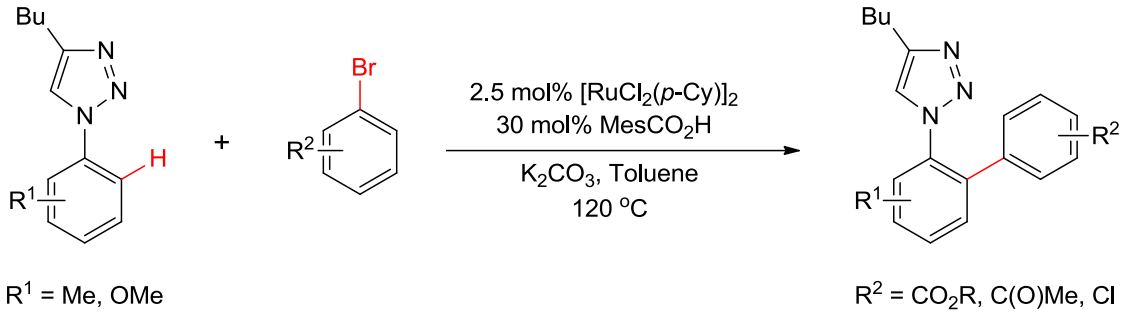

Scheme 1.43: Ru-catalysed direct arylation using $MesCO_2H$ as cocatalyst.[123]

The group of Dixneuf carried out Ru-catalysed direct arylation of 2-phenylpyridine with aryl bromides containing both electron-donating and electron-withdrawing groups.[127] The Ru catalyst was derived from a pyrimidinium NHC salt (**Fig. 1.14**) and selectively gave diarylated products in the presence of Cs_2CO_3. DFT calculations on [Ru(NHC)(phenylpyridine)] supported an AMLA type mechanism in which a proton is abstracted by the cooperative effects of the internal carbonate and metal. In a later mechanistic study however, the authors stated that external base was involved to facilitate the C-H activation.[128]

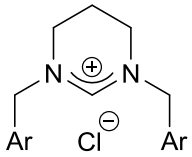

Fig. 1.14: Pyrimidinium NHC salt used to generate Ru catalyst.[127]

Dixneuf, Fischmeister and co-workers extended their studies to Ru-catalysed direct arylation using various arenes containing an *N*-heterocycle with no need for a pyrimidinium salt (**Scheme 1.44**).[129] Substituted benzenes, pyridines and thiophenes were used as coupling partners with KOPiv as cocatalyst with temperatures as low as 80 °C. In most cases the diarylated product was the major product and the authors stated the reaction proceeded via a CMD mechanism. Later the same group reported similar direct arylations in water, some even at room temperature.[130]

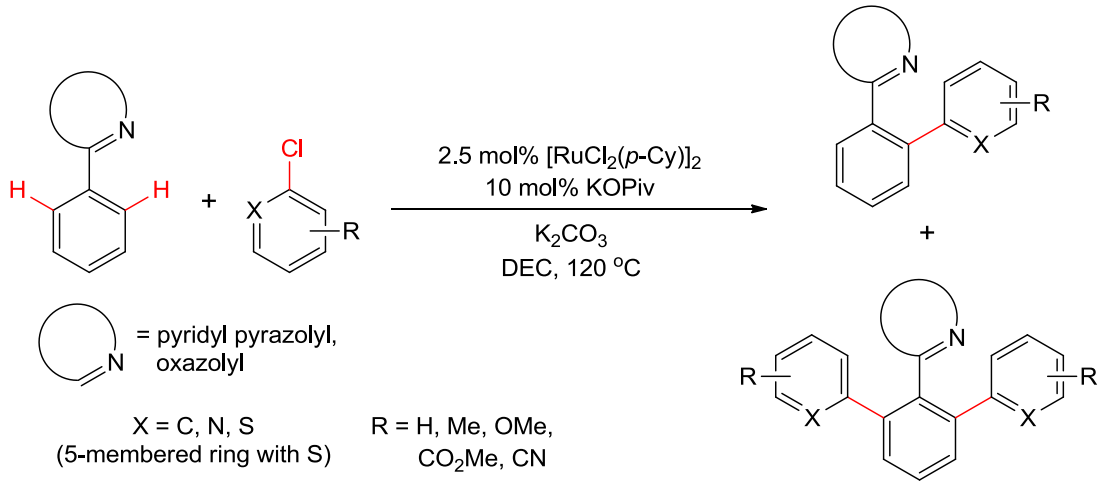

Scheme 1.44: Ru-catalysed direct arylation using DEC as solvent.[129]

Ackermann's group also reported direct arylations with other substrates such as phenyloxazolines and N-phenylpyrazoles.[100, 131] Ackermann and Mulzer investigated dehydrative direct arylation with non-halogenated substrates (**Scheme 1.45**).[132] Both C-H and C-OH bonds were functionalised in this reaction. The Ru catalyst was highly chemo- and regioselective and there was no undesired by-product formation from any nucleophilic reactivity of the phenols. The *p*-TsCl converts the phenol into a tosylate after which OA occurs. This was not emphasised by the authors.

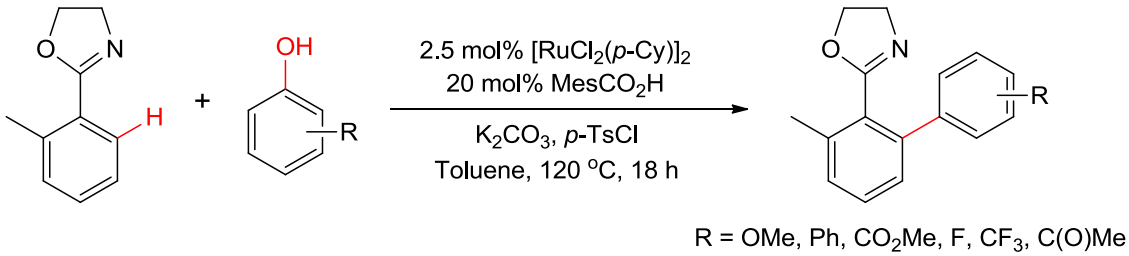

Scheme 1.45: Ru-catalysed dehydrative coupling between arenes and phenols.[132]

Carboxylate-assisted Ru-catalysed direct alkylations were also investigated by Ackermann's group. Intermolecular direct alkylation of phenylpyridine with β-hydrogen-containing alkyl halides was studied (**Scheme 1.46**).[133] As with direct arylations, the group found that NHC and phosphine additives gave poor results and carboxylic acid additives gave the highest yields with the sterically-hindered 1-adamantanecarboxylic acid (1-AdCO_2H) giving optimal results. The reactions were highly site-selective and the alkylated products were the only products observed. The system worked for alkyl chlorides, bromides and iodides with bromides giving optimal

results and chlorides giving lower yields. The scope was relatively broad with the reaction working for phenylpyrazoles and also ketimines.

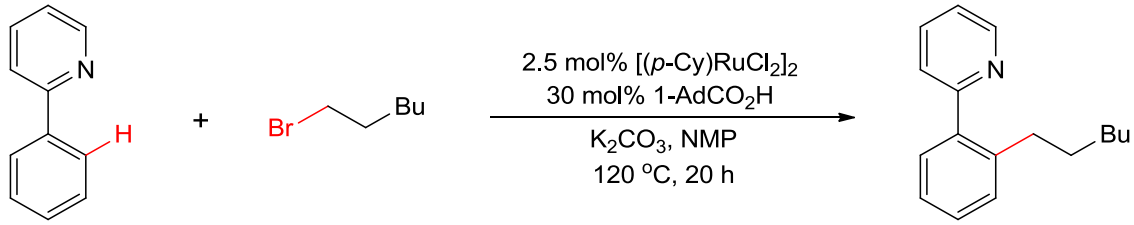

Scheme 1.46: Ru-catalysed direct alkylation of phenylpyridine.[133]

The authors proposed the mechanism shown in **Scheme 1.47** for phenylpyridine.[100] Reversible cyclometallation of the directing group takes place to give the cycloruthenated **1.38** followed by oxidative addition with the alkyl halide RX to give the Ru^{IV}(aryl)(alkyl) complex **1.39** which then undergoes reductive elimination to give the product and regenerate the Ru catalyst.

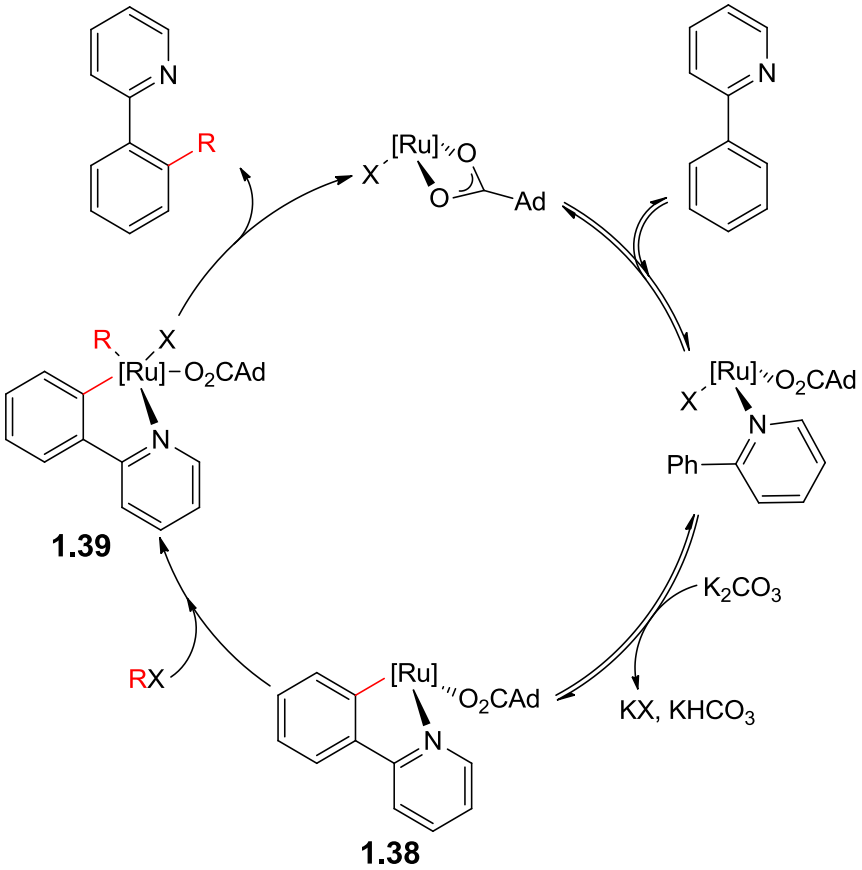

Scheme 1.47: Proposed mechanism for Ru-catalysed direct alkylations.[100]

In 2013, the same group reported the Ru-catalysed *meta*-alkylation of phenylpyridines using secondary halides.[134] The authors proposed that after C-H activation occurs, the substrate becomes activated to do an electrophilic alkylation (**Scheme 1.48**). This is due to the strong directing group effect of the Ru-C(sp^2) bond which causes functionalisation at the *para* position with respect to the Ru-C(sp^2) bond. Competition reactions using primary and secondary alkyl halides were carried out. The reactions resulted in a mixture of products where primary alkyl halides reacted to give *ortho* alkylation whereas secondary alkyl halides reacted to give *meta* alkylation.

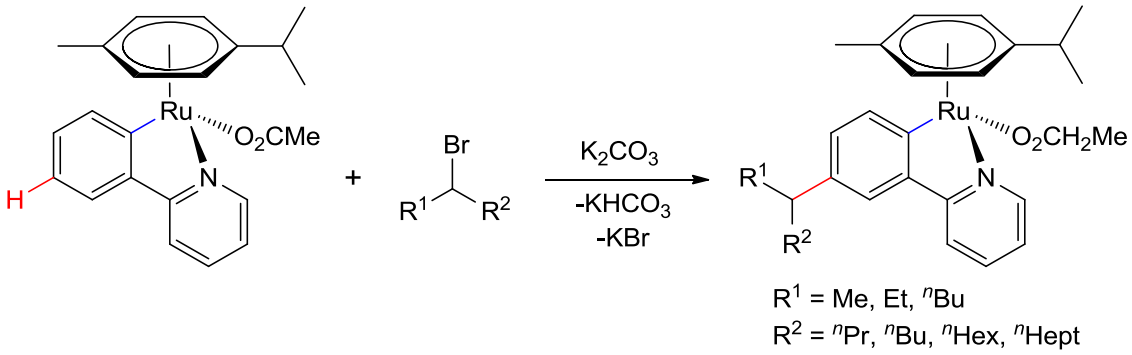

Scheme 1.48: Alkylation in the *meta* position.[134]

In conclusion, Ru-catalysed direct arylations that have been reported use C-X (X = halide, OTs) arylating agents which oxidatively add to Ru. Most of the reactions go via Ru^{II}/Ru^{IV} catalytic cycles.

Rhodium Catalysis

Rh-catalysed direct arylation has only been achieved quite recently and has only been reported for reactions using external oxidant. This is perhaps because the oxidative addition pathway would involve going from Rh^{III} to Rh^{V} which is hard.

Glorius' group reported the first oxidative Rh^{III}-catalysed biaryl formation in 2012. Various biaryls were formed from Rh-catalysed coupling of benzamides or alkylphenones with aryl halides.[135] However in this system, there is retention of the halogen substituent so oxidative addition of the C-halogen bond does not occur. Reactions involved two-fold C-H activation and were regioselective for *ortho*-arylation on the benzamide/phenone ring and *meta* on the halide-substituted ring.[136] Chloro-, bromo- and iodobenzenes made efficient coupling partners. Furthermore, H/D exchange

was observed for both coupling partners suggesting both C-H activations are reversible. Mechanistic studies led to a k_H/k_D value of 2.0 for benzamide from a **Type A** initial rates KIE experiment and 3.5 for bromobenzene from a **Type B** competition KIE experiment (**Scheme 1.49**). The authors concluded that C-H activation takes place for both substrates and that C-H cleavage of the aryl halide, a simple arene, is of substantial importance for the total rate of the reaction. It must however be noted that this conclusion has been made from a **Type B** KIE experiment which may not have given accurate evidence.

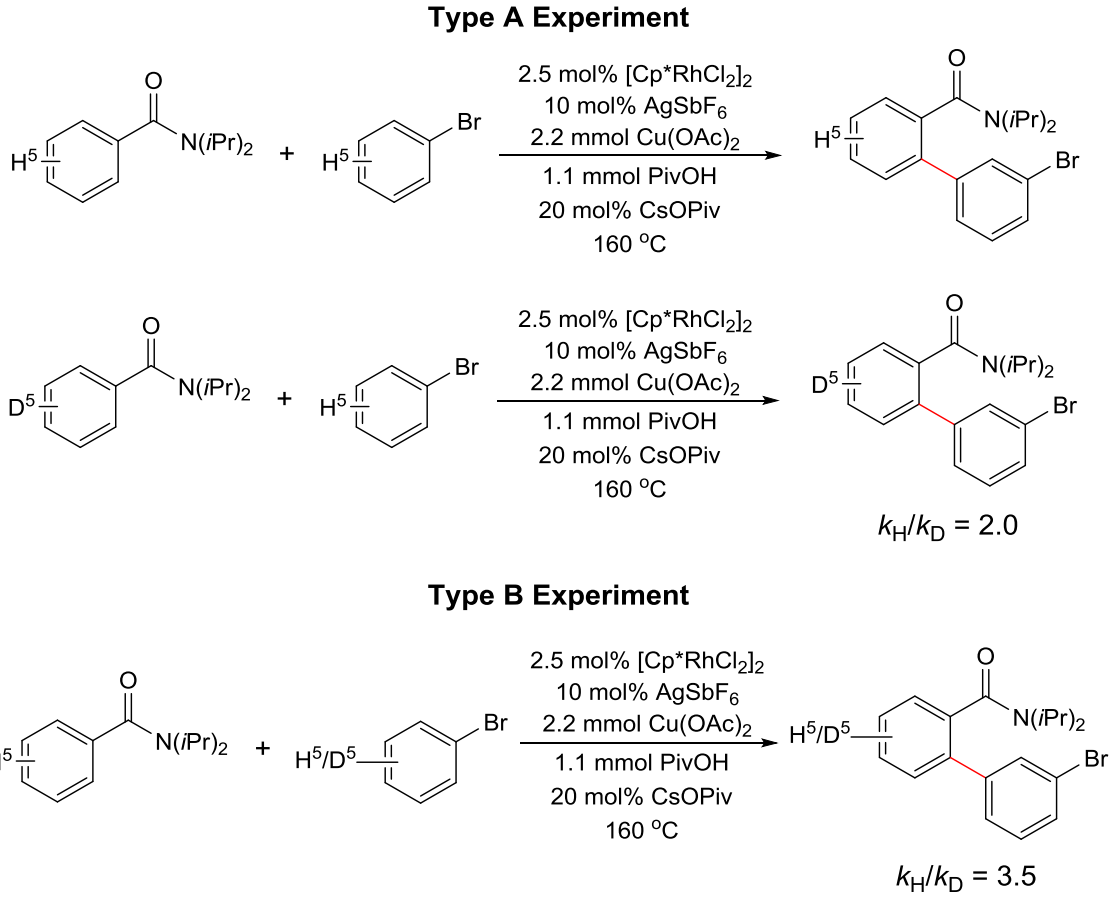

Scheme 1.49: KIE experiments for the benzamide and the aryl halide.[135]

Scheme 1.50 shows a possible mechanism for the reaction. The cyclometallation could proceed via AMLA to give **1.40**. The halobenzene then binds to the Rh in an η^2 manner to give **1.41** which can then take two pathways. The first involves C-H activation (perhaps with external base) of the halobenzene to give **1.42** which, after reductive elimination gives the product and Rh^I (reoxidised by $Cu(OAc)_2$). The other pathway involves C-H oxidative addition of the halobenzene to give a Rh^V hydride complex

(**1.43**) which then undergoes reductive elimination to give product. However, the second pathway seems less likely due to formation of Rh^{V} being hard.

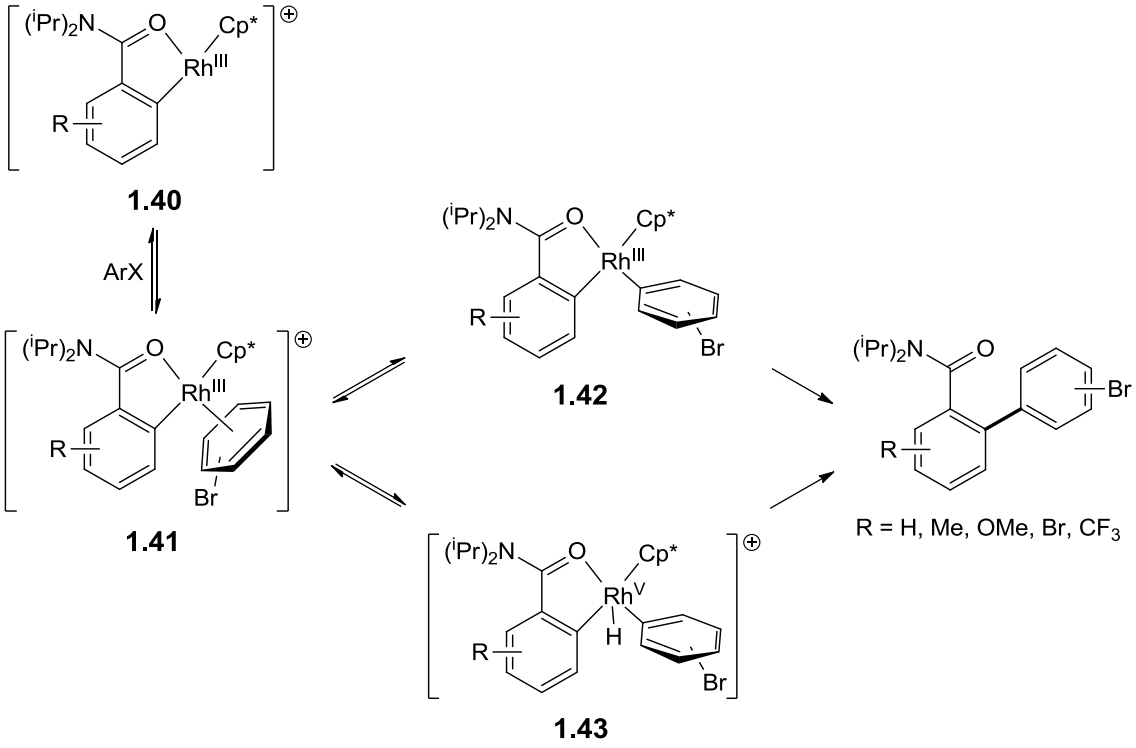

Scheme 1.50: Possible mechanism of arylation showing two possible pathways.[135]

Coupling of heteroarenes catalysed by Cp^*Rh^{III} has also been achieved (**Scheme 1.51**).[137, 138] In 2013, Lan, You and co-workers reported the first Rh-catalysed coupling involving two C-H functionalisations that works between electron-rich and electron deficient heteroarenes as well as between two electron-rich heteroarenes using the same conditions.[138] The system used Ag_2CO_3 and pivalic acid and the reaction was regioselective, with no homocoupling observed.

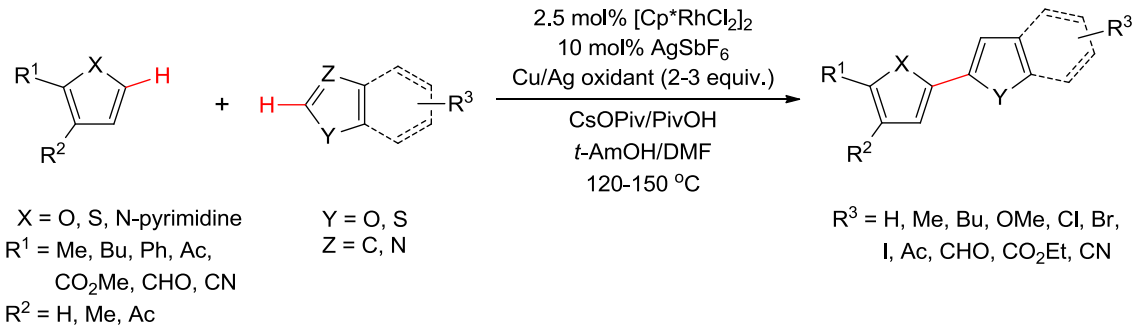

Scheme 1.51: Rh-catalysed coupling of heteroarenes.[137, 138]

Similar coupling reactions of thiophene or selenophene derivatives with N-phenylpyrazole and phenylpyridine yielded biaryl heterocyclic derivatives (**Scheme 1.52**).[139] Reactions were selective for 1:1 coupling and only trace amounts of the 1:2 coupling product were observed. The proposed mechanism involves AMLA C-H activation of the directing group.

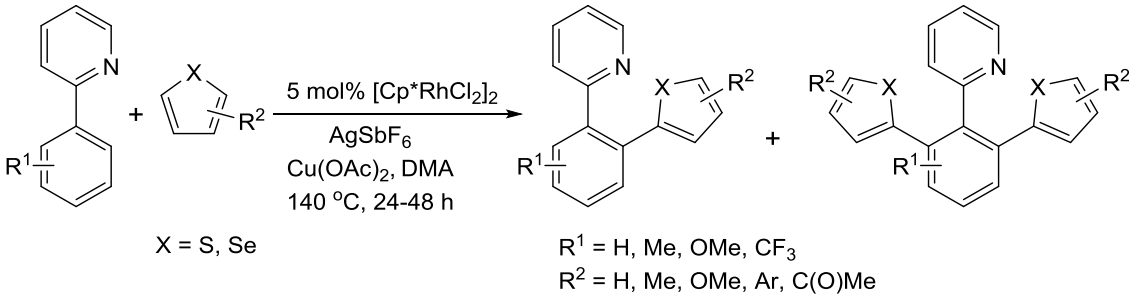

Scheme 1.52: Rh-catalysed coupling of phenylpyridines and thiophenes.[139]

Glorius' group extended their research to Rh-catalysed arylation of vinylic substrates (**Scheme 1.53**).[140] *Z*-selective coupling was observed and even highly substituted vinyls were successful. However most reactions only gave moderate to low yields and the halobenzene gives mixtures of *meta*- and *para*-substituted compounds and is required in excess.

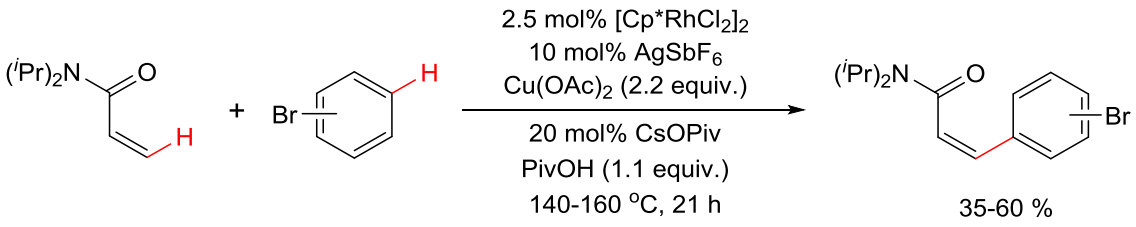

Scheme 1.53: Rh-catalysed arylation of vinylic substrates.[140]

Recently Rh-catalysed intramolecular arylation has been reported using various diaryl compounds with $Cu(OAc)_2 \cdot H_2O$ as oxidant (**Scheme 1.54**).[141, 142] With 1-amino-1,1-diarylalkanes (**1.44**), reactions proceeded to give products with retention of the NH_2 group however decarboxylation was found to occur in the case of 2,2-diarylalkanoic acids (**1.45**).

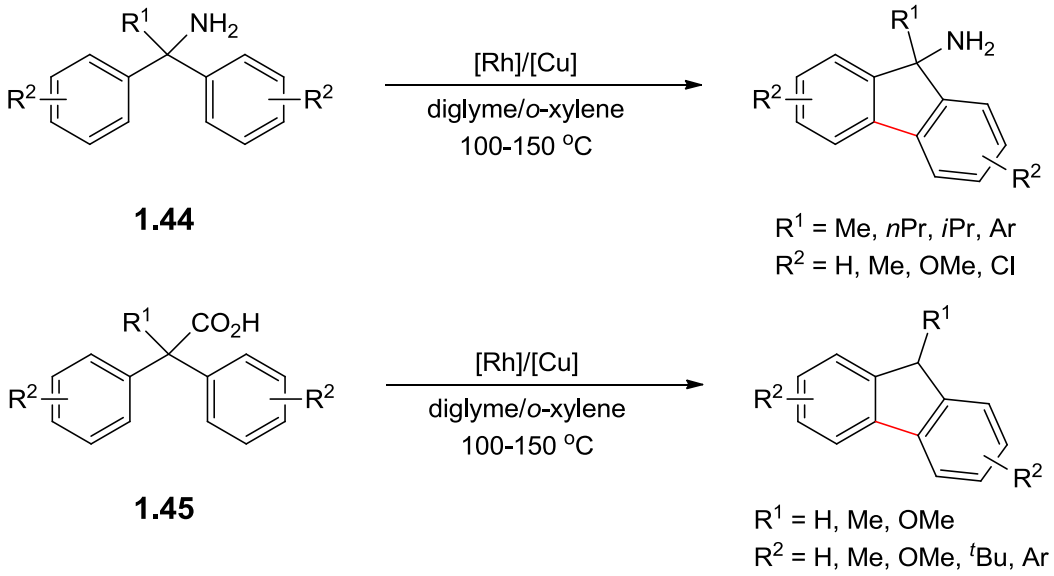

Scheme 1.54: Rh-catalysed intramolecular arylation.[141, 142]

Iridium Catalysis

There are only a few examples of Ir-catalysed direct arylations possibly because it is known to form stronger and more stable metal-carbon bonds than Rh and Ru so therefore it is harder to get catalysis. In 2013, Miura *et al.* described the intramolecular arylation of triarylmethanols using $[Cp^*IrCl_2]_2$ as catalyst and $Cu(OAc)_2.H_2O$ as oxidant.[142] $[Cp^*RhCl_2]_2$ was tested but gave diminished yields or no products at all. Reactions with Ir worked but needed temperatures as high as 170 °C. Substrates with electron-donating groups showed lower reactivity and arylation between two unsubstituted phenyl groups was favoured over reaction with a substituted phenyl. The authors postulated the mechanism shown in **Scheme 1.55**. Ir coordinates to the oxygen of the substrate to give **1.44** and cyclometallation by AMLA C-H activation follows to give **1.45**. The second cyclometallation subsequently follows to give **1.46** and the product is obtained after reductive elimination.

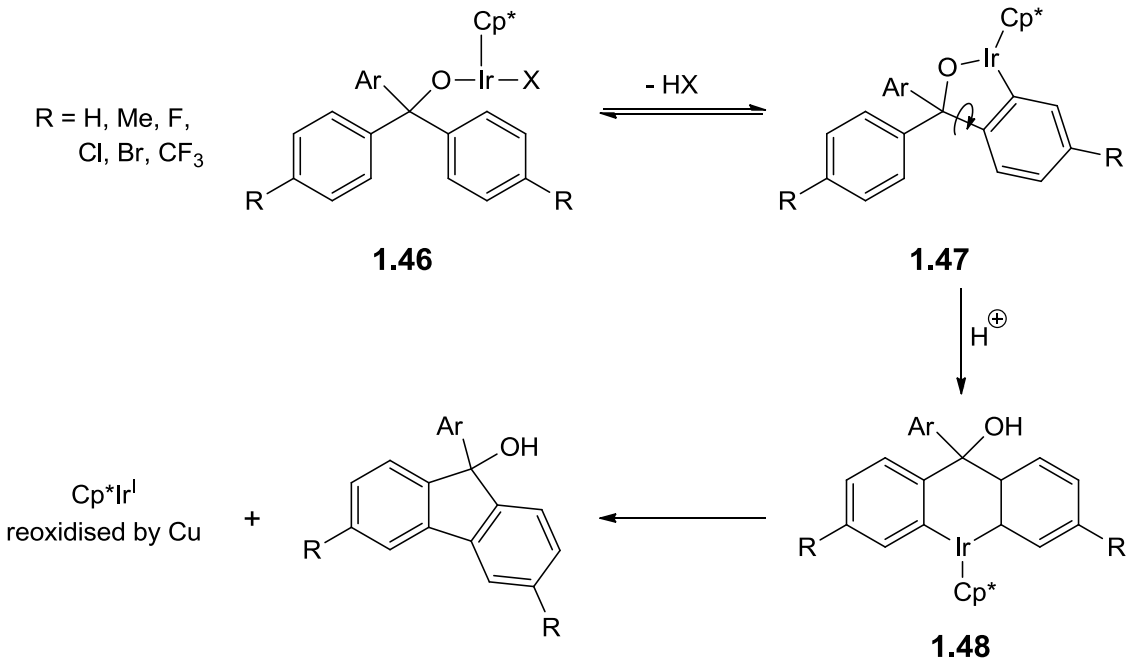

Scheme 1.55: Mechanism for Ir-catalysed intramolecular arylation of triarylmethanols.

Itami *et al.* reported the use of Crabtree's catalyst, $[Ir(cod)(py)PCy_3]PF_6$ for the direct arylation of heteroarenes with iodoarenes (**Scheme 1.56**).[143] The reactions were highly efficient in most cases, using equimolar amounts of the two coupling reagents. Diarylations were possible by using an excess of the arylating agent and diheteroarylation was also possible by reacting a diiodoarene with an excess of the heteroarene. A kinetic isotope effect of 1.9 for thiophene arylation was calculated from both intra- and intermolecular competition reactions (**Type B** and **C** experiments). The authors proposed an electrophilic metalation mechanism (S_EAr).

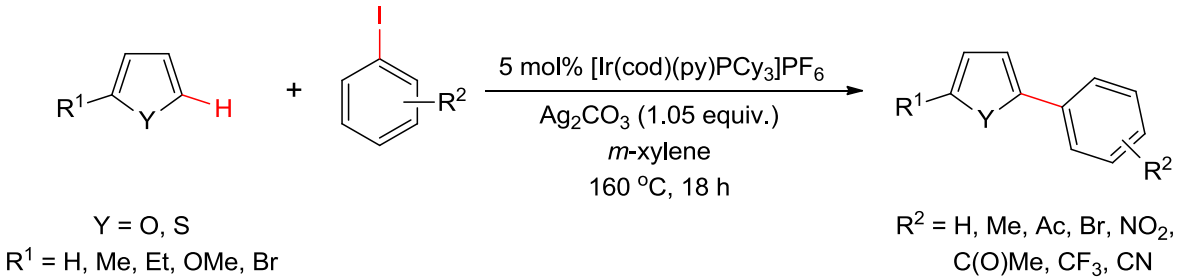

Scheme 1.56: Ir-catalysed intermolecular direct arylation of heteroarenes.[143]

A separate DFT study by Gorelsky, Woo and co-workers however disputed the S_EAr mechanism by exploring the C-H activation step for several arenes and heteroarenes

catalysed by an Ir^{III} catalyst.[144] They deduced the C-H activation mechanism to be CMD going via the transition state shown in **Fig 1.15**. A Wheland intermediate for the S_EAr pathway could not be located. They compared the data with Pd-catalysed CMD C-H activation and found that Ir has stronger interactions than Pd. There is also weaker base-proton interaction so the authors postulated that there is stronger electrophilic character in Ir-catalysed reactions.

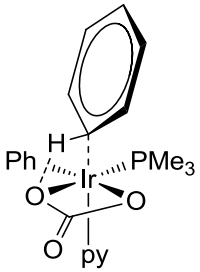

Fig. 1.15: CMD transition state for C-H activation using [Ir(Ph)(PMe_3)(py)(CO_3)].[144]

1.4.6 Conclusions on Applications of C-H Activation in Catalysis

There has been extensive progress made with C-H activation in catalysis and the field continues to grow. So far there are not many examples of catalytic C-H activation by SBM or by 1,2-addition.

Whilst stoichiometric oxidative addition of C-H bonds is very well studied it is clearly difficult to make this catalytic since as mentioned earlier, tuning the metal/ligand combination to favour OA can result in difficult reductive elimination and vice versa. Purely electrophilic activation often requires heavily acidic conditions, and can suffer from formation of unwanted byproducts. In contrast AMLA/CMD activation occurs under much milder conditions and has become extensively studied in the last decade. Indeed, some Pd-catalysed alkyne hydroarylation reactions have been reported as electrophilic activation however carboxylates are used so these may actually be AMLA.[145-147]

In general, intra- and intermolecular AMLA/CMD direct arylation reactions with Pd can be carried out efficiently under various conditions with several substrates. There are many examples using halogenated reagents whereby oxidative addition of the C-X bond is the first step followed by AMLA C-H activation. There are fewer examples of reactions with non-halogenated substrates where an external oxidant is needed for

catalyst turnover. Intermolecular direct arylation reactions with Ru have been reported but only for reactions using halogenated substrates and without external oxidant. Direct alkylations are also possible with Pd and Ru. Direct arylation using Cp^*Rh^{III}-catalysed AMLA C-H activation is quickly catching up to Pd in terms of the range of substrates used and has so far only been reported for reactions that use external oxidant. This is probably due to the difficulty in forming Rh(V) intermediates. Direct arylation with Ir has not been fully explored possibly due to strong iridium-carbon bonds that form which are quite stable and make catalysis difficult.

The AMLA/CMD process has been exploited in nitrogen or oxygen-directed oxidative coupling of various substrates with alkynes. **Chapter Two** will deal with reported examples of stoichiometric AMLA C-H activation and stoichiometric alkyne insertions followed by the results of Cp*Rh and (*p*-Cy)Ru-catalysed reactions of *C*-phenylpyrazoles with various alkynes. **Chapter Three** will include a discussion on reported stoichiometric alkene insertions followed by the results of Cp*Rh and (*p*-Cy)Ru-catalysed reactions of *C*-phenylpyrazoles with various alkenes. Following on from studies with *C*-phenylpyrazoles, **Chapter Four** will deal with Cp*Rh-catalysed reactions of selected other substrates with alkynes including phenylimidazole phenylimidazoline, phenylpyrazolidinone and phenylhydrazine to name just a few. In addition, results from various mechanistic studies and DFT calculations will be provided in **Chapters Two**-**Four** where relevant.

Bibliography

1. D. Alberico, M. E. Scott and M. Lautens, *Chem. Rev.*, 2007, **107**, 174.
2. T. Satoh and M. Miura, *Chem. Lett.*, 2007, **36**, 200.
3. D. R. Stuart and K. Fagnou, *Science*, 2007, **316**, 1172.
4. W. J. Tenn, K. J. H. Young, G. Bhalla, J. Oxgaard, W. A. Goddard and R. A. Periana, *J. Am. Chem. Soc.*, 2005, **127**, 14172.
5. Y. Feng, M. Lail, K. Barakat, T. Cundari, T. Gunnoe and J. Petersen, *J. Am. Chem. Soc.*, 2005, **127**, 14174.
6. P. J. Walsh, F. J. Hollander and R. G. Bergman, *J. Am. Chem. Soc.*, 1988, **110**, 8729.
7. C. C. Cummins, S. M. Baxter and P. T. Wolczanski, *J. Am. Chem. Soc.*, 1988, **110**, 8731.
8. D. L. Davies, S. M. A. Donald and S. A. Macgregor, *J. Am. Chem. Soc.*, 2005, **127**, 13754.
9. D. L. Davies, S. M. A. Donald, O. Al-Duaij, J. Fawcett, C. Little and S. A. Macgregor, *Organometallics*, 2006, **25**, 5976.
10. S. I. Gorelsky, D. Lapointe and K. Fagnou, *J. Am. Chem. Soc.*, 2008, **130**, 10848.
11. J. A. Labinger and J. E. Bercaw, *Nature*, 2002, **417**, 507.
12. J. Chatt and J. M. Davidson, *J. Chem. Soc.*, 1965, 843.
13. M. A. Bennett and D. L. Milner, *Chem. Commun. (London)*, 1967, 581.
14. P. Foley and G. M. Whitesides, *J. Am. Chem. Soc.*, 1979, **101**, 2732.
15. A. H. Janowicz and R. G. Bergman, *J. Am. Chem. Soc.*, 1982, **104**, 352.
16. J. K. Hoyano, A. D. McMaster and W. A. G. Graham, *J. Am. Chem. Soc.*, 1983, **105**, 7190.
17. W. Jones and F. Feher, *J. Am. Chem. Soc.*, 1984, **106**, 1650.
18. W. D. Jones and F. J. Feher, *Acc. Chem. Res.*, 1989, **22**, 91.
19. B. A. Arndtsen, R. G. Bergman, T. A. Mobley and T. H. Peterson, *Acc. Chem. Res.*, 1995, **28**, 154.
20. R. H. Crabtree, *Chem. Rev.*, 1995, **95**, 987.
21. A. H. Janowicz and R. G. Bergman, *J. Am. Chem. Soc.*, 1983, **105**, 3929.
22. P. Burger and R. G. Bergman, *J. Am. Chem. Soc.*, 1993, **115**, 10462.
23. D. M. Tellers, C. M. Yung, B. A. Arndtsen, D. R. Adamson and R. G. Bergman, *J. Am. Chem. Soc.*, 2002, **124**, 1400.

24. B. Corkey, F. Taw, R. Bergman and M. Brookhart, *Polyhedron,* 2004, **23**, 2943.
25. S. Q. Niu and M. B. Hall, *J. Am. Chem. Soc.,* 1998, **120**, 6169.
26. B. A. Arndtsen and R. G. Bergman, *J. Organomet. Chem.,* 1995, **504**, 143.
27. P. L. Watson, *J. Am. Chem. Soc.,* 1983, **105**, 6491.
28. P. L. Watson and G. W. Parshall, *Acc. Chem. Res.,* 1985, **18**, 51.
29. M. E. Thompson, S. M. Baxter, A. R. Bulls, B. J. Burger, M. C. Nolan, B. D. Santarsiero, W. P. Schaefer and J. E. Bercaw, *J. Am. Chem. Soc.,* 1987, **109**, 203.
30. D. Balcells, E. Clot and O. Eisenstein, *Chem. Rev.,* 2010, **110**, 749.
31. W. H. Lam, G. C. Jia, Z. Y. Lin, C. P. Lau and O. Eisenstein, *Chem. Eur. J.,* 2003, **9**, 2775.
32. Z. Lin, *Coord. Chem. Rev.,* 2007, **251**, 2280.
33. J. Oxgaard, R. P. Muller, W. A. Goddard and R. A. Periana, *J. Am. Chem. Soc.,* 2004, **126**, 352.
34. N. A. Foley, M. Lail, T. B. Gunnoe, T. R. Cundari, P. D. Boyle and J. L. Petersen, *Organometallics,* 2007, **26**, 5507.
35. N. J. DeYonker, N. A. Foley, T. R. Cundari, T. B. Gunnoe and J. L. Petersen, *Organometallics,* 2007, **26**, 6604.
36. N. A. Foley, T. B. Gunnoe, T. R. Cundari, P. D. Boyle and J. L. Petersen, *Angew. Chem. Int. Ed.,* 2008, **47**, 726.
37. B. A. Vastine and M. B. Hall, *J. Am. Chem. Soc.,* 2007, **129**, 12068.
38. J. Oxgaard, R. A. Periana and W. A. Goddard, *J. Am. Chem. Soc.,* 2004, **126**, 11658.
39. R. N. Perutz and S. Sabo-Etienne, *Angew. Chem. Int. Ed.,* 2007, **46**, 2578.
40. W. J. Tenn, K. J. H. Young, J. Oxgaard, R. J. Nielsen, W. A. Goddard and R. A. Periana, *Organometallics,* 2006, **25**, 5173.
41. J. Oxgaard, W. J. Tenn, R. J. Nielsen, R. A. Periana and W. A. Goddard, *Organometallics,* 2007, **26**, 1565.
42. Y. Feng, M. Lail, N. A. Foley, T. B. Gunnoe, K. A. Barakat, T. R. Cundari and J. L. Petersen, *J. Am. Chem. Soc.,* 2006, **128**, 7982.
43. T. R. Cundari, T. V. Grimes and T. B. Gunnoe, *J. Am. Chem. Soc.,* 2007, **129**, 13172.
44. M. Fryzuk, C. Montgomery and S. Rettig, *Organometallics,* 1991, **10**, 467.
45. T. R. Cundari, T. R. Klinckman and P. T. Wolczanski, *J. Am. Chem. Soc.,* 2002, **124**, 1481.

46. L. M. Slaughter, P. T. Wolczanski, T. R. Klinckman and T. R. Cundari, *J. Am. Chem. Soc.*, 2000, **122**, 7953.
47. J. Bennett and P. Wolczanski, *J. Am. Chem. Soc.*, 1997, **119**, 10696.
48. N. Ochi, Y. Nakao, H. Sato and S. Sakaki, *J. Am. Chem. Soc.*, 2007, **129**, 8615.
49. H. M. Hoyt, F. E. Michael and R. G. Bergman, *J. Am. Chem. Soc.*, 2004, **126**, 1018.
50. N. F. Gol'dshleger, M. B. Tyabin, A. E. Shilov and A. A. Shteinman, *Zh. Fiz. Khim.*, 1969, **43**, 2174.
51. N. F. Gol'dshleger, V. V. Es'cova, A. E. Shilov and A. A. Shteinman, *Zh. Fiz. Khim.*, 1972, **46**, 1353.
52. S. S. Stahl, J. A. Labinger and J. E. Bercaw, *Angew. Chem. Int. Ed.*, 1998, **37**, 2181.
53. L. A. Kushch, V. V. Lavrushko, Y. S. Misharin, A. P. Moravsky and A. E. Shilov, *Nouv. J. Chim.*, 1983, **7**, 729.
54. J. A. Labinger, A. M. Herring, D. K. Lyon, G. A. Luinstra, J. E. Bercaw, I. T. Horvath and K. Eller, *Organometallics*, 1993, **12**, 895.
55. P. E. M. Siegbahn and R. H. Crabtree, *J. Am. Chem. Soc.*, 1996, **118**, 4442.
56. S. S. Stahl, J. A. Labinger and J. E. Bercaw, *J. Am. Chem. Soc.*, 1996, **118**, 5961.
57. M. W. Holtcamp, J. A. Labinger and J. E. Bercaw, *Inorg. Chim. Acta*, 1997, **265**, 117.
58. D. D. Wick and K. I. Goldberg, *J. Am. Chem. Soc.*, 1997, **119**, 10235.
59. S. S. Stahl, J. A. Labinger and J. E. Bercaw, *J. Am. Chem. Soc.*, 1995, **117**, 9371.
60. H. A. Jenkins, G. P. A. Yap and R. J. Puddephatt, *Organometallics*, 1997, **16**, 1946.
61. Y. Boutadla, D. L. Davies, S. A. Macgregor and A. I. Poblador-Bahamonde, *Dalton Trans.*, 2009, 5820.
62. A. D. Ryabov, I. K. Sakodinskaya and A. K. Yatsimirsky, *J. Chem. Soc. Dalton Trans.*, 1985, 2629.
63. A. D. Ryabov, *Chem. Rev.*, 1990, **90**, 403.
64. M. Gómez, J. Granell and M. Martinez, *Organometallics*, 1997, **16**, 2539.
65. B. Biswas, M. Sugimoto and S. Sakaki, *Organometallics*, 2000, **19**, 3895.
66. D. L. Davies, O. Al-Duaij, J. Fawcett, M. Giardiello, S. T. Hilton and D. R. Russell, *Dalton Trans.*, 2003, 4132.

67. D. L. Davies, S. M. A. Donald, O. Al-Duaij, S. A. Macgregor and M. Pölleth, *J. Am. Chem. Soc.*, 2006, **128**, 4210.
68. M. Lafrance, C. N. Rowley, T. K. Woo and K. Fagnou, *J. Am. Chem. Soc.*, 2006, **128**, 8754.
69. M. Lafrance and K. Fagnou, *J. Am. Chem. Soc.*, 2006, **128**, 16496.
70. Y. Boutadla, D. L. Davies, S. A. Macgregor and A. I. Poblador-Bahamonde, *Dalton Trans.*, 2009, 5887.
71. D. H. Ess, S. M. Bischof, J. Oxgaard, R. A. Periana and W. A. Goddard, *Organometallics*, 2008, **27**, 6440.
72. S. M. Bischof, D. H. Ess, S. K. Meier, J. Oxgaard, R. J. Nielsen, G. Bhalla, W. A. Goddard and R. A. Periana, *Organometallics*, 2010, **29**, 742.
73. E. M. Simmons and J. F. Hartwig, *Angew. Chem. Int. Ed.*, 2012, **51**, 3066.
74. R. G. Bergman, *Nature*, 2007, **446**, 391.
75. D. A. Colby, R. G. Bergman and J. A. Ellman, *Chem. Rev.*, 2010, **110**, 624.
76. T. W. Lyons and M. S. Sanford, *Chem. Rev.*, 2010, **110**, 1147.
77. J. C. Lewis, R. G. Bergman and J. A. Ellman, *Acc. Chem. Res.*, 2008, **41**, 1013.
78. D. A. Colby, A. S. Tsai, R. G. Bergman and J. A. Ellman, *Acc. Chem. Res.*, 2012, **45**, 814.
79. R. H. Crabtree, *J. Organomet. Chem.*, 2004, **689**, 4083.
80. L. V. Desai, K. J. Stowers and M. S. Sanford, *J. Am. Chem. Soc.*, 2008, **130**, 13285.
81. F. Kakiuchi, S. Sekine, Y. Tanaka, A. Kamatani, M. Sonoda, N. Chatani and S. Murai, *Bull. Chem. Soc. Jpn.*, 1995, **68**, 62.
82. C. P. Lenges and M. Brookhart, *J. Am. Chem. Soc.*, 1999, **121**, 6616.
83. S. H. Wiedemann, J. A. Ellman and R. G. Bergman, *J. Org. Chem.*, 2006, **71**, 1969.
84. S. H. Wiedemann, J. C. Lewis, J. A. Ellman and R. G. Bergman, *J. Am. Chem. Soc.*, 2006, **128**, 2452.
85. K. M. Waltz and J. F. Hartwig, *Science*, 1997, **277**, 211.
86. H. Y. Chen, S. Schlecht, T. C. Semple and J. F. Hartwig, *Science*, 2000, **287**, 1995.
87. C. E. Webster, Y. B. Fan, M. B. Hall, D. Kunz and J. F. Hartwig, *J. Am. Chem. Soc.*, 2003, **125**, 858.
88. A. D. Sadow and T. D. Tilley, *J. Am. Chem. Soc.*, 2003, **125**, 7971.

89. R. Periana, D. Taube, S. Gamble, H. Taube, T. Satoh and H. Fujii, *Science,* 1998, **280**, 560.
90. M. Muehlhofer, T. Strassner and W. Herrmann, *Angew. Chem. Int. Ed.,* 2002, **41**, 1745.
91. V. S. Thirunavukkarasu, K. Raghuvanshi and L. Ackermann, *Org. Lett.,* 2013, **15**, 3286.
92. C. Grohmann, H. Wang and F. Glorius, *Org. Lett.,* 2012, **14**, 656.
93. C. Feng, M. Ye, K. Xiao, S. Li and J. Yu, *J. Am. Chem. Soc.,* 2013, **135**, 9322.
94. J. Park, E. Park, A. Kim, Y. Lee, K. Chi, J. H. Kwak, Y. H. Jung and I. S. Kim, *Org. Lett.,* 2011, **13**, 4390.
95. C. Pan, H. Jin, X. Liu, Y. Cheng and C. Zhu, *Chem. Commun.,* 2013, **49**, 2933.
96. J. Weng, Z. Yu, X. Liu and G. Zhang, *Tetrahedron Lett.,* 2013, **54**, 1205.
97. W. Liu and L. Ackermann, *Org. Lett.,* 2013, **15**, 3484.
98. D. Lapointe and K. Fagnou, *Chem. Lett.,* 2010, **39**, 1119.
99. J. Wencel-Delord, T. Dröge, F. Liu and F. Glorius, *Chem. Soc. Rev.,* 2011, **40**, 4740.
100. L. Ackermann, *Chem. Rev.,* 2011, **111**, 1315.
101. N. Kuhl, M. N. Hopkinson, J. Wencel-Delord and F. Glorius, *Angew. Chem. Int. Ed.,* 2012, **51**, 10236.
102. D. García-Cuadrado, A. A. C. Braga, F. Maseras and A. M. Echavarren, *J. Am. Chem. Soc.,* 2006, **128**, 1066.
103. D. García-Cuadrado, P. de Mendoza, A. A. C. Braga, F. Maseras and A. M. Echavarren, *J. Am. Chem. Soc.,* 2007, **129**, 6880.
104. S. Pascual, P. de Mendoza, A. A. C. Braga, F. Maseras and A. M. Echavarren, *Tetrahedron,* 2008, **64**, 6021.
105. L. C. Campeau and K. Fagnou, *Chem. Commun.,* 2006, 1253.
106. L. C. Campeau, M. Parisien, A. Jean and K. Fagnou, *J. Am. Chem. Soc.,* 2006, **128**, 581.
107. M. Lafrance, D. Lapointe and K. Fagnou, *Tetrahedron,* 2008, **64**, 6015.
108. M. Lafrance, S. I. Gorelsky and K. Fagnou, *J. Am. Chem. Soc.,* 2007, **129**, 14570.
109. M. Chaumontet, R. Piccardi, N. Audic, J. Hitce, J. Peglion, E. Clot and O. Baudoin, *J. Am. Chem. Soc.,* 2008, **130**, 15157.
110. L. Ackermann, A. Althammer and S. Fenner, *Angew. Chem. Int. Ed.,* 2009, **48**, 201.

111. N. Lebrasseur and I. Larrosa, *J. Am. Chem. Soc.*, 2008, **130**, 2926.
112. B. Liégault, D. Lapointe, L. Caron, A. Vlassova and K. Fagnou, *J. Org. Chem.*, 2009, **74**, 1826.
113. D. Zhao, W. Wang, S. Lian, F. Yang, J. Lan and J. You, *Chem. Eur. J.*, 2009, **15**, 1337.
114. B. Liégault, D. Lee, M. P. Huestis, D. R. Stuart and K. Fagnou, *J. Org. Chem.*, 2008, **73**, 5022.
115. T. Watanabe, S. Oishi, N. Fujii and H. Ohno, *J. Org. Chem.*, 2009, **74**, 4720.
116. K. L. Hull and M. S. Sanford, *J. Am. Chem. Soc.*, 2007, **129**, 11904.
117. X. Gong, G. Song, H. Zhang and X. Li, *Org. Lett.*, 2011, **13**, 1766.
118. D. Kalyani, N. R. Deprez, L. V. Desai and M. S. Sanford, *J. Am. Chem. Soc.*, 2005, **127**, 7330.
119. N. R. Deprez and M. S. Sanford, *J. Am. Chem. Soc.*, 2009, **131**, 11234.
120. B. C. Chary, S. Kim, Y. Park, J. Kim and P. H. Lee, *Org. Lett.*, 2013, **15**, 2692.
121. L. Y. Chan, L. Cheong and S. Kim, *Org. Lett.*, 2013, **15**, 2186.
122. S. R. Neufeldt, C. K. Seigerman and M. S. Sanford, *Org. Lett.*, 2013, **15**, 2302.
123. L. Ackermann, R. Vicente and A. Althammer, *Org. Lett.*, 2008, **10**, 2299.
124. L. Ackermann, R. Born and R. Vicente, *Chemsuschem*, 2009, **2**, 546.
125. L. Ackermann, P. Novák, R. Vicente, V. Pirovano and H. K. Potukuchi, *Synthesis-Stuttgart*, 2010, 2245.
126. L. Ackermann, E. Diers and A. Manvar, *Org. Lett.*, 2012, **14**, 1154.
127. I. Özdemir, S. Demir, B. Çetinkaya, C. Gourlaouen, F. Maseras, C. Bruneau and P. H. Dixneuf, *J. Am. Chem. Soc.*, 2008, **130**, 1156.
128. E. F. Flegeau, C. Bruneau, P. H. Dixneuf and A. Jutand, *J. Am. Chem. Soc.*, 2011, **133**, 10161.
129. P. Arockiam, V. Poirier, C. Fischmeister, C. Bruneau and P. H. Dixneuf, *Green Chem.*, 2009, **11**, 1871.
130. P. B. Arockiam, C. Fischmeister, C. Bruneau and P. H. Dixneuf, *Angew. Chem. Int. Ed.*, 2010, **49**, 6629.
131. L. Ackermann, R. Vicente, H. K. Potukuchi and V. Pirovano, *Org. Lett.*, 2010, **12**, 5032.
132. L. Ackermann and M. Mulzer, *Org. Lett.*, 2008, **10**, 5043.
133. L. Ackermann, P. Novák, R. Vicente and N. Hofmann, *Angew. Chem. Int. Ed.*, 2009, **48**, 6045.

134. N. Hofmann and L. Ackermann, *J. Am. Chem. Soc.*, 2013, **135**, 5877.
135. J. Wencel-Delord, C. Nimphius, F. W. Patureau and F. Glorius, *Angew. Chem. Int. Ed.*, 2012, **51**, 2247.
136. F. W. Patureau, J. Wencel-Delord and F. Glorius, *Aldrichim. Acta*, 2012, **45**, 31.
137. N. Kuhl, M. N. Hopkinson and F. Glorius, *Angew. Chem. Int. Ed.*, 2012, **51**, 8230.
138. X. Qin, H. Liu, D. Qin, Q. Wu, J. You, D. Zhao, Q. Guo, X. Huang and J. Lan, *Chem. Sci.*, 2013, **4**, 1964.
139. V. P. Reddy, R. Qiu, T. Iwasaki and N. Kambe, *Org. Lett.*, 2013, **15**, 1290.
140. J. Wencel-Delord, C. Nimphius, F. W. Patureau and F. Glorius, *Chem. Asian J.*, 2012, **7**, 1208.
141. K. Morimoto, M. Itoh, K. Hirano, T. Satoh, Y. Shibata, K. Tanaka and M. Miura, *Angew. Chem. Int. Ed.*, 2012, **51**, 5359.
142. M. Itoh, K. Hirano, T. Satoh, Y. Shibata, K. Tanaka and M. Miura, *J. Org. Chem.*, 2013, **78**, 1365.
143. B. Join, T. Yamamoto and K. Itami, *Angew. Chem. Int. Ed.*, 2009, **48**, 3644.
144. M. García-Melchor, S. I. Gorelsky and T. K. Woo, *Chem. Eur. J.*, 2011, **17**, 13847.
145. W. J. Lu, C. G. Jia, T. Kitamura and Y. Fujiwara, *Org. Lett.*, 2000, **2**, 2927.
146. C. G. Jia, D. G. Piao, J. Z. Oyamada, W. J. Lu, T. Kitamura and Y. Fujiwara, *Science*, 2000, **287**, 1992.
147. C. G. Jia, W. J. Lu, J. Oyamada, T. Kitamura, K. Matsuda, M. Irie and Y. Fujiwara, *J. Am. Chem. Soc.*, 2000, **122**, 7252.

Chapter Two

Oxidative Coupling of Phenylpyrazoles with Alkynes

2 Chapter Two

2.1 Introduction

AMLA C-H activation has been exploited in many different stoichiometric and catalytic C-H functionalisation reactions. Applications of AMLA in catalytic direct arylations and alkylations were explored in **Chapter One**. This introduction will deal with coupling reactions of various directing groups and alkynes via AMLA C-H activation. Firstly, further studies on stoichiometric cyclometallations by AMLA will be discussed to give a deeper mechanistic understanding of the process. Secondly, an overview of stoichiometric alkyne insertions into cyclometallated complexes will be given which has implications in catalysis. Finally, examples of catalytic coupling between a diverse range of substrates and alkynes will be dealt with, including a discussion on the different catalysts, substrates and oxidants and their effects on product selectivity.

2.2 Stoichiometric AMLA C-H Activation Studies

Cyclometallations of different substrates with metals such as Pd and Ru have been reviewed[1-4] but for the purpose of this thesis, only cyclometallation by AMLA C-H activation using Ir, Rh and Ru will be discussed. In 1998, Beck reported the first acetate-assisted C-H activation using $[Cp^*IrCl_2]_2$.[5] The reaction was carried out with an oxazolone and NaOAc, and at room temperature (**Scheme 2.1**). Product selectivity was affected by the substituent on the oxazolone, giving cyclometallated complex **2.1** as a mixture of diasteroisomers or dimeric complex **2.2** by sp^3 C-H activation.

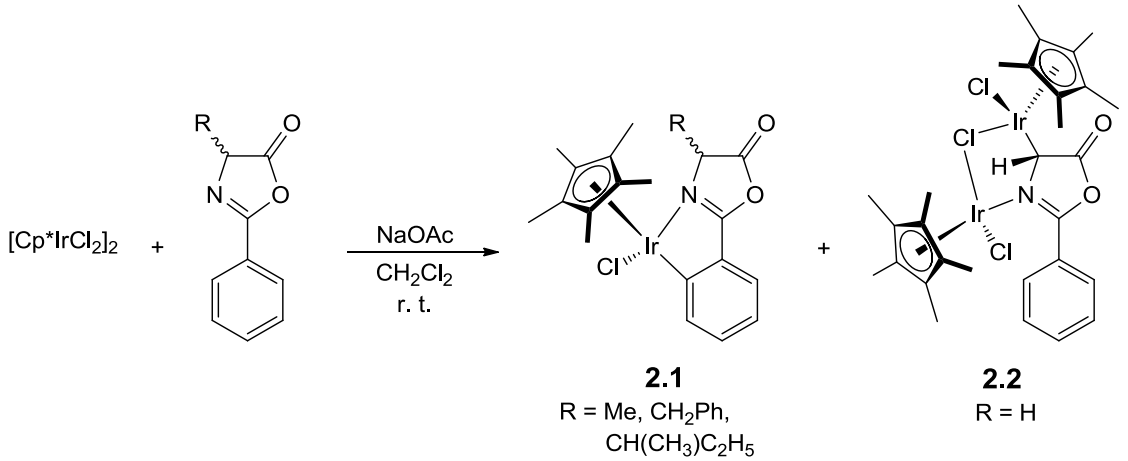

Scheme 2.1: Acetate-assisted C-H activation of oxazolones.

As mentioned in **Chapter One** (**Section 1.2.5**), Davies *et al.* in 2003 demonstrated that acetate-assisted C-H activation of amines, imines and oxazolines with $[Cp^*MCl_2]_2$ (M = Ir, Rh) and $[(p\text{-Cy})RuCl_2]_2$ occurs at room temperature.[6] The cyclometallation would not occur in the absence of acetate or with other bases like triethylamine. The isolated [(*p*-Cy)RuCl(OAc)] complex was found to carry out cyclometallation in the absence of external acetate. The authors concluded that the acetate may help the breaking of the dimer and exchange of a chloride, and also act as an intramolecular base.

Computational studies of the C-H activation step were discussed in **Chapter One**. There have now been a number of additional studies of the mechanism prior to the C-H activation step and the results of these are summarised in **Scheme 2.2**. Many substrates do not react with the metal dimers without acetate so this eliminates complex **2.3** as an intermediate and suggests acetate must react first to form **2.4**. [6] This was confirmed in a later study of cyclometallations of acetyl pyridine (see later).[7] A later study by Jones *et al.* showed the formation of the bisacetate complex (**2.5**) to be a strong possibility before reaction with the substrate L.[8] A vacant site is needed in order for C-H activation to occur so dissociation of an oxygen from **2.6** is necessary. Subsequently C-H activation goes via an AMLA process with intramolecular proton transfer to bound acetate (see **Chapter 1**, **Section 1.2.5**).

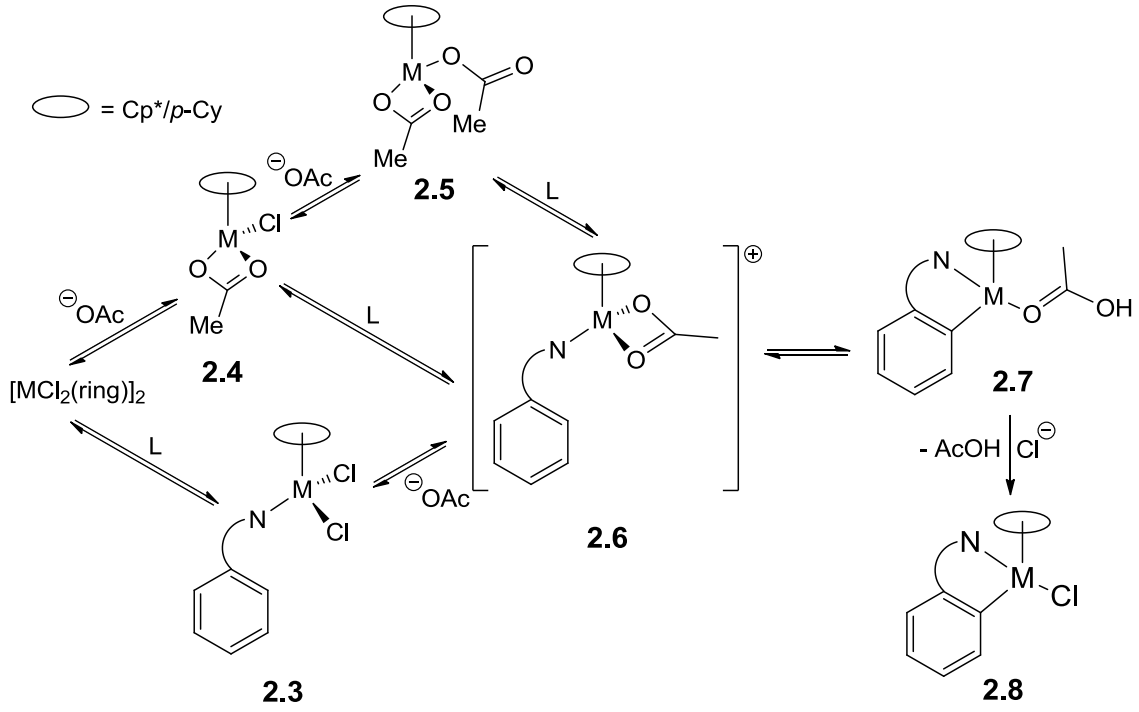

Scheme 2.2: Possible pathways for cyclometallations (M = Ir, Rh or Ru).

In 2009, Jones *et al.* investigated acetate-assisted C-H activation of *meta*-substituted phenyl imines and 2-phenylpyridines using $[Cp^*MCl_2]_2$ M = Ir and Rh (**Scheme 2.3**).[8] They found that substrates bearing electron-donating substituents reacted faster than those bearing electron-withdrawing substituents which they attributed to an electrophilic C-H activation mechanism. Similarly iridium reacted faster than rhodium suggesting the former is more electrophilic. Detailed studies showed that Cp*RhCl(OAc) and $Cp^*Rh(OAc)_2$ are in equilibrium and that reaction of the latter is retarded in the presence of added acetate. All of these observations are consistent with the key intermediate prior to C-H activation being **2.6** (see also **Fig 1.6**). A **Type A** KIE experiment showed a large KIE of >5 which the authors suggested was due to an electrophilic type C-H activation mechanism[8] with hydrogen–bonding to the acetate i.e. an AMLA reaction.[9, 10]

They also found the reactions were regioselective for the formation of isomer **2.9** rather than **2.10** and that the selectivity is very sensitive to steric effects as even when R = Me, only isomer **2.9** was formed. Formation of **2.10** was only favoured when R = F.

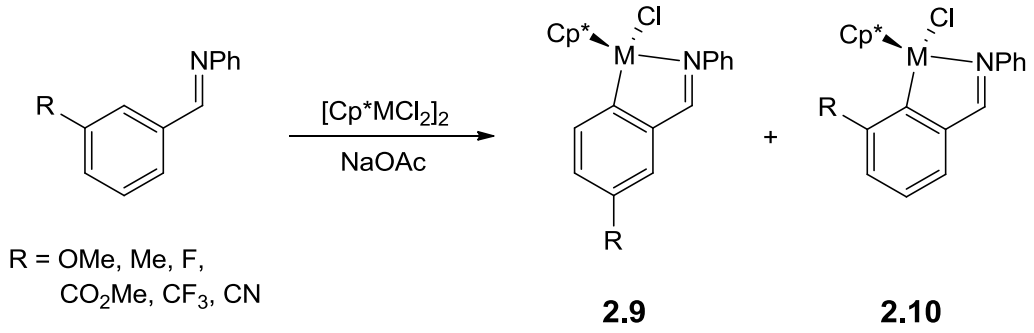

Scheme 2.3: Acetate-assisted C-H activation of *meta*-substituted phenyl imines.

Higher temperatures gave increased rates of reaction however the regioselectivity did not change.[8] Pure isomer **2.10** (R = OMe) was isolated and exposed to the reaction conditions along with acetic acid (2 equiv.). Over time, isomer **2.9** began to form which suggests the C-H activation is reversible.

Many neutral directing groups have been tested for acetate-assisted C-H activation of arene C-H bonds, some of which are illustrated in **Fig. 2.1** including 2-phenylpyridine (**2.11**)[7, 8, 11] and benzo[*h*]quinoline (**2.12**)[12, 13] that both cyclometallate with Ir, Rh and Ru. 2-Benzoylpyridine (**2.14**),[14] *N*-phenylpyrazole (**2.15**),[13, 14] oxazolines (**2.16**),[6, 13, 15] triazoles (**2.17**),[14] amines (**2.18**),[6] benzaldehyde oxime (**2.19**)[14] and imines (**2.20**)[6, 8, 13], all cyclometallate with Ir but only some with Rh and Ru. 2-Benzylpyridine (**2.13**)[8] only cyclometallates with Ir. 2-Phenylpyridine (**2.11**)[7, 8, 11] and benzo[*h*]quinoline (**2.12**)[12, 13] are therefore the best for promoting cyclometallation as they work with all three metals.

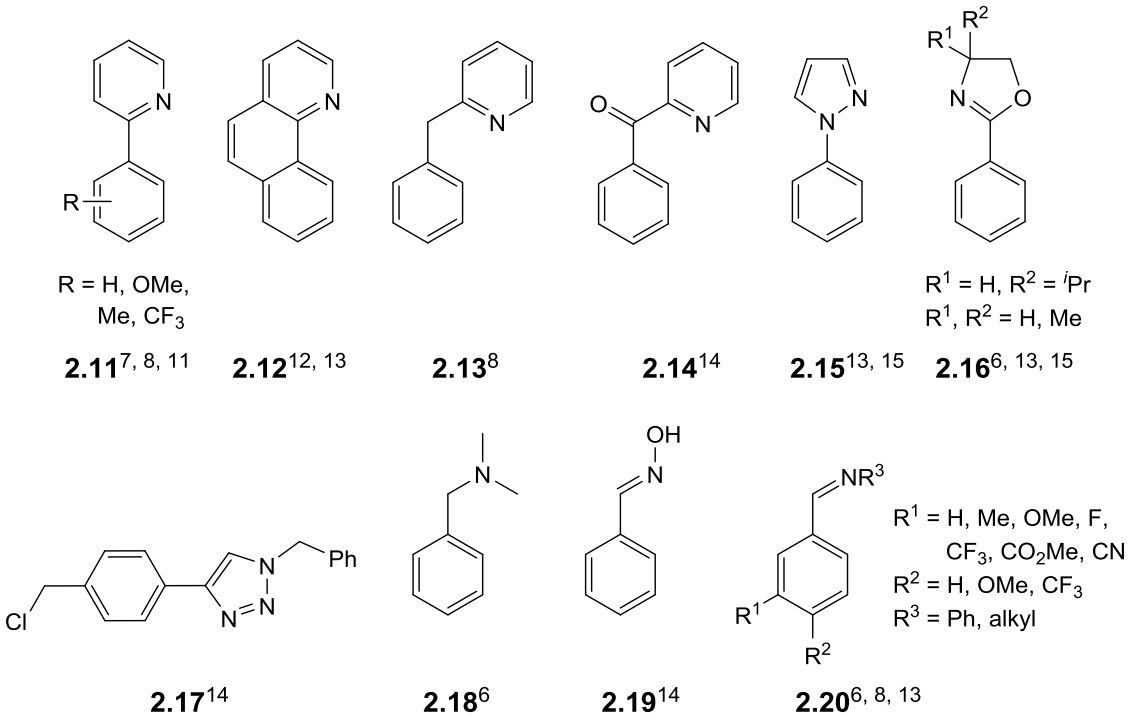

Fig 2.1: Examples of neutral directing groups used in acetate-assisted C-H activation.

AMLA C-H activation has also been carried out on heterocyclic C-H bonds (**Fig. 2.2**). Davies, Macgregor and co-workers reported the acetate-assisted cyclometallation of an *N*-methylated pyrrole imine (**2.21**) with Ir.[16] Urriolabeitia *et al.* extended this to other imine-functionalised heterocycles (**2.22**) including pyrrole, thiophene, furan and indole which successfully cyclometallated with {(*p*-Cy)Ru}.[17] Davies *et al.* later reported acetate-assisted C-H activation of an *N*-methylated benzimidazolium triazole salt (**2.23**) with Ir which affords an unusual bidentate NHC-triazole though this may not be *N*-directed.[18]

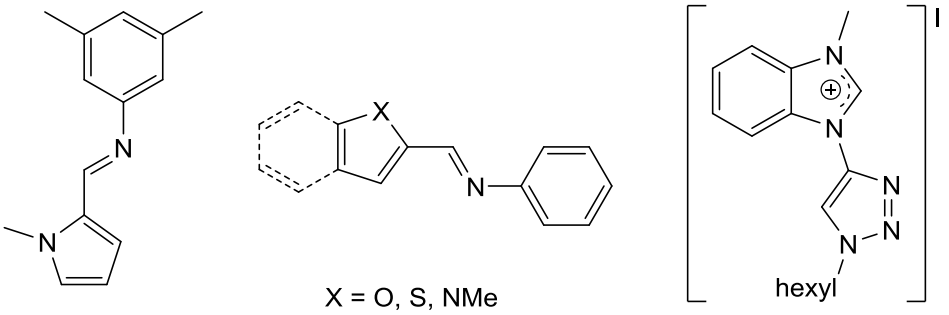

2.21 **2.22** **2.23**

Fig. 2.2: Examples of substrates used for C-H activation of heteroarene C-H bonds.

In 2009, Davies *et al.* reported a mechanistic study of acetate-assisted C-H activation of 2-substituted pyridines where either N,C cyclometallated complexes or N,O chelate complexes (**2.24**) were observed.[7] The authors found that $[Cp^*RhCl_2]_2$ did not react with 2-acetylpyridine in the absence of acetate whilst $[Cp^*IrCl_2]_2$ and $[(p\text{-Cy})RuCl_2]_2$ reacted to form equilibrium mixtures of the N,O chelate complexes (**2.24**) and starting materials (**Scheme 2.4**). When either the Ir or Ru N,O chelate complexes were treated with NaOAc no reaction occurred. The authors concluded the N,O chelate complexes are not intermediates in reactions to form N,C cyclometallated products. If the pyridine coordinates to the metal before the reaction between metal dimer and acetate, then AMLA C-H activation may not occur. The acetate must bind to the metal before the ligand in order for C-H activation to occur, ruling out complex **2.3** as an intermediate (**Scheme 2.2**).

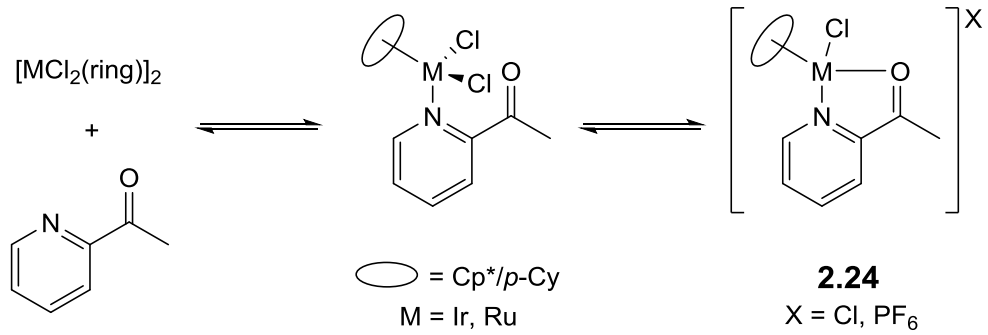

Scheme 2.4: Formation of N,O chelate complexes (**2.24**) in the absence of acetate.[7]

Acetate-assisted C-H activation of an sp^3 C-H bond was achieved using 2-acetyl pyridine and Rh (**Scheme 2.5**).[7] Surprisingly in this case the sp^3 C-H activation is more successful with Rh which contrasts with sp^2 C-H activation which is more successful

with Ir. The DFT calculations however show little difference in activation barriers between the three different metals so the difference in reactivity may not involve the C-H activation step. Attempts to cyclometallate 2-ethylpyridine with any of the metals failed. The authors suggested this is due to the less acidic proton to be activated in this substrate compared with 2-acetylpyridine, making H-bonding less favourable in the transition state. Also, there would be another sp^3 carbon in the metallacycle formed which may also make cyclometallation less favourable.

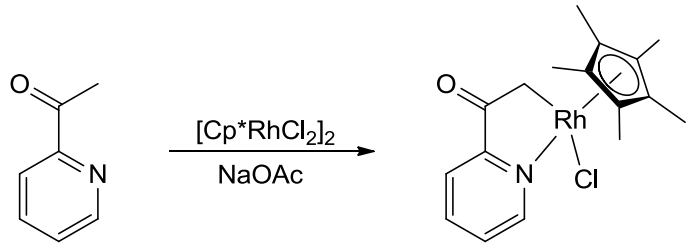

Scheme 2.5: Acetate-assisted cyclometallation of an sp^3 C-H bond.

Davies, Macgregor and co-workers investigated the competition between C-H and N-H activation using pyrrole imines.[16] With an N-methylated pyrrole imine (**2.25**, R= Me), C-H activation occurred and the cyclometallated complex was obtained in good yield. However, when an NH pyrrole imine was used instead, N-H activation was preferred over C-H activation (**Scheme 2.6**). DFT calculations showed that N-H activation is both kinetically and thermodynamically more favourable than C-H activation. It also occurs via an AMLA mechanism involving an electrophilic agostic interaction with the metal and with intramolecular H-bonding with the acetate in a six-membered transition state.

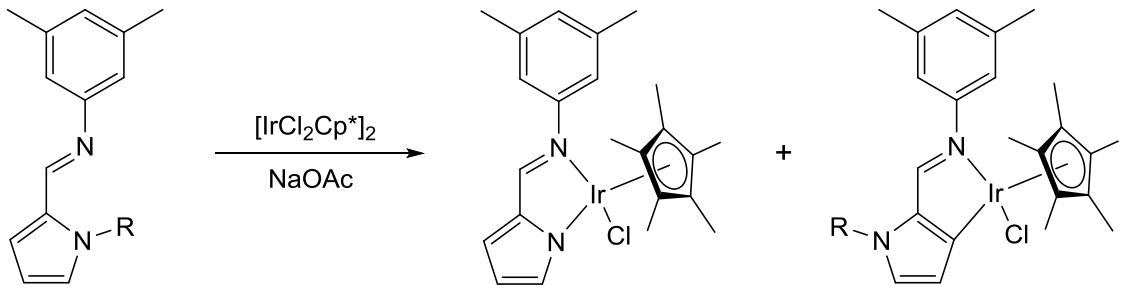

Scheme 2.6: N-H activation of a pyrrole imine.

Anionic directing groups have been studied for C-H activation (**Scheme 2.7**). In recent years, Wang *et al.* demonstrated acetate-assisted cyclometallation of isoquinolones (**2.26**) using Ir and Rh which led to cyclometallated complexes **2.27**.[19]

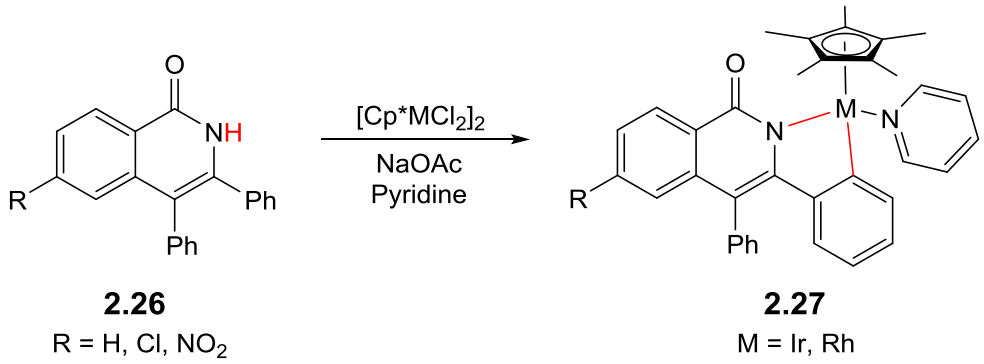

2.26
R = H, Cl, NO_2

2.27
M = Ir, Rh

Scheme 2.7: Isoquinolones used in AMLA C-H activation.

2.3 Stoichiometric Alkyne Insertions

Pfeffer *et al.* first reported insertion of alkynes into cycloruthenated complexes in 1993.[20] They demonstrated that cycloruthenated benzylamine complexes (**2.28**) react with internal alkynes to form coordinated isoquinolinium salts (**Scheme 2.8**).

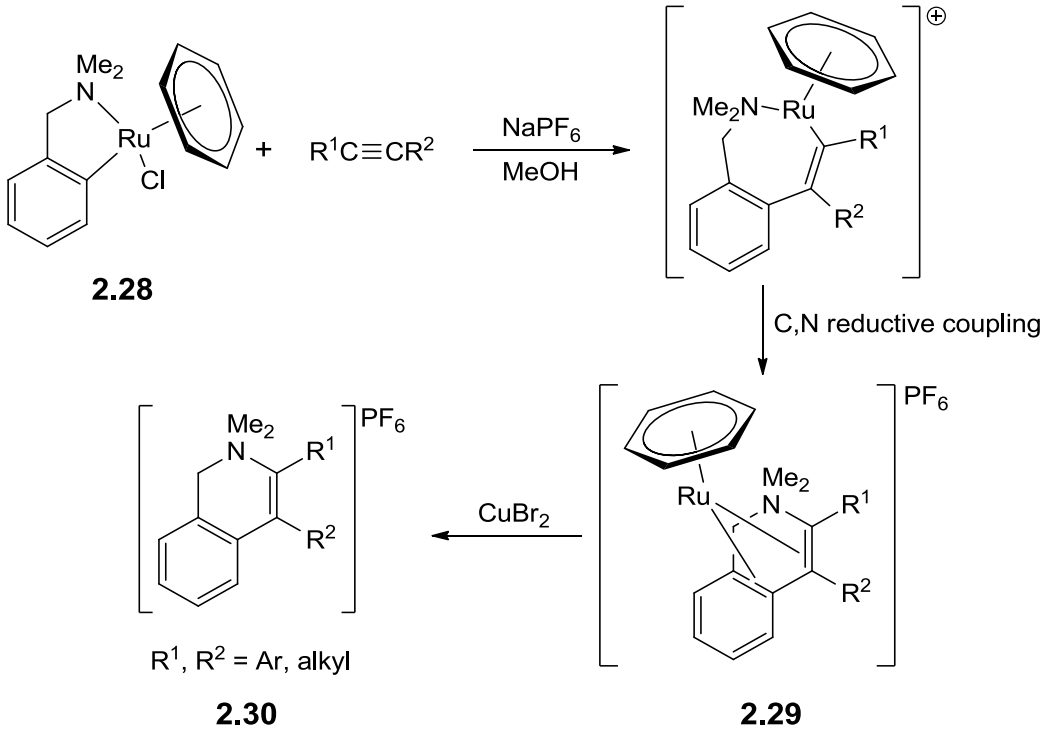

2.28

R^1, R^2 = Ar, alkyl

2.30

2.29

Scheme 2.8: Alkyne insertions into cycloruthenated benzylamine complexes.[20]

The authors postulated that the reaction goes via an alkyne-inserted intermediate followed by spontaneous C,N reductive coupling from Ru^{II} to give Ru^{0} complex **2.29**. Addition of the oxidising agent $CuBr_2$ causes reductive elimination to give an isoquinolinium salt (**2.30**). Cationic heterocycle products such as **2.30** have also been found for neutral directing groups by other researchers (see below for reactions of cyclometallated imine complexes).[12]

The reactions did not occur in dichloromethane however, using methanol and adding KPF_6 gave good yields suggesting that loss of chloride to form a reactive cationic species is necessary. This is true in related reactions of other Ir and Ru cyclometallated oxazoline complexes (see below).[15] The alkyne inserts into the M-C bond rather than the M-N bond. When electron-deficient alkynes such as dimethylacetylene dicarboxylate (DMAD) were tested, the reaction was found to stop after the insertion step. In the case of unsymmetrical alkynes, insertions were regioselective for less bulky substituents to end up next to the nitrogen atom which shows steric factors are certainly important. Using $PhC{\equiv}CCF_3$ two regioisomers were formed;[21] with the phenyl group next to the metal, C,N bond formation occurred and the isoquinolinium salt product (**2.30**) was observed. However, with the electron-withdrawing CF_3 group next to the metal, the reaction stopped after the insertion step before C-N bond formation. The authors concluded that reductive elimination depended on electronic effects at the metallated carbon whereby an electron-rich group was needed in order to attack the coordinated electrophilic amine.[20] The groups of Davies and Jones also found that electron-withdrawing groups on the alkyne make reductive elimination harder (see below). The rate of alkyne insertion was found to depend on the electron-density of the arene as the benzylamines bearing electron-donating substituents on the ring reacted faster than those bearing electron-withdrawing substituents.[22]

Jones *et al.* showed DMAD inserted into the M-C bond of Ir and Rh cyclometallated complexes of imines, 2-phenylpyridine and benzo[*h*]quinoline (**Scheme 2.9**).[12] Only mono-insertion was observed in all cases. The same result was observed using cycloruthenated *N*-phenylpyrazole with diphenylacetylene.[13] In these cases, spontaneous C,N reductive coupling did not occur.

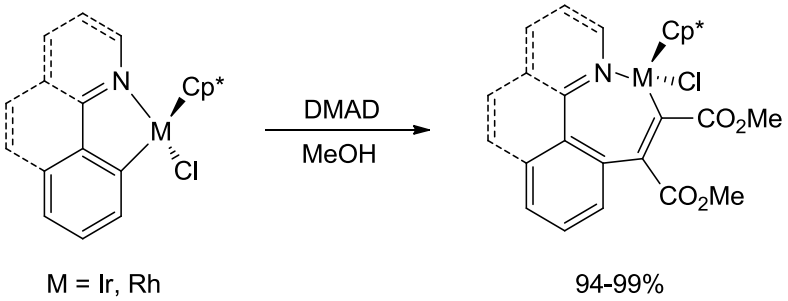

Scheme 2.9: Insertion of DMAD into Ir and Rh cyclometallated complexes.

The group of Davies successfully inserted alkynes into Ir and Ru cyclometallated oxazoline complexes with no spontaneous C,N reductive coupling.[15] Internal alkynes gave mono-inserted products and terminal alkynes gave a mixture of mono and di-inserted products (**Fig. 2.3**). If the starting cyclometallated complex was treated with acetonitrile and KPF_6, a more reactive cationic cyclometallated complex resulted and gave mono-insertion with terminal alkynes (**Scheme 2.10**). These reactions were regioselective for more electron-withdrawing groups next to the metal and showed electronic effects were important rather than just steric effects although a large range of alkynes were not studied.[20]

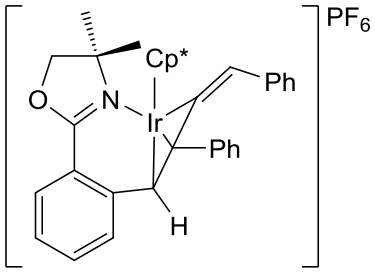

Fig. 2.3: Di-inserted products obtained with phenylacetylene.

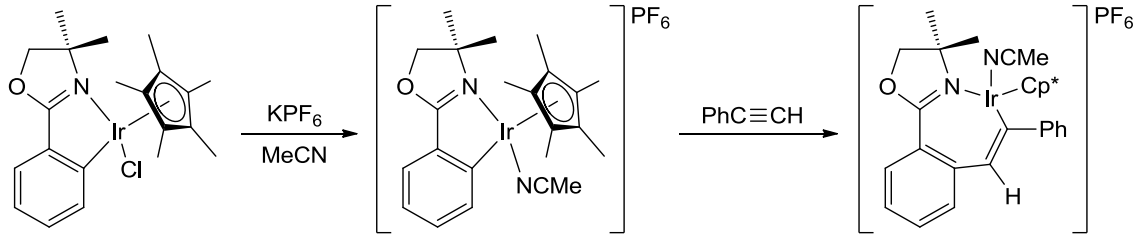

Scheme 2.10: Alkyne insertion into a cationic cyclometallated Ir complex.[15]

Davies *et al.* also observed alkyne insertions into cyclometallated *N*-phenylpyrazole complexes of Ir, Rh and Ru.[23] Diphenylacetylene and DMAD gave mono-inserted products. Phenylacetylene gave an inseparable mixture of products with Ir and Ru. With Rh however, the mono-inserted product was isolated and was regioselective for the phenyl being next to the metal, as with cyclometallated oxazolines[15] discussed earlier.

The groups of Davies and Jones studied alkyne insertions into cyclometallated imine complexes.[12, 23] Davies *et al.* found product selectivity was dependent on the substituents on the imine.[23] When R = CH_2CH_2OMe, the alkyne insertion product (**2.31**) is stable (**Scheme 2.11**). When R = Me, it was found that the insertion product was unstable so it was proposed that mono-insertion followed by reductive elimination occurs to give an isoquinolinium salt (**2.32**) but this product was not isolated. Jones *et al.* managed to isolate the DMAD-inserted analogue of **2.32** after addition of $CuCl_2$ to the DMAD-inserted Rh complex. When R = Ph, the insertion product undergoes a C-C bond formation to give the amino indene organic product (**2.33**) (**Scheme 2.11**).[23] Imino indenes[24] (dehydrogenation of **2.33**) and isoquinolines[25] have been formed from catalytic reactions of certain imines with alkynes using $[Cp^*RhCl_2]_2$ as catalyst (see **Section 2.5**). Davies *et al.* concluded that product selectivity from alkyne insertions with cyclometallated imine complexes depends on the substituent on the imine.

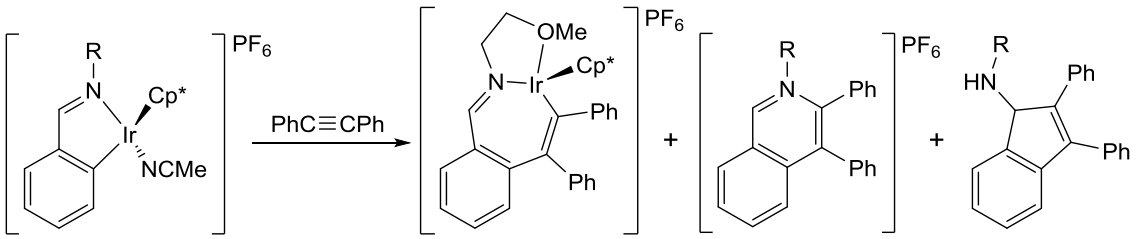

Scheme 2.11: Alkyne insertions into various cyclometallated imine complexes.

Cycloruthenated complexes from imine-functionalised heterocycles (**2.34**) undergo alkyne insertion with 3-hexyne followed by spontaneous C,N reductive coupling to afford complexes **2.35** (**Scheme 2.12**).[17] The pyrrole derivative reacted faster than the furan and thiophene derivatives. The benzannulated analogue complexes were the slowest. The authors proposed that the rate of alkyne insertion depends on the electron-density of the heteroarene, the more electron rich pyrrole derivative reacting fastest.

Pfeffer *et al.* found a similar trend for alkyne insertion into substituted benzylamines (discussed above).[22] The group was able to isolate the fused cationic heterocyclic products (**2.36**) from the oxidation reaction of **2.35** with $CuCl_2$. Jones had also adopted a similar strategy to liberate isoquinolinium salts from DMAD-inserted Rh complexes of imines, 2-phenylpyridine and benzo[*h*]quinoline.[8]

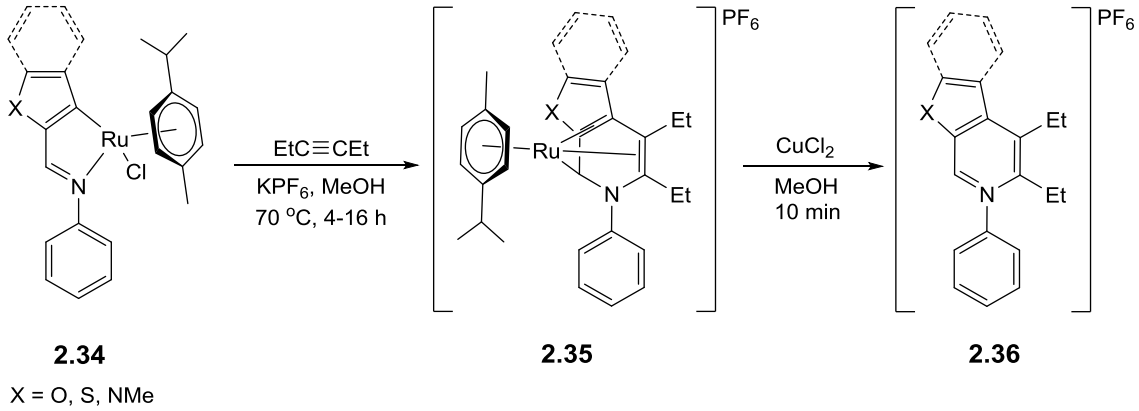

2.34

X = O, S, NMe

2.35 **2.36**

Scheme 2.12: Alkyne insertion into imine-based heterocyclic complexes.

In 2013, Wang *et al.* investigated alkyne insertions into cyclometallated complexes of anionic directing groups.[19] Isoquinolones were reacted with internal alkynes and $[Cp^*MCl_2]_2$ (M = Ir, Rh) in the presence of sodium acetate to give complexes **2.37** and **2.38** (**Scheme 2.13**). Higher yields of the inserted complexes were observed with Ir than Rh. The reaction was more favourable for isoquinolones with electron-withdrawing substituents (R = Cl, NO_2). With unsymmetrical alkynes, the reaction was highly regioselective for the more electron-withdrawing group to be next to the metal. In **2.37**, the substrate is bonded via an alkyne carbon and an η^3-amide, whilst in **2.38** with the amide is only N-bonded and there is an η^2-coordinated phenyl group. In all cases NH-deprotonation occurred, only mono-insertion was observed and all alkynes were inserted into the M-C bond. The authors observed the same results when starting from preformed cyclometallated complexes of the isoquinolones.

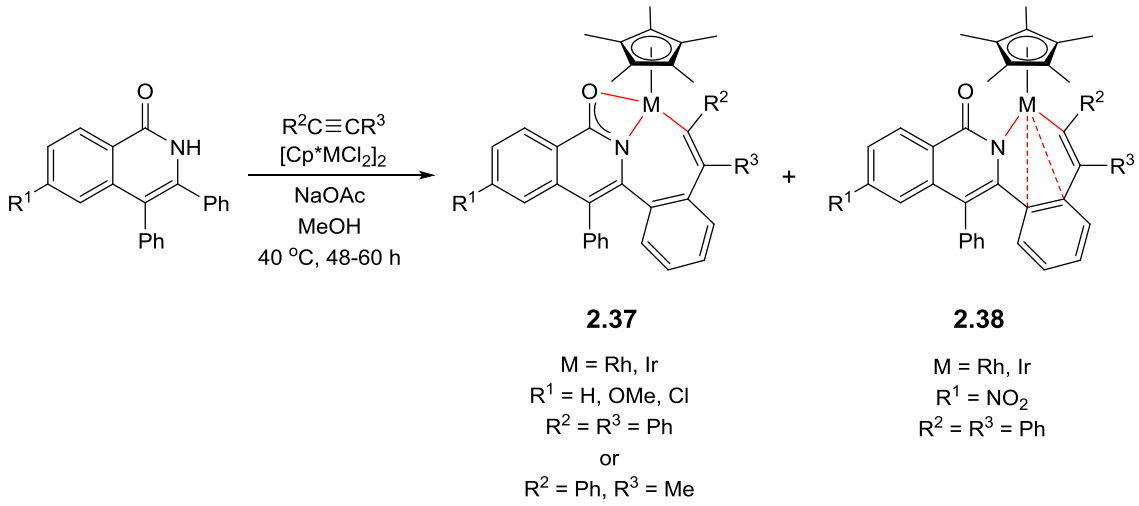

Scheme 2.13: Alkyne insertion with isoquinolones and Ir and Rh.[19]

Heating the Rh complexes **2.37** and **2.38** led to C,N reductive coupling and formation of Rh^{I} sandwich complexes (**Scheme 2.14**) however the authors did not identify this as reductive coupling. Similar reactions with the Ir analogues were unsuccessful.[19] These Rh^{I} complexes reacted with copper(II) acetate to liberate the organic products **2.39** (**Scheme 2.14**). Alternatively **2.37** and **2.38** could be converted directly to **2.39** by reaction with copper(II) acetate. Similar reactions with the Ir analogues were unsuccessful presumably because reductive elimination is harder from iridium. The catalytic reaction between isoquinolones and alkynes using 4 mol% $[Cp^*RhCl_2]_2$ also led to **2.39** in high yields (>86%). Based on their results, the authors proposed the catalytic coupling reaction goes via a Rh^{III} to Rh^{I} to Rh^{III} cycle (see **Section 2.5** for catalytic reactions).

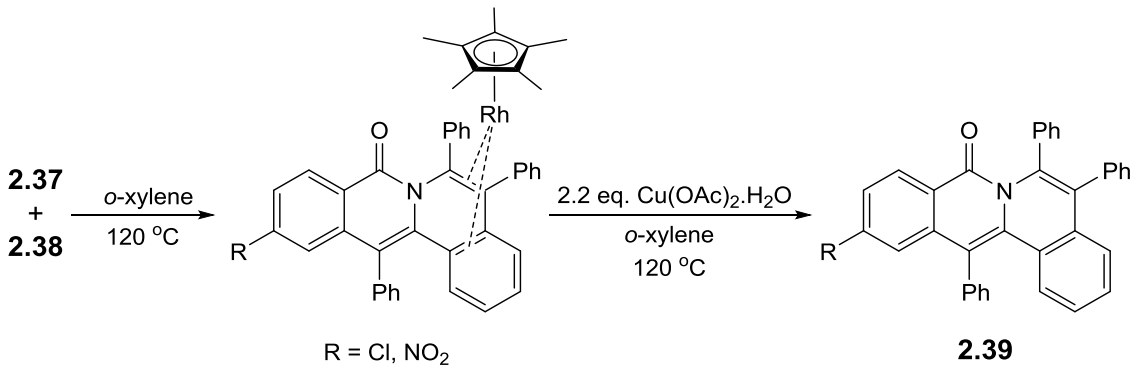

Scheme 2.14: Formation of organic products (**2.39**) via a Rh^{I} sandwich complex.[19]

2.4 Conclusions on Stoichiometric AMLA C-H Activation Studies

AMLA C-H activation has been accomplished with many different directing groups both neutral and anionic with the metals Ir, Rh and Ru. C-H activation of arene-sp^2, heteroarene-sp^2 and sp^3 C-H bonds has been achieved. The acetate must bind to the metal first before AMLA C-H activation can occur and $[Cp^*M(OAc)L]^+$ is the key species responsible for the C-H activation. Cyclometallation of most nitrogen donor directing groups is successful with Ir but not always with Rh and Ru. N-H activation is both kinetically and thermodynamically favourable compared to C-H activation, and occurs with the relevant substrates. Stoichiometric alkyne insertions into various cyclometallated Ir, Rh and Ru complexes have taken place mainly using diaryl alkynes. Dialkyl and terminal alkynes have not been fully explored. Sometimes the resulting complexes are unstable and so C,N reductive coupling or even reductive elimination to give organic products has been observed, particularly with Rh and Ru complexes. Ir^{III} complexes are more stable therefore reductive elimination is harder for these. Reductive elimination with anionic directing groups seems to be much easier. These stoichiometric studies have implications in catalysis reactions which have been predicted to go via a M^{III} to M^{I} to M^{III} (M = Rh, Ir) or Ru^{II} to Ru^{0} to Ru^{II} catalytic cycle. The next section will discuss catalysis reactions in more detail.

2.5 Catalytic AMLA Coupling Reactions with Alkynes

It has already been noted that AMLA C-H activation has been exploited in catalysis for many different types of C-H functionalisations including direct arylation reactions which were dealt with in **Chapter One**. This section will highlight catalytic coupling reactions between directing groups and alkynes which include AMLA C-H activation as part of their catalytic cycle. The effects on product selectivity of neutral and anionic directing groups, symmetrical and unsymmetrical alkynes, internal and external oxidants and Rh, Ru and Ir catalysts will be discussed. There will be a particular focus on studies with benzamide-derived directing groups to help illustrate the aforementioned differences.

Numerous heterocycles and carbocycles are now available by Rh or Ru-catalysed coupling of substrates with alkynes. In the vast majority of cases only internal alkynes work hence this is assumed in the discussion below; if reactions have been tried with

terminal alkynes these will be mentioned specifically. Substrates which have a protic directing group Y-H which can be easily deprotonated usually give heterocyclic products and their general catalytic cycle is shown in **Scheme 2.15**. The metal dimer breaks in the presence of $Cu(OAc)_2$ to form the active catalyst $[M(OAc)_2(ring)]$. Y-H (Y = O, N) and C-H bond activation (AMLA) of the substrate occurs to form a 5-membered cyclometallated complex. Alkyne association occurs followed by migratory insertion to give a 7-membered metallacycle. C-Y reductive elimination then gives the heterocyclic product. Reoxidation of the Rh(I) or Ru(0) species by $Cu(OAc)_2$ regenerates $[M(OAc)_2(ring)]$. Facile C-Y reductive elimination occurs with a directing group that can be made anionic.[26]

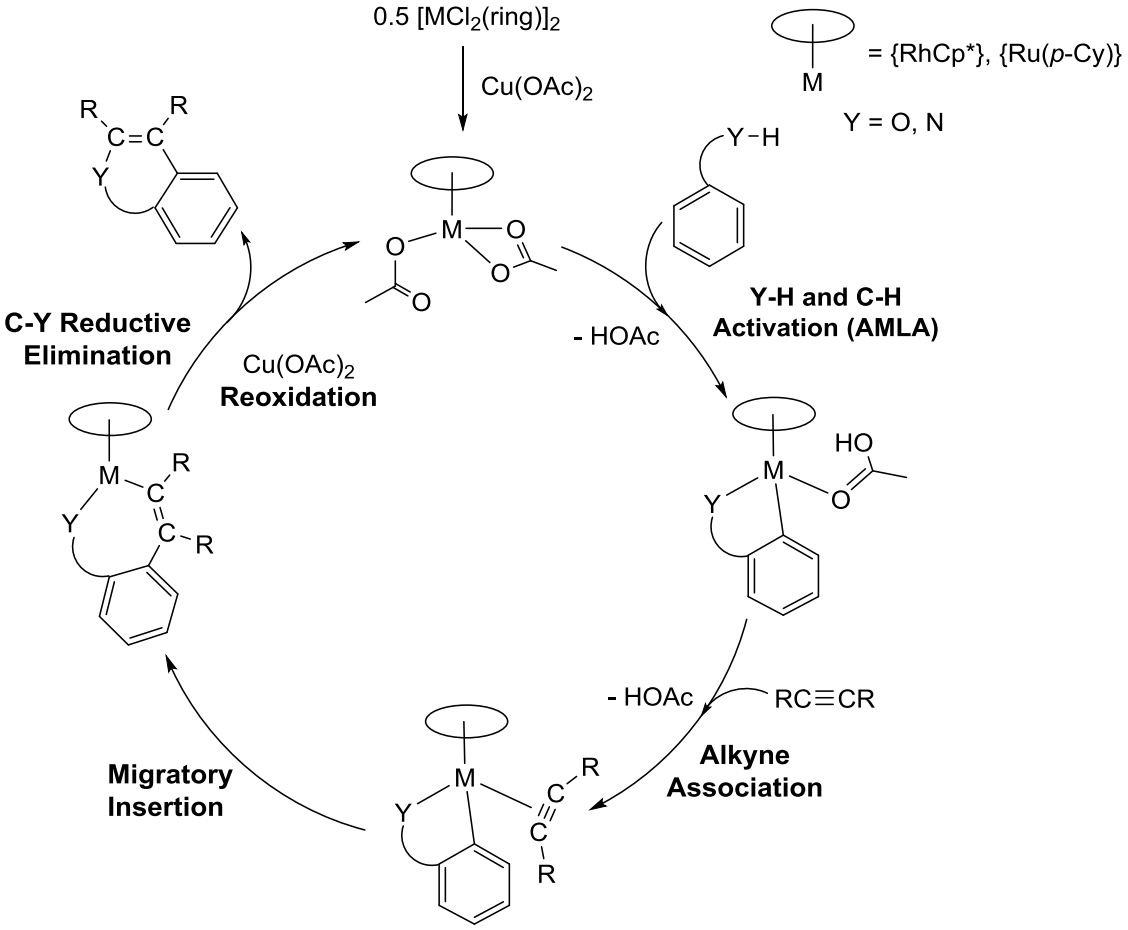

Scheme 2.15: General catalytic cycle for coupling of anionic directing groups with alkynes.

Neutral directing groups tend to give carbocyclic products. The general catalytic cycle for reactions using neutral substrates is illustrated in **Scheme 2.16**. After the first alkyne insertion C-Y reductive elimination is disfavoured as it would form a cation. If Y

dissociates from the metal[26] a second AMLA C-H activation can occur followed by a second alkyne insertion to give a new 7-membered dianionic metallacycle which undergoes C-C reductive elimination to give a carbocyclic product. An important thing to note for this type of catalysis with both types of directing groups is that there is no change in the oxidation state of the metal after the C-H (and Y-H) activation (as with direct arylations, see **Chapter One**, **Section 1.4.5**) unlike in OA catalysis.

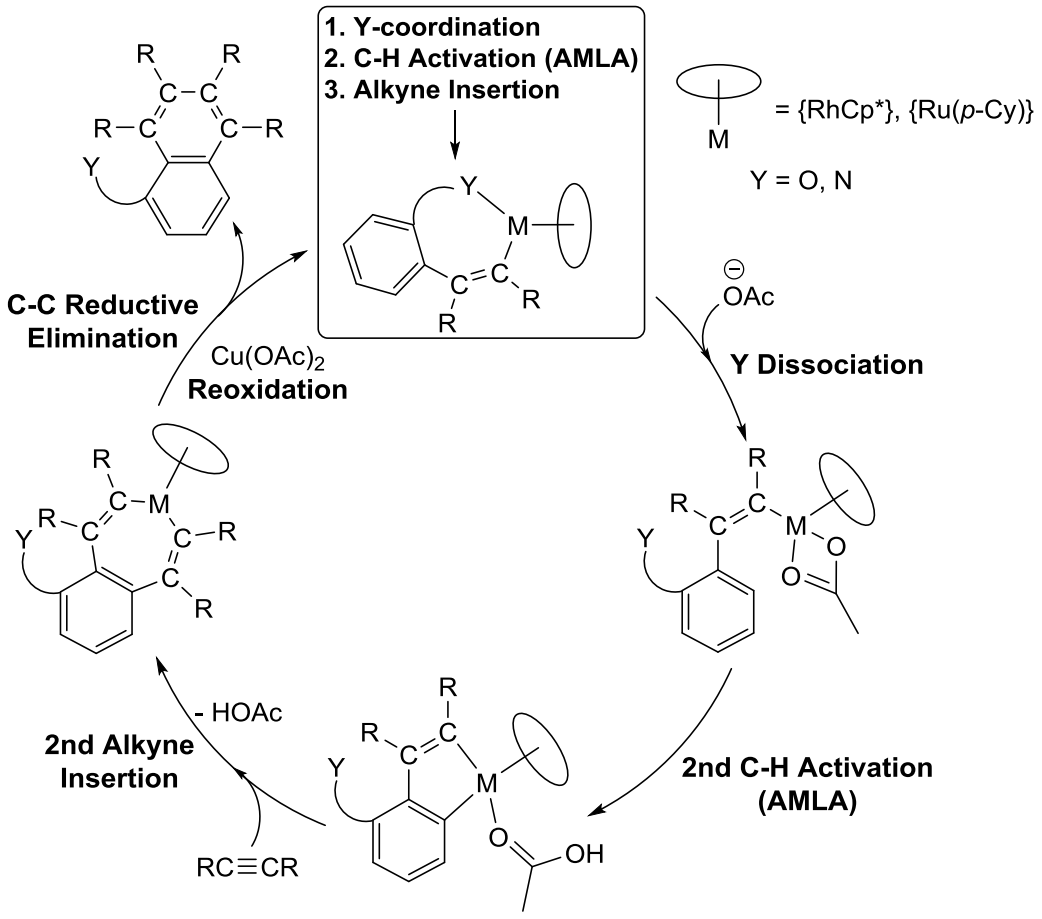

Scheme 2.16: General catalytic cycle for coupling of neutral substrates with alkynes.

In early studies using $[Cp^*RhCl_2]_2$ as a precatalyst, the groups of Miura[24, 27, 28] and Fagnou[25, 29] showed that AMLA C-H activation can be incorporated into catalytic cycles to prepare carbocycles and heterocycles. Using neutral imine directing groups and alkynes the products depend on the substituents on the imine (both C and N). *N*-aryl aldimines form imino indenes (**Scheme 2.17 A**)[24] whilst *N*-^{t}Bu imines give isoquinolines (**Scheme 2.17 B**).[25]

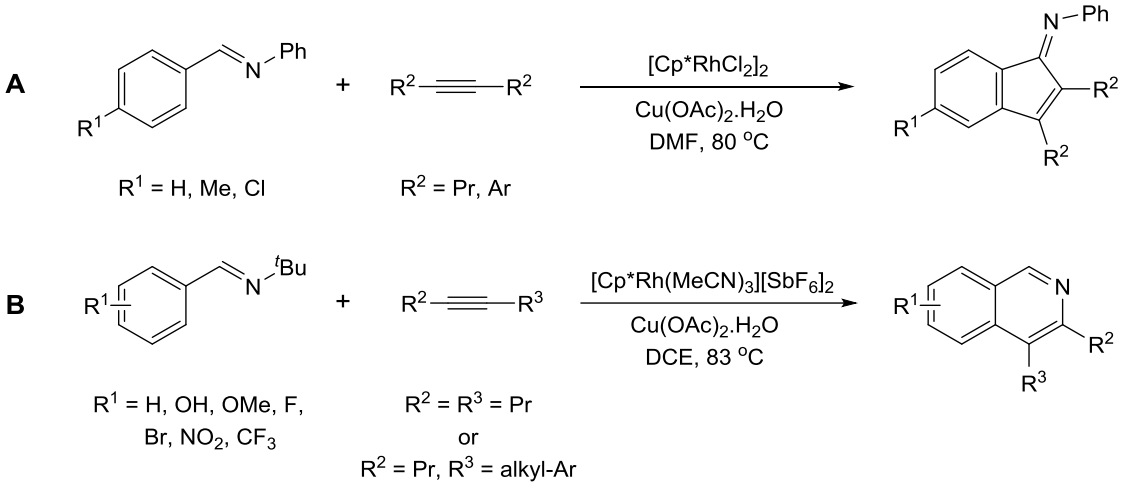

Scheme 2.17: Miura's coupling of alkynes with *N*-aryl imines (**A**)[24] and Fagnou's coupling of alkynes with *N*-*t*-butyl imines (**B**).[25]

For the *N*-aryl imine, Miura's group postulated that intramolecular insertion of the imine moiety occurs after alkyne insertion to form a C-C bond (**Scheme 2.18**). This is followed by β-hydride elimination to give the imino indene product.[24] In the case of *N*-^{t}Bu imines, C,N reductive elimination can occur after alkyne insertion with the loss of a *t*-butyl cation which gives 2-methyl-prop-1-ene and H^{+} as proposed by the authors.

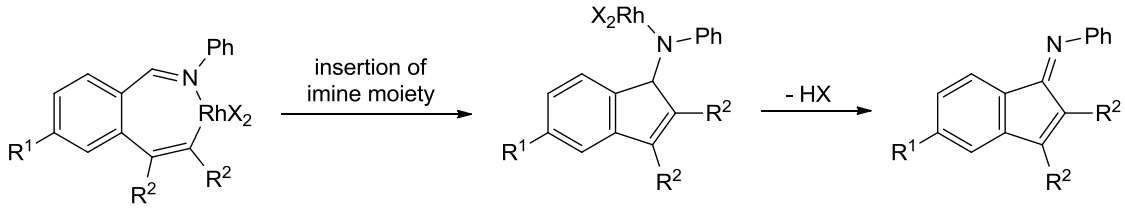

Scheme 2.18: Proposed mechanism for formation of indenone imine products.

In terms of coupling between anionic directing groups, Miura's group studied benzoic acids (**Scheme 2.19 A**)[27, 28] and Fagnou's group studied acetanilides (**Scheme 2.19 B**).[29] In both cases the directing group Y-H (Y = O, N) is deprotonated and this facilitates C-Y bond formation to form heterocyclic products. Also in the case of both directing groups with aryl-alkyl alkynes, reactions were regioselective for the phenyl substituent rather than the alkyl substituent to end up next to the heteroatom. Unsymmetrical dialkyl alkynes were also tested and were moderately regioselective for having the shorter alkyl chain next to the heteroatom.[30]

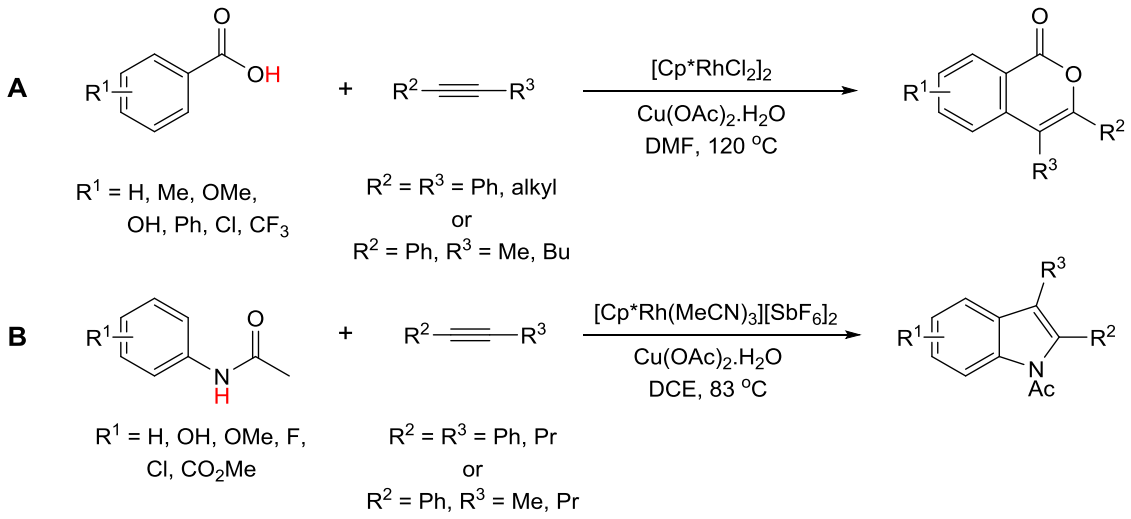

Scheme 2.19: Miura's coupling of alkynes with benzoic acids (**A**)[27, 28] and Fagnou's coupling of alkynes with acetanilides (**B**).[29]

Since the early studies by the groups of Miura and Fagnou, Rh-catalysed oxidative coupling has expanded rapidly. A wide array of neutral and anionic directing groups with alkynes has been reported and the field has been reviewed.[26, 31, 32] Selected examples are shown in **Table 2.1** with their corresponding products. All of these examples are from Cp*Rh-catalysed reactions unless otherwise stated.

These examples illustrate that C-Y (Y = O, N) bond formation is disfavoured with neutral directing groups so C-C bond occurs giving naphthalenes (**Entries 1-2**)[33-35] or even anthracenes (**Entry 2**).[33] With aryl ketones (**Entry 3**), intramolecular insertion of the C=O group presumably occurs after alkyne insertion into the metal-alkenyl bond to form a C-C bond and give indenol products.[36, 37] This is analogous to formation of imino indenes discussed above. Y-H (Y = O, N) activation can occur with anionic directing groups so C-Y (Y = O, N) reductive elimination is favourable and six-membered heterocyclic products are formed (**Entries 4-5**).[27, 28, 35, 38] However, reactions of benzoic acids with alkynes catalysed by $[Cp^*IrCl_2]_2$ and using Ag_2CO_3 as oxidant give naphthalene products (**Entry 4**). Presumably decarboxylation followed by a second alkyne insertion takes place after the first alkyne insertion.[28]

Table 2.1: Examples of different directing groups and their corresponding products obtained from metal-catalysed oxidative coupling reactions.

Entry	Directing Group	Product(s) Obtained
1	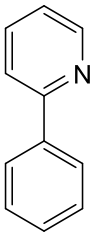	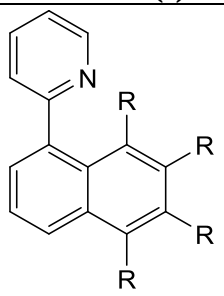 R = Ph[33]
2	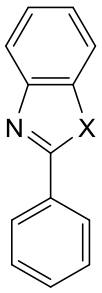 X = O, NMe	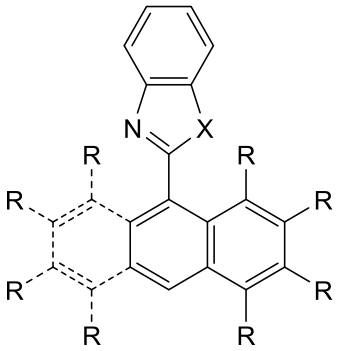 R = Ar[33, 34]
3	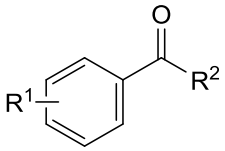 R^1 = H, Me, Ph, F, Cl, Br, I, CF_3 R^2 = Me, Et, Ph	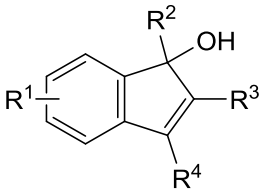 R^3/R^4 = Ar, CH_2OMe or R^3 = Ph, R^4 = Me, Et, CH_2OMe[36, 37]
4	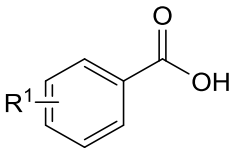 R^1 = H, Me, OMe, OH, Ph, Cl, CF_3	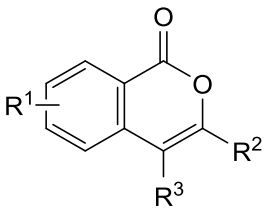 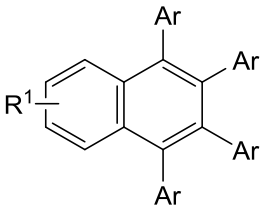 R^2/R^3 = Ph, alkyl or R^2 = Ph, R^3 = Me[27, 28]
5	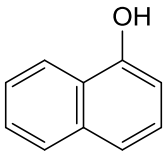	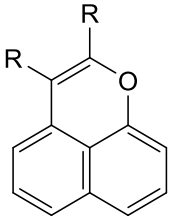 R = Ar, alkyl[35]

Benzamide directing groups which can be neutral or anionic depending on their substituents have been extensively studied. Thus, tertiary benzamides which have no N-H available for deprotonation form naphthalenes but only the reaction with diphenylacetylene has been reported (**Scheme 2.19**).[39]

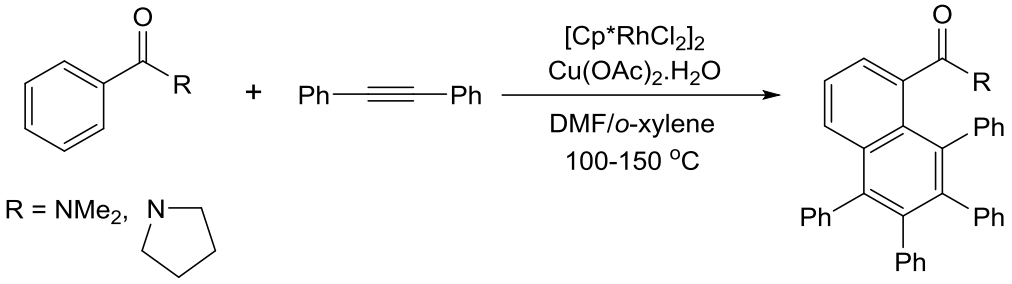

Scheme 2.20: 1:2 coupling of tertiary benzamides with diphenylacetylene.

Cp*Rh and (*p*-Cy)Ru-catalysed reactions of secondary benzamides with internal alkynes have been studied (**Scheme 2.21)**.[40-42] In general, both *N*-alkyl and *N*-aryl benzamides made efficient anionic directing groups and gave isoquinolones (**Scheme 2.20 A**). It is interesting to note that with *N*-aryl benzamides, the *N*-aryl substituent does not react at all so no indole products were formed as had been found by Fagnou *et al.* in their study with acetanilides.[29] This suggests that under neutral Cp*Rh catalyst conditions, benzamide C-H activation is faster than *N*-aryl C-H activation.

Reactions with ArC≡CR (R = alkyl) were regioselective for the aryl group to end up next to nitrogen whilst unsymmetrical dialkyl alkynes showed a preference for the smaller methyl group to end up next to the nitrogen. Unsymmetrical diaryl alkynes containing an electron-rich and an electron-poor substituent showed no regioselectivity. With bulky substituents on nitrogen (^{i}Pr, cyclohexyl) the benzamides do not undergo C,N coupling to isoquinolones instead they form naphthalenes (**Scheme 2.20 B**).[43] However, under harsher conditions and using a cationic catalyst, the naphthalene products can react further to give benzoisoquinolones (**2.40**).

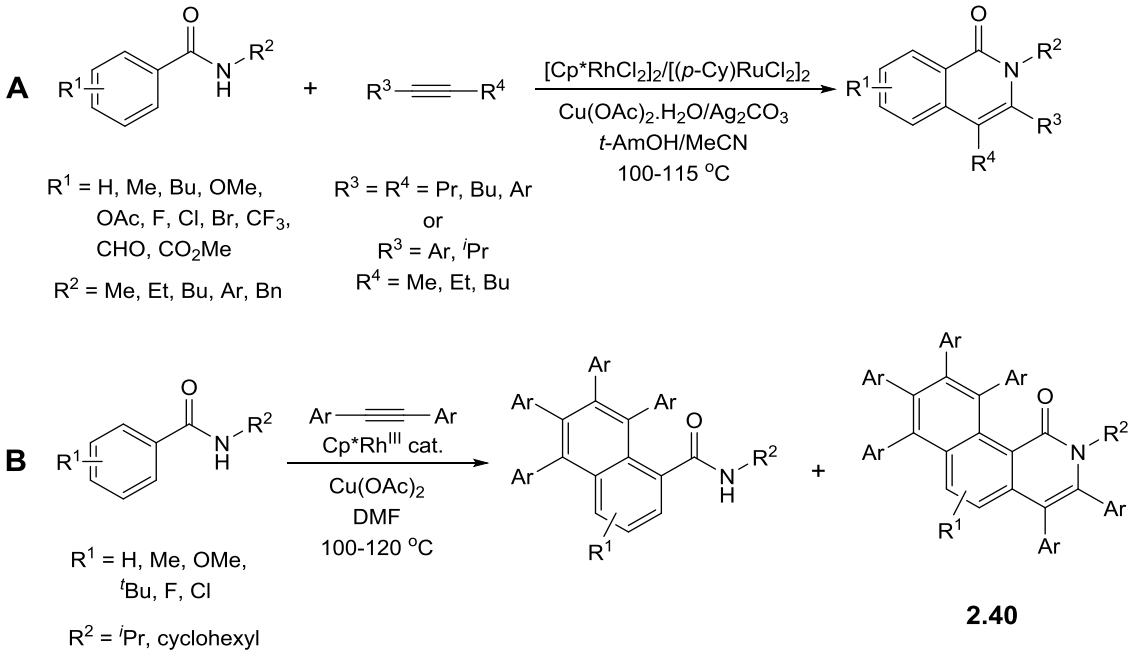

Scheme 2.21: Coupling of secondary benzamides with internal alkynes to give isoquinolones (**A**) or naphthalenes and benzoisoquinolones (**B**).

Primary benzamides react with 4-octyne to give 1:1 coupling products i.e. isoquinolones (**2.41**)[40] while reactions with aryl alkynes give mostly **2.41** and minor products (**2.42**), formed from **2.41** (**Scheme 2.22**).[39, 40] Using PhC≡CMe, the phenyl substituent ends up next to the nitrogen atom and so can react further to show the same regioselectivity.[40]

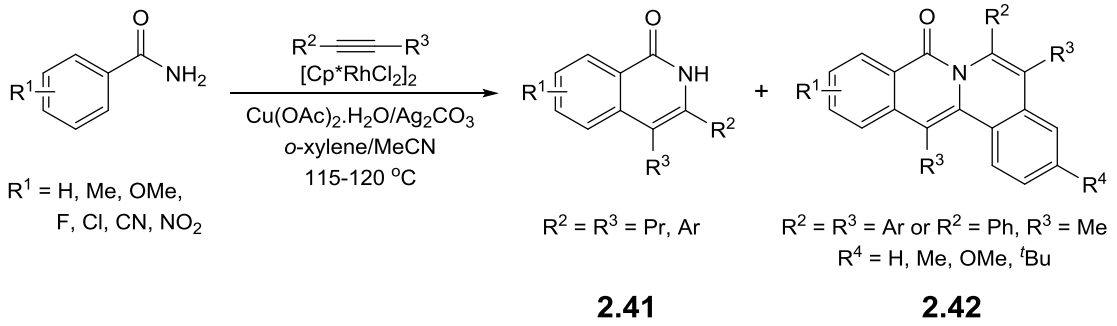

Scheme 2.22: Oxidative coupling of primary benzamides with internal alkynes.

Activation of heterocyclic C-H bonds has also been achieved catalytically. Thus, secondary heteroaryl carboxamides react with alkynes using $[Cp^*RhCl_2]_2$[39, 41] or $[(p\text{-}Cy)RuCl_2]_2$[42] as precatalyst. Reactions with PhC≡CEt were regioselective with the phenyl substituent ending up next to the nitrogen which agrees with previous results discussed above.[41] Reactions of substrates with the heteroatom *meta* to the amide

functionality resulted in the formation of a single regioisomer as product due to C-H activation at the more activated 2-position (next to the heteroatom) (**Scheme 2.23**). Yields with some substrates were low using neutral $[Cp^*RhCl_2]_2$ as precatalyst. These were vastly improved when the more activated cationic $[Cp^*Rh(MeCN)_3][SbF_6]_2$ precatalyst was employed.[41]

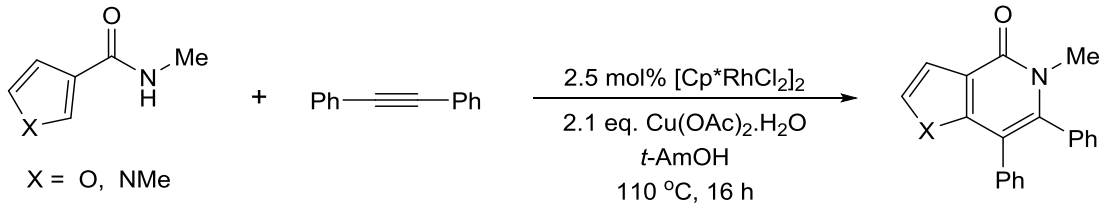

Scheme 2.23: Oxidative coupling of secondary heteroaryl carboxamides with alkynes.[41]

Activation of a vinyl sp^2 C-H bond was achieved in reactions between acrylamides and alkynes. Primary acrylamides reacted with diphenylacetylene in the same manner as primary benzamides to give fused-quinolinones (**Scheme 2.24**).[44] After the first alkyne insertion, there is still a protic NH present which acts as an anionic directing group and the second C-H activation takes place on a phenyl from the first diphenylacetylene inserted.

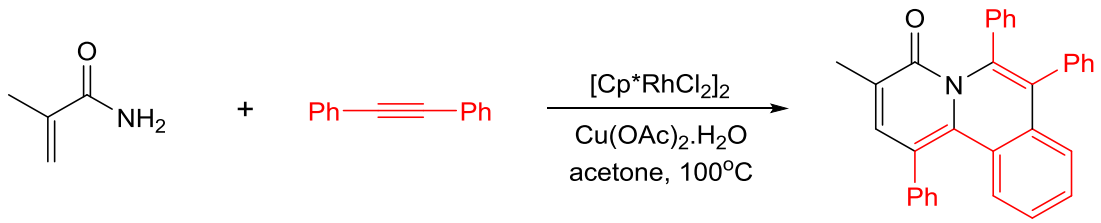

Scheme 2.24: Oxidative coupling of primary acrylamides with diphenylacetylene.

Pyridones were mostly formed from the reaction between secondary acrylamides and alkynes using $[Cp^*RhCl_2]_2$ and $[(p\text{-Cy})RuCl_2]_2$ precatalysts (**Scheme 2.25**).[44, 45] Again, reactions were regioselective for the phenyl rather than the alkyl substituent to end up next to the nitrogen. Interestingly when R^2 = Ph, no products were observed when using the Rh catalyst however the Ru catalyst afforded the pyridone product in moderate yield (**Scheme 2.25 B**). Cp*Rh-catalysed reactions with dialkyl alkynes proceeded smoothly but the analogous (*p*-Cy)Ru-catalysed reactions gave complicated mixtures of inseparable products. Reactions using $[Cp^*RhCl_2]_2$ sometimes gave indoles (**Scheme 2.25 A**),[44] depending on the substituents on the acrylamide. Reactions using [(*p*-

Cy)$RuCl_2]_2$ only gave pyridones, regardless of what the R^2 substituent was.[45] Indole formation was sluggish using neutral $[Cp^*RhCl_2]_2$ however the cationic $[Cp^*Rh(MeCN)_3][PF_6]_2$ gave full conversion. Imino esters were formed using $[Cp^*RhCl_2]_2$ with an acrylamide bearing a bulky *N*-mesityl substituent or an electron withdrawing group which presumably made C-N bond formation unfavourable (**Scheme 2.26**).[44]

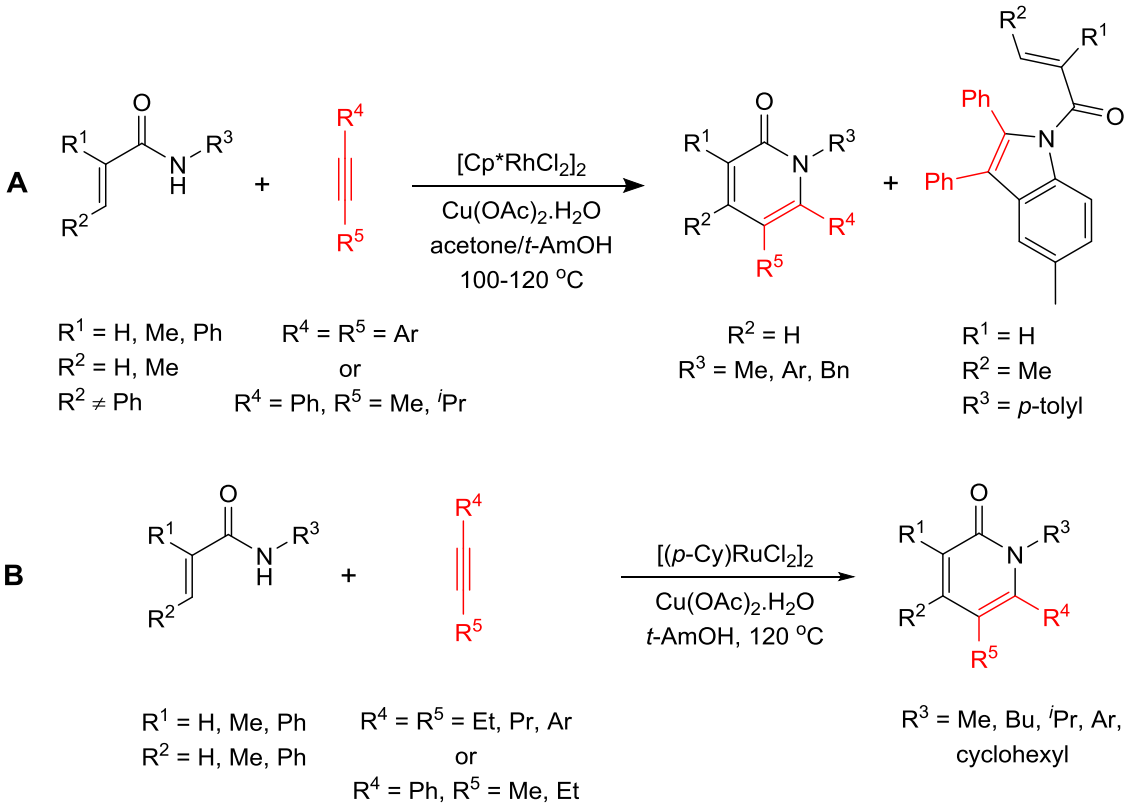

Scheme 2.25: Couplings of secondary acrylamides with alkynes using $[Cp^*RhCl_2]_2$ (**A**) and $[(p\text{-}Cy)RuCl_2]_2$ (**B**).[44, 45]

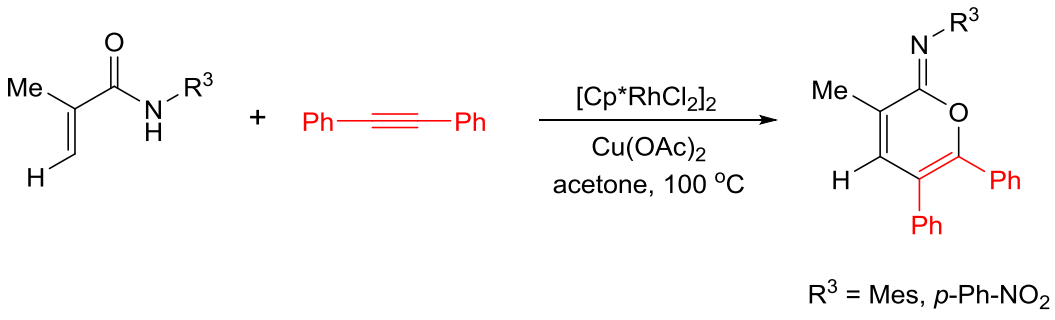

Scheme 2.26: Imino ester formation from Cp*Rh catalyst with certain secondary acrylamides.[44]

Intramolecular couplings are a very recent development. In 2013, intramolecular oxidative coupling of alkyne-tethered secondary benzamides was reported by Mascareñas *et al.* (**Scheme 2.27**).[46] Fused tricyclic isoquinolone derivatives were formed and the reaction tolerated both electron-donating and electron-withdrawing groups on the aryl substituent of the alkyne. The reaction worked efficiently with alkyl-substituted alkynes (R = Me) but did not work for terminal alkynes (R = H). The reaction also worked for acrylamides.

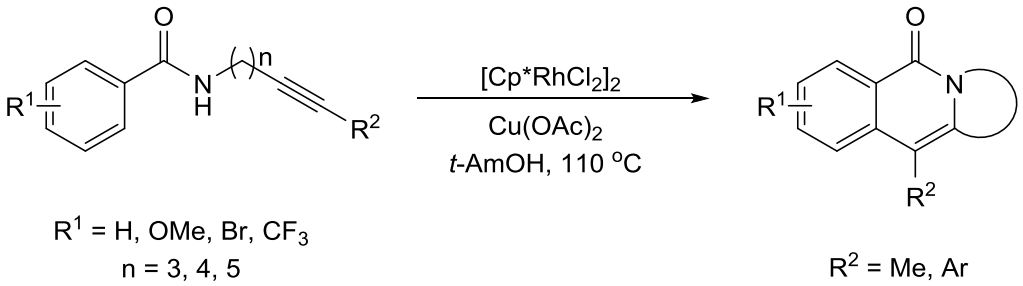

Scheme 2.27: Intramolecular oxidative coupling of alkyne-tethered benzamides.

All examples discussed thus far used stoichiometric amounts of oxidant (Cu or Ag). However catalytic copper in air/oxygen has been successfully employed with acrylamides,[47] benzoic acids[27, 28] and indoles.[48] Clearly, it would be most desirable from a green chemistry perspective if these reactions could be copper-free.

Copper-free reactions have been reported by Fagnou *et al.* for Cp*Rh-catalysed coupling of *N*-methoxy benzamides with alkynes where the methoxy group acts as an internal oxidant.[49] Reaction of benzamide itself with diphenylacetylene resulted in only stoichiometric reaction taking place giving a very low yield, proving that the *N*-substituent indeed acts as an internal oxidant and is needed for catalyst turnover.[49]

The same group later reported that *N*-acetoxy, -benzoxy and pivaloyloxy benzamides gave high yields, with the pivaloyloxy internal oxidant giving optimal results.[50] A range of alkynes reacted with *N*-pivaloyloxy benzamides to give isoquinolone products (**Scheme 2.28**) with the same regioselectivity with ArC≡CR (R = alkyl) as for reactions with copper oxidant discussed above. More importantly, these reactions occurred at room temperature with a low loading of precatalyst (0.5 mol%) compared with reactions using copper oxidants that require higher temperatures and higher catalyst loadings (2.5-5.0 mol%). This suggests reoxidation of the metal may be turnover-limiting in the

case reaction using copper oxidants. Perhaps the major advantage of this system is that it works with terminal alkynes. Terminal alkynes do not work with a copper oxidant possibly because the Cu-catalysed Glaser coupling of terminal alkynes occurs or a di-inserted product (as in **Fig. 2.3**) forms which cannot come off the metal and so kills the catalyst. Using an internal oxidant also allows reactions with internal and terminal alkenes and these will be discussed in **Chapter Three**.

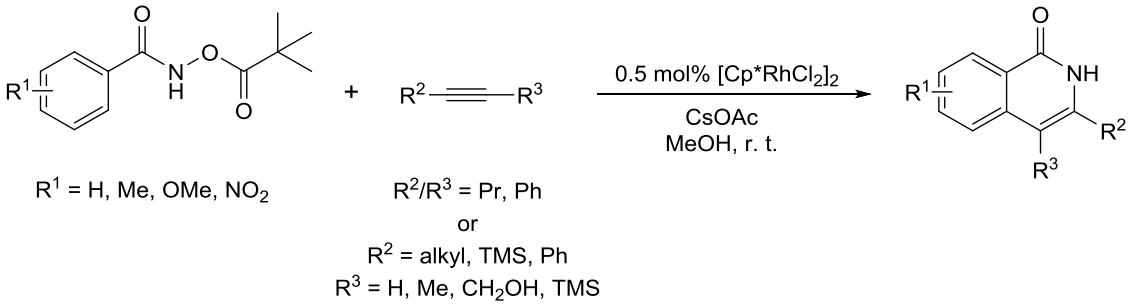

Scheme 2.28: Isoquinolone synthesis using benzamides with an internal oxidant.[50]

Reaction in deuterated methanol in the absence of alkyne resulted in deuteration at the *ortho*-positions of the benzamide substrate which suggested reversible C-H activation.[49] Reaction in deuterated methanol with alkyne present resulted in no deuterium incorporation so the authors concluded that the alkyne insertion is irreversible.[50] This result also suggests migratory insertion has a lower energy barrier than C-H activation. **Type A** KIE experiments measuring initial rates showed a very large k_H/k_D value of 15 for *N*-pivaloyloxy benzamide compared with the small k_H/k_D value of 1 for *N*-methoxy benzamide. This implied C-H activation is the rate-limiting step for *N*-pivaloyloxy benzamide and DFT calculations supported this. However it should be noted that the calculations were carried out with acetylene and not any alkynes tested experimentally, and the computations were with a Cp ligand not Cp*. The authors concluded that the rate-limiting step depends on the internal oxidant and the large KIE observed with *N*-pivaloyloxy benzamide is due to tunnelling effects.

Intramolecular coupling using an internal oxidant was realised by Park *et al.* in 2012 using alkyne-tethered hydroxamic esters (**Scheme 2.29**).[51] Products obtained were hydroxyalkyl isoquinolones unlike fused tricyclics obtained by Mascareñas *et al.* in their study of intramolecular couplings using external copper oxidant (**Scheme 2.27**).[46] The system was also successful when the arene was replaced by a heteroarene (thiophene and indole). For the arene activation the authors concluded C-H activation is

irreversible and rate-limiting. They proposed that the alkyne inserts into the M-C bond, however later studies including DFT calculations by Mascareñas *et al.* showed insertion into the M-N bond to be a strong possibility.[46] The reaction also worked for alkyne-tethered acrylamides.

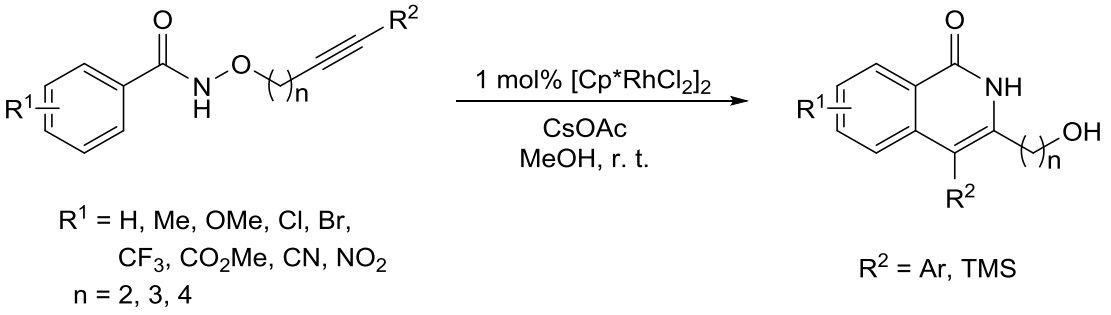

Scheme 2.29: Intramolecular coupling of benzamides containing an internal oxidant.[51]

2.6 Mechanistic Studies

Reactions of secondary benzamides with alkynes have been extensively studied by several groups and several mechanistic and labelling studies have been carried out. Competition reactions of secondary benzamides with different alkynes showed preference for diaryl alkynes over dialkyl alkynes (**Scheme 2.30**) for both Rh and Ru catalysts, and for electron-rich over electron-poor aryls (**Scheme 2.31**) for the Cp*Rh catalyst.[41, 42] Remarkably, electron poor aryls were favoured over electron-rich ones with the (*p*-Cy)Ru catalyst.[42] As expected, reactions were also selective with *meta*-substituted benzamides for attack at the least sterically-hindered site, similar to the cyclometallation of *meta*-substituted phenyl imines (see **Scheme 2.3**, **Section 2.2**).

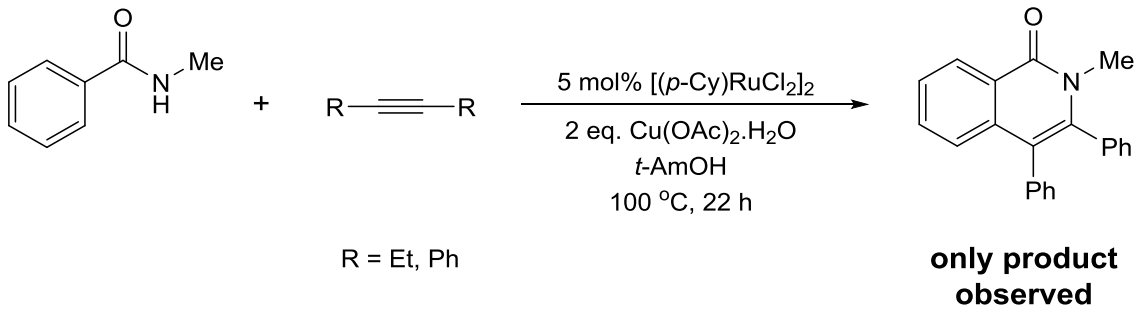

Scheme 2.30: Competition experiment with diaryl and dialkyl alkynes using Ru.[42]

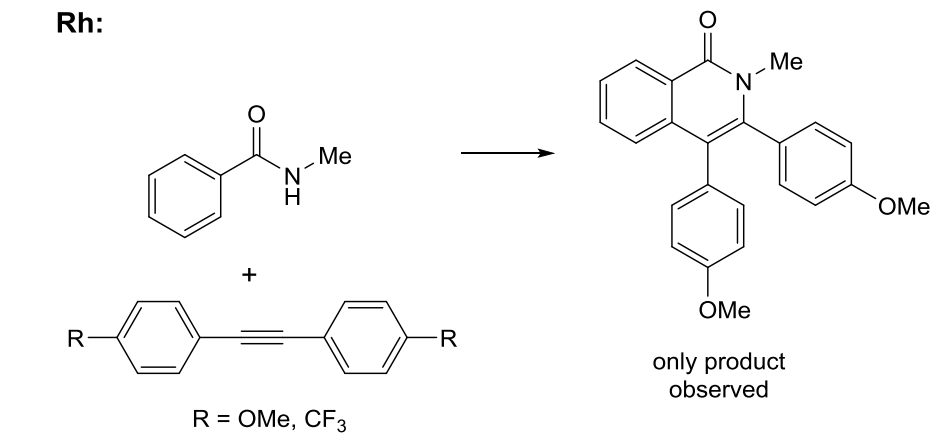

Reaction conditions: 2.5 mol% $[Cp^*RhCl_2]_2$, 2.1 eq.$Cu(OAc)_2.H_2O$, *t*-AmOH, 110 ^oC

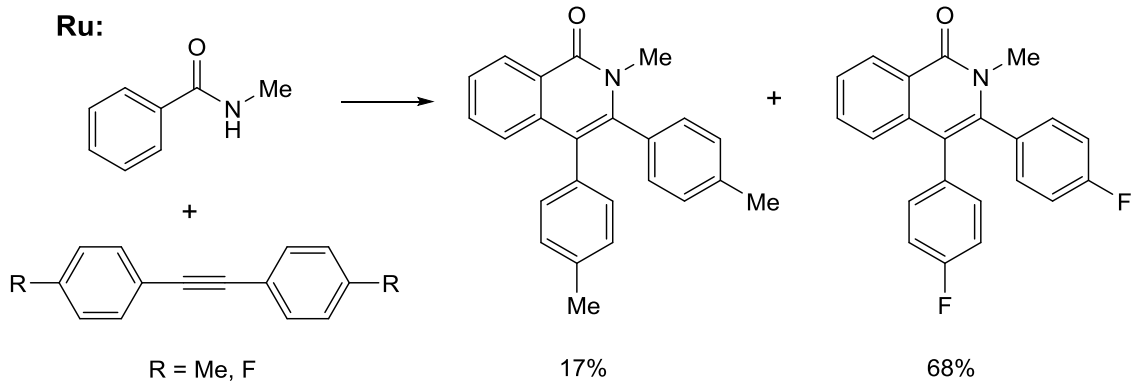

Reaction conditions: 5 mol% $[(p\text{-Cy})RuCl_2]_2$, 2 eq. $Cu(OAc)_2.H_2O$, *t*-AmOH, 100 ^oC

Scheme 2.31: Competition experiments with diaryl alkynes bearing electron-donating or electron-withdrawing groups.[41, 42]

Competition reactions between *N*-aryl benzamides containing different *N*-aryl groups showed a preference for benzamides with electron-poor aryls (**Scheme 2.32 A**).[40, 42] Similar results were observed with competition reactions comparing different R^1 groups on the phenyl being activated (**Scheme 2.32 B**).[40-42] These results agree with those reported in the later stoichiometric study by Wang *et al.* (see **Section 2.3**).[19]

H/D scrambling on the *ortho* sites of both proteo and deutero-benzamides was observed after heating them in the presence of $[Cp^*RhCl_2]_2$ without alkyne present.[40] This suggests C-H activation is reversible. Reaction between fully proteo benzamide and alkyne in deuterated solvent at low conversion showed no deuterium incorporation in either the product or unreacted benzamide so the authors concluded that C-H activation is irreversible in the catalytic system.[41]

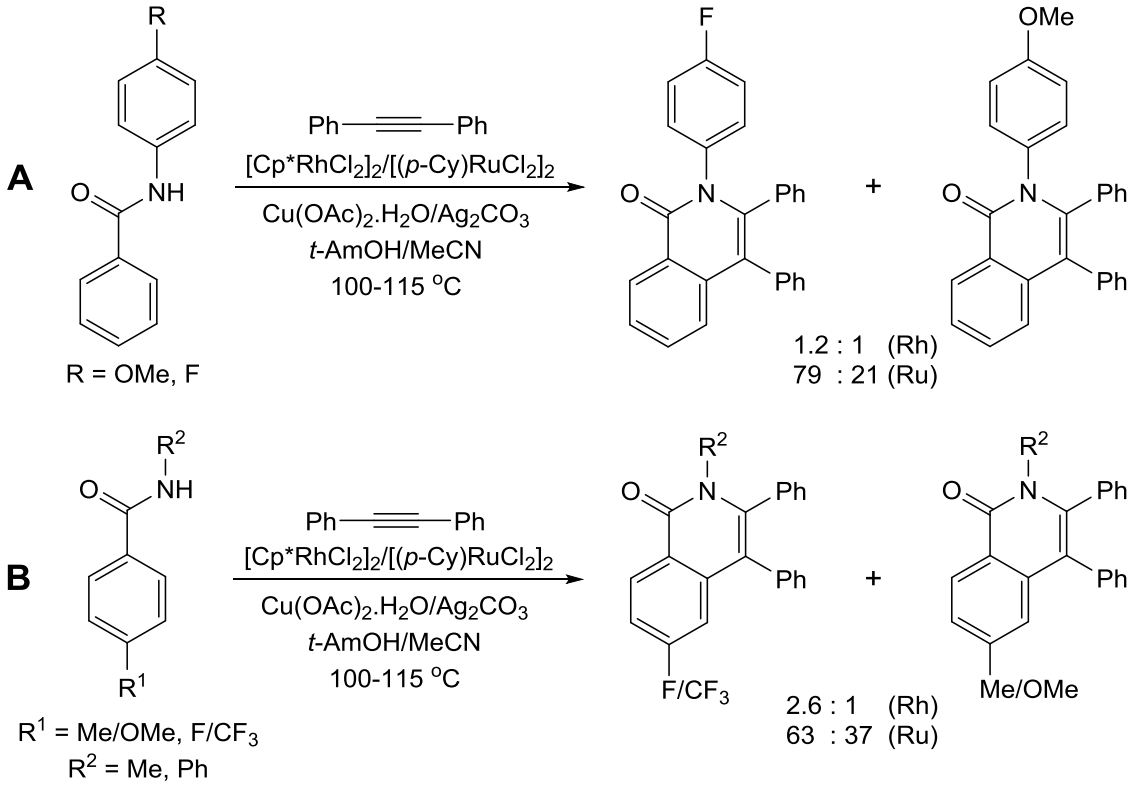

Scheme 2.32: Competition experiments with different secondary benzamides.[40-42]

Rovis *et al.* carried out a competition reaction to investigate whether C-H or N-H activation was rate-limiting. They used two different *para*-substituted benzamides (Br and CF_3), both with disparate σ_p values but with similar σ_m values (**Scheme 2.33**). It was found that products from both benzamides were formed in a nearly equimolar ratio (1:1.2), suggesting that C-H activation rather than N-H activation is the rate-limiting step. If N-H activation was rate-limiting, there would be a larger difference in the product ratios due to the greater acidity of the benzamide with the *p*-CF_3 substituent.[41]

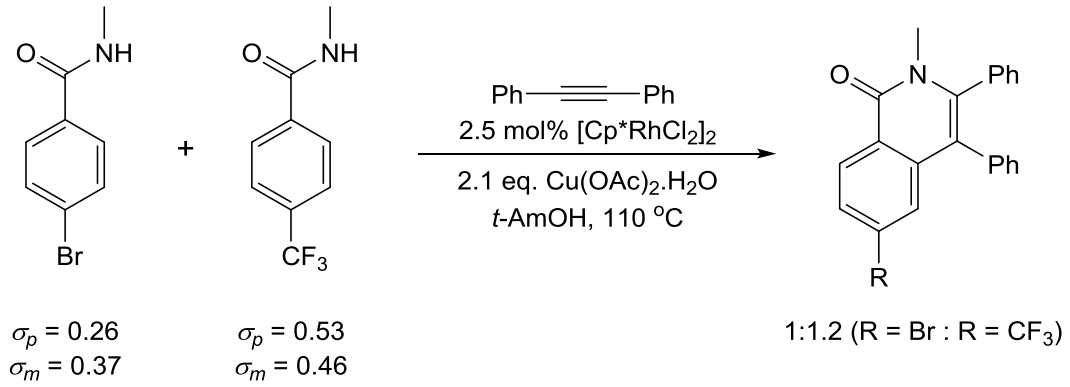

Scheme 2.33: Competition experiment to investigate the rate-limiting step.[41]

2.7 Conclusions on Catalytic AMLA Coupling Reactions with Alkynes

This section has provided an overview of Cp*Rh and (*p*-Cy)Ru-catalysed reactions of various directing groups with alkynes, with a particular focus on benzamides. In general, the mechanism goes via an AMLA C-H activation, alkyne insertion and reductive elimination catalytic cycle. Neutral directing groups tend to give carbocyclic products whilst anionic directing groups have an extra Y-H activation step and give heterocyclic products. Tertiary benzamides cannot be deprotonated so give naphthalenes. Isoquinolone (heterocyclic) products are usually obtained with primary and secondary benzamides, however they can give naphthalenes if the *N*-substituent is sterically bulky, disfavouring C-N bond formation. Further reaction of the initial products is sometimes possible. Heterocyclic amides and acrylamide substrates are also tolerated for coupling with alkynes, however product selectivity for acrylamides in Cp*Rh-catalysed reactions varies depending on the substituents. Using catalytic amounts of copper oxidant has been reported for some substrates[27, 28, 47, 48] and copper-free reactions of benzamides with internal oxidants have been studied.[49, 50] Very recently intramolecular annulations of benzamides,[46, 51] heteroarene amides[51] and acrylamides[46, 51] have been achieved with both external and internal oxidants.

2.8 Aims and Objectives

AMLA C-H activation is a promising route for the formation of carbocycles and heterocycles using various N and O directing groups with alkynes. Cp*Rh and (*p*-Cy)Ru make good catalysts for these reactions and are capable of activating sp^2 aromatic, heteroaromatic and vinyl C-H bonds.

In 2008, Satoh, Miura and co-workers reported the reaction of *N*-phenylpyrazoles with alkynes using $[Cp^*RhCl_2]_2$ to give naphthalenes (**Scheme 2.34**).[34] Reactions with PhC≡CR (R = alkyl) were always regioselective for the phenyl group to end up next to the metal which led to the formation of naphthalene products shown below. They later extended their studies to show that anthracenes are formed when using four equivalents of alkyne (**Scheme 2.34**).[33] *N*-phenylpyrazole is a neutral directing group, therefore C-N reductive elimination is disfavoured, leading to naphthalene and anthracene products.

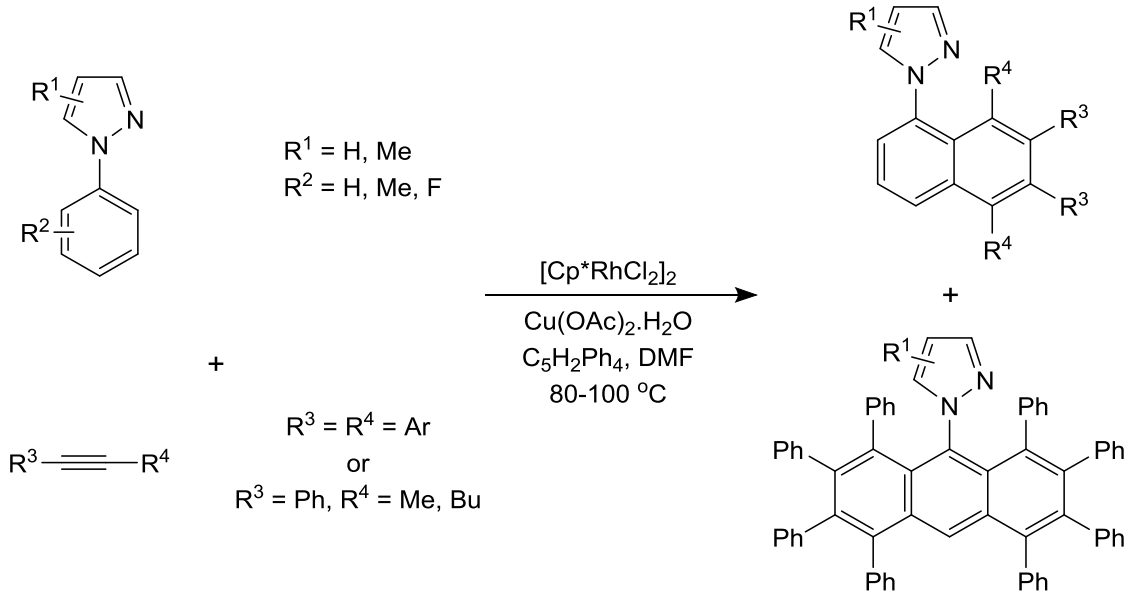

Scheme 2.34: Formation of naphthalenes and anthracenes with *N*-phenylpyrazoles.

In this work, we aimed to investigate the C-H functionalisation of *C*-phenylpyrazoles (**2.43**) and *C*-thiophenylpyrazoles (**2.44**) (**Fig. 2.4**) at Cp*Rh and (*p*-Cy)Ru centres. This chapter deals with synthetic and mechanistic studies of C-H functionalisation of *C*-phenylpyrazoles with alkynes at a Cp*Rh and (*p*-Cy)Ru centre. In contrast to *N*-phenylpyrazole which gives carbocycles, the presence of an NH proton may lead to NH deprotonation and formation of heterocyclic pyrazoloisoquinoline products. This chapter deals with synthetic and mechanistic studies of C-H functionalisation of *C*-

phenylpyrazoles with alkynes (alkenes are dealt with in **Chapter Three**) at a Cp*Rh and (*p*-Cy)Ru centre. Deuteration and competition experiments, coupled with detailed DFT calculations, have provided a detailed understanding of the mechanism of the catalysis which will be discussed. During the course of this research, some related chemistry using $[Cp^*RhCl_2]_2$ as catalyst was reported by Li[52] and similar reactions catalysed by $[(p\text{-Cy})RuCl_2]_2$ were subsequently reported by Ackermann.[53]

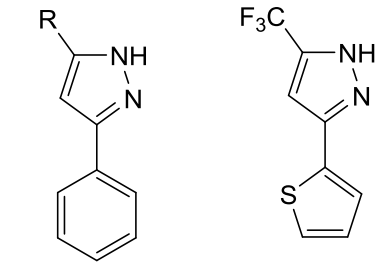

R = Me (**2.43a**)
H (**2.43b**)
Ph (**2.43c**)
CF_3 (**2.43d**)

2.44

Fig. 2.4: *C*-phenylpyrazoles and *C*-thiophenylpyrazoles used in this study.

2.9 Results and Discussion

Initially the reactions of 3-phenyl-5-methylpyrazole (**2.43a**) with 4-octyne (**a**) using different catalysts and reaction conditions were examined (**Table 2.2**). The reactions gave heterocycle **2.45aa** as product or major product in all cases. Full characterisation of **2.45aa** was carried out using ESMS, HRMS and ^{1}H, ^{13}C, COSY, NOESY and HMQC NMR spectroscopy.

The ^{1}H NMR spectrum of **2.45aa** shows signals for five protons in the aromatic region as expected; four for the phenyl protons and one for the pyrazole proton. These signals are in a 1:1 ratio with the signals for the *n*-propyl groups, showing that one equivalent of 4-octyne (**a**) has reacted with **2.43a**. Two sets of signals are seen in the alkyl region of the ^{1}H NMR spectrum for the two inequivalent *n*-propyl groups and the assignment for the two groups was determined by NOESY NMR spectroscopy which shows an NOE from one CH_2 signal to a signal from a phenyl proton from the pyrazole. The ^{13}C NMR spectrum shows the expected number of signals for all the carbon atoms and the HMQC NMR spectrum was useful for their assignment. ESMS shows ions at *m/z* 267

due to $[M+H]^+$ and HRMS (ESI) calculated 267.1861 for $[M+H]^+$ $C_{18}H_{23}N_2$ and found 267.1857. This confirms that N-H and C-H activation have occurred followed by C-N reductive elimination and there were no signs of a naphthalene product.

It is clear that $[Cp^*Rh(MeCN)_3][PF_6]_2$ (**Entry 2**, 98%) is a much better catalyst than $[Cp^*RhCl_2]_2$ (**Entry 1**, 9%), forming heterocycle **2.45aa** in quantitative yield rather than only 9%. In a recent study Li *et al.* did not report the use of dialkyl alkynes with $[Cp^*RhCl_2]_2$ as catalyst.[52] There was no catalysis in the absence of rhodium (**Entry 3**, 0%). In the absence of $Cu(OAc)_2.H_2O$ (**Entry 4**, 5%), stoichiometric formation of **2.45aa** occurred, indicating that reductive elimination can occur without prior oxidation of the metallacyclic species as seen with reactions of cyclometallated imine complexes with alkynes (see **Section 2.3**).[23] Lowering the catalyst loading to 1 mol% led to very low conversions (**Entry 5**, 8%). For comparison all reactions were left overnight to go to completion, however, detailed reaction monitoring showed that when using $[Cp^*Rh(MeCN)_3][PF_6]_2$ as catalyst, the reaction was complete in 1 hour at 83 °C. $[(p\text{-}Cy)RuCl_2]_2$ was also tested as a catalyst precursor and this also gave **2.45aa** in good yield (**Entry 6**, 65%), although under somewhat harsher conditions than rhodium. Moreover, unlike related reactions recently reported by Ackermann,[53] for **2.45aa** there was no need to use Ag^+ salts as additives. Finally both catalysts were tested with only catalytic copper, using air as the external oxidant. Using rhodium (**Entry 7**) the yield of **2.45aa** was reduced (50%) and importantly a new isomeric product **2.46aa** was also formed (24%) (see below for discussion of the characterisation). Similarly with ruthenium (**Entry 8**) the yield with catalytic copper was slightly reduced (48%). However, addition of 20 mol% $AgPF_6$ to give a cationic catalyst resulted in a 70% yield even with catalytic copper and no **2.46aa** was observed (**Entry 9**). Hence it has been demonstrated for the first time that both these catalytic systems can successfully produce heterocycles with only catalytic copper using air as the external oxidant thus improving the overall efficiency of the process.

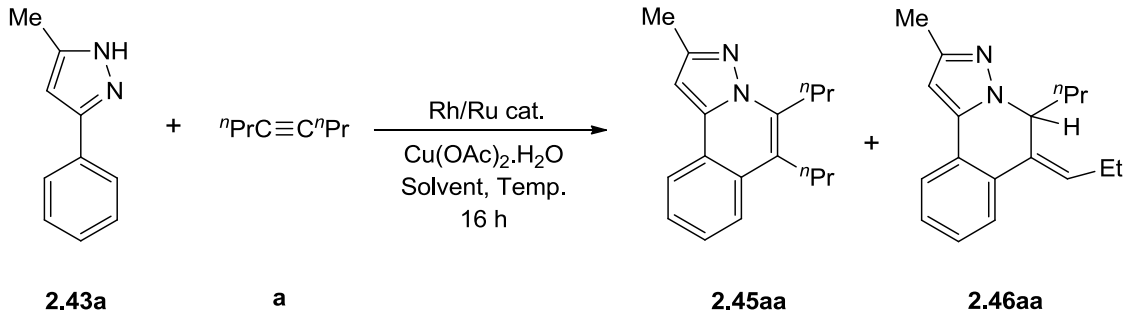

2.43a **a** **2.45aa** **2.46aa**

Table 2.2: Catalyst optimisation.

	Catalyst	mol%	Equiv. Cu	Yield/%[a]
1	$[Cp^*RhCl_2]_2$	5	2.5	9
2	$[Cp^*Rh(MeCN)_3][PF_6]_2$	5	2.5	98
3	$[Cp^*Rh(MeCN)_3][PF_6]_2$	0	2.5	0
4	$[Cp^*Rh(MeCN)_3][PF_6]_2$	5	0	5[b,c]
5	$[Cp^*Rh(MeCN)_3][PF_6]_2$	1	2.5	8[b]
6[d]	$[RuCl_2(p\text{-cymene})]_2$	5	2.5	65
7	$[Cp^*Rh(MeCN)_3][PF_6]_2$	5	0.1	50 (24)[e]
8[d]	$[RuCl_2(p\text{-cymene})]_2$	5	0.1	48
9[d]	$[RuCl_2(p\text{-cymene})]_2$[f]	5	0.1	70

Reagents: **2.43a** (1.0 mmol), **a** (1.2 mmol, 1.2 equiv.), DCE. [a]isolated yield after chromatography; [b]NMR yield using internal standard; [c]yield increased to >95% after addition of 2.5 equivalents $Cu(OAc)_2.H_2O$; [d]in *t*-AmOH 120 °C; [e]yield of isomeric product **2.46aa**; [f]20 mol% $AgPF_6$ additive

2.46aa was similarly characterised using mass spectrometry and NMR spectroscopy. The ^{1}H NMR spectrum shows signals for four aromatic protons, suggesting that one C-H of **2.43a** had been functionalised. The pyrazole proton and the pyrazole methyl substituent are observed as a 1H singlet (δ 6.29) and 3H singlet (δ 2.32). The spectrum also shows a propyl group and an ethyl group with two additional 1H peaks, a triplet at δ 6.02 (J = 7.4 Hz) and a doublet of doublets (J = 5.9, 7.8 Hz) at δ 5.34. Notably the

CH_2 groups of the propyl and ethyl groups show non-equivalent protons suggesting a lack of symmetry in the molecule. The triplet at δ 6.02 shows a COSY correlation to a CH_2 from a ethyl and so was assigned as the vinyl proton. The doublet of doublets at δ 5.34 was assigned as the N-CH proton due to the downfield shift and its COSY correlation to a CH_2 from a propyl. The ^{13}C APT NMR spectrum shows the presence of three CH_2 carbons compared to **2.45aa** which has four CH_2 carbons. The ESIMS shows an ion at *m/z* 267 due to $[M+H]^+$ and HRMS (ESI) supports the same formula as for, **2.45aa**, suggesting an isomer of **2.45aa**. An NOE from the vinyl proton to a phenyl proton from the starting substrate suggests that **2.46aa** isomer was formed as the *Z*-isomer rather than *E*.

Scope of Catalysis with Pyrazoles and Alkynes

Since the reactions with rhodium using catalytic copper led to some isomeric products, stoichiometric copper was used to explore the reactivity scope for rhodium and selected examples for ruthenium catalysis. **Scheme 2.35** shows the results of the reactions with symmetrical alkynes 4-octyne (**a**) and diphenylacetylene (**b**). Changing the substituent on the pyrazole had little effect, good yields of **2.45ba**-**2.45da** being formed in reactions with 4-octyne. Next reactions with diphenylacetylene (**b**) were explored which gave products **2.45ab**-**2.45db** in high yields (78-98%). During the course of this work Li *et al.* reported formation of **2.45ab**, **2.45bb** and **2.45cb** in broadly similar yields.[52] However, they noted reduced yields with electron withdrawing CF_3 on the pyrazole and difficulty in activating heterocyclic C-H bonds. In contrast, using $[Cp^*Rh(MeCN)_3][PF_6]_2$ as catalyst with a CF_3-substituted pyrazole we obtained **2.45db** in 90% yield. Even substrate **2.44** which requires C-H activation of a thiophene with a CF_3-substituted pyrazole (**2.44**), reacted well with 4-octyne or diphenylacetylene giving **2.47a** (79%) and **2.47b** (88%), respectively. The results with ruthenium were less consistent. Thus, though the product with 4-octyne **2.45aa** was formed in good yield (65%, **Table 2.2**, **Entry 6**) the corresponding product from diphenylacetylene, **2.45ab**, was only formed in 14% yield even in the presence of $AgPF_6$ as additive, whilst the thiophene substrate with a CF_3-substituted pyrazole with 4-octyne gave **2.47a** in 40% yield; in this case addition of $AgPF_6$ was essential.

The products **2.45ba**-**2.45da**, **2.45ab**-**2.45db**, **2.47a** and **2.47b** have all been fully characterised by ESMS, HRMS and ^1H, ^{13}C, COSY, NOESY and HMQC NMR

spectroscopy and the expected signals for all products were observed in the data. Suitable crystals were grown of **2.45cb** which allowed elemental analysis to be carried out and this showed very good agreement between calculated and obtained results. Products containing a CF_3 substituent on the pyrazole (**2.45da**, **2.45db**, **2.47a** and **2.47b**) were also analysed by ^{19}F NMR spectroscopy which showed the expected singlet at *ca.* δ -61 for all these products. Their corresponding ^{13}C APT NMR spectra showed the presence of the quaternary CF_3 carbon atoms as quartets at *ca.* δ 121 with large coupling constants between 268-300 Hz. The *C*-CF_3 carbon atoms could also sometimes be seen as small quartets between δ 142-144, with smaller coupling constants, between 35-41 Hz.

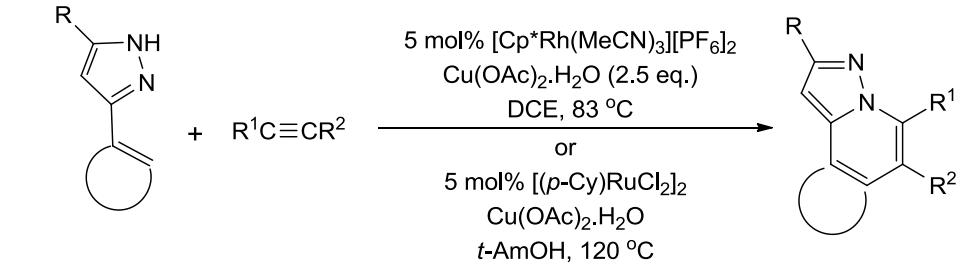

2.45ba (R = H) 87%
2.45ca (R = Ph) 91%
2.45da (R = CF_3) 80%[a]

2.45ab (R = Me) 91%
2.45bb (R = H) 78%
2.45cb (R = Ph) 98%
2.45db (R = CF_3) 90%
2.45ab (Ru; R = Me) 14%[b]

2.47a (R = ^{n}Pr) 79%[a]
2.47b (R = Ph) 88%
2.47a (Ru/Ag; R = ^{n}Pr) 40%[ab]

[a] a vinyl product is also formed
[b] 20 mol% $AgPF_6$ additive

Scheme 2.35: Scope of C-H functionalisation of pyrazoles with symmetrical alkynes.

As both dialkyl and diaryl alkynes react to give heterocyclic products, mixed aryl/alkyl alkynes were used to investigate the regioselectivity of insertion (**Scheme 2.36**). Thus, PhC≡CMe (**c**) reacted with **2.43a** to give **2.45ac** as a 9:1 ratio of the expected regioisomers in 50% combined yield along with 40% yield of another isomer **2.48ac** (see below). The isomers of **2.45ac** could be separated by chromatography and the

major isomer is that shown, with the phenyl substituent next to the nitrogen atom in the heterocycle. Interestingly this reaction with a Ru catalyst gave only **2.45ac** in 80% yield with a slightly higher selectivity of 12:1. These results imply a preference for insertion with an aryl next to the metal and is consistent with previous studies of catalytic heterocycle synthesis from alkynes with Cp*Rh and (*p*-Cy)Ru catalysts.[24-29, 34, 52-56] Unsubstituted pyrazole **2.43b** reacted similarly to give **2.45bc** in 54% combined yield as a 12:1 ratio of isomers however there was a considerable amount of unreacted **2.43b** so the yield based on **2.43b** consumed is 98%. The phenyl and trifluoromethyl substituted phenylpyrazoles reacted similarly to form **2.45cc** and **2.45dc** respectively in good yields, in the latter case a minor amount (16%) of **2.48dc** was also formed.

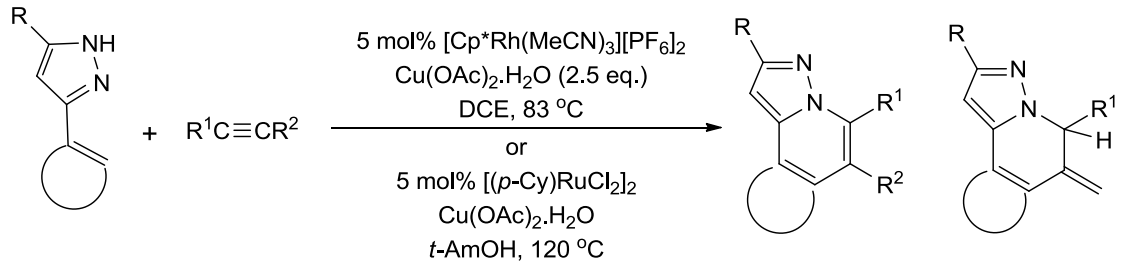

(minor isomer in parentheses)

2.45ac (R = Me) 50% (9:1)
2.45bc (R = H) 54% (12:1)[a]
2.45cc (R = Ph) 66% (3:1)
2.45dc (R = CF_3) 64% (6:1)
2.45ac (Ru; R = Me) 80% (12:1)

2.48ac (R = Me) 40%
2.48bc (R = H) trace
2.48cc (R = Ph) trace
2.48dc (R = CF_3) 16%

2.45ad (R = Me) 96% (3:1)[a]
2.45bd (R = H) trace
2.45cd (R = Ph) 83% (1:1)
2.45dd (R = CF_3) 90% (1:1)[b]

[a] minor isomer not isolated
[b] one isomer not isolated

Scheme 2.36: Scope of C-H functionalisation of pyrazoles with unsymmetrical alkynes.

The products **2.45ac-2.45dc** were all fully characterised by ESMS, HRMS and ^{1}H, ^{13}C, COSY, NOESY and HMQC NMR spectroscopy and the expected signals were observed for all the products. NOESY NMR spectra of the major isomers show an NOE from the signal of the methyl group from the alkyne to a signal from a phenyl proton from the starting phenylpyrazole. The minor isomers show NOE correlations from the

phenyl group from the alkyne to a phenyl proton from the starting phenylpyrazole. In the reactions of **2.43a** and **2.43d** another product was also formed, **2.48ac** and **2.48dc** respectively. The ^{1}H NMR spectra show two 1H signals at δ 5.49 and 5.67 for **2.48ac**, and two 1H signals at δ 5.56 and 5.76 for **2.48dc**. These correlate with one carbon signal in the HMQC spectrum for each compound and hence are assigned to an exocyclic CH_2. The ^{1}H NMR spectra also show singlets at δ 6.15 and 6.27 for **2.48ac** and **2.48dc** respectively which are assigned to C*H*(Ph) groups. Signals from the vinyl CH_2 protons show an NOE to a signal from a phenyl proton from the starting phenylpyrazole which was used to assign the phenyl protons. Products **2.48ac**-**2.48dc** are basically isomers of **2.45ac**-**2.45dc** by just a hydrogen shift and the mechanism for their formation will be discussed below in the Computational Studies section.

Products arising by formal hydrogen shifts have been noticed in rhodium oxidative couplings previously[48] and equivalent products have been realised through the use of allene coupling partners (**Scheme 2.37**).[57] Both products **2.45ac** and **2.48ac** were tested and it was found that they do not interconvert to each other when exposed to the catalyst and oxidant under catalytic conditions. In principle, compounds **2.48ac**-**2.48dc** could arise from insertion of an allene that is itself formed by isomerisation of PhC≡CMe (**c**); however DFT calculations indicate that this route is not energetically feasible as the C(sp^3)–N reductive coupling step is prohibitively high in energy. A possible alternative mechanism is discussed later (see Computational Studies section).

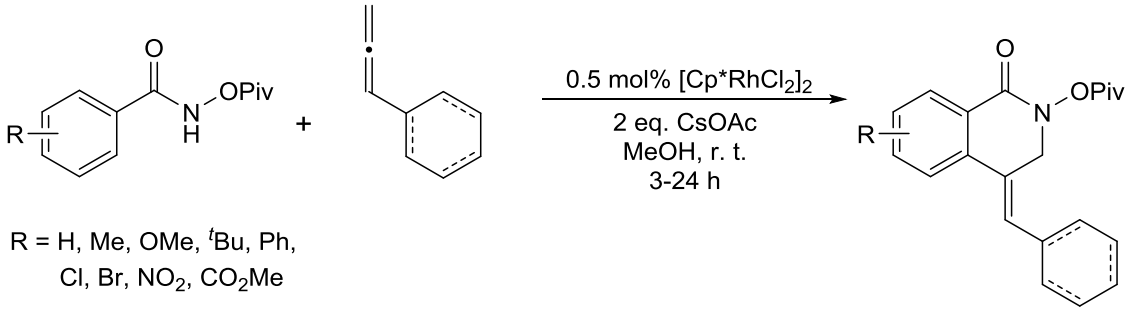

Scheme 2.37: Rh-catalysed oxidative coupling of benzamides with allenes. [57]

Aryl/alkyl alkynes containing more functionalised alkyl groups were also tested. Thus, (4-nitrophenyl)but-3-yn-1-ol (**d**) reacted with **2.43a** and **2.43c** to give **2.45ad** and **2.45cd** in high yields. Products were fully characterised by ESMS, HRMS and ^{1}H, ^{13}C, COSY, NOESY and HMQC NMR spectroscopy and the expected signals for all products were observed. For **2.45ad**, the structures of the major (**2.45ad**) and minor (**2.45ad′**) isomers were determined from the NOESY NMR spectra. The spectrum for the major isomer showed NOE correlations from one of the CH_2 proton signals to a phenyl proton from the starting phenylpyrazole. The minor isomer showed NOE correlations from the (*p*-NO_2-phenyl) proton signals to a phenyl proton from the starting phenylpyrazole. Thus, the major isomer is the one shown in **Scheme 2.36** (**2.45ad**), with the phenyl substituent next to the nitrogen atom in the heterocycle which is the same as the regioselectivity observed with PhC≡CMe (**c**).

In these reactions with alkyne **d**, there is significantly more of the isomers that have the alkyl substituent next to the pyrazole nitrogen (e.g. **2.45ad′**) than for PhC≡CMe (**c**), the isomer ratios being 3:1 for **2.45ad**, and 1:1 for **2.45cd-2.45dd** (compared to 9:1 and 3:1 for **2.45ac** and **2.45cc**, respectively). It is possible in these cases that the hydroxyethyl side chain may be able to hydrogen bond to the uncoordinated nitrogen of the pyrazole, thereby leading to a relative stabilisation of this isomer, or an intermediate that leads to this isomer. This could indeed be the case as the ^{1}H NMR spectrum for isomer **2.45cd′** shows the OH proton as a triplet at δ 4.16 whereas in isomer **2.45cd**, it appears as a broad singlet at δ 1.54. This downfield shift for **2.45cd′** is likely due to the effect of being in close proximity to the nitrogen possibly because of hydrogen bonding to the uncoordinated nitrogen of the pyrazole.

Several of the products have been characterised by X-ray crystallography. The structures of the major isomers of **2.45ac**, and **2.45dc** are shown in **Fig. 2.5** and those of **2.45da**, **2.45ab**, **2.45cb**, **2.45db**, **2.45cc**, **2.45ad**, **2.45bd** and **2.47a** are in the **Appendix**. The three fused rings are coplanar but are not completely delocalised. The central ring shows clear evidence of bond localisation[58] with the original alkyne bond C(10)—C(11) now being a double bond (C=C = 1.36(3)-1.38(5) Å) and the bond joining the phenyl or thiophene to the pyrazole being 1.43(5)-1.44(3) Å. The structures of the major isomers of **2.45c** and **2.49c** confirm that the phenyl substituent is on the carbon attached to nitrogen.

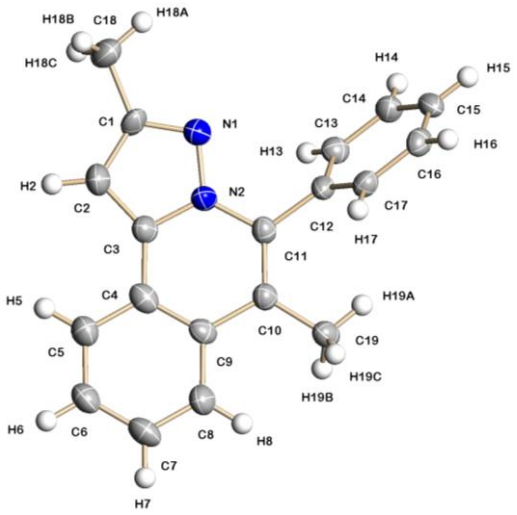

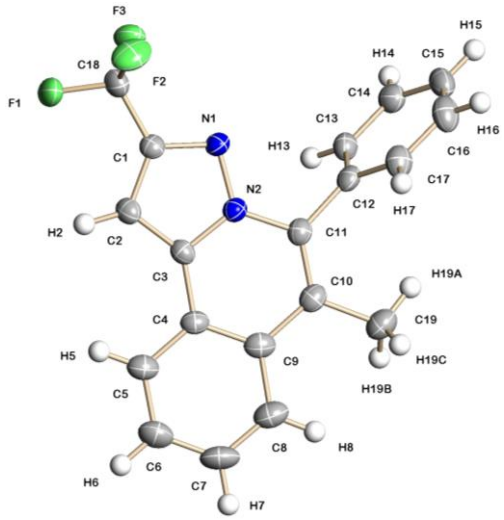

2.45ac	N(2)-C(3)	1.374(4)	C(4)-C(9)	1.388(5)
	N(2)-C(11)	1.390(4)	C(9)-C(10)	1.467(4)
	C(3)-C(4)	1.432(5)	C(10)-C(11)	1.374(5)
	C(3)-N(2)-C(11)	124.3(3)	C(3)-C(4)-C(9)	117.9(3)
	N(2)-C(11)-C(10)	118.5(3)	C(9)-C(10)-C(11)	118.9(3)
2.45dc	N(2)-C(3)	1.379(3)	C(4)-C(9)	1.402(3)
	N(2)-C(11)	1.401(3)	C(9)-C(10)	1.461(3)
	C(3)-C(4)	1.435(3)	C(10)-C(11)	1.357(3)
	C(3)-N(2)-C(11)	123.9(2)	C(3)-C(4)-C(9)	118.4(2)
	N(2)-C(11)-C(10)	118.6(2)	C(9)-C(10)-C(11)	120.2(2)

Fig. 2.5: Crystal structures of **2.45ac** (left) and **2.45dc** (right) with selected bond distances (Å) and angles (^{o}). Figures show 50% displacement ellipsoids.

All the results discussed so far have involved the formation of *N*-heterocyclic products which involve a C, N reductive elimination step. However in reactions with CF_3 substituted pyrazoles (**2.43d** and **2.44**) very small amounts of vinyl products **2.49da**, **2.49dd** and **2.50a** are also formed (**Fig 2.6**). The ^{1}H NMR spectrum for **2.49da** shows signals for four protons in the aromatic region and a singlet for the pyrazole at δ 6.72 suggesting that one C-H has been functionalised. Two sets of signals are seen in the alkyl region for two different propyl groups which are in a 1:1 ratio with the signals from the pyrazole, suggesting that one equivalent of 4-octyne (**a**) has reacted with **2.43d**. There is also a 1H triplet at δ 5.61 (J = 7.4 Hz) which shows an NOE to a phenyl proton from the starting substrate. It also couples to a CH_2 signal at δ 2.20 according to the COSY spectrum so it is assigned to the vinyl proton. The ^{13}C APT NMR spectrum

confirms the presence of four CH_2 carbons. The ESIMS shows an ion at *m/z* 323 due to $[M+H]^+$ and HRMS (ES) is correct for the monovinyl product, **2.49da** (**Fig. 2.6**). The data for monovinyl product **2.50a** is similar to that of **2.49da** and a crystal structure of **2.49dd** was obtained which confirms the structure shown below (see **Appendix**).

The CF_3 substituent on the pyrazole possibly causes C-N bond formation to be disfavoured therefore some protonation takes place before reductive elimination can take place. The protonation therefore leads to formation of these vinylic products. However it should be noted that these are only formed in very small yield therefore the C-N reductive elimination pathway is largely favoured over the protonation pathway. Li *et al.* reported reduced yields with substrates containing an electron withdrawing CF_3 substituent on the pyrazole[52] so it may be that the reductive elimination step is harder with CF_3 as a substituent.

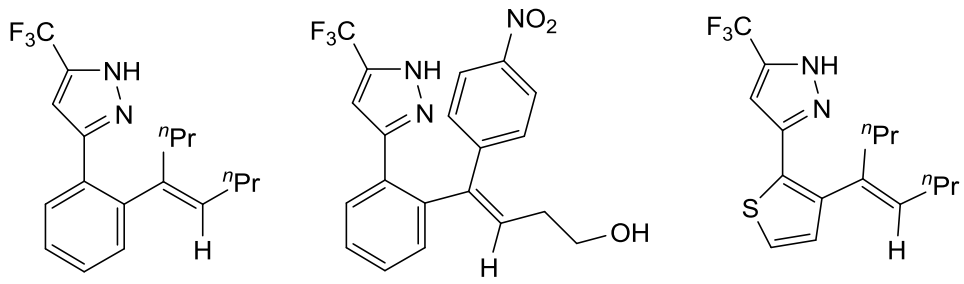

2.49da 6% **2.49dd** trace[a] **2.50a** trace[a]

[a] no pure product(s) isolated

Fig. 2.6: Vinyl phenylpyrazole minor products.

Reactions with alkynes containing electron-withdrawing groups such as dimethylacetylene dicarboxylate (**e**) or PhC≡C(CO_2Et) (**f**) were tested next. Reaction of **2.43a** with DMAD (**e**) (**Scheme 2.38**) went to 100% consumption of starting material and led to a mixture of products which made purification difficult, leading to the low isolated yields. The major product was purified by column chromatography. The ^{1}H NMR spectrum for the major product shows signals for five protons in the aromatic region and a singlet at δ 6.50 due to the pyrazole proton suggesting that no C-H's have been functionalised. A 3H singlet at δ 2.40 is assigned to the methyl group on the pyrazole and two 3H singlets at δ 3.79 and δ 3.99 are assigned to two CO_2Me groups. Therefore the pyrazole and DMAD signals are in a 1:1 ratio with each other, suggesting that one equivalent of DMAD (**e**) has reacted with **2.43a**. The pyrazole 1H singlet shows an NOE to the pyrazole methyl singlet. Additionally there is a 1H singlet at δ 6.36 which shows an NOE to a CO_2Me signal so is assigned to a vinyl proton. Neither of the CO_2Me signals show any NOEs to any phenyl protons. The ^{13}C NMR spectrum shows 14 signals as expected. The ESIMS shows an ion at *m/z* 301 due to $[M+H]^+$ and HRMS (ES) is correct for the maleate product, **2.51ae** (**Scheme 2.38**). A crystal structure was obtained to confirm which nitrogen was attached to the vinyl (see below). Data for product **2.51be** was consistent with the structure shown in **Scheme 2.38**.

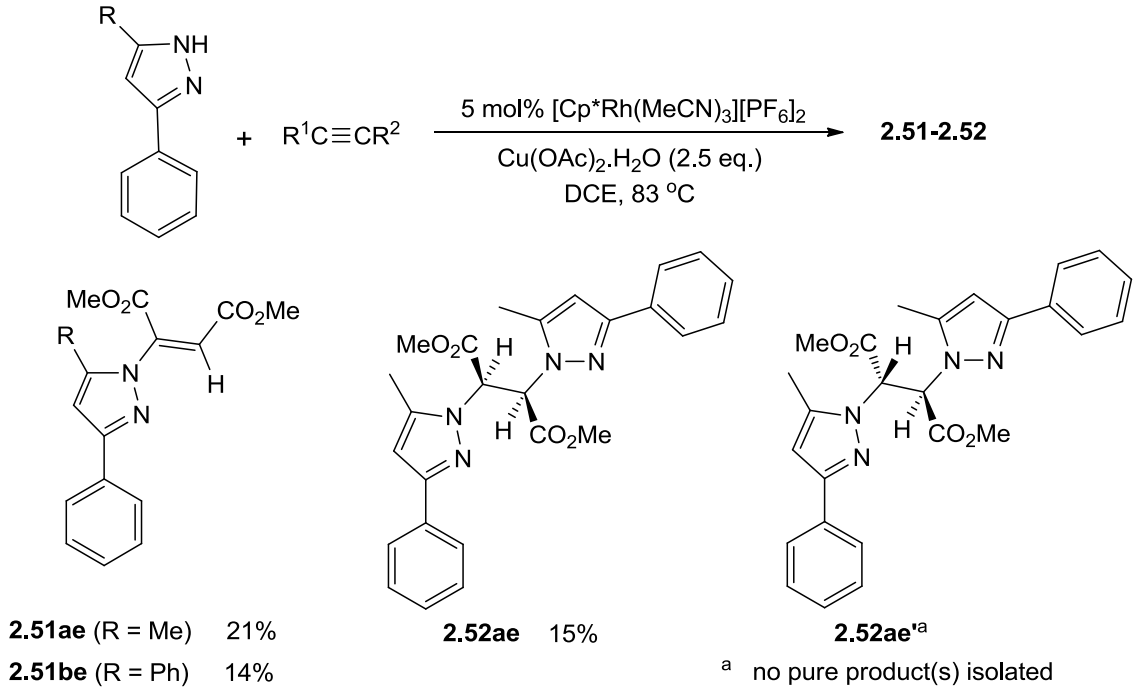

Scheme 2.38: C-H functionalisation of pyrazoles with DMAD (**e**).

As mentioned above, the crystal structure of **2.51ae** was used to determine the exact structure of the compound (**Fig 2.7**). It shows that the alkyne has attached to N(1) rather than N(2) and also shows the CO_2Me groups are on the same side of the now alkene. This therefore shows that the *E* isomer has formed rather than the *Z* isomer.

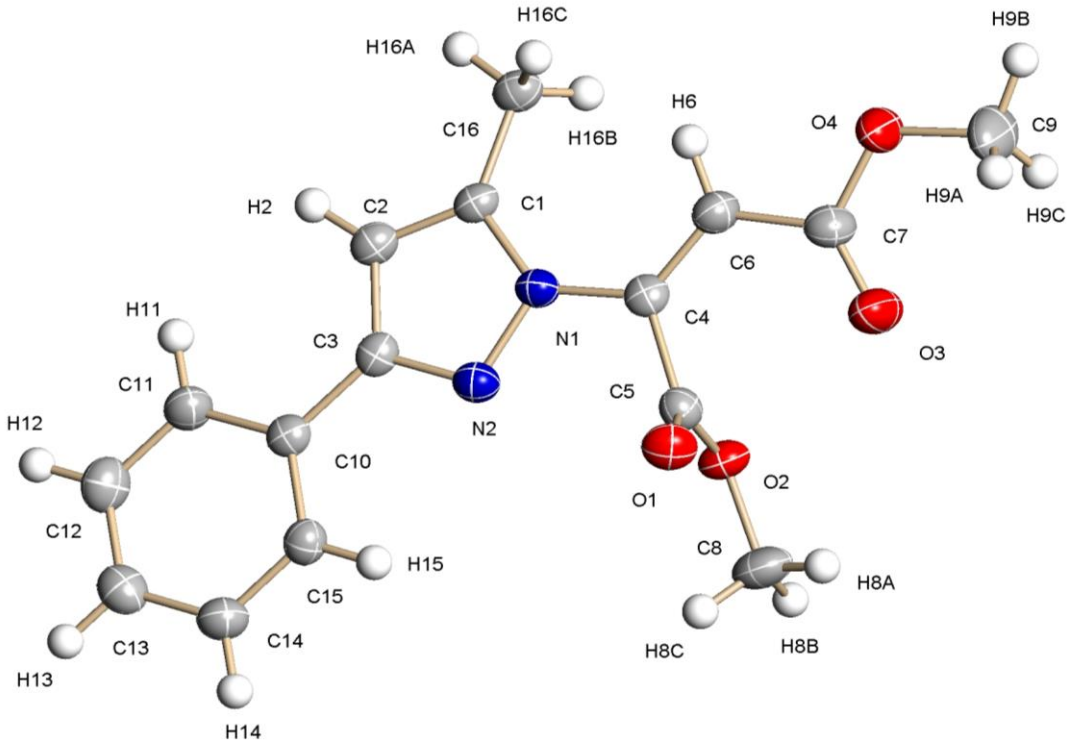

N(1)-C(4)	1.391(3)	C(4)-C(6)	1.335(3)
C(1)-N(1)-C(4)	131.8(2)	N(1)-C(4)-C(6)	125.6(2)
N(1)-C(4)-C(5)	113.1(2)	C(4)-C(6)-C(7)	122.3(2)

Fig. 2.7: Crystal structure of **2.51ae** with selected bond distances (Å) and angles (^{o}). Figures show 50% displacement ellipsoids.

On some occasions, a small amount of the dimeric product **2.52ae** was also observed. A crystal structure was obtained which helped to deduce its structure and help with assignment (see **Fig 2.8** below). As mentioned above, reaction of **2.43a** with DMAD led to a complicated mixture of products which made purification difficult. Fortunately, a crystal was obtained from a mixture which turned out to be the dimeric compound **2.52ae′** which is related to **2.52ae**. **Fig 2.8** shows the structures of both **2.52ae** and **2.52ae′**. Of these, **2.52ae** is a meso compound which contains an inversion centre and **2.52ae′** is a racemate which does not contain an inversion centre. For **2.52ae**, the

original alkyne bond C(2)—C(2A) is now a single bond (C-C = 1.54(7) Å). Similarly for **2.52ae′**, the original alkyne bond C(10)—C(11) is now a single bond (C-C = 1.52(4) Å). The structures show that DMAD attached to the nitrogen atoms furthest away from the phenyl rings for both products.

2.52ae **2.52ae′**

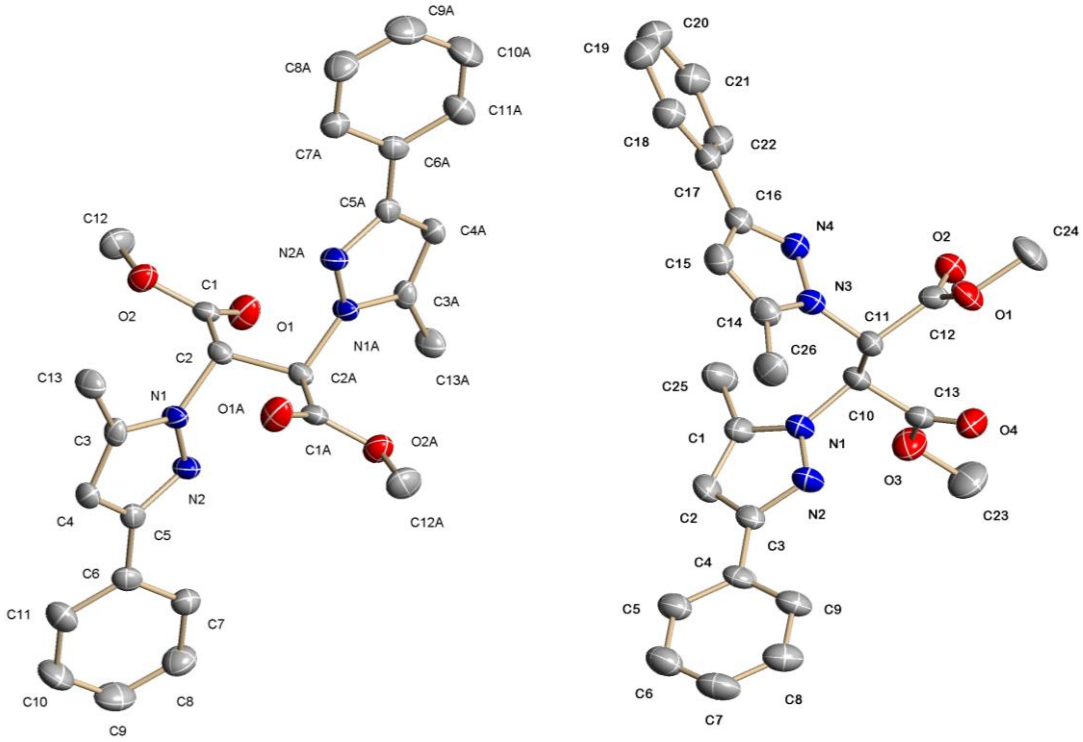

2.52ae	N(1)-C(2)	1.454(4)	C(2)-C(2A)	1.542(7)
	N(1)-C(2)-C(1)	108.2(3)	N(1)-C(2)-C(2A)	110.0(4)
2.52ae′	N(1)-C(10)	1.458(4)	C(10)-C(11)	1.523(4)
	N(3)-C(11)	1.458(4)	C(10)-C(13)	1.510(4)
	N(1)-C(10)-C(11)	109.5(2)	N(1)-C(10)-C(13)	108.6(3)
	N(3)-C(11)-C(10)	110.8(3)	N(3)-C(11)-C(12)	109.4(3)

Fig. 2.8: Crystal structures of **2.52ae** and **2.52ae′** with selected bond distances (Å) and angles (^{o}). The hydrogen atoms have been omitted from the diagram for clarity.

The ^{1}H NMR spectrum for **2.52ae** shows a 6H singlet at δ 3.57 assigned to two equivalent CO_2Me groups. There is a 6H methyl singlet at δ 2.57 for two equivalent pyrazole methyl groups and a 2H singlet at δ 6.37 for two equivalent pyrazole protons. Therefore the pyrazole and DMAD signals are in a 2:1 ratio with each other, suggesting

that one equivalent of DMAD (**e**) has reacted with two equivalents of **2.43a**. The pyrazole 2H singlet shows an NOE to the 6H pyrazole methyl singlet. Additionally there is a 2H singlet at δ 6.12 which shows an NOE to the CO_2Me signal so is assigned as the C*H*(CO_2Me) protons. Neither of the CO_2Me signals show any NOEs to any phenyl protons, consistent with the DMAD having attached to the nitrogen atoms furthest from the phenyl rings (as seen from the crystal structure in **Fig. 2.8**). The ^{13}C NMR spectrum shows 12 signals as expected. The ESIMS shows an ion at *m/z* 459 due to $[M+H]^+$ and HRMS (ES) is correct for the dimeric product, **2.52ae** (**Scheme 2.37**).

The reaction of **2.43a** with PhC≡C(CO_2Et) (**f**) had a very low conversion with mainly starting materials being recovered (**Scheme 2.39**). However, the reaction did give a mixture of the acrylate products (**2.51af**) and the pyrazoloisoquinoline products (**2.45af**) in trace amounts. Attempts to separate the regioisomers of **2.51af** and **2.45af** failed. The ^1H NMR spectrum of **2.51af** shows two singlets at δ 2.12 and δ 2.46 in a roughly 1.5:1 ratio, consistent with two pyrazole methyl signals from each isomer suggesting that the two isomers have formed in a roughly 1.5:1 ratio. There are also four singlets in the range δ 6.51-6.87, consistent with two pyrazole protons and two vinyl protons from each isomer. The pyrazole signals are accompanied by two triplets at δ 0.91 and δ 1.12 (both J = 7.0 Hz), and two quartets in the range δ 4.04-4.23 (both J = 7.0 Hz), consistent with ethyl groups from the alkyne. ESIMS shows an ion at *m/z* 333 due to $[M+H]^+$ and HRMS (ES) is correct for the acrylate product, **2.51af** (**Scheme 2.39**).

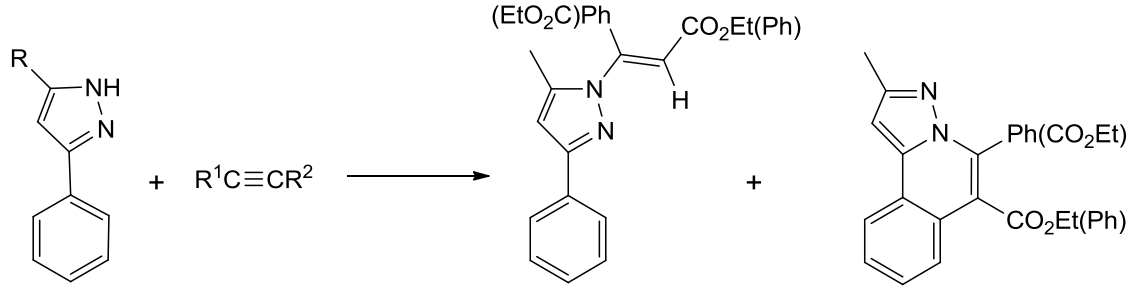

[a] no pure product(s) isolated **2.51af**[a] **2.45af** [a]

Reaction conditions: 5 mol% $[Cp^*Rh(MeCN)_3][PF_6]_2$, $Cu(OAc)_2.H_2O$ (2.5 eq.), DCE, 83 °C, 16 h

Scheme 2.39: C-H functionalisation of pyrazoles with alkyne **f**.

The ^{1}H NMR spectrum of **2.45af** shows two singlets at δ 2.37 and δ 2.39 in 3:1 ratio, consistent with two pyrazole methyl signals from each isomer, suggesting that the two isomers have formed in 3:1 ratio. Additionally, there are two singlets δ 6.31 and δ 6.34, consistent with two pyrazole protons from each isomer. The pyrazole signals are accompanied by two triplets at δ 0.87 and δ 1.07 (both J = 7.0 Hz), and two quartets at δ 3.76 and δ 3.95 (both J = 7.0 Hz), consistent with ethyl groups from the alkyne. The integrations from the signals of both major and minor products show the pyrazole and alkyne signals are in a 1:1 ratio, suggesting that one equivalent of **f** has reacted with one equivalent of **2.43a**. ESIMS shows an ion at *m/z* 331 due to $[M+H]^+$ and HRMS (ES) is correct for the product, **2.45af** (**Scheme 2.39**).

In the reactions with alkynes bearing electron-withdrawing groups (**e** and **f**), *N*-heterocycle products are disfavoured and instead maleates (**2.51ae** and **2.51be**) and acrylates (**2.51af**) are formed. Further studies on the reaction with **e**, including blank reactions without the use of Cp*Rh catalyst and $Cu(OAc)_2.H_2O$, and with added acid or base still gave the vinylic products. This suggests these products are formed by a Michael reaction and that no Rh catalysis takes place. DMAD (**e**) is known to be a good Michael acceptor. The poor conversion observed in the reaction with **f** can probably be explained by the fact it only contains one CO_2Et group and is therefore not as good a Michael acceptor as DMAD (**e**). Also the presence of the CO_2Me group may disfavour the catalysis reaction to give *N*-heterocycles of type **2.45**.

In conclusion, for all these reactions except those with alkynes **e** and **f**, only heterocyclic products are formed, and there is no trace of naphthalene-type products which were formed from *N*-phenyl pyrazole.[33] This outcome is therefore consistent with that shown in **Scheme 2.15**, i.e. N-H and C-H activation followed by alkyne insertion, C-N reductive coupling, and reoxidation of the catalyst.[52]

Experimental Mechanistic Studies

Stoichiometric cyclometallation of **2.43c** with $[Cp^*IrCl_2]_2$ has been reported by Ikariya *et al.* (**Scheme 2.40**).[59] Our attempts to cyclometallate **2.43a** with $[Cp^*RhCl_2]_2$ to form a similar product failed. In the case of **2.43c**, Ikariya *et al.* showed that the NH proton is retained in the form of the cyclometallated complex which can undergo further transformations by exposure to different conditions. In addition, it was shown that different bases and solvents cause full or partial dechlorination and NH-deprotonation which leads to the formation of various dimeric complexes (**Scheme 2.41**).

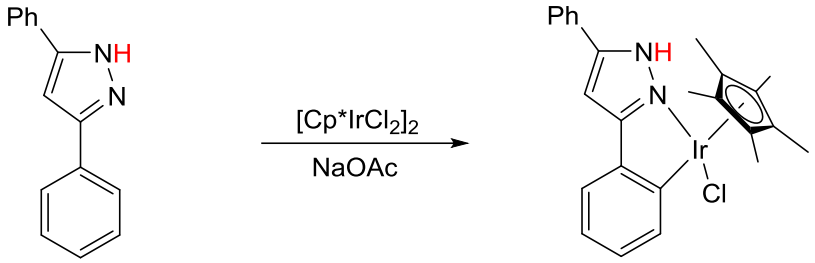

2.43c

Scheme 2.40: Stoichiometric cyclometallation of **2.43c** with $[Cp^*IrCl_2]_2$.[59]

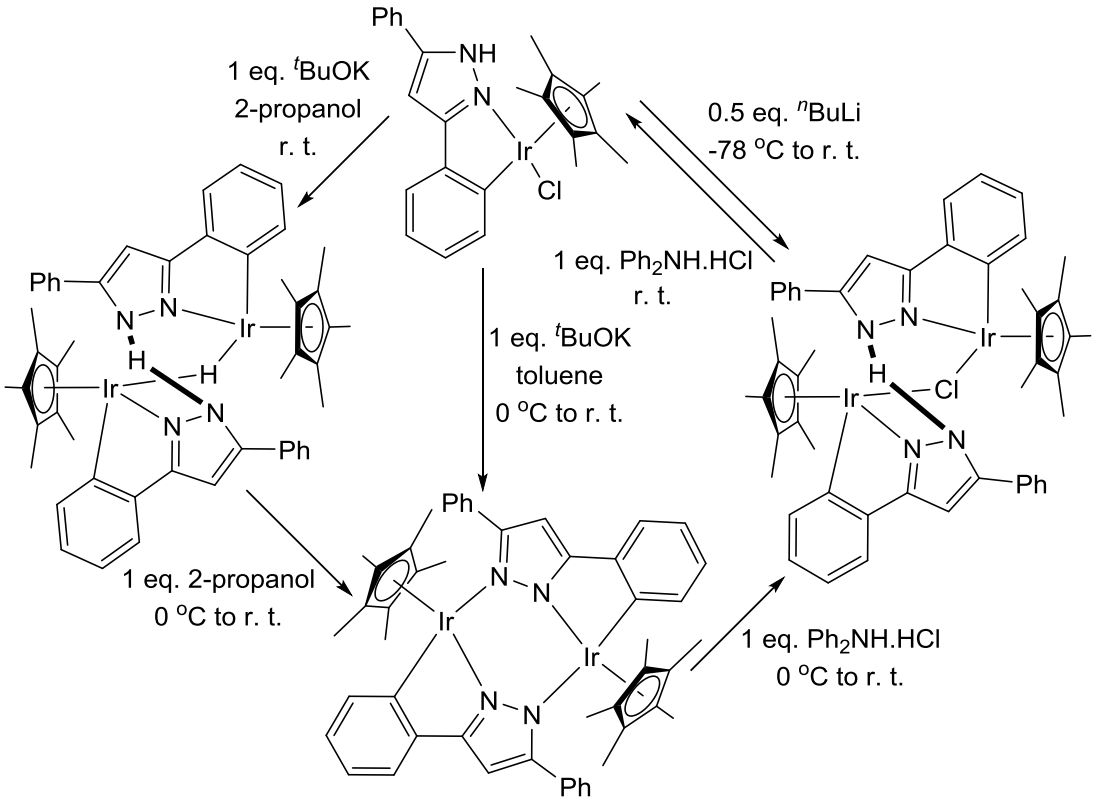

Scheme 2.41: Interconversion between different pyrazole complexes.[59]

Since isolation of possible intermediates failed, deuterium labelling experiments were used to probe the mechanism. Thus, the reversibility of the C-H activation step was assessed by treating substrate **2.43a** with $[Cp^*Rh(MeCN)_3][PF_6]_2$ (5 mol%) and NaOAc (2 equiv.) in d^4-methanol. This gave partially deuterated **2.43a** containing approximately 29% deuterium incorporation into each of the *ortho* positions after 16 h at 60 °C (**Scheme 2.42 A**). Surprisingly almost 50% deuterium exchange also occurred at the remaining pyrazole proton. Adding $Cu(OAc)_2.D_2O$ had little effect with similar deuteration being observed. As has been observed in similar cases previously[57] addition of d^1-pivalic acid increased the rate and extent of deuterium exchange. It is worth noting that to see deuterium incorporation into the ligand requires not only that N-H and C-H activation are reversible but also that exchange of free and bound pyrazole is facile under these conditions. If C-H activation is reversible but ligand exchange is not facile then only the bound ligand can undergo exchange (i.e. 5%, equivalent to the catalyst loading).

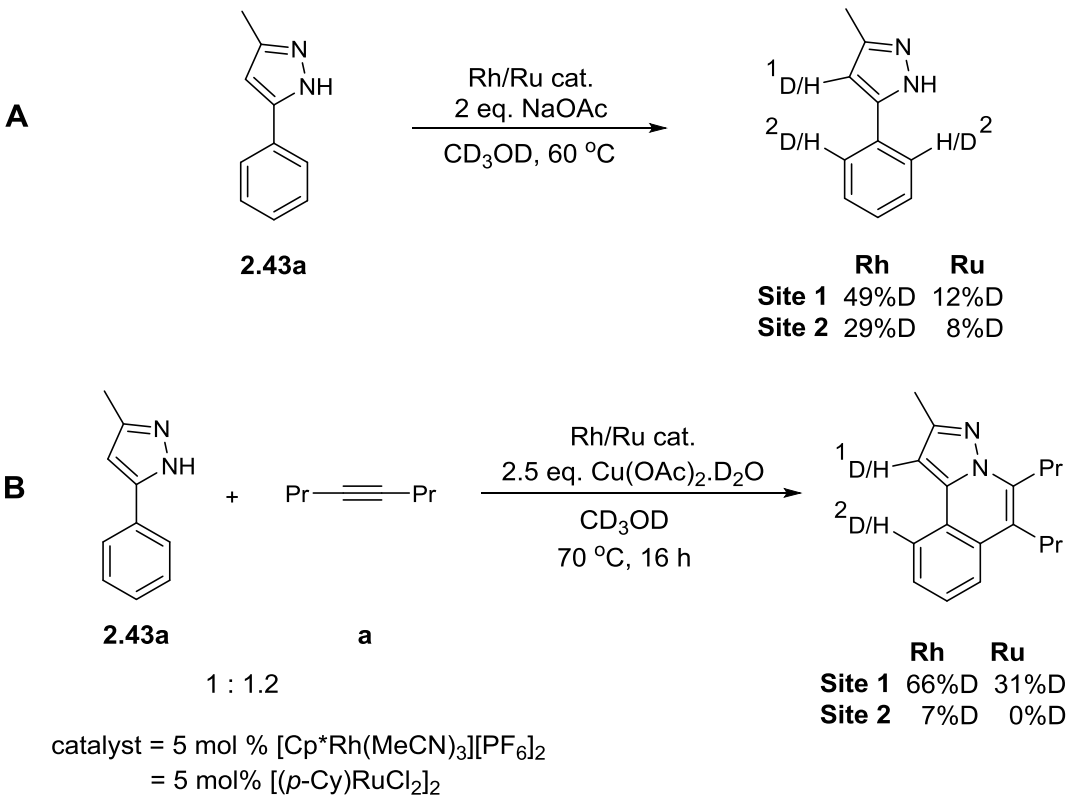

Scheme 2.42: Rh/Ru-catalysed deuteration of **2.43a** (**A**) and Rh/Ru-catalysed deuteration of **2.43a** in the presence of alkyne (**B**).

The deuteration experiment was repeated in the presence of a slight excess of alkyne and $Cu(OAc)_2.D_2O$, i.e. similar to the catalytic conditions, although using d^4-methanol as solvent in place of dichloroethane (**Scheme 2.42 B**). In this case at only low conversion (<10%) the product showed no deuterium incorporation by NMR spectroscopy suggesting that the cyclometallated intermediate is being intercepted by the alkyne rather than going back to starting material. However, if the reaction is allowed to go to completion there is deuterium incorporation in both positions, though considerably less at the *ortho* position (7%) compared to the pyrazole position (66%). Given that the alkyne is in slight excess (1.2 equiv), at high conversion the alkyne concentration is approximately 0.2 times that at the start hence at this stage the rate of H/D exchange in the *ortho* position (i.e. the reverse of C-H activation) is competitive with alkyne insertion. These observations suggest that the barriers to the forward (alkyne insertion) and reverse reactions (C-H activation) are similar in energy.

Similar deuteration experiments were carried out with ruthenium. In this case in the absence of alkyne there was significantly less deuterium incorporation, suggesting that C-H activation is less reversible for ruthenium. As for rhodium, exchange at the pyrazole position occurred as well as at the *ortho* positions of the phenyl. However, in the presence of alkyne with ruthenium even at high conversion there was only deuterium incorporation into the pyrazole position and no H/D exchange in the phenyl ring (**Site 2**).[26] This suggests that in this case alkyne insertion is significantly easier than the reverse of C-H activation (see below). Note the observation that deuterium exchange in the pyrazole position is less affected by the presence of alkyne than exchange in the phenyl positions; this is consistent with pyrazole exchange not occurring via a rollover mechanism. Note that in similar studies with nitrophenyl-substituted pyrazoles and ruthenium, Ackermann found that C-H activation was reversible and that deuterium exchange occurred even in the presence of diphenylacetylene suggesting that the relative barriers to C-H activation and alkyne insertion are substrate dependent.[53]

A possible mechanism for deuterium exchange in the pyrazole is "roll-over cyclometallation" (**Scheme 2.43**). Rollover cyclometallation of *N*-phenylpyrazole was implicated in results by Miura *et al.*.[33] However, BP86D calculations indicate that the double-cyclometallated species implicated in this pathway is too high in energy (G_{DCE} = 22.0 kcal/mol) ruling out this mechanism. It is possible that when the pyrazole is

coordinated this proton is much more acidic and so can undergo exchange without direct involvement of the rhodium.

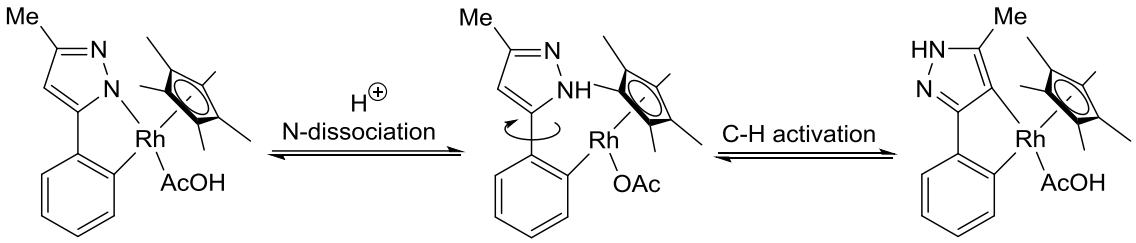

Scheme 2.43: Possible rollover cyclometallation.

A value for k_H/k_D for rhodium was measured from a Type A KIE experiment using d^3-**2.43a** and was determined to be 2.7 ± 0.5 (**Scheme 2.44**).[26] This suggests that C–H bond cleavage is likely involved in the rate determining step. To confirm this, the order of reaction with respect to alkyne was measured using initial rates and this showed near zero order in alkyne (0.07 ± 0.1), again consistent with C–H bond cleavage being rate limiting. Similar deuteration studies and a KIE were carried out for ruthenium. The k_H/k_D was determined to be 1.1 ± 0.2 which could be interpreted as indicating that C-H bond activation is not rate determining; this reaction is also zero order in alkyne (0.0 ± 0.1). Further interpretation of the KIE will be discussed in the computational section. (see below).

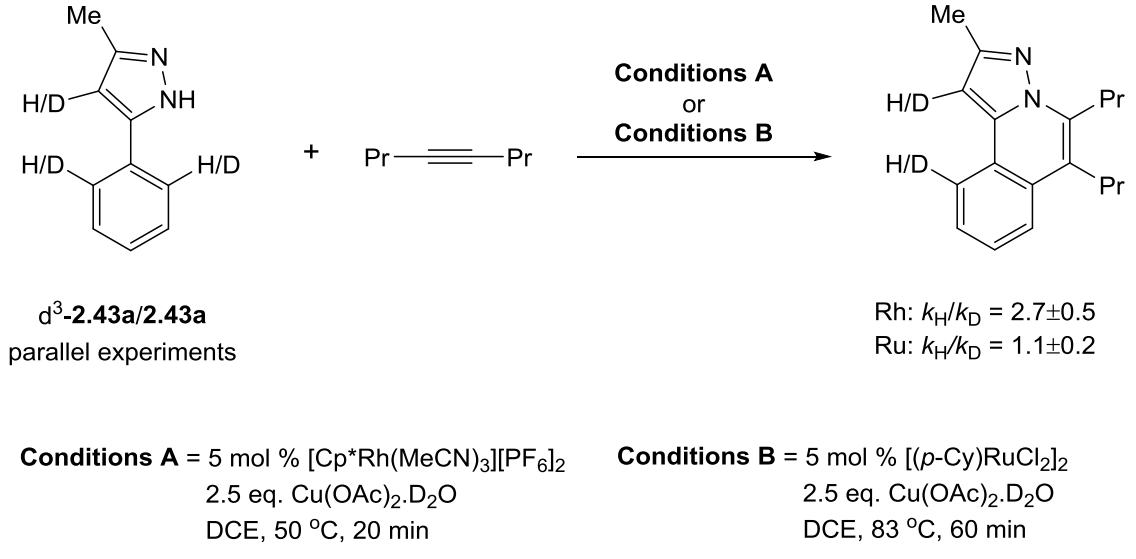

Scheme 2.44: Determination of KIE.

To probe the alkyl/aryl selectivity further, competition reactions were carried out in which **2.43a** or **2.43b** were each reacted with a mixture containing 5 equivalents each of the alkynes 4-octyne (**a**) and diphenylacetylene (**b**) (**Scheme 2.45**). These reactions gave mixtures of the expected products (**2.45aa**/**2.45ab** from **2.43a** and **2.45ba**/**2.45bb** from **2.43b**). The reaction with **2.43a** showed no selectivity giving a 1:1 ratio of **2.45aa** and **2.45ab**. **2.43b** gave a ratio of 1:0.7 showing a small preference for the product from 4-octyne (**2.44ba**), suggesting that this alkyne reacts slightly faster than diphenylacetylene. Similar results have also been reported with a nitrophenyl pyrazole and ruthenium catalyst.[53] A competition reaction between 4-octyne (**a**) and dimethylacetylene dicarboxylate (**e**) was also carried out using **2.43a**. In this case, the Michael reaction with **e** to form **2.51ae** was favoured and no **2.45aa** was observed.

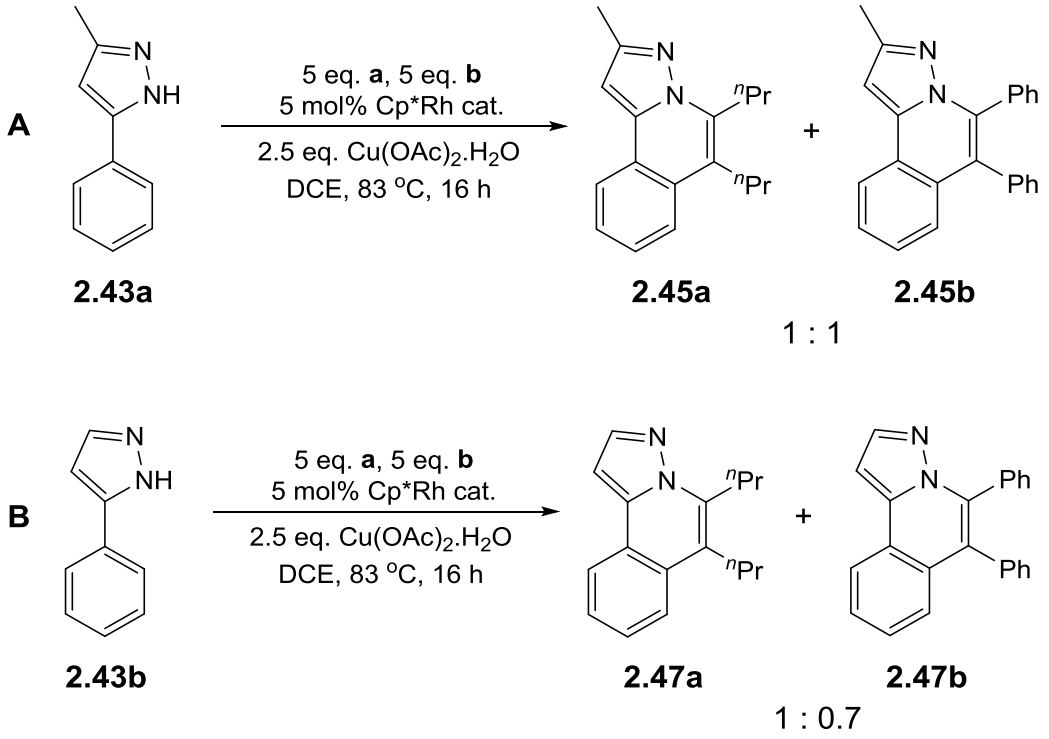

Scheme 2.45: Alkyne competition reactions with **2.43a** (**A**) and **2.43b** (**B**).

Computational Studies

DFT calculations have been performed by the group of Prof S. A. Macgregor to assess the mechanism of the coupling of alkynes with *C*-phenylpyrazoles using {Cp*Rh} and {(*p*-Cy)Ru} catalysts. The computed catalytic cycle starts with adduct **A**, where the pyrazole substrate, **2.43a**, is H-bonded to the pendant oxygen of the κ^1-acetate ligand in $Rh(OAc)_2(Cp^*)$ (**Fig. 2.9**). N-H activation in **A** proceeds in two steps, first formation of

the Rh–N^2 bond (with κ^2- κ^1 displacement of the second acetate ligand) to give **INT(A-B)**, followed by N^1-H^1 bond cleavage induced by acetate dissociation via elongation of the Rh-O^2 bond. This forms **B·HOAc** where acetic acid is H-bonded to N^1 and the spectator acetate has reverted to a κ^2-binding mode. Loss of HOAc then gives **B** which can undergo C-H activation via an agostic intermediate, **INT(B-C)**, formed via κ^2-κ^1 displacement of acetate by the approaching *ortho* C-H bond of **2.43a**. This allows for intramolecular H–bonding to acetate which promotes C-H bond cleavage via **TS(B-C)2**. Together, these two steps comprise AMLA C-H bond activation.[2d] The cyclometallated intermediate **C1** is initially formed from which a more stable form, **C2**, can be readily accessed via rotation about the Rh–O^4 bond. HOAc/alkyne exchange then forms **D** which undergoes migratory insertion (**D→E**) followed by C-N reductive coupling to give **F** where the pyrazoloisoquinoline product, **H**, is η^4-bound to the Rh centre. Experimentally, this last step was shown to occur in the absence of $Cu(OAc)_2.H_2O$ (see above) and so rules out any need for prior oxidation of the Rh. Release of the *N*-heterocyclic product completes the cycle with reoxidation of unspecified Rh^I species, **G**.

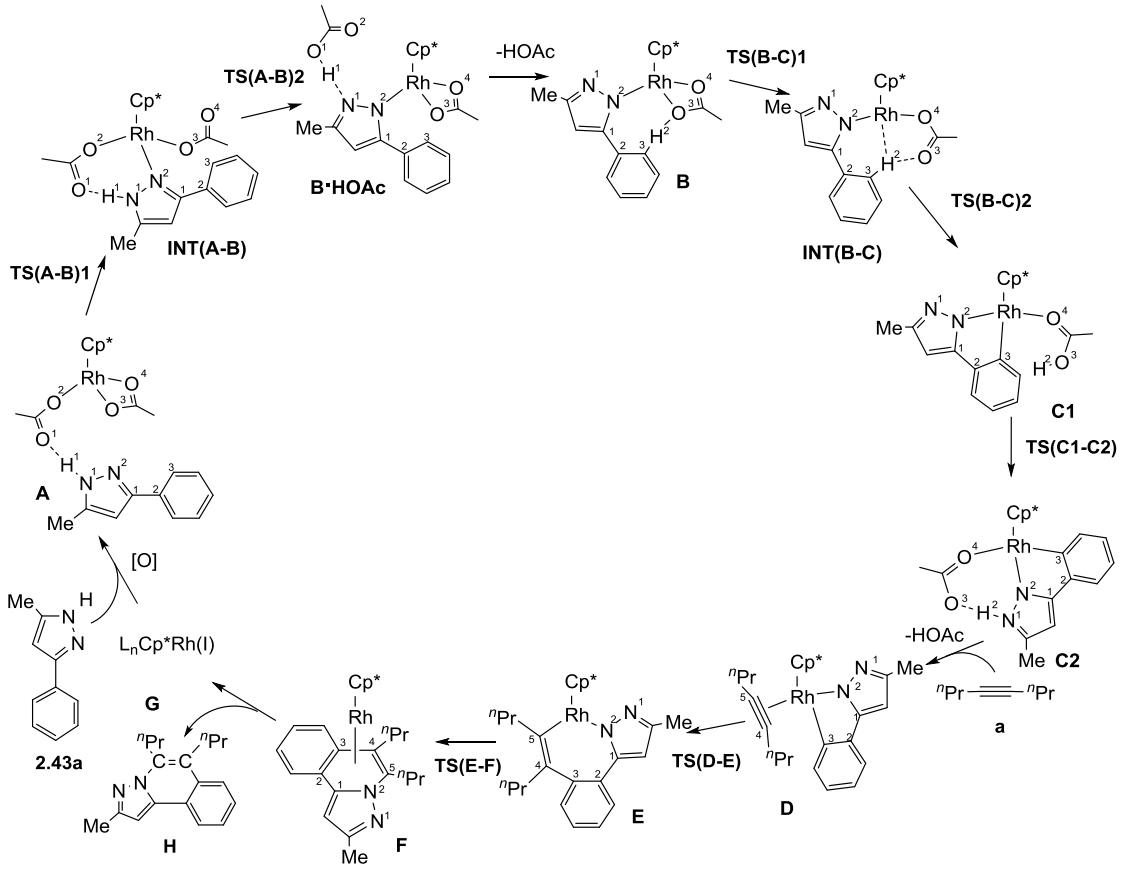

Fig. 2.9: Computed cycle for Cp*Rh-catalysed coupling of **a** with *C*-phenylpyrazoles.

The reaction profile was computed for the Rh-catalysed coupling of 4-octyne (**a**) with **2.43a** (**Fig. 2.10**). It shows that N-H activation is easy as it has a barrier of -7.0 kcal mol^{-1}. C-H activation follows with **TS(B–C)2** being the highest barrier (G_{DCE} = +14.8 kcal mol^{-1}). This leads to **D** which undergoes migratory insertion with a barrier of 14.0 kcal mol^{-1}. Finally, reductive elimination occurs with a barrier of +8.3 kcal mol^{-1}. It is important to note that **TS(D–E)** (G_{DCE} = +14.6 kcal mol^{-1}) is at a similar energy to the C-H activation high point (**TS(B–C)2**, G_{DCE} = +14.8 kcal mol^{-1}). This is consistent with reduced *ortho*-H/D exchange in the presence of alkyne as the two processes (reverse C-H activation and migratory insertion) are competing with each other.

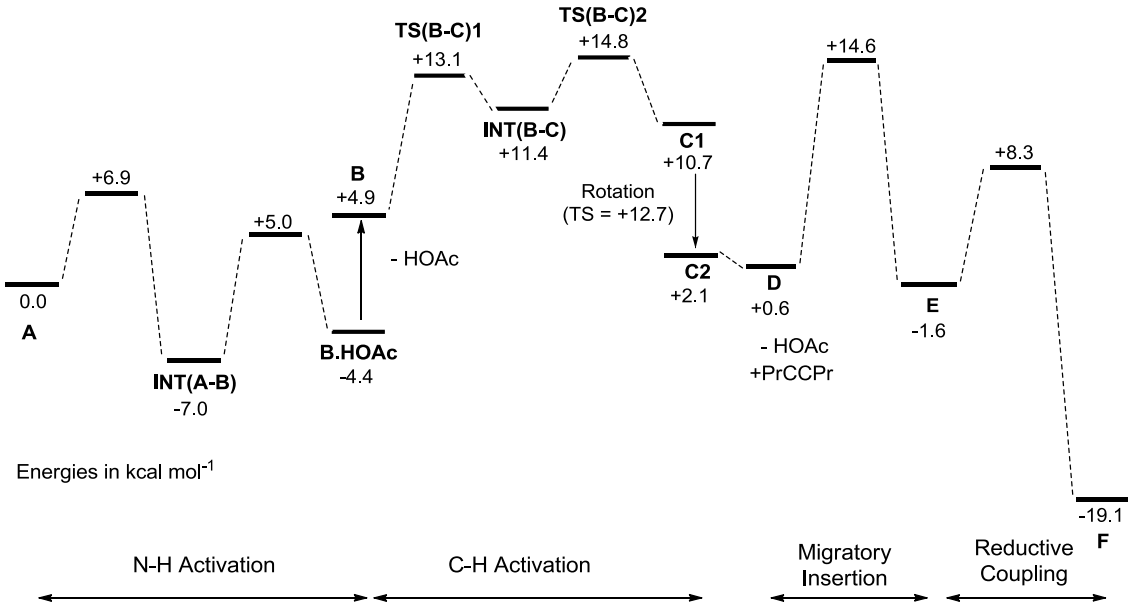

Fig. 2.10: Reaction profile for the Cp*Rh-catalysed coupling of 4-octyne with **2.43a**.

To interpret the observed k_H/k_D value of 2.7 ± 0.5 the geometries of the two transition states associated with the AMLA C-H bond activation process were computed (**Fig. 2.11**). **TS(B–C)1** corresponds to the initial κ^2-κ^1 displacement of acetate by the incoming substrate and, the C^3-H^2 bond shows little bond elongation (1.11 Å). In contrast, the transition state for C-H bond cleavage, **TS(B–C)2**, exhibits significant bond elongation ($C^3\cdots H^2$= 1.30 Å). In this case, as **TS(B–C)2** is higher in energy than **TS(B–C)1** it corresponds to the rate-determining transition state and the elongation of the C^3-H^2 bond leads to a computed k_H/k_D value of 5.48 for the forward reaction. This is consistent with the significant observed equilibrium k_H/k_D value.

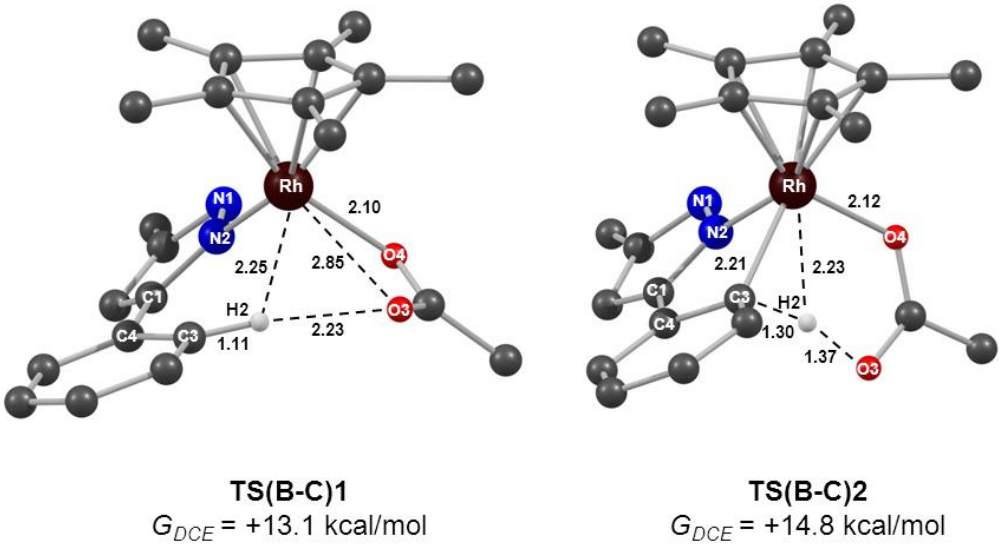

Fig. 2.11: Computed structures of the AMLA C-H bond activation transition states, **TS(B-C)1** and **TS(B-C)2**, with selected distances (Å) and relative free energies in solution (kcal mol^{-1}). Spectator hydrogen atoms are omitted for clarity.

Reaction profiles have also been computed for the coupling of diphenylacetylene (**b**) and MeC≡CPh (**c**) with **2.43a** at $Rh(OAc)_2Cp^*$. These give very similar profiles in each case. With MeC≡CPh (**c**), **TS(D–E)** is 2.4 kcal mol^{-1} more stable when migratory insertion proceeds with the phenyl group adjacent to the metal, and so correctly models the regioselectivity observed experimentally. A similar preference of 1.9 kcal mol^{-1} is also computed with the BP86 functional alone which indicates that dispersion effects and hence steric effects, are not important in determining the regioselectivity. Instead electronic effects are important. Similar regioselectivity has been observed for alkyne insertion into 5-membered phosphanickelacycles.[60-62] In that case, DFT calculations linked this preference to the asymmetric distribution of the frontier molecular orbitals of MeC≡CPh, where both the π-bonding HOMO and π-antibonding LUMO have a greater contribution on the Me-substituted carbon. Both of these orbitals participate in C-C bond formation in the migratory insertion transition state, therefore this structure is stabilised when the C(Me) centre is involved in this process, i.e. when the Ph-substituent carbon is adjacent to the metal, as is the preference seen experimentally.

DFT calculations were also carried out for $Ru(OAc)_2$(*p*-Cy). The reaction profile computed for the coupling of **2.43a** with 4-octyne (**a**) at $Ru(OAc)_2$(*p*-Cy) is shown in **Fig. 2.12**. Experimentally the (*p*-Cy)Ru system is characterised by slower H/D exchange in the absence of alkyne and this is reflected in the computed barriers to both the forward C-H activation (25.9 kcal mol^{-1}) and the reverse process (17.1 kcal mol^{-1}), respectively 4.1 kcal mol^{-1} and 4.8 kcal mol^{-1} higher than for the Cp*Rh system. The major difference is the higher energy of **TS(B-C)1** (G_{DCE} = +17.3 kcal mol^{-1}). This corresponds to the κ^2- κ^1 acetate dissociation step and presumably reflects stronger Ru-OAc bonding in this case. Similarly the energies of **TS(A-B)1** and **TS(A-B)2** are both about 4 kcal mol^{-1} higher than their Cp*Rh counterparts and both involve cleavage of an M-O bond. Once the agostic/H-bonded AMLA intermediate **INT(B–C)** is formed the subsequent C-H bond cleavage is barrierless.

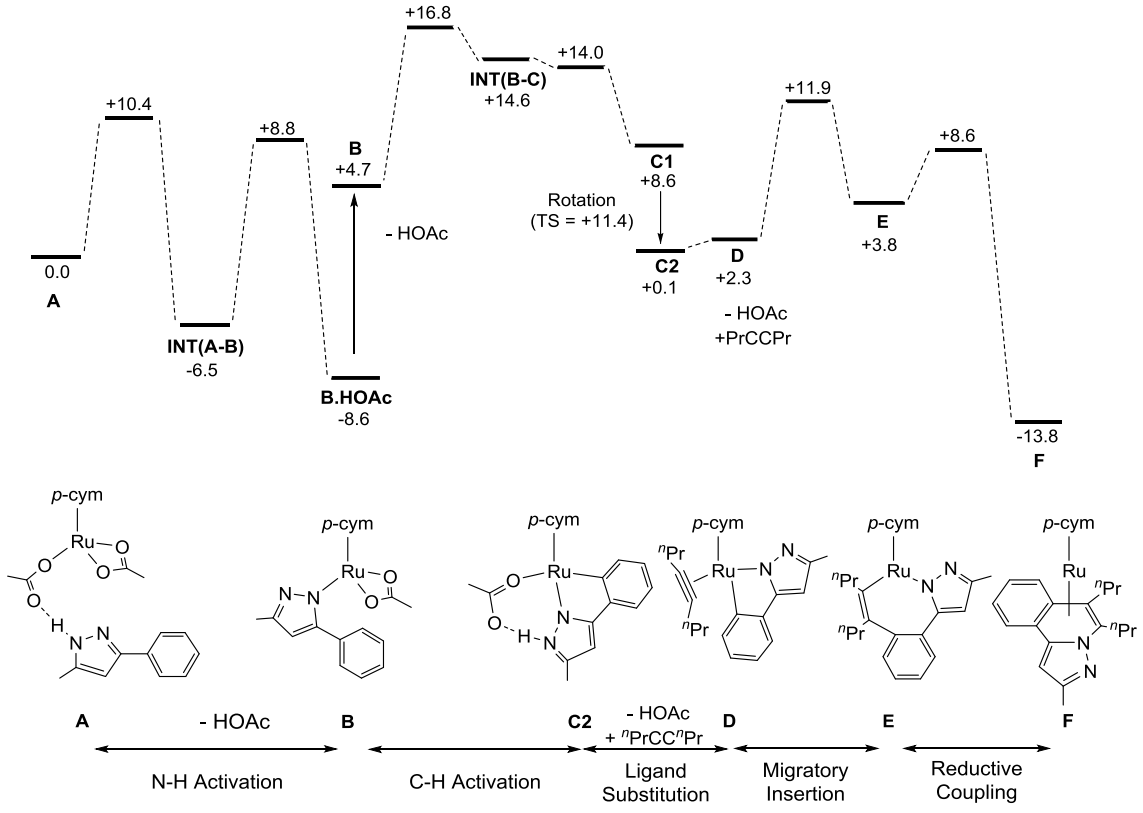

Fig. 2.12: Reaction profile for coupling of **2.43a** with 4-octyne (**a**) at $Ru(OAc)_2$(*p*-Cy).

The migratory insertion has a lower barrier than at Cp*Rh (9.6 kcal mol^{-1} vs 14.0 kcal mol^{-1}) and this, along with the facile reductive coupling means that the C-H activation process is still the rate-limiting process in the Ru catalysis. The overall barrier for the coupling process is 25.4 kcal mol^{-1}, 4.0 kcal mol^{-1} higher than for $Rh(OAc)_2Cp^*$ which

is consistent with the harsher conditions required experimentally. The geometry of the rate-determining transition state, **TS(B-C)1**, is very similar to that computed at Cp*Rh in **Fig. 2.11** and so features minimal C-H bond elongation. Thus, despite the fact that the AMLA C-H bond activation process is rate-limiting, it does not follow that a significant k_H/k_D should be expected and indeed the experimentally determined value is only 1.1 ± 0.2 and the computed value is 1.23.

As mentioned earlier, **2.48ac** is formed in the reaction of **2.43a** with MeC≡CPh (**c**) as a significant side product. An analogous side product, **2.46** is also seen with 4-octyne (**a**), particularly when catalytic $Cu(OAc)_2.H_2O$ was employed. This implies that side product formation is enhanced when re-oxidation of the Rh^I species based on **F** is slow and hence that reorganisation of **F** may be linked to side product formation. One such possible rearrangement is shown in **Scheme 2.46.** Slippage of the η^4-bound species $\mathbf{F_{MePh}}$ to an η^2-bound species $\mathbf{F2_{MePh}}$ is accompanied by formation of an agostic interaction with one C^6-H bond. This readily undergoes β-H transfer to give a hydrido allyl intermediate $\mathbf{F3_{MePh}}$. Oxidation of $\mathbf{F3_{MePh}}$ can induce C-H reductive elimination, either with reformation of the C^6-H bond (to give **2.45ac**) or with C^5-H bond formation (to give **2.48ac**).

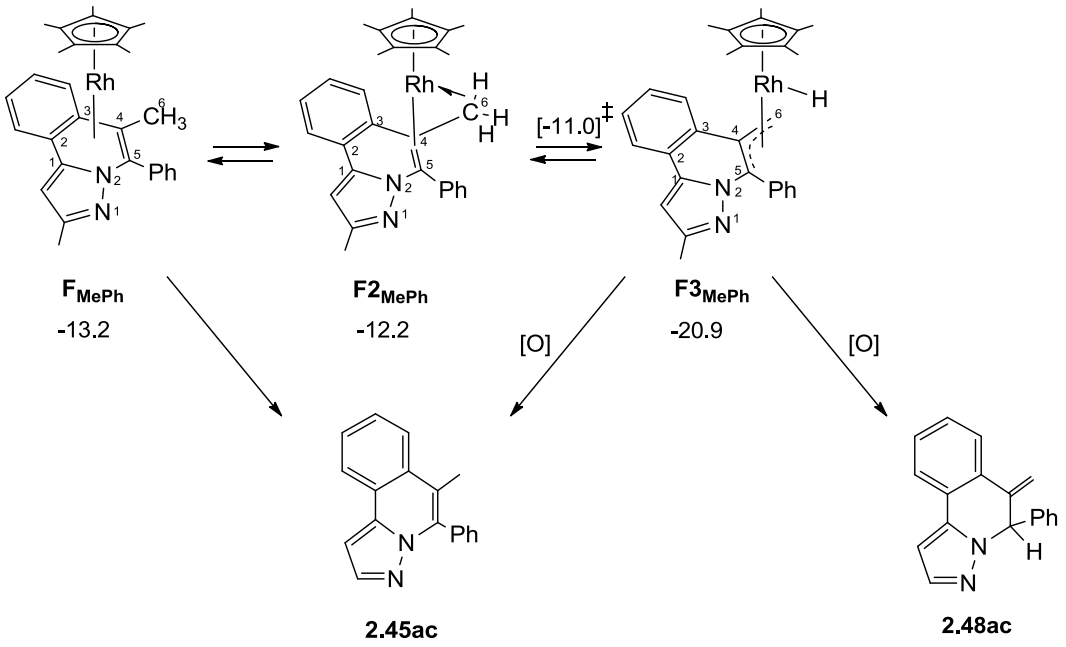

Scheme 2.46: Possible mechanism of formation of isomerised product **2.48ac**. Energies are delta G.

2.10 Conclusions

The Rh- and Ru-catalysed formation of a range of pyrazoloisoquinolines has been demonstrated using a C-H functionalisation strategy based on the coupling of 3-phenylpyrazoles with aryl and alkyl alkynes. Vinyl phenylpyrazoles are obtained as minor products in reactions with pyrazoles containing an electron-withdrawing substituent. Also, reactions with alkynes that contain electron-withdrawing groups lead to the formation of maleates or acrylates as products due to a Michael reaction taking place. In the rhodium catalysis, $[Cp^*Rh(MeCN)_3][PF_6]_2$ is shown to be a more effective catalyst precursor than $[Cp^*RhCl_2]_2$ with efficient catalysis achieved at 83 ^oC, while catalysis with $[(p\text{-}Cy)RuCl_2]_2$ requires higher temperatures. The reactions can be carried out for both metals using catalytic rather than stoichiometric copper as the reoxidant. Deuteration and competition experiments on the rhodium catalysis show that C-H activation is reversible and rate limiting, but that the subsequent reaction with alkynes can be competitive with this process. For ruthenium C-H bond activation is much less reversible and in the presence of alkyne is essentially irreversible. Alkyne competition reactions show there is very little preference between dialkyl and diaryl alkynes, with dialkyl only being favoured slightly in one case.

DFT calculations on both Rh and Ru catalysis indicate a mechanism involving sequential N-H and AMLA-6 C-H bond activation, HOAc/alkyne exchange, migratory insertion and C-N reductive coupling. A significantly higher overall barrier to catalysis is computed for ruthenium, in which the rate-limiting process also corresponds to C-H activation. This is consistent with the harsher reaction conditions used experimentally and reflects the need to dissociate a stronger Ru–O bond in order to generate a κ^1-acetate ligand that is that is needed for AMLA C-H bond cleavage.

The DFT calculations correctly reproduce the close competition between C-H bond activation and alkyne migratory insertion seen in the Rh system, as well as identifying C-H bond activation as being rate limiting for Ru. The calculations show that the observed deuterium isotope effects (Rh: k_H/k_D = 2.7 ± 0.5; Ru: 1.1 ± 0.2) can both be consistent with rate-limiting C-H activation due to the two-step (acetate dissociation and C-H bond cleavage) nature of the AMLA mechanism. For Rh the higher lying transition state corresponds to C-H bond cleavage with significant bond elongation. However, for Ru the highest lying transition state involves the κ^2-κ^1 displacement of acetate which

occurs without any significant lengthening of the C-H bond. Thus for AMLA C-H activation reactions the non-observation of a significant kinetic isotope effect does not provide sufficient grounds to rule out C-H bond activation as the rate determining step.

2.11 Experimental

General

The electrospray (ESI) mass spectra were recorded using a micromass Quattra LC mass spectrometer with acetonitrile or methanol as the matrix. FAB mass spectra (including high resolution) were recorded on Kratos Concept spectrometer with NBA as the matrix. The infrared spectra were recorded in the solid state with Universal ATR sampling accessories on a Perkin Elmer Spectrum One FTIR instrument. NMR spectra were recorded on a Bruker DRX400 spectrometer operating at 400.13 (^{1}H), 376.50 (^{19}F) and 100.61 MHz (^{13}C) or a Bruker DRX500 spectrometer at 500 (^{1}H) and 125 MHz (^{13}C) at ambient temperature; chemical shifts (ppm) are referred to the residual protic solvent peaks and coupling constants are expressed in Hertz (Hz). Assignments of ^{1}H NMR and ^{13}C NMR signals were made where possible, using DEPT or APT experiments. Quaternary carbon NMR chemical shifts will usually be given without assignment. Elemental analyses were performed at the Science Technical Support Unit, London Metropolitan University. The reagents 4-octyne, diphenylacetylene, 1-phenyl-3-propyne, methyl acrylate, styrene, methyl vinyl ketone and crotonaldehyde were purchased from Aldrich Chemical Co. and used without further purification. Copper(II) acetate monohydrate was purchased from Alfa Aesar and used without further purification. Dimethyl acetylenedicarboxylate was purchased from Lancaster and distilled prior to use. $[Cp^*Rh(MeCN)_3][PF_6]_2$,[63] 3-phenyl-1*H*-pyrazole,[64] 3-phenyl-5-methyl-1*H*-pyrazole,[65] 3,5-diphenyl-1*H*-pyrazole,[65] 3-phenyl-5-(trifluoromethyl)-1H-pyrazole,[66] 3-(thiophen-2-yl)-5-(trifluoromethyl)-1H-pyrazole[66] and (4-nitrophenyl)but-3-yn-1-ol[67] were prepared using literature procedures.

General procedure for catalysis reactions with Rh

$[Cp^*Rh(MeCN)_3][PF_6]_2$ (33 mg, 5 mol%), the appropriate directing ligand (1 eq.), $Cu(OAc)_2.H_2O$ (2.5 eq.), appropriate alkyne (1.2 eq.) and DCE (10 ml) were added to a Schlenk flask. The Schlenk flask was sealed with a screw-cap and then transferred to a preheated oil bath and stirred at 83 °C for 16 hours. The reaction mixture was cooled to

room temperature with continuous stirring and diluted with Et_2O (10 ml).The mixture was transferred to separating funnel and ammonium hydroxide solution (10 ml, 2M) was added. The aqueous layer was extracted with Et_2O (3 x 10 ml) and the organic layers were combined and dried over $MgSO_4$. The drying agent was removed by filtration and solvent was removed under reduced pressure.

General procedure for catalysis reactions with Ru

[(*p*-Cy)$RuCl_2$]$_2$ (31 mg, 5 mol%), the appropriate directing ligand (1 eq.), $Cu(OAc)_2.H_2O$ (2.5 eq.), appropriate alkyne (1.2 eq.) and *t*-AmOH (3 ml) were added to a Schlenk flask. The Schlenk flask was sealed with a screw-cap and then transferred to a preheated oil bath and stirred at 120 °C for 16 hours. The reaction mixture was cooled to room temperature with continuous stirring and diluted with Et_2O (10 ml).The mixture was transferred to separating funnel and ammonium hydroxide solution (10 ml, 2M) was added. The aqueous layer was extracted with Et_2O (3 x 10 ml) and the organic layers were combined and dried over $MgSO_4$. The drying agent was removed by filtration and solvent was removed under reduced pressure.

Reaction of 2.43a with 4-octyne (a)

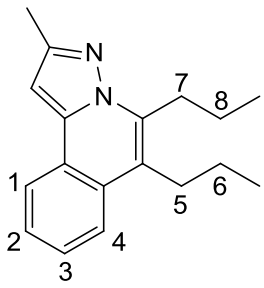

Following the general procedure, a Schlenk flask was loaded with [Cp*Rh(MeCN)$_3$][PF_6]$_2$ (22 mg, 5 mol%), 3-phenyl-5-methyl-1*H*-pyrazole (**2.43a**, 108 mg, 0.68 mmol), $Cu(OAc)_2.H_2O$ (341 mg, 1.71 mmol), 4-octyne (**a**, 90 mg, 0.43 mmol) and DCE (10 ml). The product was purified by column chromatography eluting with 70% dichloromethane in hexane to give **2.45aa** as a white solid (108 mg, 60%, 0.41 mmol). Mp: 62-64 °C. **2.45aa** was also obtained with [(*p*-Cy)$RuCl_2$]$_2$ as catalyst (173 mg, 65%, 0.65 mmol). ^{1}H NMR (400 MHz, $CDCl_3$): δ 1.08 (t, *J* = 7.4 Hz, 6H, CH_2CH_2*Me*), 1.63-1.72 (m, 2H, H^6), 1.77-1.87 (m, 2H, H^8), 2.52 (s, 3H, *Me*), 2.88-2.92 (m, 2H, H^5), 3.22-3.26 (m, 2H, H^7), 6.74 (s, 1H, *Pz-H*), 7.44 (td, *J* = 1.2, 7.8, 8.2 Hz, 1H, H^2), 7.50 (td, *J* = 1.6, 7.0, 8.2 Hz, 1H, H^3), 7.79 (brd, *J* = 8.6 Hz, 1H, H^4), 8.01 (dd, *J* = 1.2, 7.8 Hz, 1H, H^1), ^{13}C {^{1}H} NMR (100 MHz, $CDCl_3$): δ 14.2 (CH_2CH_2*Me*), 14.3 (CH_2CH_2*Me*), 14.4 (*Me*), 21.3 (C^8), 23.8 (C^6), 29.6 (C^5), 29.9 (C^7), 96.7 (Pz), 117.8, 123.5, 123.8 (C^4), 123.9 (C^1), 125.9 (C^2/C^3), 127.3 (C^2/C^3),

129.0, 136.7, 138.6, 149.4. ESIMS: *m/z* 267 $[M+H]^+$. HRMS (ESI): Calcd for $C_{18}H_{23}N_2$ $[M+H]^+$ 267.1861, found 267.1857.

Reaction of 2.43a with 4-octyne (a) with catalytic copper

A Schlenk flask was loaded with $[Cp^*Rh(MeCN)_3][PF_6]_2$ (22 mg, 5 mol%), 3-phenyl-5-methyl-1*H*-pyrazole (**2.43a**, 108 mg, 0.68 mmol), $Cu(OAc)_2.H_2O$ (10 mg, 10 mol%, 0.05 mmol), 4-octyne (**a**, 90 mg, 0.43 mmol) and DCE (10 ml). The crude ^1H NMR spectrum showed the presence of two products in a 3:1 ratio. The products were purified by column chromatography eluting from 100% dichloromethane to 10 % ethyl acetate in dichloromethane to give **2.45aa** (133 mg, 50%, 0.50 mmol) and **2.46aa** as yellow oil (65 mg, 24%, 0.24 mmol).

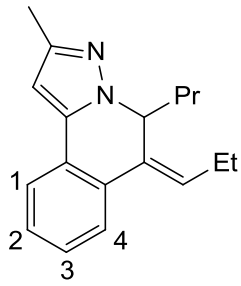

2.46aa: ^1H NMR (400 MHz, $CDCl_3$): δ 0.82 (t, *J* = 7.4 Hz, 3H, CH_2CH_2*Me*), 1.10 (t, *J* = 7.4 Hz, 3H, CH_2*Me*), 1.23-1.31 (m, 2H, CH_2CH_2Me), 1.51-1.61 (m, 1H, C*H*$_2$$CH_2$Me), 1.67-1.76 (m, 1H, C*H*$_2$$CH_2$Me), 2.23 (sex, *J* = 7.4 Hz, 1H, C*H*$_2$Me), 2.32 (s, 3H, *Me*), 2.38 (sex, *J* = 7.4 Hz, 1H, C*H*$_2$Me), 5.34 (dd, *J* = 5.9, 7.8 Hz, 1H, N-C*H*), 6.02 (t, *J* = 7.4 Hz, 1H, C=C*H*), 6.29 (s, 1H, *Pz-H*), 7.23-7.30 (m, 2H, H^2, H^3), 7.46-7.49 (m, 1H, H^1), 7.51-7.54 (m, 1H, H^4), ^{13}C {^1H} NMR (125 MHz, $CDCl_3$): δ 13.7 (CH_2CH_2*Me*), 14.0 (CH_2*Me*), 14.0 (*Me*), 18.7 (CH_2*C*H_2Me), 21.2 (*C*H_2Me), 38.8 (*C*H_2CH_2Me), 57.9 (N-*C*H), 99.7 (Pz), 123.5 (C^1), 125.0 (C^4), 125.2, 127.8 (C^2/C^3), 128.2 (C^2/C^3), 131.9, 132.6, 132.7 (C=*C*H), 138.0, 148.3. ESIMS: *m/z* 267 $[M+H]^+$. HRMS (ESI): Calcd for $C_{18}H_{23}N_2$ $[M+H]^+$ 267.1861, found 267.1849.

Reaction of 2.43b with 4-octyne (a)

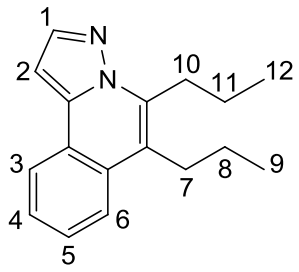

Following the general procedure, a Schlenk flask was loaded with $[Cp^*Rh(MeCN)_3][PF_6]_2$ (33 mg, 5 mol%), 3-phenyl-1*H*-pyrazole (**2.43b**, 144 mg, 1 mmol), $Cu(OAc)_2.H_2O$ (500 mg, 2.5 mmol), 4-octyne (**a**, 132 mg, 1.2 mmol) and DCE (10 ml). The product was purified by column chromatography eluting with 50% ethyl acetate in hexane to give **2.45ba** as a white solid (219 mg, 87%, 0.87 mmol). ^1H NMR (400 MHz, $CDCl_3$): δ 1.11 (t, *J* = 7.0, 7.4 Hz, 6H, H^9, H^{12}), 1.70 (sex, *J* = 7.0, 7.8 Hz, 2H, H^8), 1.83 (sex, *J* = 7.4, 8.2 Hz, 2H, H^{11}), 2.93-2.97 (m, 2H, H^7), 3.26-3.30 (m, 2H, H^{10}), 6.99 (d, *J* = 2.3 Hz, 1H, H^2), 7.50

(td, J = 1.6, 7.8 Hz, 1H, H^4), 7.55 (td, J = 1.2, 8.2 Hz, 1H, H^5), 7.84 (br dd, J = 0.8, 8.2 Hz, 1H, H^6), 7.95 (d, J = 2.3 Hz, 1H, H^1), 8.11 (dd, J = 1.6, 7.8 Hz, 1H, H^3), ^{13}C {^{1}H} NMR (100 MHz, $CDCl_3$): δ 14.4 (C^9), 14.5 (C^{12}), 21.3 (C^{11}), 23.8 (C^8), 29.7 (C^7), 30.1 (C^{10}), 97.1 (C^2), 119.1, 123.9, 124.0 (C^3, C^6), 126.3 (C^5), 127.6 (C^4), 129.0, 136.8, 137.8, 139.9 (C^1). ESIMS: *m/z* 253 $[M+H]^+$. HRMS (ESI): Calcd for $C_{17}H_{21}N_2$ $[M+H]^+$ 253.1705, found 253.1705.

Reaction of 2.43c with 4-octyne (a)

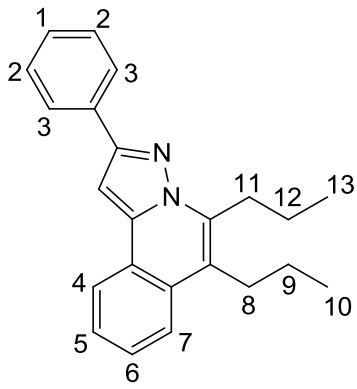

Following the general procedure, a Schlenk flask was loaded with $[Cp^*Rh(MeCN)_3][PF_6]_2$ (33 mg, 5 mol%), 3,5-diphenyl-1*H*-pyrazole (**2.43c**, 220 mg, 1 mmol), $Cu(OAc)_2.H_2O$ (500 mg, 2.5 mmol), 4-octyne (**a**, 132 mg, 1.2 mmol) and DCE (10 ml). The product was purified by column chromatography eluting from 40% dichloromethane in petroleum spirit (40-60 °C) to give **2.45ca** as a white solid (298 mg, 91%, 0.91 mmol). Mp: 85-87 °C. ^{1}H NMR (300 MHz, $CDCl_3$): δ 1.11 (t, J = 5.6, 7.3 Hz, 3H, H^{10}), 1.14 (t, J = 5.6, 7.3 Hz, 3H, H^{13}), 1.65-1.78 (m, 2H, H^9), 1.83-1.96 (m, 2H, H^{12}), 2.93-2.98 (m, 2H, H^8), 3.31-3.36 (m, 2H, H^{11}), 7.28 (s, 2H, *Pz-H*), 7.35 (tt, J = 1.2, 7.4, 8.6 Hz, 1H, H^1), 7.46 (tt, J = 1.2, 7.4 Hz, 2H, H^2), 7.50 (td, J = 1.6, 7.4, 8.6 Hz, 1H, H^6), 7.55 (br td, J = 1.6, 7.0, 8.6 Hz, 1H, H^5), 7.84 (dd, J = 1.6, 7.4 Hz, 1H, H^7), 8.06 (dd, J = 1.2, 8.2 Hz, 2H, H^3), 8.13 (dd, J = 2.0, 7.0 Hz, 1H, H^4), ^{13}C {^{1}H} NMR (100 MHz, $CDCl_3$): δ 14.5 (C^{10}, C^{13}), 21.3 (C^{12}), 23.8 (C^9), 29.8 (C^8), 30.0 (C^{11}), 94.1 (Pz), 119.0, 123.8, 123.9 (C^4), 124.0 (C^7), 126.2, 126.3 (C^3), 127.6 (C^5), 127.9 (C^6), 128.7 (C^2), 129.1 (C^1), 133.9, 137.0, 139.0, 151.3. ESIMS: *m/z* 329 $[M+H]^+$. FAB MS: *m/z* 329 $[M+H]^+$, 299 $[M-2(Me)]^+$, 271 $[M-2(Me)-2(CH_2)]^+$. HRMS (ESI): Calcd for $C_{23}H_{25}N_2$ $[M+H]^+$ 329.2018, found 329.2012.

Reaction of 2.43d with 4-octyne (a)

Following the general procedure, a Schlenk flask was loaded with $[Cp^*Rh(MeCN)_3][PF_6]_2$ (33 mg, 5 mol%), 3-phenyl-5-(trifluoromethyl)-1H-pyrazole (**2.43d**, 212 mg, 1.0 mmol), $Cu(OAc)_2.H_2O$ (500 mg, 2.5 mmol), 4-octyne (**a**, 110 mg, 1.2 mmol) and DCE (10 ml). The crude ^{1}H NMR spectrum showed the presence of two

products in a 17:1 ratio. The products were purified by column chromatography eluting from 50% dichloromethane in petroleum ether (40-60 °C) to 100% dichloromethane to give **2.45da** as a white powder (255 mg, 80%, 0.80 mmol) (Mp: 63-65 °C) and **2.49da** as clear oil (18 mg, 6%, 0.09 mmol).

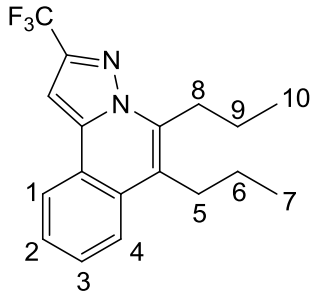

2.45da: ^{1}H NMR (400 MHz, $CDCl_3$): δ 1.09 (t, *J* = 7.4 Hz, 3H, H^{10}), 1.11 (t, *J* = 7.4 Hz, 3H, H^{7}), 1.65-1.75 (m, 2H, H^{6}), 1.77-1.86 (m, 2H, H^{9}), 2.93-2.98 (m, 2H, H^{5}), 3.25-3.29 (m, 2H, H^{8}), 7.21 (s, 1H, *Pz-H*), 7.54 (td, *J* = 7.0, 7.4 Hz, 1H, H^{2}), 7.60 (td, *J* = 7.0, 7.4 Hz, 1H, H^{3}), 7.87 (br d, *J* = 2.0 Hz, 1H, H^{4}), 8.08 (dt, *J* = 2.0 Hz, 1H, H^{1}), ^{13}C {^{1}H} NMR (100 MHz, $CDCl_3$): δ 14.2 (C^{7}/C^{10}), 14.4 (C^{7}/C^{10}), 21.2 (C^{9}), 23.7 (C^{6}), 29.8 (C^{5}, C^{8}), 95.6 (Pz), 121.4, 121.9 (q, *J* = 273.6 Hz,*C*F_3), 123.5, 123.2, 123.9 (C^{1}), 124.2 (C^{4}), 126.9 (C^{2}), 128.4 (C^{3}), 129.1, 136.8, 138.5, 142.4 (q, *J* = 39.2 Hz,*C*-CF_3), ^{19}F {^{1}H} NMR (376 MHz, $CDCl_3$): δ -61.4 (CF_3). ESIMS: *m/z* 321 $[M+H]^+$. HRMS (ESI): Calcd for $C_{18}H_{20}N_2F_3$ $[M+H]^+$ 321.1579, found 321.1566. The product was recrystallised from dichloromethane/hexane to give **2.45da** as clear needles.

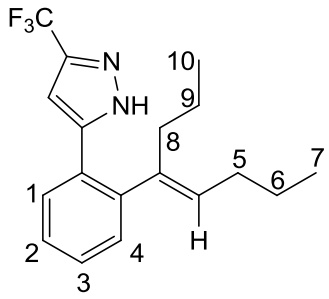

2.49da: ^{1}H NMR (400 MHz, $CDCl_3$): δ 0.79 (t, *J* = 7.4 Hz, 3H, H^{10}), 1.00 (t, *J* = 7.4 Hz, 3H, H^{7}), 1.18 (sex, *J* = 7.4 Hz, 2H, H^{9}), 1.50 (sex, *J* = 7.4 Hz, 2H, H^{6}), 2.05 (t, *J* = 7.4 Hz, 2H, H^{8}), 2.20 (q, *J* = 7.4 Hz, 2H, H^{5}), 5.61 (t, *J* = 7.4 Hz, 1H, C=C*H*), 6.72 (s, 1H, *Pz-H*), 7.18-7.21 (m, 1H, H^{4}), 7.32-7.37 (m, 2H, H^{2} + H^{3}), 7.44-7.48 (m, 1H, H^{1}), 10.65 (br s, 1H, N*H*), ^{13}C {^{1}H} NMR (100 MHz, $CDCl_3$): δ 12.9 (C^{7}/C^{10}), 13.0 (C^{7}/C^{10}), 20.4 (C^{9}), 21.8 (C^{6}), 29.3 (C^{5}), 32.3 (C^{8}), 101.5 (Pz), 124.5, 120.5 (q, *J* = 271.5 Hz,*C*F_3), 126.5 (C^{2}/C^{3}), 127.6 (C^{1}), 128.0 (C^{2}/C^{3}), 130.0 (C^{4}), 131.7 (C=*C*H), 140.9, 141.6, 143.5, ^{19}F {^{1}H} NMR (376 MHz, $CDCl_3$): δ -62.1 (CF_3). ESIMS: *m/z* 323 $[M+H]^+$. HRMS (ESI): Calcd for $C_{18}H_{22}N_2F_3$ $[M+H]^+$ 323.1735, found 323.1727. Could not assign *C*-CF_3 carbon atom.

Reaction of 2.44 with 4-octyne (a)

Following the general procedure, a Schlenk flask was loaded with $[Cp^*Rh(MeCN)_3][PF_6]_2$ (33 mg, 5 mol%), 3-(thiophen-2-yl)-5-(trifluoromethyl)-1H-pyrazole (**2.44**, 222 mg, 1.0 mmol), $Cu(OAc)_2.H_2O$ (500 mg, 2.5 mmol), 4-octyne (**a**, 132 mg, 1.2 mmol) and DCE (10 ml). The crude ^1H NMR spectrum showed the presence of two products in a 4:1 ratio. The products were purified by column chromatography eluting from 50% dichloromethane in petroleum ether (40-60 °C) to 100% dichloromethane to give **2.47a** as a white solid (261 mg, 79%, 0.79 mmol) (Mp: 79-82 °C) and **2.50a** as yellow oil (impure). In the reaction with $[(p\text{-Cy})RuCl_2]_2$ as catalyst and 20 mol% $AgPF_6$ added, **2.47a** and **2.50a** were obtained in a 1:1 ratio (261 mg, 80% combined yield, 0.80 mmol).

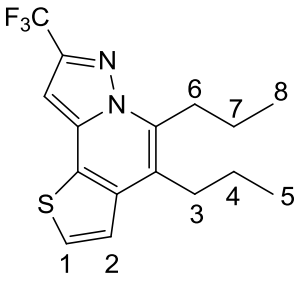

2.47a: ^1H NMR (400 MHz, $CDCl_3$): δ 1.06 (t, *J* = 7.4 Hz, 3H, H^5), 1.07 (t, *J* = 7.0, 7.4 Hz, 3H, H^8), 1.65-1.74 (m, 2H, H^4), 1.76-1.85 (m, 2H, H^7), 2.89-2.93 (m, 2H, H^3), 3.22-3.26 (m, 2H, H^6), 6.90 (s,1H, *Pz-H*), 7.38 (d, *J* = 5.5 Hz, 1H, H^2), 7.52 (d, *J* = 5.1 Hz, 1H, H^1), ^{13}C {^1H} NMR (100 MHz, $CDCl_3$): δ 14.2 (C^5/C^8), 14.3 (C^5/C^8), 20.8 (C^7), 24.0 (C^4), 29.4 (C^6), 31.6 (C^3), 93.8 (Pz), 120.5, 121.8 (q, *J* = 270.4 Hz,CF_3), 123.2 (C^2), 125.9, 126.7 (C^1), 135.7, 135.9, 136.6, 142.8 (q, *J* = 39.9 Hz,*C*-CF_3), ^{19}F {^1H} NMR (376 MHz, $CDCl_3$): δ -61.2 (CF_3). ESIMS: *m/z* 327 $[M+H]^+$. HRMS (ESI): Calcd for $C_{16}H_{18}N_2F_3S_1$ $[M+H]^+$ 327.1143, found 327.1158. The product was recrystallised from dichloromethane/hexane to give **2.50a** as clear needles.

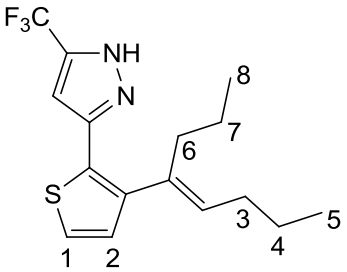

2.50a: This was obtained in a mixture with **2.47a**. ^1H NMR (400 MHz, $CDCl_3$): δ 0.86 (t, *J* = 7.0, 7.4 Hz, 3H, H^5/H^8), 0.95 (t, *J* = 7.0, 7.4 Hz, 3H, H^5/H^8), 1.31 (sex, *J* = 7.4 Hz, 2H, H^4/H^7), 1.45 (sex, *J* = 7.4 Hz, 2H, H^4/H^7), 2.18 (q, *J* = 7.4 Hz, 2H, H^3), 2.29 (t, *J* = 7.4 Hz, 2H, H^6), 5.60 (t, *J* = 7.4 Hz, 1H, C=C*H*), 6.65 (s, 1H, *Pz-H*), 6.90 (d, *J* = 5.1 Hz, 1H, H^2/H^2), 7.28 (d, *J* = 5.1 Hz, 1H, H^2/H^2) ESIMS: *m/z* 329 $[M+H]^+$. HRMS (ESI): Calcd for $C_{16}H_{20}N_2F_3S_1$ $[M+H]^+$ 329.1299, found 329.1305.

Reaction of 2.43a with diphenylacetylene (b)

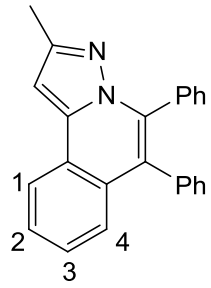

Following the general procedure, a Schlenk flask was loaded with $[Cp^*Rh(MeCN)_3][PF_6]_2$ (10 mg, 5 mol%), 3-phenyl-5-methyl-1*H*-pyrazole (**2.43a**, 50 mg, 0.32 mmol), $Cu(OAc)_2.H_2O$ (161 mg, 0.81 mmol), diphenylacetylene (**b**, 68 mg, 0.38 mmol) and DCE (10 ml). The product was purified by column chromatography eluting from 70% dichloromethane in hexane to give **2.45ab** as an orange solid (97 mg, 91%, 0.29 mmol). **U**sing $[(p\text{-Cy})RuCl_2]_2$ as catalyst with 20 mol% $AgPF_6$ added also gave **2.45ab** (47 mg, 14%, 0.14 mmol). ^{1}H NMR (400 MHz, $CDCl_3$): δ 3.71 (s, 3H, *Me*), 6.89 (s, 1H, *Pz-H*), 7.15-7.18 (dd, *J* = 1.2, 7.4 Hz, 2H, *Ar-H*), 7.21-7.27 (m, 4H, *Ar-H*), 7.31-7.33 (m, 3H, *Ar-H*), 7.37-7.39 (m, 2H, *Ar-H*), 7.50-7.54 (m, 2H, H^2, *Ar-H*), 8.11 (d, *J* = 7.4 Hz, 1H, H^1), ^{13}C {^{1}H} NMR (100 MHz, $CDCl_3$): δ 43.4 (*Me*), 97.4 (Pz), 122.9 (Ar), 123.3 (Ar), 123.5 (Ar), 126.6 (Ar), 127.0 (Ar), 127.1 (Ar), 127.5 (Ar), 127.7 (Ar), 127.9 (Ar), 128.2 (Ar), 128.2 (Ar), 128.3 (Ar), 128.7, 130.0 (Ar), 131.1 (Ar), 131.6 (Ar), 131.7 (Ar), 133.2 (Ar), 136.2 (Ar), 136.5, 139.4, 150.7. ESIMS: *m/z* 335 $[M+H]^+$. HRMS (ESI): Calcd for $C_{24}H_{19}N_2$ $[M+H]^+$ 335.1548, found 335.1541. The product was recrystallised from dichloromethane/hexane to give **2.45ab** as orange blocks.

Reaction of 2.43b with diphenylacetylene (b)

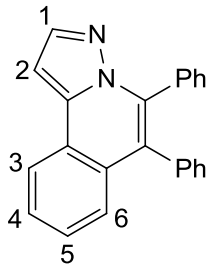

Following the general procedure, a Schlenk flask was loaded with $[Cp^*Rh(MeCN)_3][PF_6]_2$ (33 mg, 5mol %), 3-phenyl-1*H*-pyrazole (**2.43b**, 144 mg, 1 mmol), $Cu(OAc)_2.H_2O$ (500 mg, 2.5 mmol), diphenylacetylene (**b**, 214 mg, 1.2 mmol) and DCE (10 ml). The product was purified by column chromatography with ethyl acetate/dichloromethane as eluant to give **2.45bb** as a white solid (250 mg, 78 %, 0.78 mmol). ^{1}H NMR (400 MHz, $CDCl_3$): δ 7.13 (d, *J* = 2.0 Hz, 1H, H^2), 7.19-7.22 (m, 2H, *Ar-H*), 7.26-7.35 (m, 8H, *Ar-H*), 7.40-7.43 (m, 1H, *Ar-H*), 7.44 (td, *J* = 1.2, 6.7, 7.0 Hz, 1H, H^5), 7.58 (td, *J* = 2.0, 6.7, 8.2 Hz, 1H, H^4), 7.98 (d, *J* = 2.0 Hz, 1H, H^1), 8.21 (m, 1H, H^3), ^{13}C {^{1}H} NMR (100 MHz, $CDCl_3$): δ 97.6 (C^2), 123.6 (C^3), 124.1, 126.7 (C^5), 127.2 (C^4), 127.4, 127.7, 127.9, 128.01, 128.4, 130.9, 131.6, 141.1 (C^1). ESIMS: *m/z* 321 $[M+H]^+$. HRMS (ESI): Calcd for $C_{23}H_{17}N_2$ $[M+H]^+$ 321.1392, found 321.1394.

Reaction of 2.43c with diphenylacetylene (b)

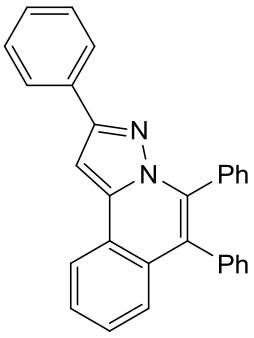

Following the general procedure, a Schlenk flask was loaded with $[Cp^*Rh(MeCN)_3][PF_6]_2$ (33 mg, 5 mol%), 3,5-diphenyl-1*H*-pyrazole (**1c**, 220 mg, 1.0 mmol), $Cu(OAc)_2.H_2O$ (500 mg, 2.5 mmol), diphenylacetylene (**b**, 214 mg, 1.2 mmol) and DCE (10 ml). The product was purified by column chromatography eluting from 100% dichloromethane to give **2.45cb** as an orange solid (390 mg, 98%, 0.98 mmol). ^{1}H NMR (400 MHz, $CDCl_3$): δ 7.21 (dd, *J* = 1.6, 7.4 Hz, 2H, *Ar-H*), 7.26-7.34 (m, 6H), 7.36-7.44 (m, 6H, *Ar-H*), 7.42 (s, 1H *Pz-H*), 7.56-7.60 (m, 1H, *Ar-H*), 7.92 (dd, *J* = 1.2, 7.0 Hz, 2H, *Ar-H*), 8.23 (d, *J* = 7.8 Hz, 1H, *Ar-H*), ^{13}C {^{1}H} NMR (100 MHz, $CDCl_3$): δ 94.6 (Pz), 123.6, 124.0, 126.8, 127.1, 127.3, 127.5, 127.7, 128.0, 128.1, 128.4, 128.6, 130.0, 131.4, 131.8, 133.0,133.5, 136.4,139.9, 152.3. ESIMS: *m/z* 397 $[M+H]^+$. HRMS (ESI): Calcd for $C_{29}H_{21}N_2$ $[M+H]^+$ 397.1705, found 397.1711. The product was recrystallised from standing in chloroform to give **2.45cb** as orange blocks. Anal. Calc. for ($C_{29}H_{21}N_2$): C, 87.85; H, 5.08; N, 7.07. Found: C, 87.99; H, 4.95; N, 6.95 %.

Reaction of 2.43d with diphenylacetylene (b)

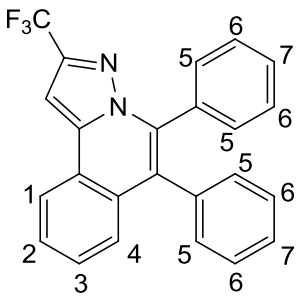

Following the general procedure, a Schlenk flask was loaded with $[Cp^*Rh(MeCN)_3][PF_6]_2$ (16 mg, 5 mol%), 3-phenyl-5-(trifluoromethyl)-1H-pyrazole (**2.43d**, 106 mg, 0.50 mmol), $Cu(OAc)_2.H_2O$ (250 mg, 1.25 mmol), diphenylacetylene (**b**, 107 mg, 0.60 mmol) and DCE (5 ml). The product was purified by column chromatography eluting from 50% dichloromethane in petroleum ether (40-60 °C) to give **2.45db** as a white powder (175 mg, 90%, 0.45 mmol). ^{1}H NMR (400 MHz, $CDCl_3$): δ 7.18 (dd, *J* = 2.3, 7.8 Hz, 2H, H^5), 7.24-7.33 (m, 8H, *Ar-H*), 7.36 (s, 1H, *Pz-H*), 7.45 (dd, *J* = 1.6, 8.2 Hz, 1H, H^4), 7.49 (td, *J* = 1.2, 7.0, 8.2 Hz, 1H, H^3), 7.62 (td, *J* = 1.2, 7.0, 8.2 Hz, 1H, H^2), 8.20 (dd, *J* = 1.2, 8.2 Hz, 1H, H^1), ^{13}C {^{1}H} NMR (125 MHz, $CDCl_3$): δ 95.9 (Pz), 121.6 (q, *J* = 270.1 Hz, CF_3), 123.4 (C^1), 123.6, 126.0, 126.9 (C^4), 127.3 (Ar), 127.6 (Ar), 127.8 (C^2), 128.0 (Ar), 128.3 (C^3), 128.4 (Ar), 129.9, 131.0 (Ar), 131.2 (C^5), 131.8, 135.5, 136.2, 139.2, 143.3 (q, *J* = 38.0 Hz, CF_3), ^{19}F {^{1}H} NMR (376 MHz, $CDCl_3$): δ -61.3 (CF_3). ESIMS: *m/z* 389 $[M+H]^+$. HRMS (ESI): Calcd for $C_{24}H_{16}N_2F_3$ $[M+H]^+$ 389.1266, found

389.1263. The product was recrystallised from dichloromethane/hexane to give **2.45db** as clear crystals.

Reaction of 2.44 with diphenylacetylene (b)

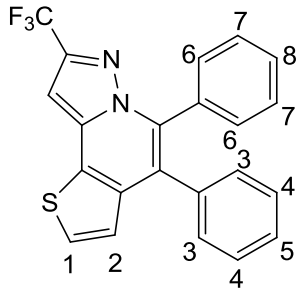

Following the general procedure, a Schlenk flask was loaded with $[Cp^*Rh(MeCN)_3][PF_6]_2$ (16 mg, 5 mol%), 3-(thiophen-2-yl)-5-(trifluoromethyl)-1H-pyrazole (**2.44**, 222 mg, 1.0 mmol), $Cu(OAc)_2.H_2O$ (250 mg, 1.25 mmol), diphenylacetylene (**b**, 214 mg, 1.2 mmol) and DCE (10 ml). The product was purified by washing with hexane to give **2.47b** as an orange powder (348 mg, 88%, 0.88 mmol). Mp: 230-232 °C. ^{1}H NMR (500 MHz, $CDCl_3$): δ 7.04 (s, 1H, *Pz-H*), 7.09 (d, *J* = 5.1 Hz, 1H, H^3), 7.19 (dd, *J* = 2.7, 7.0 Hz, 2H, H^3), 7.24-7.30 (m, 6H, H^4, H^5, H^7, H^8), 7.35 (dd, *J* = 2.7, 7.0 Hz, 2H, H^6), 7.48 (d, *J* = 5.5 Hz, 1H, H^1), ^{13}C {^{1}H} NMR (125 MHz, $CDCl_3$): δ 94.2 (Pz), 121.5 (q, *J* = 270.1 Hz, CF_3), 123.9, 125.3 (C^2), 126.8 (C^1), 127.0, 127.5 (C^5/C^8), 127.9 (C^4/C^7), 128.2 (C^4/C^7), 128.7 (C^5/C^8), 130.7 (C^3), 131.5 (C^6), 131.8, 135.4, 136.5, 136.6, 136.9, 143.8 (q, *J* = 39.7 Hz, CF_3), ^{19}F {^{1}H} NMR (376 MHz, $CDCl_3$): δ -61.3 (CF_3). ESIMS: *m/z* 395 $[M+H]^+$. HRMS (ESI): Calcd for $C_{22}H_{14}N_2F_3S_1$ $[M+H]^+$ 395.0830, found 395.0839.

Reaction of 2.43a with 1-phenyl-1-propyne (c)

Following the general procedure, a Schlenk flask was loaded with $[Cp^*Rh(MeCN)_3][PF_6]_2$ (33 mg, 5 mol%), 3-phenyl-5-methyl-1*H*-pyrazole (**2.43a**, 158 mg, 1.00 mmol), $Cu(OAc)_2.H_2O$ (500 mg, 2.50 mmol), 1-phenyl-1-propyne (**c**, 139 mg, 1.20 mmol) and DCE (10 ml). The crude ^{1}H NMR spectrum showed the presence of three products in a 12:9:1 ratio. The products were purified by column chromatography eluting with 30% ethyl acetate in hexane to give **2.45ac** as an orange powder (122 mg, 45%, 0.45 mmol) (Mp: 98-101 °C), **2.45ac′** as orange oil (impure) and **2.48ac** as an orange powder (110 mg, 40%, 0.40 mmol). **2.45ac** and **2.45ac′** were obtained with $[(p\text{-Cy})RuCl_2]_2$ as catalyst in a 12:1 ratio and purified by column chromatography to give a mixture of **2.45ac** and **2.45ac′** (218 mg, 80%, 0.80 mmol). Some **2.45ac** was obtained pure (182 mg, 67%, 0.67 mmol).

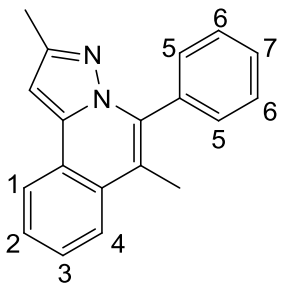

2.45ac: ^{1}H NMR (400 MHz, $CDCl_3$): δ 2.29 (s, 3H, C=C*Me*), 2.41 (s, 3H, *Me*), 6.79 (s, 1H, *Pz-H*), 7.45-7.50 (m, 5H, H^5, H^6, H^7), 7.51-7.56 (m, 2H, H^2, H^3), 7.84-7.86 (m, 1H, H^4), 8.06-8.09 (m, 1H, H^1), ^{13}C {^{1}H} NMR (100 MHz, $CDCl_3$): δ 14.3 (*Me*), 15.0 (C=C*Me*), 97.0 (Pz), 115.0, 123.8 (C^1), 123.9, 124.3 (C^4), 127.0 (C^2/C^3), 127.6 (C^2/C^3), 128.5 (C^5/C^6), 128.7 (C^7), 129.9, 130.6 (C^5/C^6), 134.0, 135.8, 138.9, 150.0. ESIMS: *m/z* 273 $[M+H]^+$. HRMS (ESI): Calcd for $C_{19}H_{17}N_2$ $[M+H]^+$ 273.1392, found 273.1392. The product was recrystallised from dichloromethane/hexane to give **2.45ac** as orange crystals.

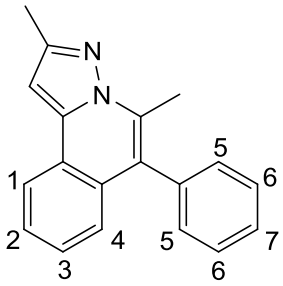

2.45ac′: This product was purified by preparative TLC eluting with 30% ethyl acetate in hexane to give **2.45ac′** as orange oil (13 mg, 5%, 0.05 mmol). ^{1}H NMR (400 MHz, $CDCl_3$): δ 2.56 (s, 3H, C=C*Me*), 2.59 (s, 3H, *Me*), 6.88 (s, 1H, *Pz-H*), 7.24 (br d, *J* = 7.8 Hz, 1H, H^4), 7.34 (dt, *J* = 2.0, 6.7, 8.6 Hz, 2H, H^5), 7.35-7.39 (m, 1H, H^3), 7.44-7.53 (m, 4H, H^2, H^6, H^7), 8.08 (dd, *J* = 0.8, 7.8 Hz, 1H, H^1), ^{13}C {^{1}H} NMR (100 MHz, $CDCl_3$): δ 14.2 (*Me*), 15.9 (C=C*Me*), 97.4 (Pz), 121.6, 122.8, 123.4 (C^1), 126.0 (C^4), 126.2 (Ar), 127.4 (C^3), 127.6 (Ar), 128.6 (C^6), 129.9, 131.0 (C^5), 133.1, 137.1, 139.0, 150.3. ESIMS: *m/z* 273 $[M+H]^+$. HRMS (ESI): Calcd for $C_{19}H_{17}N_2$ $[M+H]^+$ 273.1392, found 273.1409.

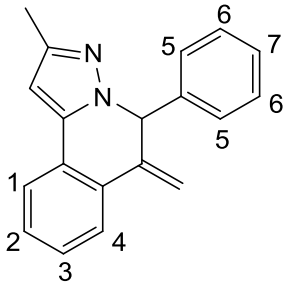

2.48ac: ^{1}H NMR (400 MHz, $CDCl_3$): δ 2.32 (s, 3H, *Me*), 5.49 (s, 1H, C=CH_2), 5.67 (s, 1H, C=CH_2), 6.15 (s, 1H, C*H*(Ph)), 6.42 (s, 1H, *Pz-H*), 6.94 (dd, *J* = 2.3, 8.2 Hz, 2H, H^5), 7.14-7.20 (m, 3H, H^6, H^7), 7.22 (td, *J* = 1.2, 7.4, 7.8 Hz, 1H, H^3), 7.32 (td, *J* = 1.2, 7.4, 7.8 Hz, 1H, H^2), 7.52 (dd, *J* = 1.2, 7.8 Hz, 1H, H^4), 7.54 (dd, *J* = 1.2, 7.8 Hz, 1H, H^1),^{13}C {^{1}H} NMR (100 MHz, $CDCl_3$): δ 13.8 (*Me*), 66.4 (*C*H(Ph)), 100.5 (Pz), 115.3 (C=*C*H_2), 123.7 (C^4), 125.5 (C^5), 125.5, 127.6 (C^7), 128.4 (C^3), 128.5 (C^2), 128.6 (C^6), 128.8 (C^1), 129.1, 129.8, 139.0, 140.6, 142.3, 149.6. ESIMS: *m/z* 273 $[M+H]^+$. HRMS (ESI): Calcd for $C_{19}H_{17}N_2$ $[M+H]^+$ 273.1392, found 273.1391.

Reaction of 2.43b with 1-phenyl-1-propyne (c)

Following the general procedure, a Schlenk flask was loaded with $[Cp^*Rh(MeCN)_3][PF_6]_2$ (33 mg, 5 mol%), 3-phenyl-1*H*-pyrazole (**2.43b**, 144 mg, 1 mmol), $Cu(OAc)_2.H_2O$ (500 mg, 2.5 mmol), 1-phenyl-1-propyne (**c**, 139 mg, 1.2 mmol) and DCE (10 ml). The crude ^1H NMR spectrum showed the presence of free pyrazole and two products in a 12:1 ratio. The products were purified by column chromatography eluting from 100% dichloromethane to 20% ethyl acetate in petroleum ether (40-60 °C) to give **2.45bc′** as orange oil (impure) and **2.45bc** as an orange powder (111 mg, 79% (based on 54% conversion), 0.43 mmol).

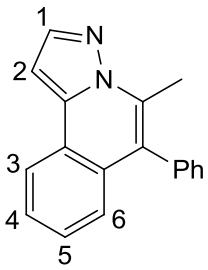

2.45bc′: This was obtained in a mixture with **2.45bc**. ^1H NMR (400 MHz, $CDCl_3$): δ 2.59 (s, 3H, *Me*), 7.09 (d, *J* = 2.3 Hz, 1H, H^2), 7.24-7.27 (m, 1H, *Ar-H*), 7.33 (dd, *J* = 1.6, 8.2 Hz, 1H, H^3/H^6), 7.39 (td, *J* = 1.6, 7.0, 8.2 Hz, 1H, H^4/H^5), 7.45-7.62 (m, 6H, *Ar-H*), 8.04 (d, *J* = 2.0 Hz, 1H, H^1).

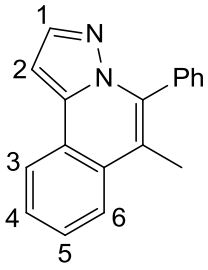

2.45bc: ^1H NMR (400 MHz, $CDCl_3$): δ 2.35 (s, 3H, *Me*), 7.03 (d, *J* = 2.3 Hz, 1H, H^2), 7.46-7.57 (m, 5H, *Ar-H*), 7.58-7.61 (m, 2H, H^4, H^5), 7.88 (d, *J* = 2.0 Hz, 1H, H^1), 7.89-7.92 (m, 1H, H^6), 8.15-8.17 (m, 1H, H^3), ^{13}C {^1H} NMR (100 MHz, $CDCl_3$): δ 14.8 (*Me*), 97.1 (C^2), 116.1, 123.7 (C^3), 124.0, 124.3 (C^6), 127.0 (C^4/C^5), 127.7 (C^4/C^5), 128.5, 128.7 (Ar), 129.7 (Ar), 130.2 (Ar), 133.7, 135.8, 137.8, 140.3 (C^1). HRMS (ESI): Calcd for $C_{18}H_{14}N_2$ $[M+H]^+$ 259.1341, found 259.1336.

Reaction of 2.43c with 1-phenyl-1-propyne (c)

Following the general procedure, a Schlenk flask was loaded with $[Cp^*Rh(MeCN)_3][PF_6]_2$ (33 mg, 5 mol%), 3,5-diphenyl-1*H*-pyrazole (**2.43c**, 220 mg, 1 mmol), $Cu(OAc)_2.H_2O$ (500 mg, 2.50 mmol), 1-phenyl-1-propyne (**c**, 139 mg, 1.20 mmol) and DCE (10 ml). The crude ^1H NMR spectrum showed the presence of two products in a 3:1 ratio. The products were purified by column chromatography eluting from 50 % dichloromethane in petroleum ether (40-60 °C) to 100% dichloromethane to give **2.45cc** and **2.45cc′** (219 mg, 66% combined yield, 0.66 mmol). **2.45cc′** was obtained pure as a brown solid (35 mg, 10%, 0.10 mmol) and **2.45cc** as an orange solid (147 mg, 44%, 0.44 mmol) (Mp: 145-148 °C).

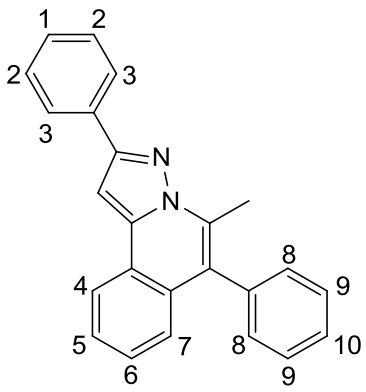

2.45cc′: ^{1}H NMR (400 MHz, $CDCl_3$): δ 2.64 (s, 3H, *Me*), 7.26 (d, *J* = 8.2 Hz, 1H, H^7), 7.34-7.42 (m, 4H, H^1, H^6, H^8), 7.39 (s, 1H, *Pz-H*), 7.46-7.55 (m, 6H, H^2, H^5, H^9, H^{10}), 8.07 (dd, *J* = 1.6, 8.6 Hz, 2H, H^3), 8.18 (br dt, *J* = 1.2, 2.0, 7.8 Hz, 1H, H^4), ^{13}C {^{1}H} NMR (100 MHz, $CDCl_3$): δ 15.8 (*Me*), 94.8 (Pz), 122.5, 123.2, 123.5 (C^4), 126.2 (C^7), 126.4 (C^3), 127.6 (Ar), 127.7 (Ar), 128.2 (Ar), 128.7 (C^2/C^9), 128.7 (C^2/C^9), 130.0, 131.0 (C^8), 133.6, 133.7, 137.1, 139.5, 152.2. ESIMS: *m/z* 334 $[M+H]^+$. HRMS (ESI): Calcd for $C_{24}H_{19}N_2$ $[M+H]^+$ 335.1548, found 335.1557.

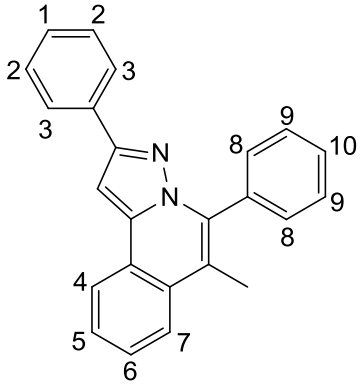

2.45cc: ^{1}H NMR (400 MHz, $CDCl_3$): δ 2.37 (s, 3H, *Me*), 7.27 (tt, *J* = 1.2, 2.7, 6.7, 8.2 Hz, 1H, H^1), 7.32 (s, 1H, *Pz-H*), 7.35-7.37 (m, 2H, H^2), 7.50-7.55 (m, 5H, H^8, H^9, H^{10}), 7.57-7.60 (m, 1H, H^5/H^6), 7.60-7.62 (m, 1H, H^5/H^6), 7.87 (dd, *J* = 1.2, 8.2 Hz, 2H, H^3), 7.89-7.91 (m, 1H, H^7), 8.16-8.20 (m, 1H, H^4), ^{13}C {^{1}H} NMR (125 MHz, $CDCl_3$): δ 15.2 (*Me*), 94.3 (Pz), 116.1, 123.7 (C^4), 123.8, 124.1 (C^7), 124.5 (C^3), 127.2 (C^1/C^5/C^6), 127.8 (C^1/C^5/C^6), 127.9 (C^1/C^5/C^6), 128.2 (C^2/C^9), 128.5 (C^2/C^9), 128.6 (C^{10}), 130.0, 130.9 (C^8), 133.6, 133.7, 136.1, 139.3, 151.6. ESIMS: *m/z* 334 $[M+H]^+$. HRMS (ESI): Calcd for $C_{24}H_{19}N_2$ $[M+H]^+$ 335.1548, found 335.1560. The product was recrystallised from dichloromethane/hexane to give **2.45cc** as orange blocks.

Reaction of 2.43d with 1-phenyl-1-propyne (c)

Following the general procedure, a Schlenk flask was loaded with $[Cp^*Rh(MeCN)_3][PF_6]_2$ (33 mg, 5 mol%), 3-phenyl-5-(trifluoromethyl)-1H-pyrazole (**2.43d**, 212 mg, 1.0 mmol), $Cu(OAc)_2.H_2O$ (500 mg, 2.5 mmol), 1-phenyl-1-propyne (**c**, 139 mg, 1.2 mmol) and DCE (10 ml). The crude ^{1}H NMR spectrum showed the presence of three products in a 7:2:1 ratio. The products were purified by column chromatography eluting from 50% dichloromethane in petroleum ether (40-60 °C) to give **2.45dc′** as an orange solid (30 mg, 9%, 0.09 mmol), **2.45dc** as an orange powder (178 mg, 55%, 0.55 mmol) (Mp:135-137 °C) and **2.48dc** as orange oil (impure).

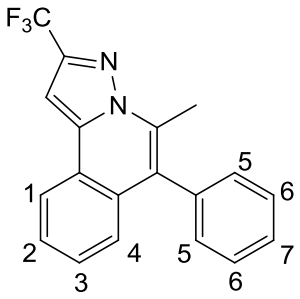

2.45dc′: ^{1}H NMR (400 MHz, $CDCl_3$): δ 2.60 (s, 3H, *Me*), 7.28-7.34 (m, 4H, *Pz-H*, H^4, H^5), 7.44-7.58 (m, 5H, H^2, H^3, H^6, H^7), 8.16 (d, *J* = 7.4 Hz, 1H, H^1), ^{13}C {^{1}H} NMR (100 MHz, $CDCl_3$): δ 15.7 (*Me*), 96.2 (Pz), 119.3 (q, *J* = 299.8 Hz, CF_3), 123.0, 123.5 (C^1), 124.8, 126.5 (Ar), 127.2 (Ar), 128.1 (Ar), 128.4 (Ar), 128.8 (Ar), 130.0, 130.7 (Ar), 133.5, 136.3, 138.9, 143.1 (q, *J* = 35.9 Hz, *C*-CF_3), ^{19}F {^{1}H} NMR (376 MHz, $CDCl_3$): δ -61.4 (CF_3). HRMS (ESI): Calcd for $C_{19}H_{14}N_2F_3$ $[M+H]^+$ 327.1109, found 327.1109.

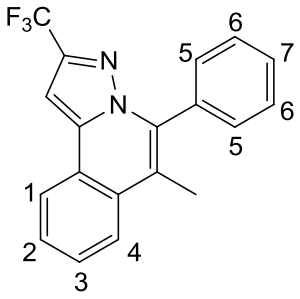

2.45dc: ^{1}H NMR (400 MHz, $CDCl_3$): δ 2.37 (s, 3H, *Me*), 7.25 (s, 1H, *Pz-H*), 7.45 (dd, *J* = 2.0, 7.8 Hz, 2H, H^5), 7.49-7.55 (m, 3H, H^6, H^7), 7.60-7.67 (m, 2H, H^2, H^3), 7.91-7.94 (m, 1H, H^4), 8.12-8.14 (m, 2H, H^1), ^{13}C {^{1}H} NMR (100 MHz, $CDCl_3$): δ 15.3 (*Me*), 95.9 (Pz), 118.7, 121.7 (q, *J* = 268.9 Hz, CF_3), 123.8, 123.8 (C^1), 124.7 (C^4), 127.8 (C^2/C^3), 128.5 (C^6), 128.7 (C^2/C^3), 129.0 (C^7), 129.9, 130.8 (C^5), 132.7, 135.9, 138.8, 143.1 (q, *J* = 39.5 Hz, *C*-CF_3), ^{19}F {^{1}H} NMR (376 MHz, $CDCl_3$): δ -61.2 (CF_3). HRMS (ESI): Calcd for $C_{19}H_{14}N_2F_3$ $[M+H]^+$ 327.1109, found 327.1114. The product was recrystallised from dichloromethane/hexane to give **2.49c** as orange blocks.

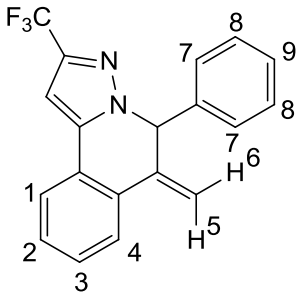

2.48dc: This product was obtained by preparative TLC eluting from 50% dichloromethane in petroleum ether (40-60 °C) to give **2.48dc** as orange oil (53 mg, 16%, 0.16 mmol). ^{1}H NMR (400 MHz, $CDCl_3$): δ 5.56 (d, *J* = 0.8 Hz, 1H, H^6), 5.76 (s, 1H, H^5), 6.27 (s, 1H, N-C*H*), 6.87 (s, 3H, *Pz-H*), 6.94-6.96 (m, 2H, H^7), 7.17-7.21 (m, 3H, H^8, H^9), 7.32 (td, *J* = 1.6, 7.4 Hz, 1H, H^2/H^3), 7.38 (td, *J* = 1.6, 7.4, 7.8 Hz, 1H, H^2/H^3), 7.56-7.60 (m, 2H, H^1, H^4), ^{13}C {^{1}H} NMR (100 MHz, $CDCl_3$): δ 67.0 (N-*C*H), 99.4 (Pz), 116.8 (C=*C*H_2), 121.4 (q, *J* = 268.7 Hz,*C*F_3), 124.0 (C^1/C^4), 124.3, 125.5 (C^7), 125.7 (C^1/C^4), 128.0 (C^8/C^9), 128.5 (C^8/C^9), 129.0 (C^2/C^3), 129.5 (C^2/C^3), 129.6, 139.1, 139.7, 141.1, 142.8 (q, *J* = 40.9 Hz, *C*-CF_3), ^{19}F {^{1}H} NMR (376 MHz, $CDCl_3$): δ -61.9 (CF_3).HRMS (ESI): Calcd for $C_{19}H_{14}N_2F_3$ $[M+H]^+$ 327.1109, found 327.1123.

Reaction of 2.43a with (4-nitrophenyl)but-3-yn-1-ol (d)

Following the general procedure, a Schlenk flask was loaded with $[Cp^*Rh(MeCN)_3][PF_6]_2$ (26 mg, 5 mol%), 3-phenyl-5-methyl-1*H*-pyrazole (**2.43a**, 125 mg, 0.79 mmol), $Cu(OAc)_2.H_2O$ (395 mg, 1.98 mmol), (4-nitrophenyl)but-3-yn-1-ol (**d**, 182 mg, 0.95 mmol) and DCE (10 ml). The crude ^{1}H NMR spectrum showed the presence of two products in a 3:1 ratio. Column chromatography eluting from 1% ethyl acetate in dichloromethane gave a mixture of regioisomers **2.45ad** and **2.45ad′** (264 mg, 96 %, 0.76 mmol). Recrystallisation from dichloromethane/hexane gave **2.45ad** as yellow crystals (200 mg, 73%, 0.73 mmol). Mp: 170-172 °C

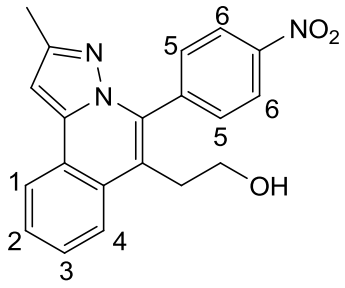

2.45ad: ^{1}H NMR (400 MHz, $CDCl_3$): δ 1.36 (br s, 1H, O*H*), 2.39 (s, 3H, *Me*), 3.00 (t, *J* = 7.0 Hz, 2H, CH_2CH$_2$OH), 3.83 (br t, *J* = 5.9 Hz, 2H, CH$_2$CH_2OH), 6.83 (s, 1H, *Pz-H*), 7.60 (t, *J* = 3.1 Hz, 1H, H^2/H^3), 7.62 (t, *J* = 3.5 Hz, 2H, H^2/H^3), 7.69 (d, *J* = 9.0 Hz, 2H, H^5), 7.93 (dd, *J* = 3.1 Hz, 1H, H^4), 8.11 (dd, *J* = 3.1 Hz, 1H, H^1), 8.42 (d, *J* = 9.0 Hz, 2H, H^6), ^{13}C {^{1}H} NMR (100 MHz, $CDCl_3$): δ 14.2 (*Me*), 31.3 (*C*H$_2$CH$_2$OH), 62.3 (CH$_2$*C*H$_2$OH), 97.5 (Pz), 115.9, 124.0 (C^6), 124.3 (C^1), 124.3 (C^4), 124.4, 127.7 (C^2/C^3), 128.0 (C^2/C^3), 128.4, 131.8 (C^5), 135.0, 139.1, 140.4, 148.1, 150.8. ESIMS: *m/z* 348 $[M+H]^+$. HRMS (ESI): Calcd for $C_{20}H_{18}N_3O_3$ $[M+H]^+$ 348.1348, found 348.1348. The product was recrystallised from dichloromethane/hexane to give **2.45ad** as orange needles. Anal. Calc. for ($C_{20}H_{17}N_3O_3$): C, 69.15; H, 4.93; N, 12.10. Found: C, 68.99; H, 4.80; N, 11.98%.

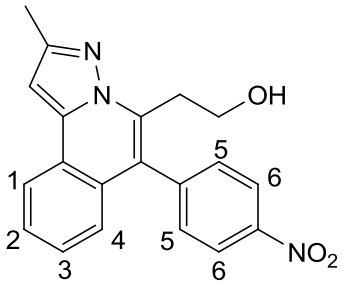

2.45ad′: Recrystallisation with dichloromethane/hexane left a filtrate of **2.45ad′** in a mixture with **2.45ad**. ^{1}H NMR (400 MHz, $CDCl_3$): δ 1.36 (br s, 1H, O*H*), 2.39 (s, 3H, *Me*), 3.00 (t, *J* = 7.0 Hz, 2H, CH_2CH$_2$OH), 3.83 (br t, *J* = 5.9 Hz, 2H, CH$_2$CH_2OH), 6.83 (s, 1H, *Pz-H*), 7.04 (d, *J* = 8.2 Hz, 1H, H^1/H^4), 7.93-7.43 (m, 1H, H^2/H^3), 7.53-7.56 (m, 1H, H^2/H^3), 7.54 (d, *J* = 9.0 Hz, 2H, H^5), 8.11 (d, *J* = 7.4 Hz, 1H, H^1/H^4), 8.41 (d, *J* = 9.0 Hz, 2H, H^6).

Reaction of 2.43b with (4-nitrophenyl)but-3-yn-1-ol (d)

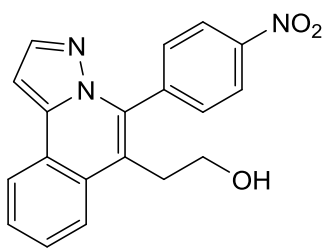

Following the general procedure, a Schlenk flask was loaded with $[Cp^*Rh(MeCN)_3][PF_6]_2$ (16 mg, 5 mol%), 3-phenyl-1*H*-pyrazole (**2.43b**, 72 mg, 0.5 mmol), $Cu(OAc)_2.H_2O$ (250 mg, 1.25 mmol), (4-nitrophenyl)but-3-yn-1-ol (**d**, 115 mg, 0.6 mmol) and DCE (5 ml). The crude ^{1}H NMR spectrum showed the presence of a trace amount of two products in a 3:1 ratio. An orange crystal of **2.45bd** formed in $CDCl_3$ when drying the sample.

Reaction of 2.43c with (4-nitrophenyl)but-3-yn-1-ol (d)

Following the general procedure, a Schlenk flask was loaded with $[Cp^*Rh(MeCN)_3][PF_6]_2$ (16 mg, 5 mol%), 3,5-diphenyl-1*H*-pyrazole (**2.43c**, 110 mg, 0.5 mmol), $Cu(OAc)_2.H_2O$ (250 mg, 1.25 mmol), (4-nitrophenyl)but-3-yn-1-ol (**d**, 115 mg, 0.6 mmol) and DCE (5 ml). The crude ^{1}H NMR spectrum showed the presence of two products in a 3:1 ratio. The products were purified by column chromatography eluting with 50% ethyl acetate in hexane to give **2.45cd** as a yellow solid (90 mg, 44%, 0.22 mmol) (Mp: 200-202 °C) and **2.45cd′** as a yellow solid (80 mg, 39%, 0.20 mmol) (Mp: 175-178 °C).

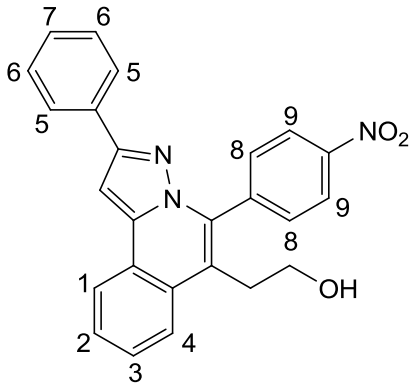

2.45cd: ^{1}H NMR (400 MHz, $CDCl_3$): δ 1.54 (br s,1H, O*H*), 3.08 (t, *J* = 7.0 Hz, 2H, C*H*$_2$CH$_2$OH), 3.87 (br q, *J* = 6.7 Hz, 2H, CH$_2$C*H*$_2$OH), 7.30 (tt, *J* = 1.2, 7.4, 8.6 Hz, 1H, *H*^{7}), 7.35 (s, 1H, *Pz-H*), 7.37 (tt, *J* = 1.2, 1.6, 7.0, 7.4 Hz, 2H, *H*^{6}), 7.62-7.68 (m, 2H, *H*^{2}, *H*^{3}), 7.76 (d, *J* = 8.6 Hz, 2H, *H*^{8}), 7.83 (dd, *J* = 1.6, 7.0 Hz, 2H, *H*^{5}), 7.97-8.00 (m, 1H, *H*^{4}), 8.21-8.24 (m, 1H, *H*^{1}), 8.42 (d, *J* = 8.6 Hz, 2H, *H*^{9}), ^{13}C {^{1}H} NMR (100 MHz, $CDCl_3$): δ 31.2 (*C*H$_2$CH$_2$OH), 62.0 (CH$_2$*C*H$_2$OH), 94.5 (Pz), 116.8, 123.5 (*C*^{9}), 124.1 (*C*^{1}), 124.3 (*C*^{4}), 124.5, 126.1 (*C*^{5}), 127.7 (*C*^{2}/*C*^{3}), 128.0 (*C*^{2}/*C*^{3}), 128.1 (*C*^{7}), 128.3, 128.4 (*C*^{6}), 131.9 (*C*^{8}), 132.8, 135.0, 139.4, 139.9, 147.9, 152.2. ESIMS: *m/z* 410 $[M+H]^+$. HRMS (ESI): Calcd for $C_{25}H_{20}N_3O_3$ $[M+H]^+$ 410.1505, found 410.1502.

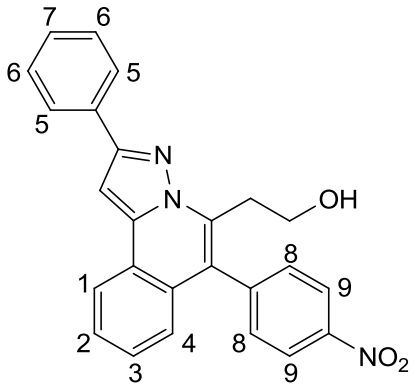

2.45cd′: ^{1}H NMR (400 MHz, $CDCl_3$): δ 3.32 (t, *J* = 5.5 Hz, 2H, C*H*$_2$CH$_2$OH), 4.02 (q, *J* = 5.5 Hz, 2H,CH$_2$C*H*$_2$OH), 4.16 (t, *J* = 5.5 Hz, 1H, O*H*), 7.09 (d, *J* = 7.8 Hz, 1H, *H*^{4}), 7.42 (s, 1H, *Pz-H*), 7.41-7.51 (m, 4H, *H*^{3}, *H*^{6}, *H*^{7}), 7.56-7.61 (m, 1H, *H*^{2}), 7.57 (dd, *J* = 6.7, 9.0 Hz, 2H, *H*^{8}), 8.02 (dd, *J* = 1.6, 7.0 Hz, 2H, *H*^{5}), 8.21 (d, *J* = 8.2 Hz, 1H, *H*^{1}), 8.41 (dd, *J* = 6.7, 8.6 Hz, 2H, *H*^{9}), ^{13}C {^{1}H} NMR (100 MHz, $CDCl_3$): δ 31.6 (*C*H$_2$CH$_2$OH), 61.0 (CH$_2$*C*H$_2$OH), 94.3 (Pz), 120.9, 122.3, 122.8 (*C*^{1}), 123.0 (*C*^{9}), 124.8 (*C*^{4}), 125.4 (*C*^{5}), 126.5 (Ar), 127.3 (Ar), 127.7 (Ar), 127.9 (*C*^{6}), 128.1, 131.2 (*C*^{8}), 131.6, 134.3, 139.0, 142.6, 146.7, 151.7. ESIMS: *m/z* 410 $[M+H]^+$. HRMS (ESI): Calcd for $C_{25}H_{20}N_3O_3$ $[M+H]^+$ 410.1505, found 410.1494.

Reaction of 2.43d with (4-nitrophenyl)but-3-yn-1-ol (d)

Following the general procedure, a Schlenk flask was loaded with $[Cp^*Rh(MeCN)_3][PF_6]_2$ (16 mg, 5 mol%), 3-phenyl-5-(trifluoromethyl)-1H-pyrazole (**2.43d**, 106 mg, 0.5 mmol), $Cu(OAc)_2.H_2O$ (250 mg, 1.25 mmol), 4-nitrophenyl)but-3-yn-1-ol (**d**, 115 mg, 0.6 mmol) and DCE (5 ml). The crude ^{1}H NMR spectrum showed the presence of two products in a 1:1 ratio. The products were purified by column chromatography eluting from 10% ethyl acetate in dichloromethane to give **2.45dd** and **2.45dd′** (163 mg, 90% combined yield, 0.45 mmol). **2.45dd′** was obtained as an orange solid (18 mg, 9%, 0.05 mmol) and **2.45dd** as an orange solid (impure).

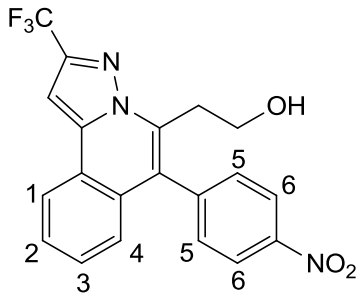

2.45dd′: ^{1}H NMR (400 MHz, $CDCl_3$): δ 2.40 (br s, 1H, O*H*), 3.28 (t, *J* = 5.9 Hz, 2H, C*H*$_2$CH$_2$OH), 4.02 (br q, *J* = 5.9 Hz, 2H, CH$_2$C*H*$_2$OH), 7.11 (d, *J* = 8.2 Hz, 1H, *H*^{4}), 7.36 (s, 1H, *Pz-H*), 7.48-7.53 (m, 1H, *H*^{3}), 7.59 (dt, *J* = 2.3, 9.0 Hz, 2H, *H*^{5}), 7.62-7.66 (m, 1H, *H*^{2}), 8.19 (d, *J* = 7.8 Hz, 1H, *H*^{1}), 8.42 (dt, *J* = 2.3, 8.6 Hz, 2H, *H*^{6}), ^{13}C {^{1}H} NMR (100 MHz, $CDCl_3$): δ 32.4 (*C*H$_2$CH$_2$OH), 60.9 (CH$_2$*C*H$_2$OH), 96.7 (Pz), 123.3, 123.8 (*C*^{1}), 124.1 (*C*^{6}), 124.4, 126.1 (*C*^{4}), 128.2 (*C*^{2}), 129.1 (*C*^{3}), 129.2, 132.1 (*C*^{5}), 134.5, 139.5, 142.9, 148.0, ^{19}F {^{1}H} NMR (376 MHz, $CDCl_3$): δ -61.6 (C*F*$_3$). ESIMS: *m/z* 402 $[M+H]^+$. HRMS (ESI): Calcd for $C_{20}H_{15}N_3F_3O_3$ $[M+H]^+$ 402.1066,

found 402.1067. Could not assign CF_3 and *C*-CF_3 carbon atoms due to small amount of product isolated.

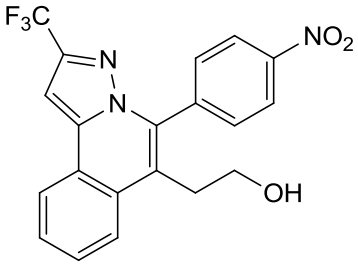

2.45dd: This was obtained in a mixture with **2.45dd′**. ^{1}H NMR (400 MHz, $CDCl_3$): δ 3.07 (t, *J* = 5.9 Hz, 2H, C*H*$_2$CH$_2$OH), 3.88 (t, *J* = 5.9 Hz, 2H, CH$_2$C*H*$_2$OH), 6.76 (s, 1H, *Pz-H*), 7.40-8.19 (multiplets, 7H, *Ar-H*), 8.34 (dt, *J* = 2.3, 8.6 Hz, 2H, *Ar-H*). ESIMS: *m/z* 402 $[M+H]^+$, 386 $[M-O]^+$.

Reaction of 2.43a with DMAD (e)

Following the general procedure, a Schlenk flask was loaded with $[Cp^*Rh(MeCN)_3][PF_6]_2$ (33 mg, 5 mol%), 3-phenyl-5-methyl-1*H*-pyrazole (**2.43a**, 158 mg, 1 mmol), $Cu(OAc)_2.H_2O$ (500 mg, 2.5 mmol), dimethyl acetylenedicarboxylate (**e**, 170 mg, 1.2 mmol) and DCE (10 ml). The product was purified by column chromatography eluting from 10 % ethyl acetate in dichloromethane to give **2.51ae** as a white powder (64 mg, 21 %, 0.21 mmol). On some occasions **2.52ae** was isolated as white powder (56 mg, 12 %, 0.12 mmol).

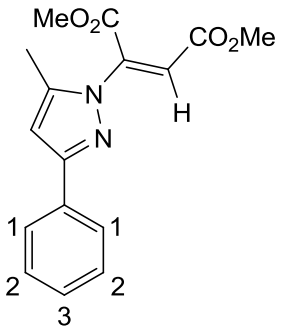

2.51ae: ^{1}H NMR (400 MHz, $CDCl_3$): δ 2.40 (s, 3H, *Me*), 3.79 (s, 3H, =CH(CO$_2$*Me*)), 3.99 (s, 3H, CO$_2$*Me*), 6.36 (s, 1H, =C*H*(CO$_2$Me)), 6.50 (s, 1H, *Pz-H*), 7.39 (m, 3H, *H*^{2}, *H*^{3}), 7.79 (d, *J* = 7.0 Hz, 1H, *H*^{1}), ^{13}C {^{1}H} NMR (100 MHz, $CDCl_3$): δ 13.0 (*Me*), 52.1 (=CH(CO$_2$*Me*)), 53.2 (CO$_2$*Me*), 107.9 (Pz), 108.2 (=*C*H(CO$_2$Me)), 126.1 (*C*^{1}), 128.6 (*C*^{2}), 128.8 (*C*^{3}), 131.9, 142.2, 143.5, 153.4, 163.5 (*C*O$_2$Me), 165.4 (*C*O$_2$Me). ESIMS: *m/z* 301 $[M+H]^+$. HRMS (ESI): Calcd for $C_{16}H_{17}N_2O_4$ $[M+H]^+$ 301.1194, found 301.1188. The product was recrystallised from dichloromethane/hexane to give **2.51ae** as clear needles.

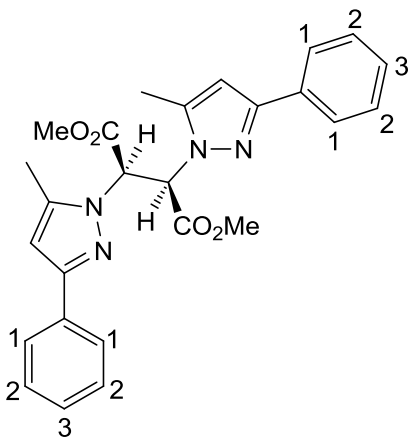

2.52ae: ^{1}H NMR (400 MHz, $CDCl_3$): δ 2.57 (s, 6H, *Me*), 3.57 (s, 6H, CO_2*Me*), 6.12 (s, 2H, C*H*(CO_2Me)), 6.37 (s, 2H, *Pz-H*), 7.29 (t, *J* = 7.4 Hz, 2H, H^3), 7.38 (t, *J* = 7.4 Hz, 4H, H^2), 7.79 (dd, *J* = 1.6, 8.2 Hz, 4H, H^1), ^{13}C {^{1}H} NMR (100 MHz, $CDCl_3$): δ 11.2 (*Me* (Pz)), 52.8 (CO_2*Me*)), 59.0 (*C*H(CO_2Me)), 103.2 (Pz), 108.22 (=*C*H(CO_2Me)), 125.8 (C^1), 127.7 (C^3), 128.5 (C^2), 133.5, 141.9, 151.6, 167.0 (*C*O_2Me). ESIMS: *m/z* 459 $[M+H]^+$. HRMS (ESI): Calcd for $C_{26}H_{27}N_4O_4$ $[M+H]^+$ 459.2032, found 459.2027. The product was recrystallised from dichloromethane/hexane to give **2.52ae** as clear needles.

Reaction of 2.43b with DMAD (e)

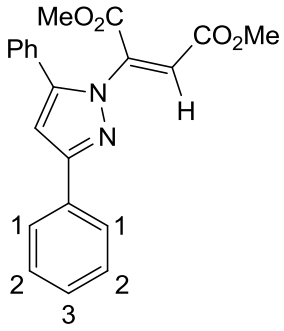

Following the general procedure, a Schlenk flask was loaded with $[Cp^*Rh(MeCN)_3][PF_6]_2$ (33 mg, 5 mol%), 3,5-diphenyl-1*H*-pyrazole (**2.43b**, 220 mg, 1 mmol), $Cu(OAc)_2.H_2O$ (500 mg, 2.5 mmol), dimethyl acetylenedicarboxylate (**e**, 170 mg, 1.2 mmol) and DCE (10 ml). The product was purified by preparative TLC eluting from 75 % dichloromethane in hexane to give **2.51be** as white powder (51 mg, 14 %, 0.14 mmol). ^{1}H NMR (400 MHz, $CDCl_3$): δ 3.64 (s, 3H, CO_2*Me*), 3.72 (s, 3H, =CH(CO_2*Me*)), 6.14 (s, 1H, =C*H*(CO_2Me)), 6.74 (s, 1H, *Pz-H*), 7.45 (m, 7H, *Ar-H*), 7.86 (dd, *J* = 1.6, 6.7 Hz. 2H, H^1), ^{13}C {^{1}H} NMR (100 MHz, $CDCl_3$): δ 52.10 (=CH(CO_2*Me*)), 52.85 (CO_2*Me*), 107.96 (Pz), 113.12 (=*C*H(CO_2Me)), 126.17 (C^5), 128.23 (Ar), 128.72 (Ar), 128.85 (Ar), 129.14 (Ar), 129.44 (Ar), 131.88 (Ar), 142.16, 146.14, 153.51, 162.93 (*C*O_2Me), 164.95 (*C*O_2Me). ESIMS: *m/z* 363 $[M+H]^+$, 332 $[M-2(Me)-H]^+$. HRMS (ESI): Calcd for $C_{21}H_{19}N_2O_4$ $[M+H]^+$ 363.1345, found 363.1354.

Competition Experiments

Following the general procedure for catalysis reactions, a Schlenk flask was loaded with $[Cp^*Rh(MeCN)_3][PF_6]_2$ (16 mg, 5 mol%), the relevant pyrazole (1, 1.0 mmol), $Cu(OAc)_2.H_2O$ (500 mg, 2.5 mmol), 4-octyne (**a**, 550 mg, 5.0 mmol), diphenylacetylene (**b**, 890 mg, 5.0 mmol), 1,3,5-trimethoxybenzene (8.4 mg, 0.05 mmol, 5 mol%) as internal standard and DCE (10 ml). The pyrazole was added after the alkynes and the Rh catalyst was added last.

General Procedure for Deuteration of Pyrazoles

A Schlenk flask equipped with a stirrer bar was evacuated and backfilled with nitrogen. It was loaded with the relevant pyrazole (1.0 mmol), the relevant metal catalyst (0.05 eq. of metal), NaOAc (164 mg, 2.0 mmol, 2 eq.) and CD_3OD (2.5 ml). The flask was sealed with a screw cap and transferred to a preheated oil bath at 60 °C to stir overnight. Monitoring by ^1H NMR spectroscopy showed some deuteration had occurred. PivOD (16 mg, 0.2 mmol, 0.2 eq.) was added and the reaction was stirred at 60 °C with further monitoring.

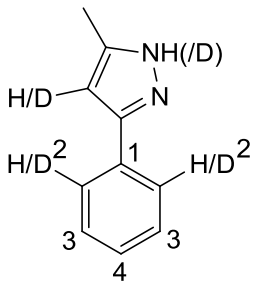

d^3-2.43a: This was formed using 5-methyl-3-phenyl-1H-pyrazole (**2.43a**, 158 mg, 1.0 mmol) and $[Cp^*Rh(MeCN)_3][PF_6]_2$ (33 mg, 0.050 mmol, 5 mol%) or $[Cp^*RhCl_2]_2$ (15 mg, 0.025 mmol, 2.5 mol%). Changing the CD_3OD twice showed 97% deuteration. The product was purified by column chromatography eluting with 50% ethyl acetate in dichloromethane to give **d^3-2.43a** as a brown powder (157 mg, 98 %, 0.98 mmol). **d^3-2.43a** was also formed from reaction with the catalyst $[(p\text{-Cy})RuCl_2]_2$ (15 mg, 0.025 mmol, 2.5 mol%). ^1H NMR (400 MHz, $CDCl_3$): δ 2.29 (s, 3H, *Me*), 7.29 (t, *J* = 7.0 Hz, 1H, H^4), 7.36 (d, *J* = 7.0 Hz, 2H, H^3), 10.00 (br s, 1H, N*H*), ^2H NMR (77 MHz, CD_3OD): 6.40 (s, 1H, *Pz-D*), 7.72 (s, 2H, D^2), ^{13}C {^1H} NMR (125 MHz, CD_3OD): δ 11.8 (*Me*), 102.7 (t, *J* = 24.5 Hz, Pz), 126.5 (t, *J* = 23.9 Hz, C^2), 128.9 (C^4), 129.7 (C^3), 133.5 (C^1), 144.9, 150.6. ESIMS: *m/z* 160 [**d^1-2.43a**+H]$^+$, 161 [**d^2-2.43a**+H]$^+$, 162 [**d^3-2.43a**+H]$^+$, 160 [**d^4-2.43a**+H]$^+$.

Deuteration in the Presence of Alkyne

Following the general procedure for catalysis reactions, a Schlenk flask was loaded with $[Cp^*Rh(MeCN)_3][PF_6]_2$ (16 mg, 5 mol%), 3-phenyl-5-methyl-1*H*-pyrazole (**2.43a**, 79 mg, 0.50 mmol), $Cu(OAc)_2.H_2O$ (250 mg, 1.25 mmol), 4-octyne (**a**, 66 mg, 0.60 mmol) and CD_3OD (3 ml) and transferred to a preheated oil bath at 70 °C. This gave **d^2-2.45a** as a brown solid (124 mg, 93%, 0.47 mmol). Reaction with the catalyst $[(p\text{-Cy})RuCl_2]_2$ (15 mg, 0.025 mmol, 2.5 mol%) gave **d^1-2.45a** as a brown solid (130 mg, in a mixture with **2.43**).

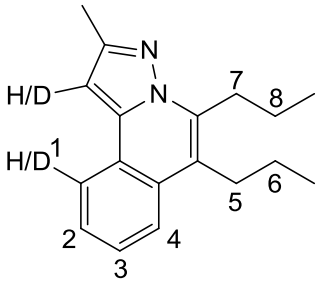

d^2-2.45a: ^{1}H NMR (400 MHz, $CDCl_3$): δ 1.08 (t, *J* = 7.4 Hz, 6H, CH_2CH_2*Me*), 1.63-1.72 (m, 2H, *H*^{6}), 1.77-1.87 (m, 2H, *H*^{8}), 2.52 (s, 3H, *Me*), 2.88-2.92 (m, 2H, *H*^{5}), 3.22-3.26 (m, 2H, *H*^{7}), 7.44 (td, *J* = 1.2, 7.8, 8.2 Hz, 1H, *H*^{2}), 7.50 (td, *J* = 1.6, 7.0, 8.2 Hz, 1H, *H*^{3}), 7.79 (br d, *J* = 8.6 Hz, 1H, *H*^{4}), ^{2}H NMR (77 MHz, $CDCl_3$): 6.81 (s, 1H, *Pz-D*), 8.07 (s, 1H, *D*^{2}). ESIMS: *m/z* 267 [**2.45a**+H]$^+$ 268 [**d^1-2.45a**+H]$^+$ 269 [**d^2-2.45a**+H]$^+$. HRMS (ESI): Calcd for $C_{18}H_{23}N_2$ [**2.45a**+H]$^+$ 267.1861, found 267.1867, Calcd for $C_{18}H_{22}D_1N_2$ [**d^1-2.45a**+H]$^+$ 268.1924, found 268.1916, Calcd for $C_{18}H_{21}D_2N_2$ [**d^2-2.45a**+H]$^+$ 269.1987, found 269.1980.

Bibliography

1. A. D. Ryabov, *Chem. Rev.*, 1990, **90**, 403.
2. P. Steenwinkel, R. A. Gossage and G. van Koten, *Chem. Eur. J.*, 1998, **4**, 759.
3. J. Dupont, C. S. Consorti and J. Spencer, *Chem. Rev.*, 2005, **105**, 2527.
4. J. Djukic, J. Sortais, L. Barloy and M. Pfeffer, *Eur. J. Inorg. Chem.*, 2009, 817.
5. W. Bauer, M. Prem, K. Polborn, K. Sünkel, W. Steglich and W. Beck, *Eur. J. Inorg. Chem.*, 1998, 485.
6. D. L. Davies, O. Al-Duaij, J. Fawcett, M. Giardiello, S. T. Hilton and D. R. Russell, *Dalton Trans.*, 2003, 4132.
7. Y. Boutadla, O. Al-Duaij, D. L. Davies, G. A. Griffith and K. Singh, *Organometallics*, 2009, **28**, 433.
8. L. Li, W. W. Brennessel and W. D. Jones, *Organometallics*, 2009, **28**, 3492.
9. D. L. Davies, S. M. A. Donald and S. A. Macgregor, *J. Am. Chem. Soc.*, 2005, **127**, 13754.
10. D. L. Davies, S. M. A. Donald, O. Al-Duaij, S. A. Macgregor and M. Pölleth, *J. Am. Chem. Soc.*, 2006, **128**, 4210.
11. C. Scheeren, F. Maasarani, A. Hijazi, J. Djukic, M. Pfeffer, S. D. Zaric, X. Le Goff and L. Ricard, *Organometallics*, 2007, **26**, 3336.
12. L. Li, W. W. Brennessel and W. D. Jones, *J. Am. Chem. Soc.*, 2008, **130**, 12414.
13. B. Li, T. Roisnel, C. Darcel and P. H. Dixneuf, *Dalton Trans.*, 2012, **41**, 10934.
14. Y. Boutadla, D. L. Davies, R. C. Jones and K. Singh, *Chem. Eur. J.*, 2011, **17**, 3438.
15. D. L. Davies, O. Al-Duaij, J. Fawcett and K. Singh, *Organometallics*, 2010, **29**, 1413.
16. D. L. Davies, S. M. A. Donald, O. Al-Duaij, J. Fawcett, C. Little and S. A. Macgregor, *Organometallics*, 2006, **25**, 5976.
17. L. Cuesta, T. Soler and E. P. Urriolabeitia, *Chem. Eur. J.*, 2012, **18**, 15178.
18. G. A. Burley, Y. Boutadla, D. L. Davies and K. Singh, *Organometallics*, 2012, **31**, 1112.
19. N. Wang, B. Li, H. Song, S. Xu and B. Wang, *Chem. Eur. J.*, 2013, **19**, 358.
20. H. C. L. Abbenhuis, M. Pfeffer, J. P. Sutter, A. Decian, J. Fischer, H. L. Ji and J. H. Nelson, *Organometallics*, 1993, **12**, 4464.
21. M. Pfeffer, J. Sutter and E. Urriolabeitia, *Bull. Soc. Chim. Fr.*, 1997, **134**, 947.

22. W. Ferstl, I. K. Sakodinskaya, N. Beydoun-Sutter, G. Le Borgne, M. Pfeffer and A. D. Ryabov, *Organometallics,* 1997, **16**, 411.
23. Y. Boutadla, D. L. Davies, O. Al-Duaij, J. Fawcett, R. C. Jones and K. Singh, *Dalton Trans.,* 2010, **39**, 10447.
24. T. Fukutani, N. Umeda, K. Hirano, T. Satoh and M. Miura, *Chem. Commun.*, 2009, 5141.
25. N. Guimond and K. Fagnou, *J. Am. Chem. Soc.,* 2009, **131**, 12050.
26. G. Song, F. Wang and X. Li, *Chem. Soc. Rev.,* 2012, **41**, 3651.
27. K. Ueura, T. Satoh and M. Miura, *Org. Lett.,* 2007, **9**, 1407.
28. K. Ueura, T. Satoh and M. Miura, *J. Org. Chem.,* 2007, **72**, 5362.
29. D. R. Stuart, M. Bertrand-Laperle, K. M. N. Burgess and K. Fagnou, *J. Am. Chem. Soc.,* 2008, **130**, 16474.
30. D. R. Stuart, M. Bertrand-Laperle, K. M. N. Burgess and K. Fagnou, *J. Am. Chem. Soc.,* 2010, **132**, 17973.
31. T. Satoh and M. Miura, *Chem. Eur. J.,* 2010, **16**, 11212.
32. J. Wencel-Delord, T. Dröge, F. Liu and F. Glorius, *Chem. Soc. Rev.,* 2011, **40**, 4740.
33. N. Umeda, K. Hirano, T. Satoh, N. Shibata, H. Sato and M. Miura, *J. Org. Chem.,* 2011, **76**, 13.
34. N. Umeda, H. Tsurugi, T. Satoh and M. Miura, *Angew. Chem. Int. Ed.,* 2008, **47**, 4019.
35. S. Mochida, M. Shimizu, K. Hirano, T. Satoh and M. Miura, *Chem. Asian J.,* 2010, **5**, 847.
36. K. Muralirajan, K. Parthasarathy and C. Cheng, *Angew. Chem. Int. Ed.,* 2011, **50**, 4169.
37. F. W. Patureau, T. Besset, N. Kuhl and F. Glorius, *J. Am. Chem. Soc.,* 2011, **133**, 2154.
38. K. Morimoto, K. Hirano, T. Satoh and M. Miura, *Chem. Lett.,* 2011, **40**, 600.
39. S. Mochida, N. Umeda, K. Hirano, T. Satoh and M. Miura, *Chem. Lett.,* 2010, **39**, 744.
40. G. Song, D. Chen, C. Pan, R. H. Crabtree and X. Li, *J. Org. Chem.,* 2010, **75**, 7487.
41. T. K. Hyster and T. Rovis, *J. Am. Chem. Soc.,* 2010, **132**, 10565.

42. L. Ackermann, A. V. Lygin and N. Hofmann, *Angew. Chem. Int. Ed.*, 2011, **50**, 6379.
43. Z. Shi, C. Tang and N. Jiao, *Adv. Synth. Catal.*, 2012, **354**, 2695.
44. Y. Su, M. Zhao, K. Han, G. Song and X. Li, *Org. Lett.*, 2010, **12**, 5462.
45. L. Ackermann, A. V. Lygin and N. Hofmann, *Org. Lett.*, 2011, **13**, 3278.
46. N. Quiñones, A. Seoane, R. García-Fandiño, J. Luis Mascareñas and M. Gulías, *Chem. Sci.*, 2013, **4**, 2874.
47. T. K. Hyster and T. Rovis, *Chem. Sci.*, 2011, **2**, 1606.
48. K. Morimoto, K. Hirano, T. Satoh and M. Miura, *Org. Lett.*, 2010, **12**, 2068.
49. N. Guimond, C. Gouliaras and K. Fagnou, *J. Am. Chem. Soc.*, 2010, **132**, 6908.
50. N. Guimond, S. I. Gorelsky and K. Fagnou, *J. Am. Chem. Soc.*, 2011, **133**, 6449.
51. X. Xu, Y. Liu and C. Park, *Angew. Chem. Int. Ed.*, 2012, **51**, 9372.
52. X. Li and M. Zhao, *J. Org. Chem.*, 2011, **76**, 8530.
53. W. Ma, K. Graczyk and L. Ackermann, *Org. Lett.*, 2012, **14**, 6318.
54. M. Shimizu, K. Hirano, T. Satoh and M. Miura, *J. Org. Chem.*, 2009, **74**, 3478.
55. S. Mochida, K. Hirano, T. Satoh and M. Miura, *J. Org. Chem.*, 2009, **74**, 6295.
56. N. Umeda, K. Hirano, T. Satoh and M. Miura, *J. Org. Chem.*, 2009, **74**, 7094.
57. H. Wang and F. Glorius, *Angew. Chem. Int. Ed.*, 2012, **51**, 7318.
58. E. Clar, *Polycyclic Hydrocarbons*, Academic Press, London, 1964.
59. Y. Kashiwame, S. Kuwata and T. Ikariya, *Chem. Eur. J.*, 2010, **16**, 766.
60. M. A. Bennett, S. A. Macgregor and E. Wenger, *Helv. Chim. Acta*, 2001, **84**, 3084.
61. A. J. Edwards, S. A. Macgregor, A. D. Rae, E. Wenger and A. C. Willis, *Organometallics*, 2001, **20**, 2864.
62. S. A. Macgregor and E. Wenger, *Organometallics*, 2002, **21**, 1278.
63. C. White, S. J. Thompson and P. M. Maitlis, *J. Chem. Soc. Dalton Trans.*, 1977, 1654.
64. A. K. Pleier, H. Glas, M. Grosche, P. Sirsch and W. R. Thiel, *Synthesis-Stuttgart*, 2001, 55.
65. F. Texier-Boullet, B. Klein and J. Hamelin, *Synthesis-Stuttgart*, 1986, 409.
66. S. Guillou, F. J. Bonhomme, M. S. Ermolenko and Y. L. Janin, *Tetrahedron*, 2011, **67**, 8451.
67. J. H. Li, Y. Liang and Y. X. Xie, *J. Org. Chem.*, 2005, **70**, 4393.

Chapter Three

Oxidative Coupling of Phenylpyrazoles with Alkenes

3 Chapter Three

3.1 Introduction

Coupling reactions of various directing groups and alkynes via AMLA C-H activation for the formation of carbocycles and heterocycles were explored in **Chapter Two**. This introduction will deal with similar reactions with alkenes. An overview of stoichiometric alkene insertions into cyclometallated complexes is given followed by selected examples of catalytic coupling with alkenes including a discussion on the different factors affecting product selectivity.

3.1.1 Stoichiometric Alkene Insertions

Pfeffer *et al.* first reported insertion of alkenes into cycloruthenated DMBA complexes in 2000.[1] The Ru-DMBA complexes (**3.1**) reacted with ethylene to give alkene-inserted complexes (**3.2**) and the organic vinylation compound (**3.3**), resulting from the β-hydrogen elimination, as the major products (**Scheme 3.1**). The ratios of the two products varied depending on solvent; use of the cationic complex **3.1b** gave a higher yield of **3.2b** compared to use of the chloride complex **3.1a**.

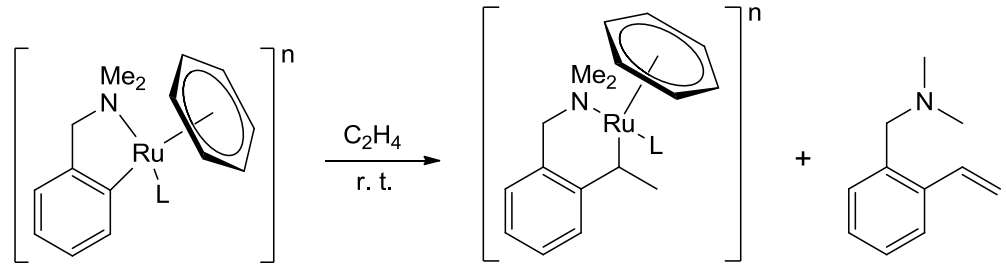

3.1a L = Cl, n = 0 **3.2a, 3.2b** **3.3**
3.1b L = MeCN, n = Cl

Scheme 3.1: Reaction of cycloruthenated DMBA complexes with ethylene.[1]

Interestingly, complexes **3.2** are six-membered metallacycles as opposed to seven-membered metallacycles which usually forms in stoichiometric alkyne insertions (see **Chapter 2**, **Section 2.3**). A likely mechanism for the formation of **3.2** and **3.3** is depicted in **Scheme 3.2**. Insertion of ethylene into **3.1** initially gives a seven-membered metallacycle which undergoes β-hydride elimination to give an alkene-hydride complex. This can then undergo reinsertion to give **3.2** or ligand dissociation can occur

to give **3.3**. The authors concluded that the coordination of L controlled the outcome of the reaction. If L displaces the alkene from coordination in the intermediate after β-hydrogen elimination, **3.3** is formed. However, if reinsertion occurs before re-coordination of L, **3.2** is formed.

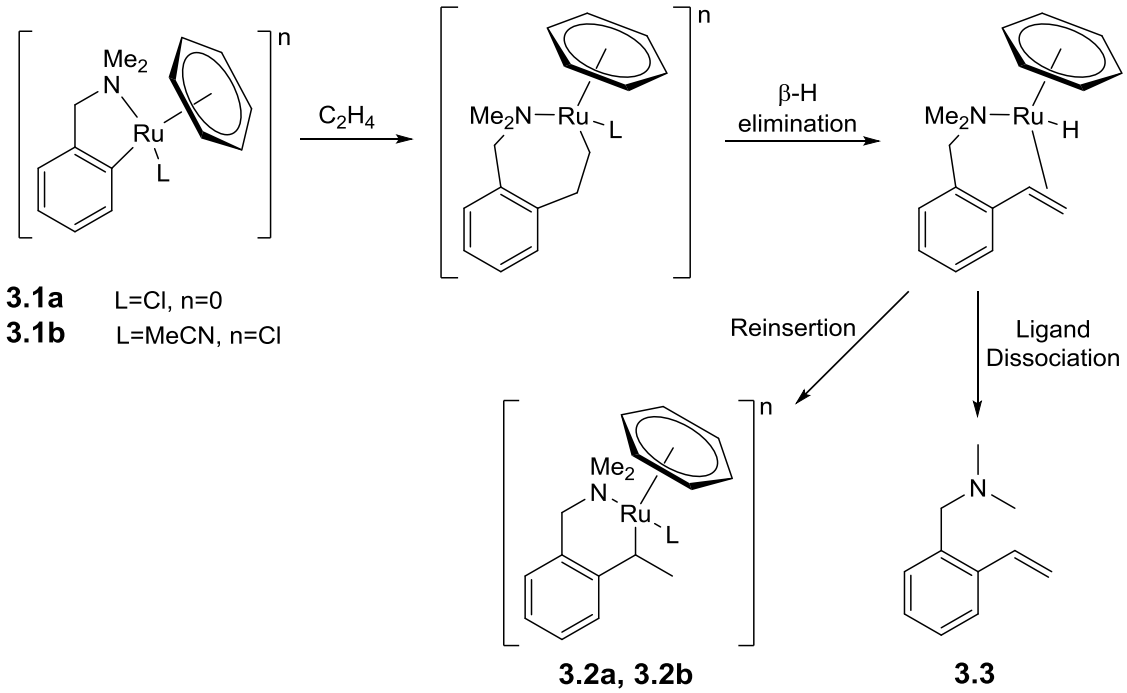

Scheme 3.2: Possible pathway for formation of **3.2** and **3.3**.[1, 2]

A similar insertion of propylene into **3.1** required the reaction to be carried out at 45 °C and after 3 hours gave **3.4** in good yield (**Scheme 3.3**).[2] After some time, **3.4** reacted further with another equivalent of propylene to give **3.5**. The regioselectivity of these propylene insertions is interesting in that **3.4** results from an unconventional insertion of propylene with the methyl next to phenyl rather than next to the metal, followed by β-hydrogen elimination and reinsertion. **3.5** presumably results from **3.4** via a conventional alkene insertion with the methyl next to the metal followed by β-hydrogen elimination and reinsertion. It is not clear why insertion occurs one way round to form **3.4** and then the opposite way round to form **3.5** (**Scheme 3.3**).

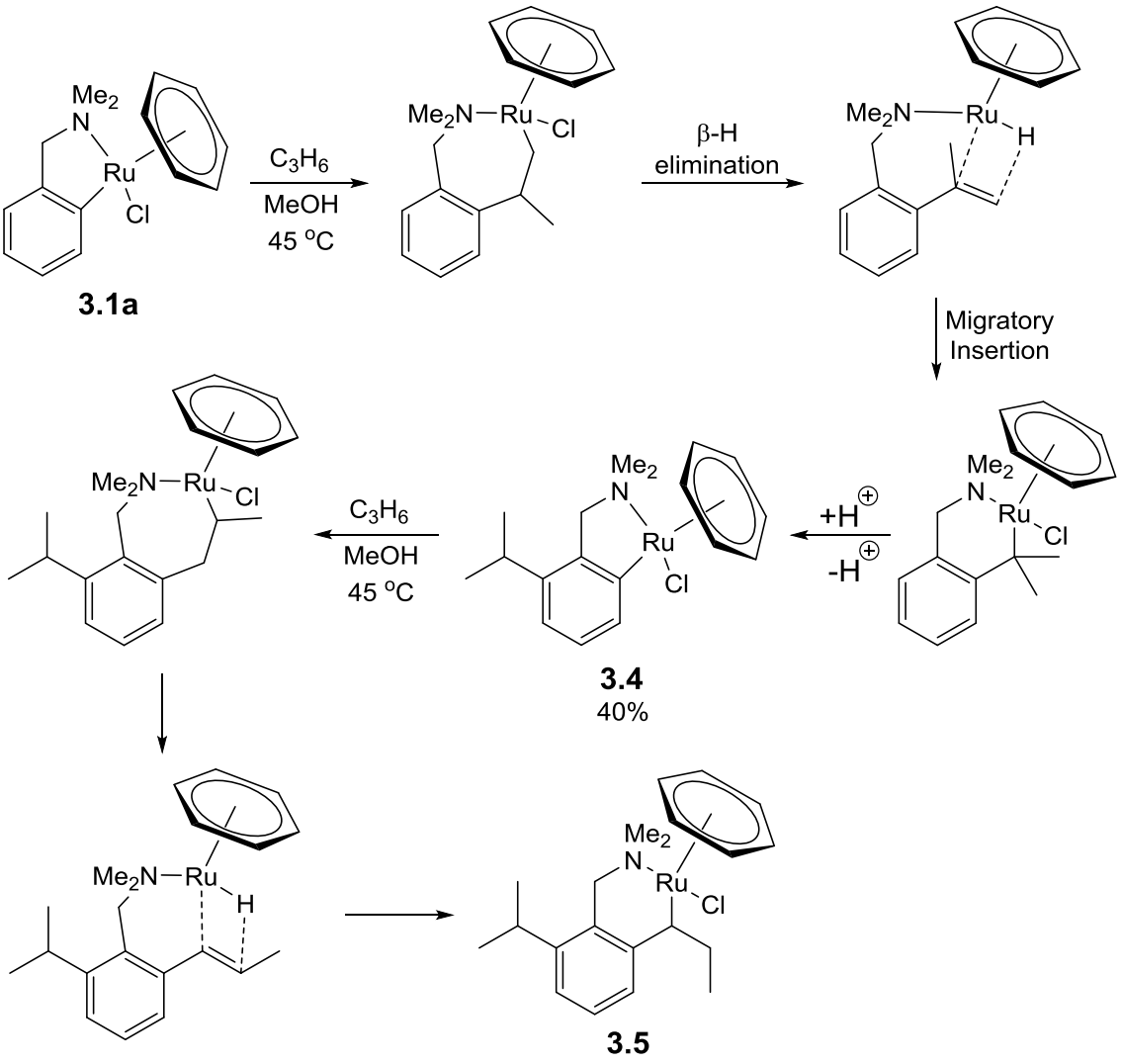

Scheme 3.3: Insertion of propylene into **3.1**.[2]

Ethylene and propylene insertions were later investigated by the group of Jones for cyclometallated pyridine and imine complexes of Ir and Rh (**Scheme 3.4**).[3] Reactions with ethylene showed that only coordination occurred with cyclometallated Ir complexes whereas insertion occurred with the analogous Rh complexes.[3] As for the Ru complexes mentioned above, the insertion product (**3.7**) is formed via an insertion, β-H elimination and reinsertion sequence. Complexes **3.6** and **3.7** did not react further with ethylene to give any di-inserted products which is unlike the case with the Ru-DMBA complexes and propylene described earlier.

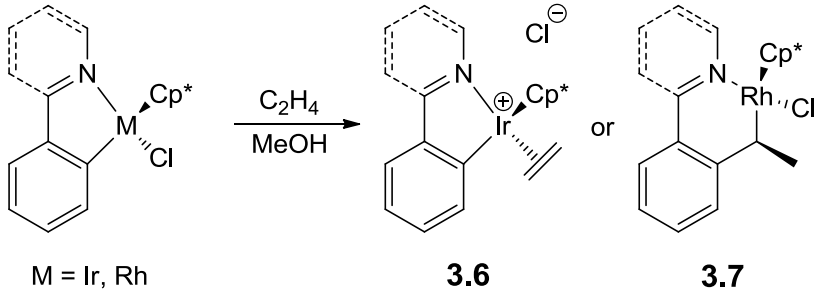

Scheme 3.4: Reaction of cyclometallated complexes of Ir and Rh with ethylene.[3]

Reactions with propylene gave similar results where only coordination occurred with Ir complexes and insertion occurred with the analogous Rh complexes.[3] The insertion product (**3.8**) is formed via a propylene insertion, β-H elimination and reinsertion from the alkene-hydride complex (**Scheme 3.5**). This is the same sequence as that described for Ru earlier (**Scheme 3.3**) except the regioselectivity of the first alkene insertion is different. In this case the propylene inserts with the methyl next to the metal but in the first insertion with Ru it inserted next to the phenyl.

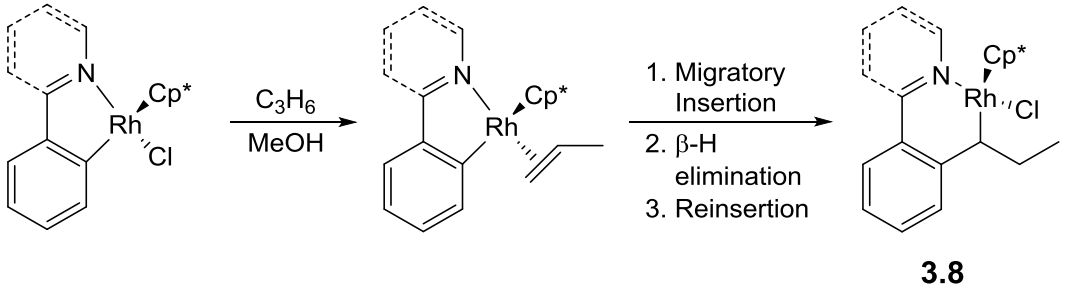

Scheme 3.5: Reaction of propylene with cyclometallated Rh complexes.[3]

Overall, limited stoichiometric alkene reactions have been reported. Ethylene and propylene react with Ir, Rh and Ru cyclometallated complexes however only coordination occurs with Ir complexes. Jones *et al.* suggested that since Ir-C bonds are stronger than Rh-C bonds, alkene insertion does not take place for iridium. The isolated insertion products contain six-membered rings probably formed by rearrangement of initially formed 7-membered ring products. Ru complexes can react further to give di-inserted complexes or β-hydrogen elimination can occur to give purely organic compounds.

3.1.2 Catalytic AMLA Coupling Reactions with Alkenes

Chapter Two covered catalytic AMLA coupling reactions with alkynes. In the last few years alkene catalysis incorporating AMLA C-H activation has been extensively studied. The general catalytic cycle for most coupling reactions of anionic directing groups with alkenes is shown in **Scheme 3.6**. The early stages of the catalytic cycle, namely Y-H (Y = O, N) activation and C-H activation are exactly the same as with alkyne catalysis (see **Chapter Two**, **Section 2.5**, **Scheme 2.14**). These are followed by alkene association and then regioselective migratory insertion, where the substituted carbon atom ends up next to the metal as found in reported Heck reactions.[4] After the insertion step C-Y reductive elimination is a possibility, however it is disfavoured and β-H elimination usually occurs instead (see later) to give a metal hydride species. If the directing group is anionic, reductive elimination occurs which leads to a vinylic product that can react further and the metal is reoxidised by copper.

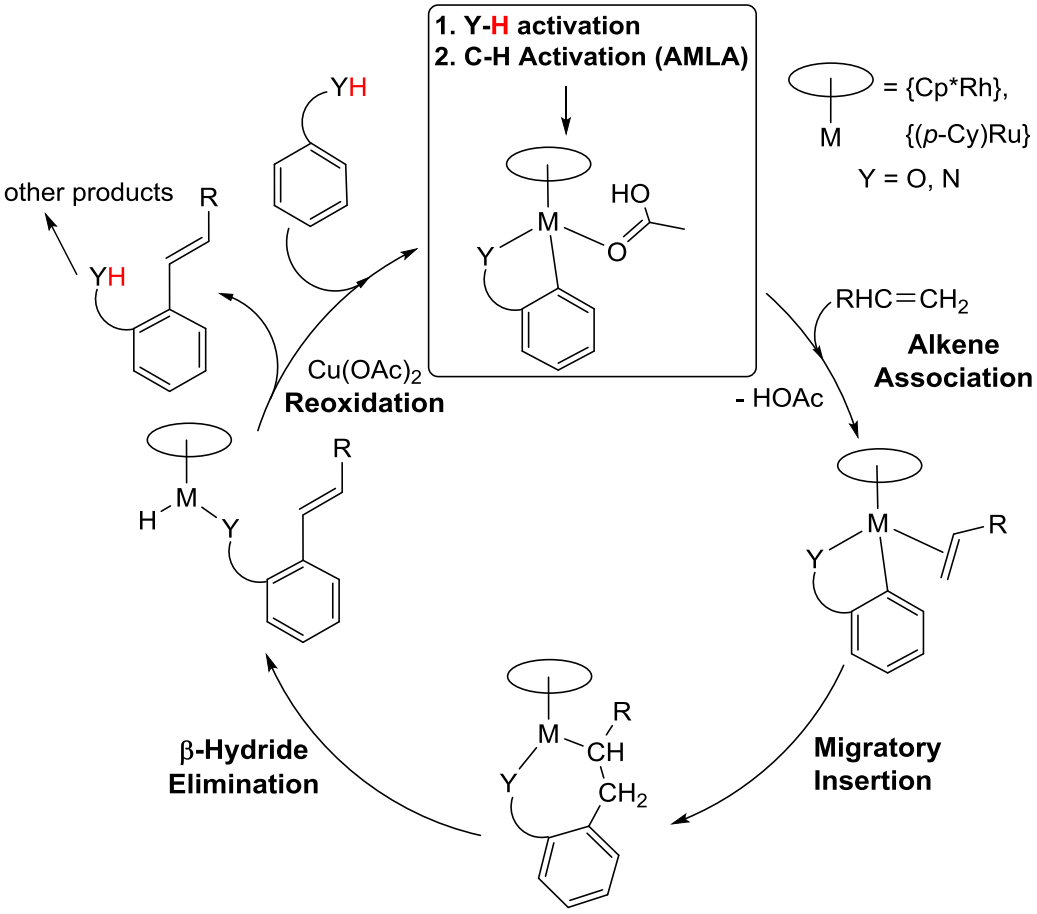

Scheme 3.6: General catalytic cycle for coupling of anionic directing groups with alkenes.

The general catalytic cycle for most coupling reactions of neutral directing groups with alkenes is shown in **Scheme 3.7**. The catalytic cycle is similar to above, namely coordination of Y (Y = O, N) with no Y-H activation, then C-H activation (see **Chapter Two**, **Section 2.5**, **Scheme 2.15**). These are followed by alkene association, migratory insertion and β-H elimination steps as with anionic substrates. However the directing group is neutral, therefore simple ligand dissociation can occur to give a vinylic product that can react further, leaving $[Cp^*RhH]^+$ which can re-enter the catalytic cycle.

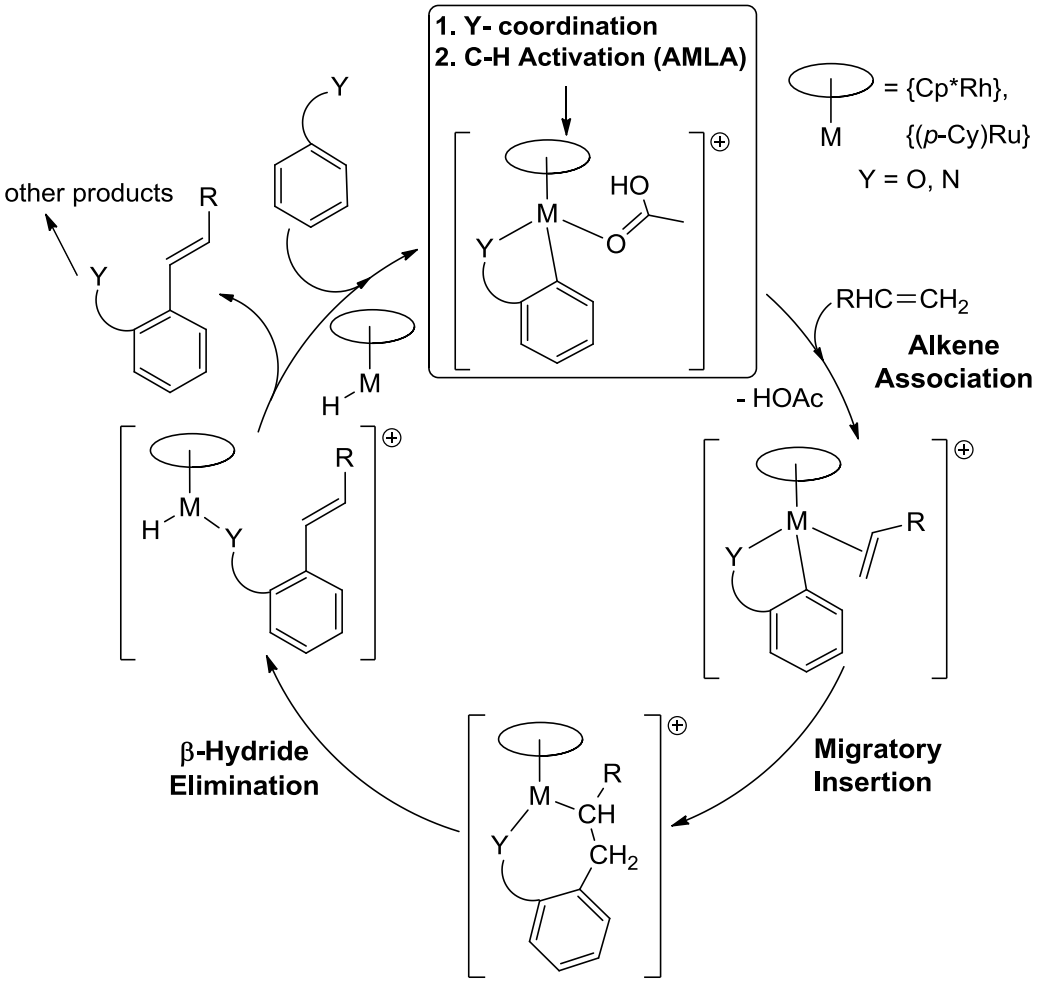

Scheme 3.7: General catalytic cycle for coupling of neutral directing groups with alkenes.

In most cases, alkene catalysis leads to vinylic products as opposed to alkyne catalysis which gives heterocycles or carbocycles as products. The initial vinylic products (**3.9**) can potentially coordinate via the Y (Y = O, N) atom and react further to give a divinyl compound (**3.10**) (**Scheme 3.8**). Moreover, if the directing group is a YH (Y = O, N)

and if R is electron withdrawing, **3.9** or **3.10** may undergo a Michael reaction to give a cyclised compound **3.12** or **3.11** respectively.

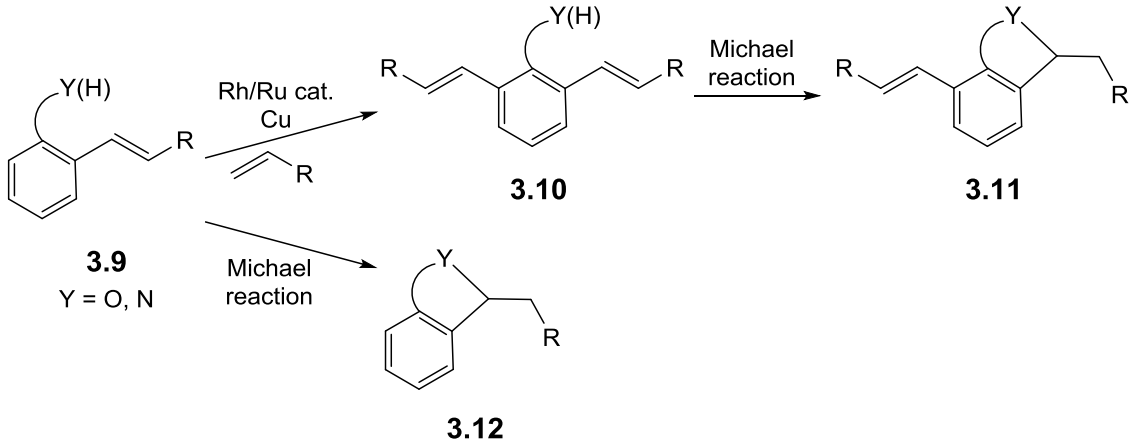

Scheme 3.8: Further reactions from vinylic product **3.9**.

A few examples of catalysis involving alkene insertion are discussed below. An early study by the group of Miura involved the Cp*Rh-catalysed reaction of alkenes with *N*-phenylpyrazoles (**Scheme 3.9**).[5] Only vinylic products were formed as *N*-phenylpyrazole is a neutral directing group and so does not contain an N-H proton for cyclisation by aza Michael addition to occur. When the alkene was the limiting reagent, only monovinylation occurred, however, when the alkene was used in excess, only the divinyl product was observed. This observation enabled the group to carry out further reactions to install two different vinyl groups onto the substrate in a simple stepwise process.

In a later study using $[(p\text{-Cy})RuCl_2]_2$ as catalyst, it was found that monovinylation occurred selectively even when excess alkene was used and divinylation was only detected in trace amounts in a few cases.[6] Tertiary benzamides and their derivatives have also been shown to only give vinylic products[7-9] and a DFT study in 2013 on these reactions supported AMLA/CMD C-H activation taking place in the catalytic cycle.[10]

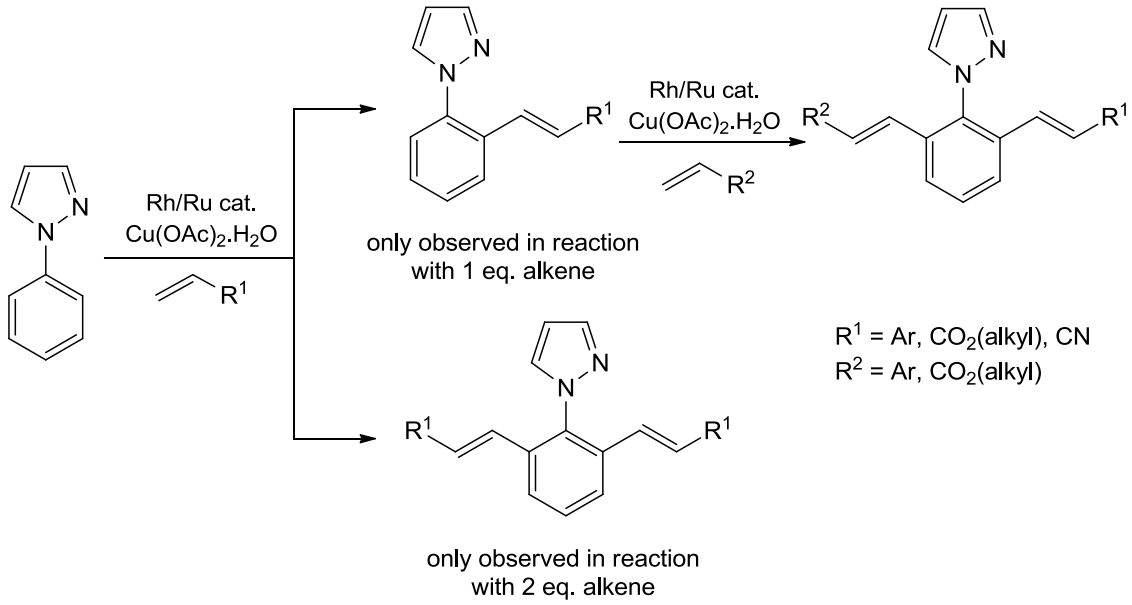

Scheme 3.9: Mono- and divinylation of *N*-phenylpyrazoles.[5, 6]

Anionic directing groups such as benzoic and acrylic acids were also reported in early studies on catalysis with alkenes.[11-13] Benzoic acids reacted with excess alkene to give products of type **3.11** (**Scheme 3.8**) where divinylation followed by cyclisation occurred (**Scheme 3.10 A**). Also, a small amount of the dehydrogenated isomer of the major product was recovered. Acrylic acids reacted with excess alkene to give butenolide products where vinylation followed by cyclisation occurred (**Scheme 3.10 B**).

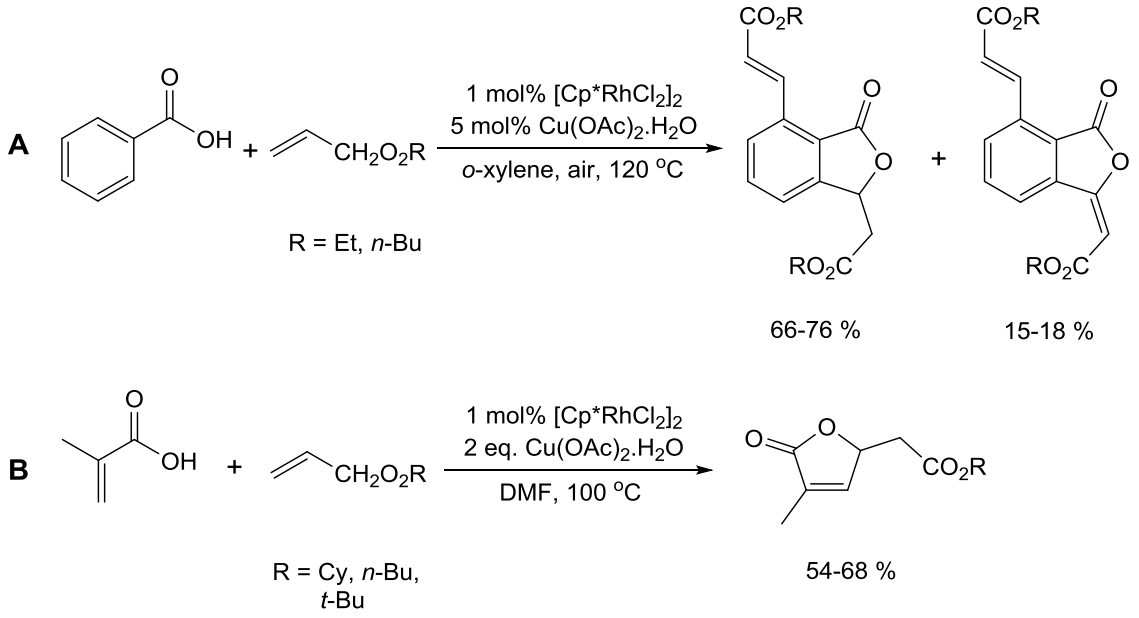

Scheme 3.10: Cp*Rh-catalysed reaction of benzoic acids (**A**) and acrylic acids (**B**) with an excess of alkenes.[11-13]

In general, these reactions gave cyclised products because the substrates have a protic directing group O-H which can be easily deprotonated, leading to cyclisation by Michael addition. Furthermore, acrylates were used as the alkenes which are good Michael acceptors. Similar results have been observed in Cp*Rh-catalysed reactions of primary and secondary benzamides where cyclisation occurred when using good Michael acceptors and vinylation occurred when the alkene substituent was a simple aryl or alkyl.[9, 14-17] Similarly, Cp*Rh-catalysed reactions of heteroaryl amides with acrylates were reported to produce similar cyclised products of types **3.11** and **3.12**.[18] Additionally, both Cp*Rh and (*p*-Cy)Ru complexes have been shown to successfully catalyse the vinylation of acrylamides which involves AMLA C-H activation of vinyl sp^2 C-H bonds.[19] Interestingly, no cyclisation was observed even when acrylates were used as the alkene.

As discussed for alkyne reactions (**Chapter 2**, **Section 2.5)**, an internal oxidant also works for alkenes (**Scheme 3.11**).[20] More importantly, these reactions gave rise to dihydroisoquinolone products (**3.13a** and **3.13b**) arising from alkene insertion and C (sp^3), N reductive elimination (**Scheme 3.11**). A mixture of regioisomers was obtained when R ≠ H. The reaction was highly selective (20:1) for the sp^2 substituents (R = Ph, CO_2Me) to be on the carbon next to the nitrogen (**3.13a**), as found with alkyne catalysis. However the reaction was less selective (~2:1, **3.13a**:**3.13b**) for the alkenes with sp^3 substituents (R = CH_2OH, CH_2Ph). This methodology also gave the first examples of the reaction with cyclic alkenes such as cyclohexadiene and norbornadiene, however the reaction did not work with acyclic internal alkenes.

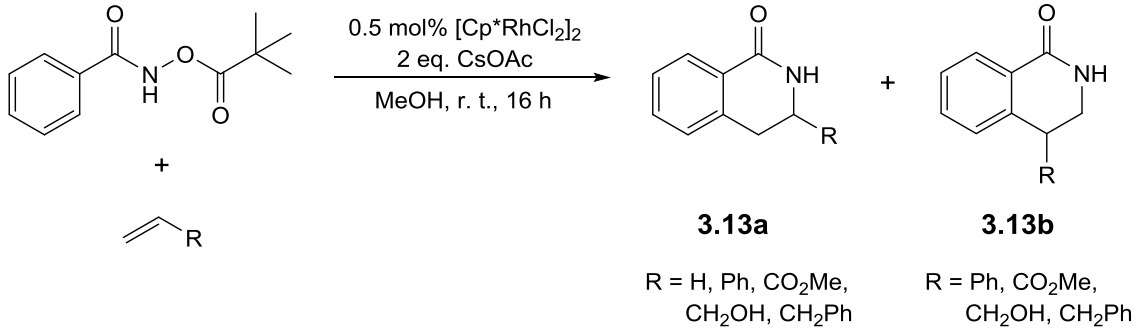

Scheme 3.11: Formation of dihydroisoquinolones from *N*-pivaloyloxy benzamide.[20]

Similar results were reported by Cramer's group in their study of benzamides with an internal oxidant using a Rh catalyst bearing a chiral Cp ring to give enantioselective alkene insertions.[21] In 2012, the group of Glorius reported the Cp*Rh-catalysed reaction of *N*-pivaloyloxy benzamides and their heterocyclic derivatives with allenes to give dihydroisoquinolones.[22] A recent DFT study by Xia *et al.* on alkene catalysis with *N*-pivaloyloxy benzamides showed that after alkene insertion coordination of the OPiv moiety to the Rh centre stabilises the intermediate and makes β-H elimination higher in energy than C, N reductive elimination, leading to dihydroisoquinolone products.[23]

In conclusion, very few examples of catalytic CH activation followed by alkene insertion were reported before 2010, though extensive progress has been made since then. Both neutral and anionic directing groups have been reported to react with alkenes. Mono- and divinylation of substrates can occur depending on the substrate and on the equivalents of alkene used. In addition, protic directing groups can react to give cyclised products due to vinylation followed by a Michael reaction, particularly when the alkenes used are good Michael acceptors. For substrates with an internal oxidant, C-Y (Y = N, O) bond formation occurs, leading to heterocyclic products. In some cases, internal oxidants also allow the use of cyclic alkenes.

3.2 Results and Discussion

The reactions of *C*-phenylpyrazoles **2.43a**-**2.43d** with alkenes were tested using the same reaction conditions as for alkyne catalysis and with selected examples with ruthenium catalysis. The results are divided according to the type of alkene, methyl acrylate (**a**), styrene (**b**), methyl vinyl ketone (**c**) and crotonaldehyde (**d**). Unless otherwise stated, the products were all fully characterised by ESIMS, HRMS and ^{1}H, ^{13}C, COSY, NOESY and HMQC NMR spectroscopy.

Methyl Acrylate

Reaction of **2.43a** with methyl acrylate (**a**) (**Scheme 3.12**) led to a mixture of four products which were purified by column chromatography. The ^{1}H NMR spectrum for the major component shows signals for four protons in the aromatic region and a singlet for the pyrazole at δ 6.41 suggesting that one C-H has been functionalised. Two 3H singlets at δ 2.33 and δ 3.81 are assigned to the methyl group on the pyrazole and the OMe group respectively. There are also two mutually coupled 1H doublets at δ 5.06 and δ 6.47 (J = 13.7 Hz) assigned to a *cis* alkene suggesting that one equivalent of methyl acrylate (**a**) has reacted with **2.43a**. The 1H doublet at δ 5.06 shows an NOE to a phenyl proton from the starting substrate and also to the pyrazole methyl so is assigned to the CH next to the aryl rather than next to the CO_2Me. The ^{13}C NMR spectrum shows 14 signals as expected. The ESIMS shows an ion at *m/z* 243 due to $[M+H]^+$ and HRMS (ES) is correct for the monovinyl product, **3.14aa′** (**Scheme 3.12**).

The ^{1}H NMR spectrum for one of the minor products is very similar to that of **3.14aa′** except the vinyl protons are observed as two 1H doublets at δ 6.39 and δ 8.13 with a coupling of 16.0 Hz, compared to δ 5.06 and δ 6.47 with a coupling of 13.7 Hz in **3.14aa′**. Thus, the chemical shifts of the vinyl protons are considerably downfield compared with **3.14aa′**, hence this compound is assigned as the *trans* isomer **3.14aa** which was isolated in 14% yield (**Scheme 3.12**). As expected ESIMS shows an ion at *m/z* 243 due to $[M+H]^+$ the same as for **3.14aa'**. The vinyl proton next to the CO_2Me group is assigned as the 1H doublet at δ 8.13 as it showed a long-range correlation to the C=O carbon signal. Both vinyl protons show an NOE to the CO_2Me signal as expected.

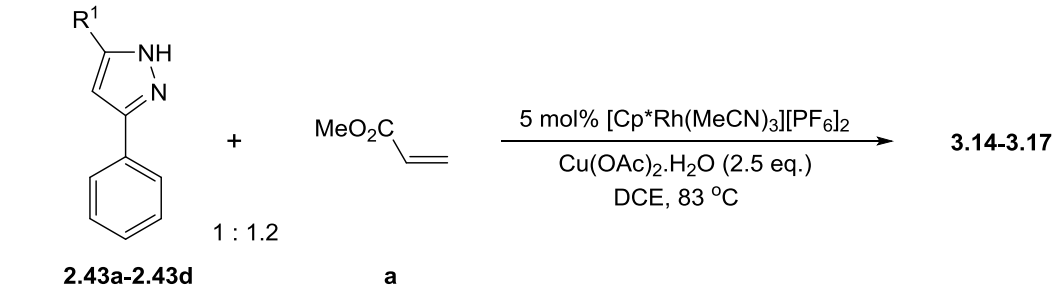

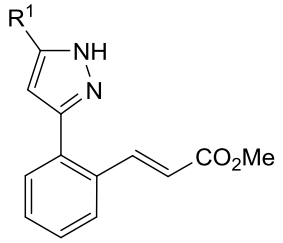

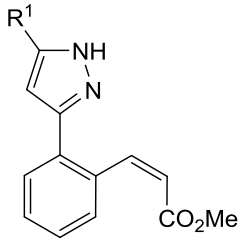

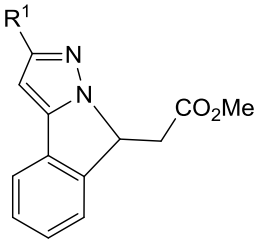

3.14aa (R^1 = Me)	14%	**3.14aa'** (R^1 = Me)	51%	**3.15aa** (R^1 = Me)	17%
3.14ba (R^1 = H)	trace	**3.14da'** (R^1 = CF_3)	11%	**3.15ba** (R^1 = H)	trace
3.14ca (R^1 = Ph)	35%			**3.15ca** (R^1 = Ph)	4%
3.14da (R^1 = CF_3)	73%			**3.15da** (R^1 = CF_3)	trace

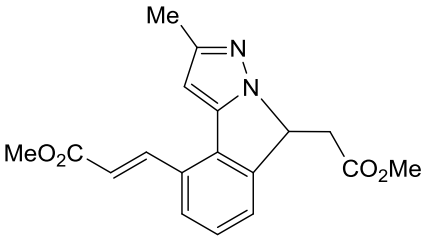

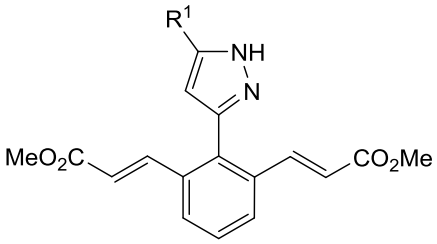

3.16aa (R^1 = Me) 16%

3.17aa (R^1 = Me) 23%[a]

3.17ca (R^1 = Ph) 15%

[a] only observed in some cases

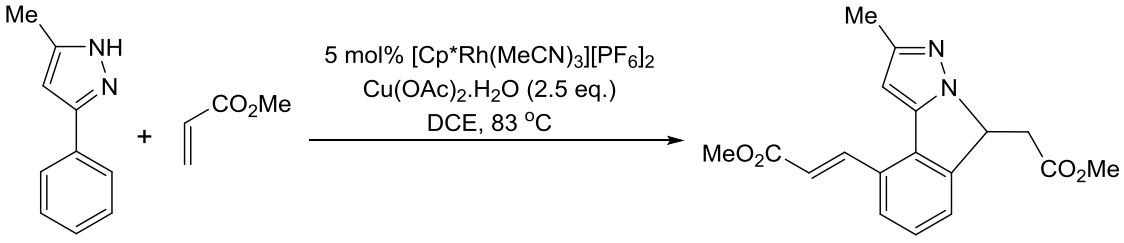

2.43a

1 : 2.2

3.16aa 86%

Scheme 3.12: C-H functionalisation of pyrazoles with 1.2 or 2.2 equivalents of methyl acrylate **a**.

The ^{1}H NMR spectrum for the second minor product shows two doublets and two triplets corresponding to 4H in the aromatic region. The expected 1H and 3H singlets for the pyrazole are present as is a 3H singlet at δ 3.77 corresponding to a CO_2Me group. In addition there are three mutually coupled doublets of doublets at δ 5.49, 3.30 and 2.77, each for 1H. Notably, none of the doublet of doublets signals show an NOE to a phenyl proton, which suggests this is not a six-membered saturated N-heterocyclic product, formed by C(sp^3)-N coupling. DFT calculations suggest C(sp^3)-N reductive elimination would be too high in energy (see Computational Studies later). The ^{13}C NMR spectra show the presence of a CH group at δ 58.8 which correlates (HMQC) with the ^{1}H NMR signal at δ 5.49, and a CH_2 group at δ 38.7 which correlates with the signals at δ 3.30 and 2.77; hence, these data show the presence of a $CHCH_2$ group. Furthermore, the two CH_2 signals show a long-range correlation to the C=O carbon signal, suggesting that the CH_2 carbon is next to the C=O carbon. The HRMS shows the same mass as the vinyl complexes. Based on these data and the crystal structure of related compound **3.15ca** (see later), the structure was deduced to be the five-membered heterocyclic compound **3.15aa** (**Scheme 3.12**) formed from **3.14aa** and/or **3.14aa′** by an intramolecular Michael reaction. Pyrazoles have been reported to undergo aza-Michael additions using various organocatalysts.[24, 25] Indeed Rh could possibly catalyse the reaction as found with the reaction of amines with ethylene.[26]

The ^{1}H NMR spectrum for the final compound shows a triplet and two doublets between δ 7.30 and 7.60 for three phenyl protons and two singlets at δ 6.36 (1H) and 2.38 (3H) for the pyrazole. In addition there are two 3H singlets at δ 3.76 and 3.85 for two CO_2Me groups, suggesting that two equivalents of methyl acrylate (**a**) have reacted with **2.43a**. There are two mutually coupled doublets at δ 6.52 and δ 8.04 (J = 16.0 Hz) assigned to a *trans* alkene. Both the doublets show an NOE to a phenyl proton and to one of the CO_2Me signals. Additionally there are three mutually coupled 1H doublets of doublets at δ 2.70, 3.22 and 5.42 similar to **3.15aa,** that all show an NOE to the other CO_2Me signal. The HMQC and ^{13}C APT NMR spectra show that these three doublet of doublets correspond to a $CHCH_2$ group. ESIMS shows an ion at *m/z* 327 assigned to $[M+H]^+$. Based on these data, the structure of the product was deduced to be the cyclic monovinyl compound **3.16aa**. This product arises by formation of the divinylation product **3.17aa** (see below) followed by an aza-Michael cyclisation. This product could

be independently prepared in 86% yield by the reaction of **2.43a** with 2.2 equivalents of methyl acrylate (**Scheme 3.12**). During the course of this work Li *et al.* carried out reactions of **2.43b** with two equivalents of acrylate to form cyclic monovinyl products of type **3.16** (**Scheme 3.12**) however they used ethyl and butyl acrylate.[27]

On some occasions the divinyl product **3.17aa** was also observed as a product after chromatography. The ^{1}H NMR spectrum for this product shows a 3H singlet at δ 2.25 for the pyrazole methyl and a 6H singlet at δ 3.65 for two equivalent CO_2Me substituents suggesting two equivalents of methyl acrylate (**a**) have reacted with **2.43a**. A singlet at δ 5.98 is assigned as the pyrazole proton. There are two mutually coupled doublets corresponding to four vinyl protons, one at δ 6.26 (J = 15.7 Hz) and the other at δ 7.59 (part of a 4H multiplet). The low field shift and large coupling constant, suggesting a *trans* vinyl. Two of the aromatic protons overlap with the doublet at δ 7.59, the other aromatic proton is observed as a 1H triplet at δ 7.33. The HRMS (ES) is consistent with $[M+H]^+$. Based on these data, the structure of the minor product was deduced to be the symmetrical *trans* divinyl compound **3.17aa** (**Scheme 3.12**). This compound was unstable in solution and readily isomerised to **3.16aa** via a non-catalysed Michael addition within two days. The cyclisation of divinyl compound **3.17aa** to **3.16aa** is easier than cyclisation of monovinyl compounds **3.14aa** and **3.14aa′** to **3.15aa** as the monovinyl compounds are stable in solution for longer than two days. All of the compounds observed from the reaction of **2.43a** with methyl acrylate (**a**) result from regioselective insertion of the alkene in the catalytic cycle where the CO_2Me substituent ends up next to the metal (see Computational Studies below).

Surprisingly, substrate **2.43b** (R^1 = H) showed only very low reactivity with methyl acrylate. In the ^{1}H NMR spectrum of the crude reaction mixture two mutually coupled doublets at δ 6.40 and δ 8.12 (both J = 16.0 Hz) are consistent with a trace amount of the *trans* monovinyl product and the mass spectrum showed an ion of the appropriate mass (*m/z* = 229). Additionally, three doublet of doublets are seen at δ 2.84 (J = 7.8, 16.4 Hz), δ 3.26 (J = 5.5, 16.4 Hz) and δ 5.57 (J = 5.5, 7.8 Hz) which are consistent with the cyclic product **3.15ba** which would also give *m/z* = 229 in the ESIMS. During the course of this work Li *et al.* reported reactions of substrate **2.43b** with one or two equivalents of acrylate which gave a product of type **3.16** (**Scheme 3.12**).[27] Their conditions involved the use of neutral $[Cp^*RhCl_2]_2$ catalyst at 120 °C with ethyl, butyl

and benzyl acrylates; they did not report methyl acrylate (**a**). As noted in **Chapter Two** substrate **2.43b** seems to show reduced reactivity with alkynes, this appears to also be the case with alkenes.

A similar reaction between **2.43c** and methyl acrylate (**a**) gave the corresponding monovinyl (**3.14ca**), cyclised (**3.15ca**) and divinyl (**3.17ca**) products in approximately a 3:3:1 crude ratio and the products were isolated in 54% combined yield. The aryl protons are difficult to fully assign in the ^{1}H NMR spectra of these products due to overlapping signals but the integrations still sum up to give the correct number of protons.

The alkene protons of **3.14ca** are observed in the ^{1}H NMR spectrum as two mutually coupled 1H doublets at δ 6.43 and δ 8.11 with a coupling constant of ca. 16.0 Hz and are assigned to *trans* vinyl protons. The corresponding protons in **3.17ca** are observed at δ 6.39 and δ 8.04, again with coupling constants of 16.0 Hz. The NH proton was also observed in this case at δ 10.27. For **3.15ca**, three 1H doublet of doublets are observed at δ 2.76, δ 3.29 and δ 5.55 showing that intramolecular Michael reaction has occurred as for **3.15aa** discussed above. In addition the structure of **3.15ca** was determined by X-ray diffraction (see **Fig. 3.1** later).

Reaction of **2.43d** with methyl acrylate (**a**) gave monovinyl compounds **3.14da** and **3.14da'** in 73% and 11% isolated yields respectively. In the major product the two vinyl protons appear as doublets at δ 6.42 and δ 7.81, with a coupling constant of 16.0 Hz, hence this is assigned as the *trans* isomer. In this case, the NH proton was observed at δ 11.52. The CF_3 carbon signal is visible as a quartet at δ 121.2 (J_{CF} = 270.6 Hz). For the *cis* isomer (**3.14da′**) the vinyl protons are observed as two 1H doublets more upfield at δ 5.26 and 6.71 with coupling constants of 14.1 Hz.

Styrene

Since the cationic catalyst $[Cp^*Rh(MeCN)_3][PF_6]_2$, gave increased reactivity with alkynes, reactions of substrates **2.43** with styrene (**b**) were attempted. Notably Li *et al.* reported that reactions of **2.43b** with styrene under their conditions failed.[27] The reaction of **2.43a** with styrene worked to give a mixture of mono- and divinyl products (**3.14ab** and **3.17ab**) in a 3:1 ratio and 80% overall yield which were purified by column chromatography. The ^{1}H NMR spectrum for the major component shows a 3H singlet at

δ 2.35 for the methyl group on the pyrazole. One vinyl proton is observed as a doublet at δ 7.06 (J = 16.0 Hz) which shows a COSY cross peak with a doublet at δ 7.45 (note this lies on top of a multiplet). The large coupling constant and chemical shifts are consistent with it being the *trans* vinyl compound **3.14ab**. The ESIMS shows an ion at *m/z* 261 due to $[M+H]^+$ consistent with the monovinyl compound **3.14ab** (**Scheme 3.13**). A minor component was also isolated but not fully characterised. The ESIMS shows an ion at *m/z* 363 due to $[M+H]^+$ and the HRMS (ESI) is consistent with the formula $C_{26}H_{23}N_2$ suggesting two equivalents of styrene (**b**) have reacted with **2.43a** to give the divinyl compound (**3.17ab**). As observed in reactions with methyl acrylate (**a**), products observed from reactions with styrene (**b**) result from regioselective insertion of the alkene where the Ph substituent ends up next to the metal

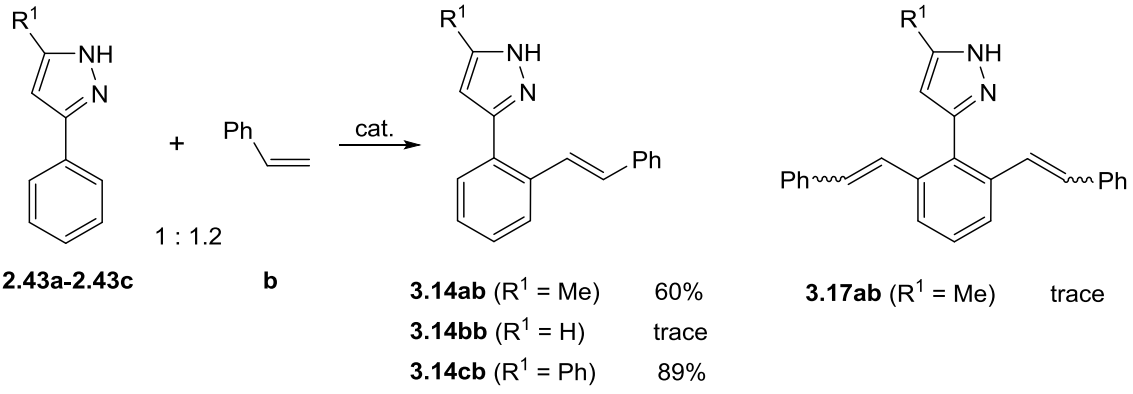

Reactions conditions: 5 mol% $[Cp^*Rh(MeCN)_3][PF_6]_2$, $Cu(OAc)_2.H_2O$ (2.5 eq.), DCE, 83 °C

Scheme 3.13: C-H functionalisation of pyrazoles with 1.2 equivalents of styrene (**b**).

The reaction of **2.43b** with styrene (**b**) was unsuccessful with only some evidence in the mass spectrum (*m/z* = 247) of the monovinyl product **3.14bb** but no evidence was obtained in the NMR spectrum. Li *et al.* were unable to isolate any products from the reaction of **2.43b** with styrene.[27]

The reaction of diphenyl pyrazole (**2.43c**) with styrene gave only the monovinyl product **3.14cb** in 89% yield. This was characterised by the same NMR and mass spectrometry techniques and all the expected signals were observed in the data. The two vinyl protons appear as doublets at δ 7.03 and δ 7.28, both with a *trans* coupling constant of 16.0 Hz. The NH proton is observed at δ 10.40. The ESIMS shows an ion at *m/z* 323 due to

$[M+H]^+$ and the HRMS (ESI) is consistent with the product being **3.14cb** (**Scheme 3.13**).

Overall, reactions of the pyrazoles with styrene gave monovinyl products as the major products in all cases. There was only one instance of a divinyl compound being observed as a minor product which was with pyrazole **2.43a**. The styrene insertion occurred regioselectively with the phenyl next to the metal. The results are less complicated when compared with reactions with methyl acrylate (**a**) since no cyclised products are observed consistent with the fact that styrene is not as good a Michael acceptor as methyl acrylate.

Methyl Vinyl Ketone

Reactions of **2.43a** and **2.43c** with methyl vinyl ketone (**c**) were next attempted. Reaction of **2.43a** with methyl vinyl ketone (**c**) gave the cyclised product **3.15ac** as the major product (70%) and a simple Michael addition product **3.18ac** as the minor product (8%) (**Scheme 3.14**). The ^{1}H NMR spectrum of **3.15ac** shows the expected 1H and 3H singlets for the pyrazole at δ 6.01 and δ 2.25 and an additional methyl at δ 2.07. In addition there are three mutually coupled doublets of doublets at δ 2.72 (J = 8.6, 18.0 Hz), 3.30 (J = 3.9, 18.0 Hz), and 5.41 (J = 3.9, 8.6 Hz) due to a $CHCH_2$ group, as seen in **3.15aa**, the signal at δ 5.41 being due to the proton next to the pyrazole nitrogen. The presence of the CH_2 group is confirmed by the HMQC spectrum which shows correlations from the doublet of doublets at δ 2.72 and δ 3.30 to the same carbon signal at δ 47.9.

For the simple Michael addition product (**3.18ac**), there are signals for five protons in the aromatic region due to the phenyl suggesting that C-H functionalisation has not occurred. A 1H singlet at δ 6.25 is assigned to the pyrazole proton and two 3H singlets at δ 2.13 and δ 2.30 to the two methyl groups. The pyrazole singlet shows an NOE to the 3H singlet at δ 2.30 which is therefore assigned as the pyrazole methyl. In addition there are two 2H triplets in the alkyl region for the two CH_2 units, both with a coupling constant of 6.7 Hz. The ^{13}C APT NMR spectrum confirms the presence of two CH_2 carbon atoms. The CH_2 triplet at δ 4.24 shows an NOE to the methyl signal of the pyrazole the other CH_2 triplet at δ 3.06 shows an NOE to the other methyl signal of the ketone. Hence the CH_2 triplet at δ 4.24 is assigned as the one next to the nitrogen which

is as expected on chemical shift grounds. The CH_2 triplets do not show an NOE to any phenyl protons, hence the alkyl chain must be on the nitrogen furthest away from the phenyl ring.

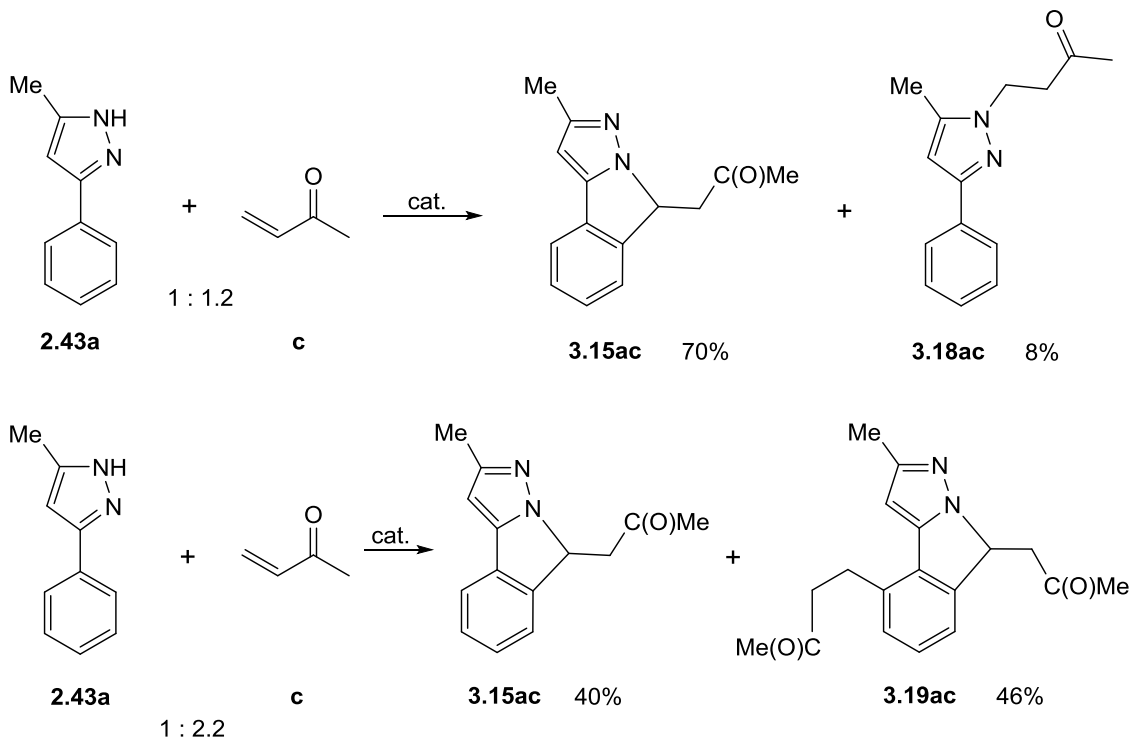

Reactions conditions: 5 mol% $[Cp^*Rh(MeCN)_3][PF_6]_2$, $Cu(OAc)_2.H_2O$ (2.5 eq.), DCE, 83 °C

Scheme 3.14: C-H functionalisation of **2.43a** with 1.2 or 2.2 equivalents of methyl vinyl ketone (**c**).

Reaction of **2.43a** with 2.2 equivalents of methyl vinyl ketone (**c**) gave two products in a roughly 1:1 ratio and 86% combined yield. One of the products isolated was cyclic compound **3.15ac** (40%) as found in the reaction with just 1.2 equivalents. The ^1H NMR spectrum for the second product shows only three signals in the aromatic region for the phenyl protons and a singlet at δ 6.12 for the pyrazole proton suggesting that two C-H activations have occurred. There are three 3H singlets between δ 2.17 and 2.37 due to methyl groups on the pyrazole and two from the alkene. In addition, there are multiplets for seven other protons. A doublet of doublets at δ 5.56 couples to doublets of doublets at δ 2.87 and 3.45, the latter two are clearly a CH_2 group as seen in the HMQC and ^{13}C APT spectrum. Hence these signals constitute a $CHCH_2$ unit formed by the aza-Michael reaction. Finally there are two triplets at δ 2.81 (J = 7.6 Hz) and δ 3.09 (J = 7.6 Hz) each for two protons that couple with each other according to the COSY

NMR spectrum; the HMQC confirms these are two CH_2 groups. ESIMS shows an ion at *m/z* 297 due to $[M+H]^+$ supporting that two equivalents of methyl vinyl ketone (**c**) have reacted with **2.43a**. Based on these data, the structure of the product was deduced to be the compound **3.19ac** which was obtained in 46% yield (**Scheme 3.14**).

Similarly **2.43c** gave solely **3.15cc** in very high yield (92%) (**Scheme 3.15**). This was characterised by the same NMR and mass spectrometry techniques and all the expected signals were observed in the data. The characteristic three doublets of doublets at δ 2.83, 3.46 and 5.59 confirm the presence of a $CHCH_2$ moiety formed by C-H activation followed by the aza-Michael reaction.

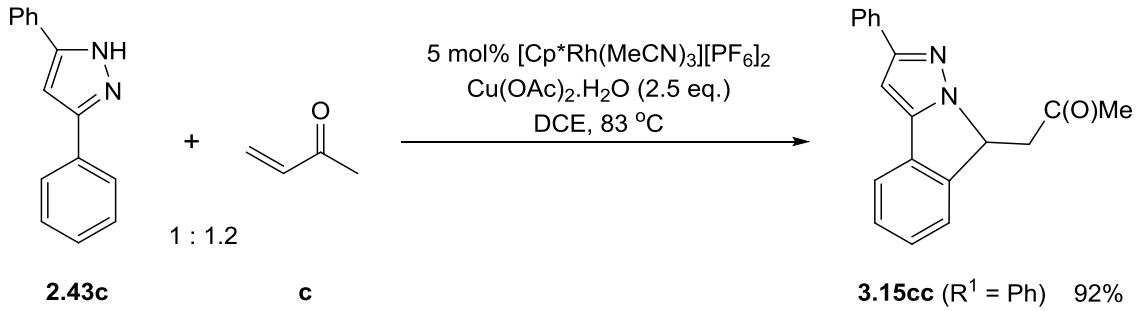

Scheme 3.15: C-H functionalisation of **2.43c** with 1.2 equivalents of methyl vinyl ketone (**c**).

It is likely that **3.15ac** forms via mono-vinylation followed by aza-Michael addition. In this reaction, there is competition between the catalytic reaction to form **3.15ac** and the direct aza-Michael addition to give **3.18ac**. In contrast, with methyl acrylate (**a**) monovinylation is mainly observed and the cyclic compound (**3.15aa**) formed from aza-Michael addition is only observed as a minor product. This is as expected since methyl vinyl ketone is a better Michael acceptor than methyl acrylate hence cyclisation to form **3.15cc** is faster than to form **3.15ac**. In addition because methyl acrylate is a weaker Michael acceptor there is no direct Michael reaction to form a product of type **3.18**. The results of the reaction of **2.43a** with 2.2 equivalents of methyl vinyl ketone can be explained by the mechanism shown in **Scheme 3.16**. C-H activation, alkene insertion and β-H elimination lead to an alkene-hydride complex (**3.20**). The alkene dissociates from the metal and, following rotation about the phenyl to pyrazole bond, a second C-H activation takes place. This is followed by a second alkene insertion to give **3.21** from which reductive elimination and addition of H_2 occur to give **3.22** that undergoes aza-

Michael addition to give **3.19ac**. The second alkene must add before the substrate dissociates from the metal since if it dissociates after one alkene insertion, it is likely to give **3.15ac** which has no directing group for the second C-H activation step. The higher concentration of alkene helps favour addition of the second alkene. In addition, in contrast to the reaction with 1.2 equivalents of alkene, excess alkene leads to less competition with the direct aza-Michael addition, so no **3.18ac** is formed. The reaction of **2.43a** with 2.2 equivalents of methyl acrylate was more selective than that with methyl vinyl ketone, giving just one product. In this case the monovinyl has much less tendency to cyclise so divinylation occurs, this then has a higher tendency to cyclise giving only one product (**3.16aa**).

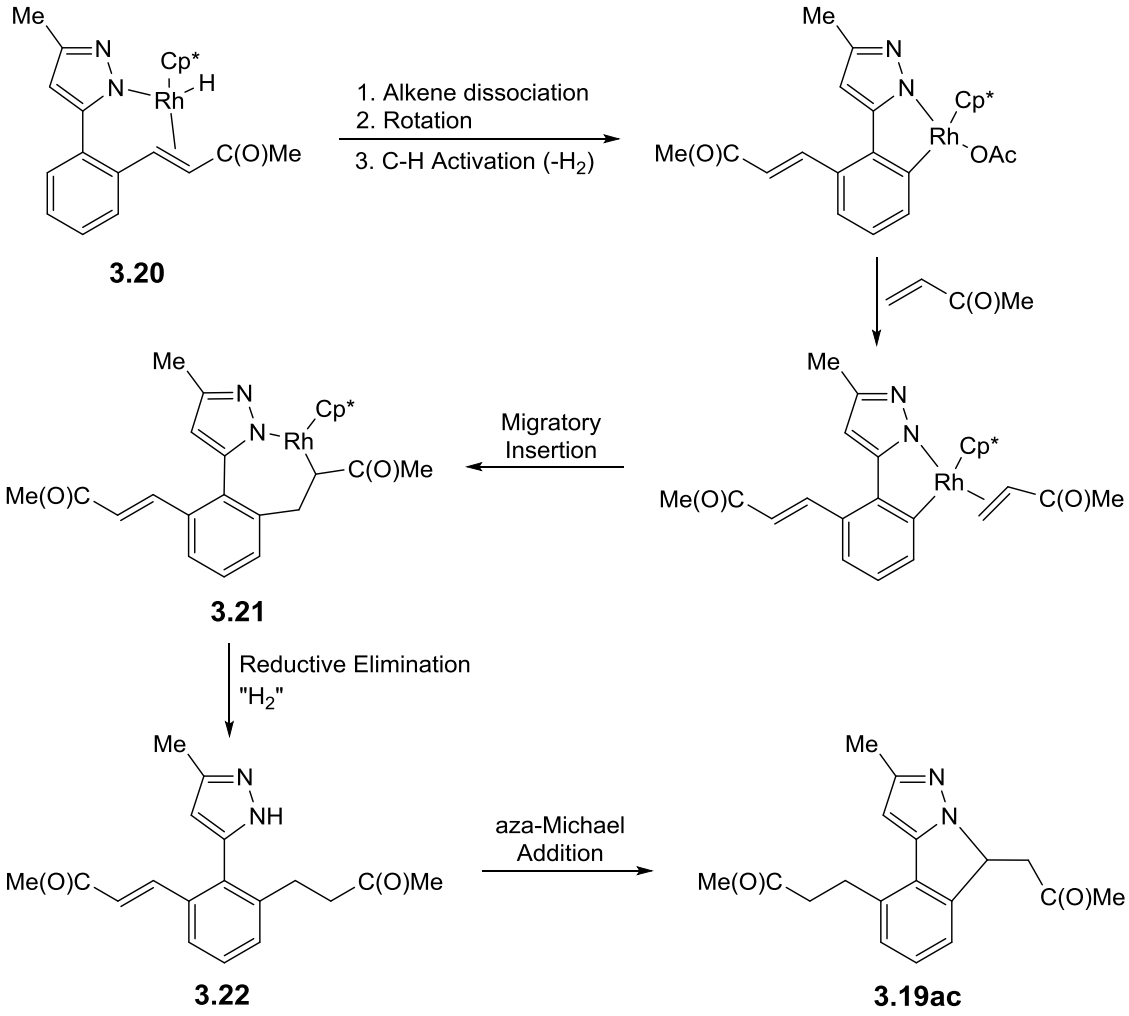

Scheme 3.16: Possible mechanism for formation of **3.19ac**.

Crotonaldehyde

Reaction of **2.43a** with internal alkene crotonaldehyde (**d**) was also attempted. The ^{1}H NMR spectrum of the product shows signals for five phenyl protons, so no C-H activation, and two singlets (1H and 3H) at δ 6.19 and 2.29 for the pyrazole. In addition there is a 1H singlet at δ 9.69, three 1H multiplets at δ 4.74, 3.38 and 2.83 and a 3H doublet at δ 1.42, suggesting that one equivalent of crotonaldehyde (**d**) has reacted with **2.43a**. The 3H doublet (J = 7.8 Hz) couples to the 1H multiplet at δ 4.74, which is assigned to the CH group next to nitrogen. The two doublet of doublets at δ 2.83 (J = 8.2, 16.8 Hz) and δ 3.38 (J = 5.1, 16.8 Hz) correspond to the two inequivalent CH_2 protons which, based on the COSY NMR spectrum, couple with each other and to the 1H multiplet at δ 4.74, and both of these correlate to the same carbon signal in the HMQC spectrum. Both CH_2 protons also show an NOE to the methyl doublet and the aldehyde proton at δ 9.69. The ESIMS shows an ion at *m/z* 229 due to $[M+H]^+$ consistent with the simple Michael addition product **3.24ad** (**Scheme 3.17**) which was isolated in 54% yield. None of the protons originally from the alkene show an NOE to any phenyl protons hence the alkyl chain is likely to be on the nitrogen furthest away from the phenyl ring. The formation of a simple aza-Michael addition product (**3.24ad**) from this reaction suggests that insertion of a disubstituted alkene is less favourable than a mono-substituted alkene.

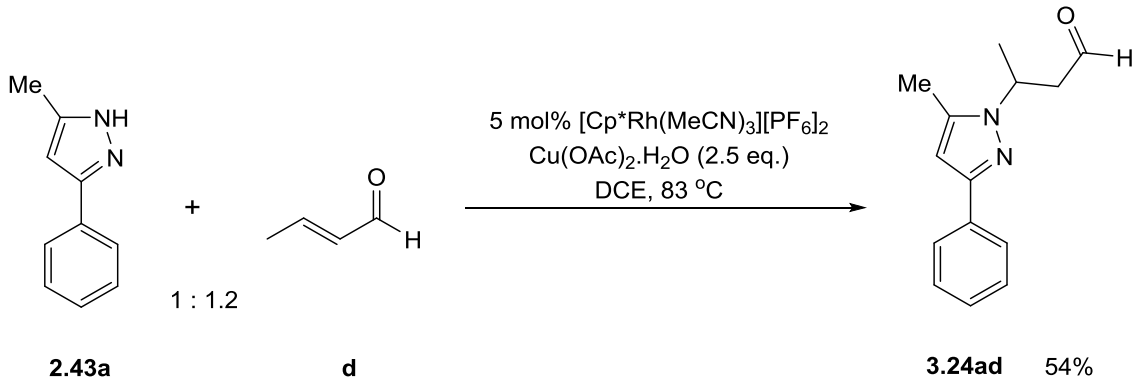

Scheme 3.17: Reaction of pyrazole **2.43a** with 1.2 equivalents of crotonaldehyde (**d**).

X-Ray Structures

Most of the products obtained in these reactions with alkenes are oils. However, crystals of **3.15ca** were obtained and the X-ray crystal structure is shown in **Fig. 3.1**. The structure clearly shows that one equivalent of methyl acrylate has reacted with **2.43c** and that an intramolecular Michael reaction has occurred to give a new 5-membered ring. The original alkene bond C(2)—C(3) is now a single bond (C-C = 1.515(4) Å - average).

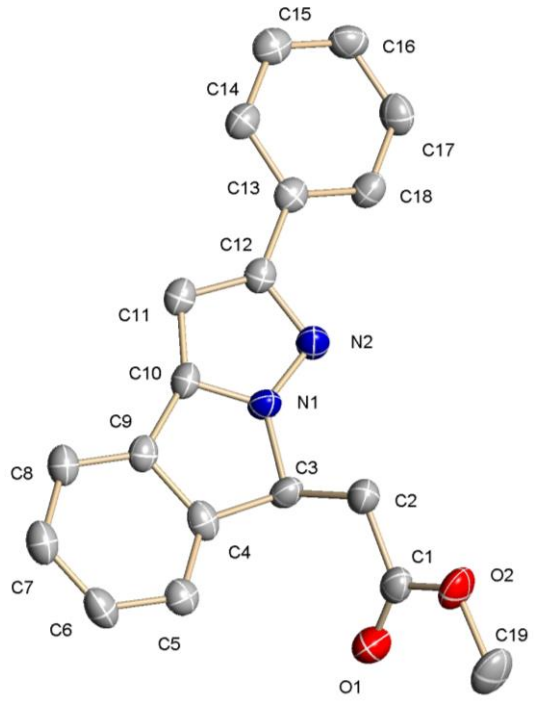

N(1)-C(3)	1.472(4)	C(4)-C(9)	1.422(5)
N(1)-C(10)	1.351(4)	C(9)-C(10)	1.456(4)
C(3)-C(4)	1.520(4)	C(2)-C(3)	1.515(4)
C(3)-N(1)-C(10)	115.3(3)	N(1)-C(3)-C(4)	99.4(3)
C(3)-C(4)-C(9)	110.7(3)	C(1)-C(2)-C(3)	112.2(3)

Fig. 3.1: Crystal structure of one of the two unique molecules of **3.15ca** with selected average bond distances (Å) and angles (°). Hydrogen atoms omitted for clarity.

Mechanistic Studies

All of the results described above are consistent with the mechanism shown in **Scheme 3.6**. C-H activation is followed by alkene insertion then β-hydride elimination and dissociation followed by reoxidation. Sometimes the vinyl product(s) reacts further via an intramolecular aza Michael reaction to give fused heterocycle products such as **3.15**, **3.16** and **3.19**. In order to gain further insight into the reaction mechanisms some further experiments and DFT studies have been carried out.

To confirm that **3.18ac** and **3.24ad** are formed via Michael addition taking place, the reactions of **2.43a** with 1.2 equivalents of **c** or **d** were repeated in the absence of $[Cp^*Rh(MeCN)_3][PF_6]_2$ and $Cu(OAc)_2.H_2O$. As expected, the reaction of **2.43a** with **c** proceeded to give **3.18ac** as the sole product in 94% isolated yield (**Scheme 3.18 A**). The reaction of **2.43a** with **d** gave **3.24ad** as the major product (56%) with minor products in trace amounts (**Scheme 3.18 B**). These results therefore confirm that **3.18ac** and **3.24ad** are formed via Michael addition without the need for Rh or Cu.

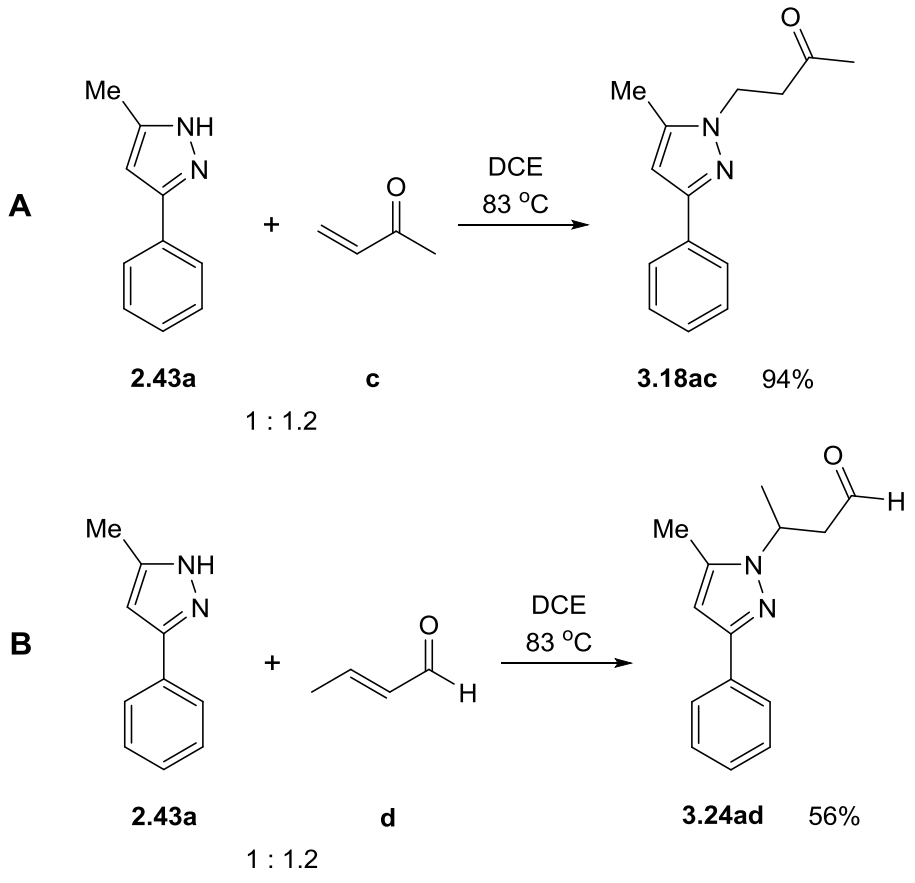

Scheme 3.18: Blank reactions of **2.43a** with 1.2 equivalents of **a** and **c**.

The cyclisation of the vinyl products was also investigated. It has already been mentioned that divinyl compound **3.17aa** spontaneously cyclises to give the monovinyl cyclic product **3.16aa**. This isomerisation is complete within two days in solution at room temperature. The monovinyl product **3.14aa′** however is stable even after one week so the cyclisation of monovinyl compounds **3.14aa′** and **3.14ca** was attempted by adding base (**Scheme 3.19**)**.** For **3.14aa′**, no reaction occurred after addition of ^{t}BuOK or after addition of K_2CO_3 and heating at 70 °C. Following this, the reaction of $[Cp^*Rh(MeCN)_3][PF_6]_2$ (5 mol%) and $Cu(OAc)_2.H_2O$ (2.5 equiv.) with **3.14aa′** was tested to see if the cyclisation is metal catalysed. The mixture was heated at 83 °C in DCE overnight and following aqueous work-up, the *trans* isomer (**3.14aa**) was isolated in 46% yield with no evidence for cyclised product **3.15aa**.

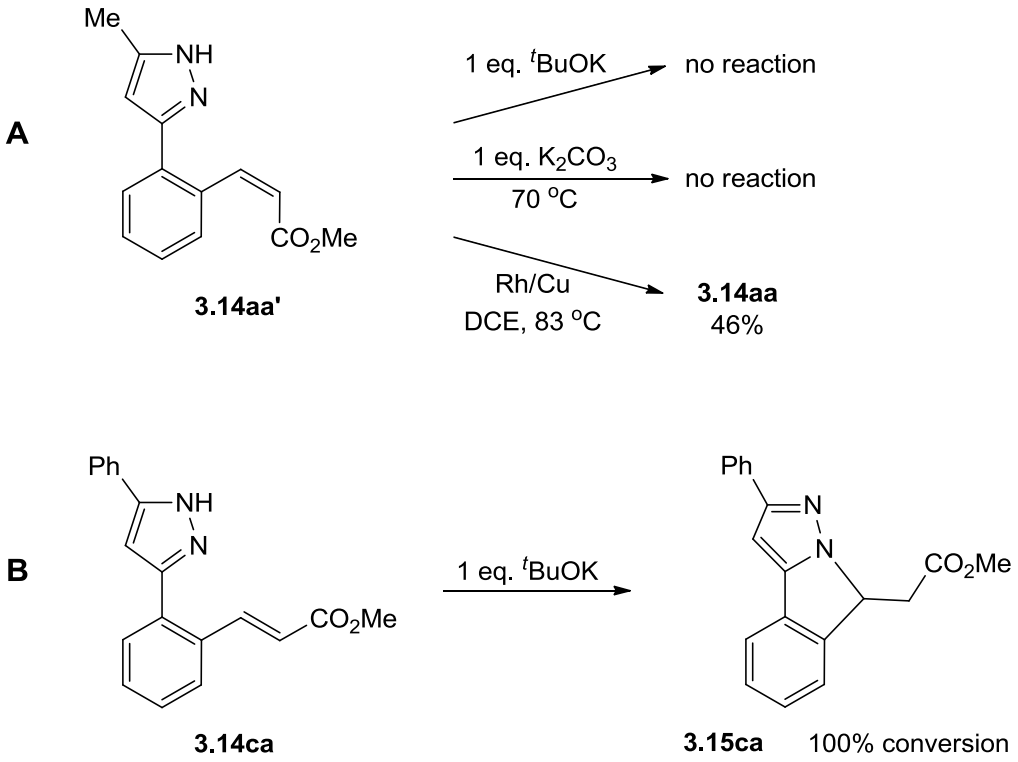

Scheme 3.19: Attempted cyclisation of **3.14aa′** and **3.14ca**.

Addition of ^{t}BuOK to **3.14ca** gave cyclised product **3.15ca** (**Scheme 3.19 B**). This may be because the phenyl substituent on the pyrazole makes the NH proton more acidic and therefore more prone to deprotonation compared with a methyl substituent on the pyrazole. It is also worthy to note that **3.14ca** is a *trans* alkene as opposed to **3.14aa′** which is a *cis* alkene which may have an effect on the cyclisation.

Computational Studies

Density functional theory (DFT) calculations have been performed to study the mechanism of the coupling of *C*-phenylpyrazoles with the alkenes methyl acrylate (**a**) and styrene (**b**) at catalysts based on {Cp*Rh} fragments. The N-H and C-H activation steps are the same as discussed in **Chapter Two** (**Figs. 2.9** and **2.10**) the alkene reactions are therefore considered from the alkene adduct. **Fig. 3.2** shows the energies calculated for different intermediates and transition states in the reaction of **2.43a** with methyl acrylate (**a**) to give monovinyl products **3.14aa** and **3.14aa′**.

	A	TS(A-B)	B	TS(B-D)	D	TS(D-E)	E	TS(B-C)	C
Y = a	+1.0	+23.6	+11.1	+19.6	+13.2	+13.2	+6.6	+64.5	+20.7
Y = b	+0.5	+23.3	+17.4	+18.2	+13.2	+14.8	+6.0	+61.0	+18.3
Y = c	+0.0	+16.8	+2.1	+10.5	+4.0	+5.4	+2.9	+58.9	+20.4
Y = d	+1.9	+16.3	+5.3	+15.5	+8.3	+8.6	+3.9	+56.4	+21.4

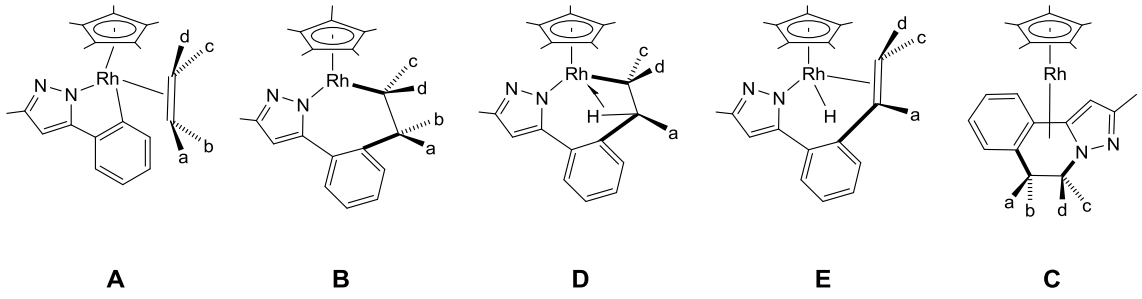

Fig. 3.2: Computed energies for the reaction of **2.43a** with methyl acrylate (**a**).

The energies were calculated for the CO_2Me substituent (Y) located in each site (a, b, c or d). Firstly, it is clear that the transition state leading to intermediate **C** (**TS(B-C)**) has very high energies (56.4-64.5 kcal mol^{-1}) which implies formation of intermediate **C** is not feasible. This is consistent with the experimental results as intermediate **C** corresponds to the six-membered *N*-heterocyclic product which is not observed. Secondly, these results show that it would be higher in energy for the methyl acrylate to insert with the CO_2Me substituent next to the phenyl (a/b = CO_2Me in intermediate **B**) rather than next to the metal (c/d = CO_2Me in intermediate **B**). This is also consistent with the experimental results as all products obtained from the catalysis have formed via regioselective alkene insertion where the CO_2Me substituent ends up next to the metal.

Finally, **Fig. 3.2** shows that Y = c corresponds to the *trans* monovinyl product (**3.14aa**) whereas Y = d corresponds to the *cis* monovinyl product (**3.14aa′**). The calculations show that the *trans* product E_c is thermodynamically more stable than the *cis* product E_d, however the transition state for the migratory insertion step leading to the *trans* product (**TS(A-B)**) has a larger energy gap than for the *cis* product (ΔG_{DCE} = 16.8 kcal mol^{-1} compared to 14.4 kcal mol^{-1}) as well as a higher absolute barrier (16.8 vs 16.3 kcal mol^{-1}). These data suggest that formation of the *cis* product may be more feasible that the *trans* product which is also consistent with the experimental results as the *cis* product (**3.14aa′**) is favoured over the *trans* (**3.14aa**) in approximately a 4:1 ratio.

The reaction profile for the Cp*Rh-catalysed coupling of **2.43a** with methyl acrylate (**a**) is shown in **Fig. 3.3** starting from the alkene-associated intermediate **A**. This profile further illustrates that migratory insertion is regioselective for the CO_2Me substituent (Y) to end up next to the metal in intermediate **B** and that the barrier to intermediate **B** is lower in energy for the *cis* rather than *trans* product. It shows that the barrier to intermediate **C** is very high in energy (56.4-58.9 kcal mol^{-1}) therefore β-H elimination takes place leading to intermediate **E**.

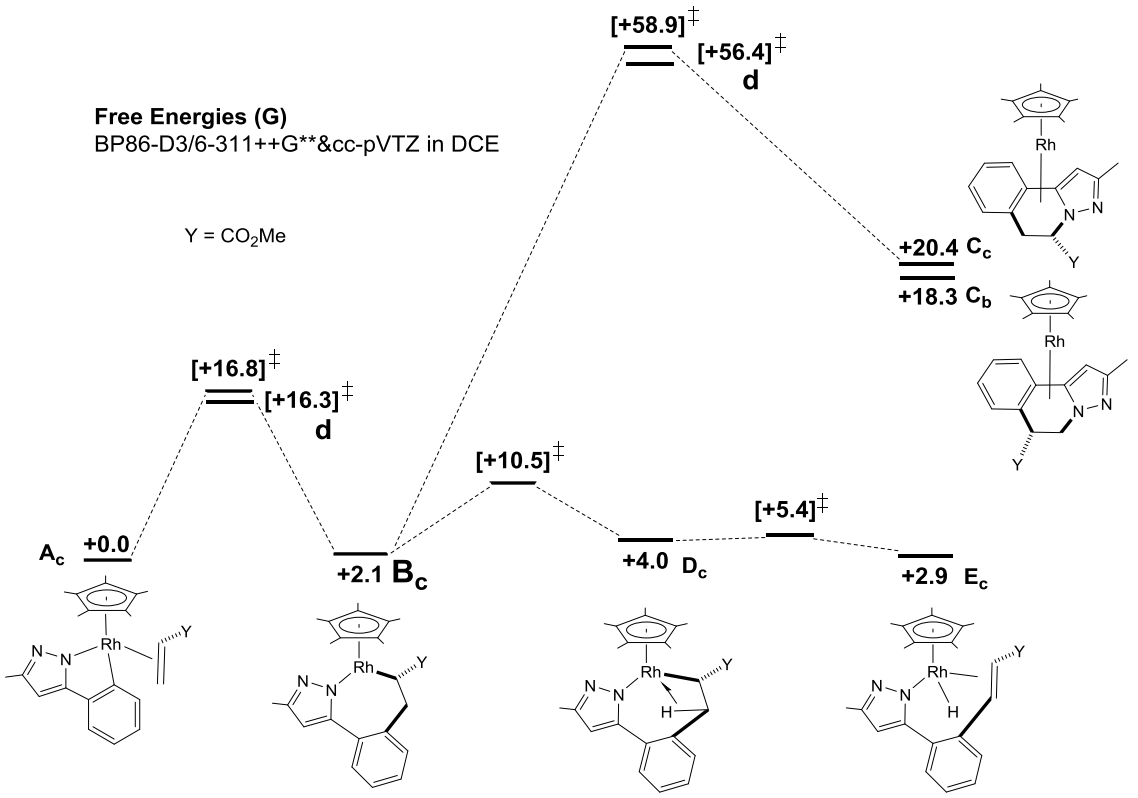

Fig. 3.3: Reaction profile for the Cp*Rh-catalysed coupling of **2.43a** with **a**.

The energies calculated for the different intermediates and transition states in the reaction of **2.43a** with styrene (**b**) to give monovinyl product **3.14ca** are shown in **Fig. 3.4**. The energies were calculated for each site (a, b, c or d) the Ph substituent (Y) could be located. Again, the results show that it would be higher in energy for the alkene to insert with the substituent next to the phenyl (a/b = Ph in intermediate **B**) rather than next to the metal (c/d = Ph in intermediate **B**) therefore the calculations for Y = a and Y = b have been omitted from **Fig 3.4**. Again, it is clear that the transition state leading to intermediate **C** (**TS(B-C)**) has very high energies (58.2-60.0 kcal mol^{-1}) which implies formation of intermediate **C** (six-membered *N*-heterocyclic product) is not feasible, consistent with the experimental results. Finally, these calculations show that the *trans* product (Y = c) is thermodynamically more stable than the *cis* product (Y = d). The transition state (**TS(A-B)**) for the migratory insertion step leading to the *trans* product has a larger energy gap than for the *cis* product (ΔG_{DCE} 19.5 vs 17.8 kcal mol^{-1}) which suggests that *cis* product formation may be more facile than *trans* product, however this route would be uphill and would lead to higher energy intermediates than for the *trans* product (e.g. +9.6 vs -2.6 kcal mol^{-1} for intermediate **B**). This suggests the *trans* product route is kinetically and thermodynamically more favourable than *cis* in the case of styrene (**b**) which is consistent with the experimental results as the *trans* product (**3.14ca**) is observed but not the *cis* product.

	A	TS(A-B)	B	TS(B-D)	D	TS(D-E)	E	TS(B-C)	C
Y = c	+0.0	+19.5	-2.6	-1.8	-2.5	+7.0	+3.4	+58.2	+19.8
Y = d	+1.3	+19.1	+9.6	+17.6	+11.7	+11.3	+5.2	+60.0	+19.3

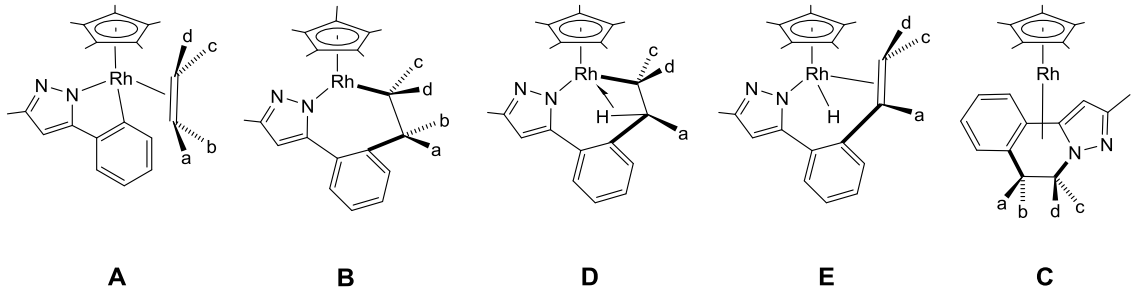

Fig. 3.4: Computed energies for the reaction of **2.43a** with styrene (**b**).

In conclusion, DFT calculations have been performed to study the mechanism of the coupling of *C*-phenylpyrazoles with the alkenes methyl acrylate (**a**) and styrene (**b**) at catalysts based on {Cp*Rh} fragments. The calculations suggest oxidative coupling to form six-membered *N*-heterocyclic products is very high in energy and therefore not feasible which supports the experimental results as six-membered *N*-heterocycles are not observed. The calculations also show that migratory insertion is regioselective for the carbon with the substituent to end up next to the metal which is consistent with the observed experimental results. For methyl acrylate (**a**), the barrier for migratory insertion is lower in energy for the *cis* rather than *trans* product and so the *cis* product is favoured as found experimentally. For styrene (**b**), the *cis* product route would be uphill, leading to higher energy intermediates compared with the *trans* product, therefore the *trans* product is favoured, consistent with the experimental results.

3.3 Conclusion

The results presented in this chapter have illustrated that by using the cationic Cp*Rh catalyst and milder reaction conditions compared to that used by Li *et al.*,[27] acrylates can react with *C*-phenylpyrazoles to incorporate only one equivalent of alkene in the product, though the reactions with 2.2 equivalents give similar results to Li *et al.*. Reactions with methyl acrylate are not particularly selective, giving rise to complicated mixtures of both *cis* and *trans* isomers of the monovinyl products, cyclised products (likely formed via chelation-assisted vinylation followed by aza-Michael addition) and divinyl products which readily cyclise via aza-Michael addition. In addition, less reactive alkenes such as styrene react to give mono or divinyl products depending on the substituent on the pyrazole. Good Michael acceptors such as methyl vinyl ketone react to give cyclised products likely formed via chelation-assisted vinylation followed by Michael addition. In this case direct Michael reaction before C-H activation can also compete if the reaction is carried out with only 1.2 equivalents of alkene. In the case of crotonaldehyde the simple non-catalysed Michael addition is now even more favoured. Some of the vinylic products were successfully cyclised by the addition of base, depending on the substituent on the pyrazole.

Apart from the direct Michael addition products, the products observed from the reactions of *C*-phenylpyrazoles with alkenes resulted from regioselective insertion of the alkene in the catalytic cycle where the carbon atom with a substituent ends up next to the metal. DFT calculations have been performed to study the mechanism of the coupling of *C*-phenylpyrazoles with certain alkenes. The calculations support the non-observation of six-membered *N*-heterocyclic products and show that migratory insertion is regioselective for the carbon with the substituent to end up next to the metal, also in support of the observed experimental results. Finally the calculations support formation of the *cis* monovinyl product being favoured with methyl acrylate (**a**) and the *trans* monovinyl product being favoured with styrene (**b**).

3.4 Experimental

See Experimental section of **Chapter Two** for general characterisation methods and preparation of non-commercial substrates and catalysts. In addition, the infrared spectra were recorded in the solid state with Universal ATR sampling accessories on a Perkin Elmer Spectrum One FTIR instrument. The reagents methyl acrylate, styrene, methyl vinyl ketone and crotonaldehyde were purchased from Aldrich Chemical Co. and used without further purification.

General procedure for catalysis reactions with Rh

$[Cp^*Rh(MeCN)_3][PF_6]_2$ (33 mg, 5 mol%), the appropriate directing ligand (1 eq.), $Cu(OAc)_2.H_2O$ (2.5 eq.), appropriate alkene (1.2 eq.) and DCE (10 ml) were added to a Schlenk flask. The Schlenk flask was sealed with a screw-cap and then transferred to a preheated oil bath and stirred at 83 °C for 16 hours. The reaction mixture was cooled to room temperature with continuous stirring and diluted with Et_2O (10 ml). The mixture was transferred to separating funnel and ammonium hydroxide solution (10 ml, 2M) was added. The aqueous layer was extracted with Et_2O (3 x 10 ml) and the organic layers were combined and dried over $MgSO_4$. The drying agent was removed by filtration and solvent was removed under reduced pressure.

Reaction of 2.43a with methyl acrylate (a) (1.2 equiv.)

Following the general procedure, a Schlenk flask was loaded with $[Cp^*Rh(MeCN)_3][PF_6]_2$ (33 mg, 5 mol%), 3-phenyl-5-methyl-1*H*-pyrazole (**2.43a**, 158 mg, 1 mmol), $Cu(OAc)_2.H_2O$ (500 mg, 2.5 mmol), methyl acrylate (**a**, 103 mg, 1.2 mmol) and DCE (10 ml). The products were purified by column chromatography eluting from 100% dichloromethane to 20% ethyl acetate in hexane to give **3.14aa′** as light brown oil (123 mg, 51%, 0.51 mmol), **3.15aa** as yellow oil (40 mg, 17%, 0.17 mmol), **3.16aa** as a brown oily solid (52 mg, 16%, 0.16 mmol) and **3.14aa** as yellow oil (34 mg, 14%, 0.14 mmol).

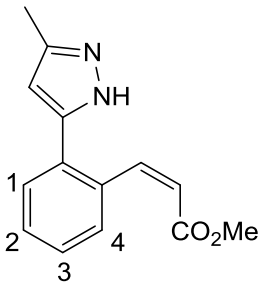

3.14aa′: ^{1}H NMR (400 MHz, $CDCl_3$): δ 2.33 (s, 3H, *Me* (Pz)), 3.81 (s, 3H, CO_2*Me*), 5.06 (d, *J* = 13.7 Hz, 1H, *H*C=CH(CO_2Me)), 6.41 (s, 1H, *Pz-H*), 6.47 (d, *J* = 13.7 Hz, 1H, =C*H*(CO_2Me)), 7.19-7.28 (m, 2H, H^3 + H^4), 7.35 (t, *J* = 7.0, 7.4 Hz, 1H, H^2), 7.47 (d, *J* = 7.4 Hz, 1H, H^1), ^{13}C {^{1}H} NMR (100 MHz, $CDCl_3$): δ 13.7 (*Me*), 52.0 (CO_2*Me*), 77.8 (H*C*=CH(CO_2Me)), 94.6 (=*C*H(CO_2Me)), 102.4 (*C*-H (Pz)), 127.2 (C^1), 127.6 (C^3/C^4), 128.6 (C^3/C^4), 128.9 (C^2), 130.9, 134.4, 150.7, 151.5, 167.8 (*C*CO_2Me). ESIMS: *m/z* 243 $[M+H]^+$. HRMS (ES): Calcd for $C_{14}H_{15}N_2O_2$ $[M+H]^+$ 243.1134, found 243.1137.

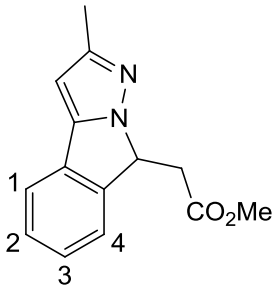

3.15aa: ^{1}H NMR (400 MHz, $CDCl_3$): δ 2.36 (s, 3H, *Me* (Pz)), 2.77 (dd, *J* = 7.8, 16.0 Hz, 1H, CH_2), 3.30 (dd, *J* = 3.1, 16.4 Hz, 1H, CH_2), 3.77 (s, 3H, CO_2*Me*), 5.49 (br dd, *J* = 3.1 Hz, 1H, CH_2C*H*), 6.16 (broad s, 1H, *Pz-H*), 7.30 (t, *J* = 7.4 Hz, 1H, H^2/H^3), 7.39 (t, *J* = 7.4 Hz, 1H, H^2/H^3), 7.45 (d, *J* = 7.4 Hz, 1H, H^1/H^4), 7.53 (d, *J* = 7.4 Hz, 1H, H^1/H^4), ^{13}C {^{1}H} NMR (125 MHz, $CDCl_3$): δ 14.5 (*Me*), 38.7 (*C*H_2), 52.1 (CO_2*Me*), 58.8 (CH_2*C*H), 120.4 (C^1/C^4), 123.5 (C^1/C^4), 127.3 (C^2/C^3), 128.7 (C^2/C^3), 130.6, 144.2 (3C), 170.7 (*C*CO_2Me). ESIMS: *m/z* 243 $[M+H]^+$. HRMS (ES): Calcd for $C_{14}H_{15}N_2O_2$ $[M+H]^+$ 243.1134, found 243.1140. Pyrazole CH not observed in normal ^{13}C spectrum.

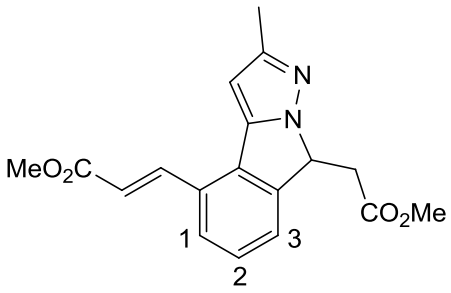

3.16aa: ^{1}H NMR (400 MHz, $CDCl_3$): δ 2.38 (s, 3H, *Me* (Pz)), 2.70 (dd, *J* = 8.6, 16.4 Hz, 1H, CH_2), 3.22 (dd, *J* = 4.7, 16.4 Hz, 1H, CH_2), 3.76 (s, 3H, CO_2*Me*), 3.85 (s, 3H, CO_2*Me*), 5.42 (dd, *J* = 4.7, 8.2 Hz, 1H, CH_2C*H*), 6.36 (s, 1H, *Pz-H*), 6.52 (d, *J* = 16.0 Hz, 1H, *H*C=CH(CO_2Me)), 7.30 (t, *J* = 7.4, 7.8 Hz, 1H, H^2), 7.46 (d, *J* = 7.4 Hz, 1H, H^3), 7.60 (d, *J* = 7.8 Hz, 1H, H^1), 8.04 (d, *J* = 16.0 Hz, 1H, =C*H*(CO_2Me)), ^{13}C {^{1}H} NMR (100 MHz, $CDCl_3$): δ 11.4 (*Me*), 38.6 (*C*H_2), 51.9 (CO_2*Me*), 52.1 (CO_2*Me*), 58.7 (CH_2*C*H), 99.5 (*C*-H (Pz)), 119.9 (H*C*=CH(CO_2Me)), 124.8 (C^3), 125.7 (C^1), 127.7 (C^2), 130.9, 140.4 (=*C*H(CO_2Me)), 144.9, 167.0 (*C*CO_2Me), 170.5 (*C*CO_2Me). ESIMS: *m/z* 327 $[M+H]^+$. HRMS (ES): Calcd for $C_{18}H_{19}N_2O_4$ $[M+H]^+$ 327.1345, found 327.1338. In some ^{1}H NMR spectra, signals for the CH_2CH protons are broad.

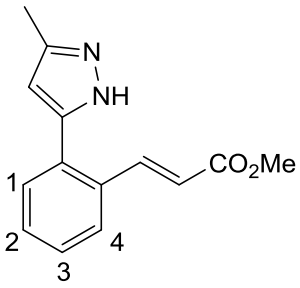

3.14aa: ^{1}H NMR (400 MHz, $CDCl_3$): δ 2.33 (s, 3H, *Me* (Pz)), 3.77 (s, 3H, CO_2*Me*), 6.19 (s, 1H, *Pz-H*), 6.39 (d, *J* = 16.0 Hz, 1H, *H*C=CH(CO_2Me)), 7.36 (td, *J* = 1.6, 7.4 Hz, 1H, H^3), 7.40 (td, *J* = 1.6, 7.4 Hz, 1H, H^2), 7.55 (dd, *J* = 1.6, 7.4 Hz, 1H, H^1), 7.65 (dd, *J* = 1.6, 7.8 Hz, 1H, H^4), 8.13 (d, *J* = 15.7 Hz, 1H, =C*H*(CO_2Me)), ^{13}C {^{1}H} NMR (125 MHz, $CDCl_3$): δ 11.5 (*Me*), 51.7 (CO_2*Me*), 105.9 (*C*-H (Pz)), 118.9 (H*C*=CH(CO_2Me)), 127.0 (C^4), 128.2 (C^3), 129.7 (C^2), 129.9 (C^1), 132.9 (2C), 133.6, 144.3 (=*C*H(CO_2Me)), 167.5 (*C*O_2Me). ESIMS: *m/z* 243 $[M+H]^+$, 211 $[M-H-OMe]^+$, 169 $[M-CO_2Me-Me]^+$.

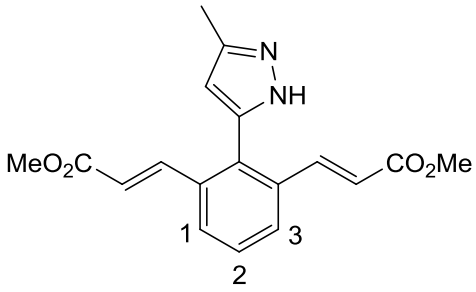

3.17aa: This was sometimes observed in reactions but cyclised to **3.16aa**. ^{1}H NMR (400 MHz, $CDCl_3$): δ 2.25 (s, 3H, *Me* (Pz)), 3.65 (s, 6H, CO_2*Me*), 5.98 (s, 1H, *Pz-H*), 6.26 (d, *J* = 15.7 Hz, 2H, 2 x *H*C=CH(CO_2Me)), 7.33 (t, *J* = 7.8 Hz, 1H, H^2), 7.55-7.61 (m, 4H, 2 x C*H*(CO_2Me) + H^1 + H^3), ^{13}C {^{1}H} NMR (100 MHz, $CDCl_3$): δ 13.3 (*Me*), 50.6 (CO_2*Me*), 106.9 (*C*-H (Pz)), 118.8 (H*C*=CH(CO_2Me)), 124.7 (C^2), 126.8 (Ar), 126.7 (Ar), 139.4 (=*C*H(CO_2Me)), 169.5 (*C*O_2Me). FAB MS: *m/z* 327 $[M+H]^+$, 295 $[M-OMe]^+$, 267 $[M-CO_2Me]^+$, 207 $[M-2(CO_2Me)]^+$, 154 $[M-2(CH=CH(CO_2Me))]^+$. HRMS (ES): Calcd for $C_{18}H_{19}N_2O_4$ $[M+H]^+$ 327.1345, found 327.1338. Quaternary carbons were difficult to assign as **3.17aa** had mostly isomerised to **3.16aa** at the time the spectrum was recorded.

Reaction of 2.43a with methyl acrylate (a) (2.2 equiv.)

Following the general procedure, a Schlenk flask was loaded with $[Cp^*Rh(MeCN)_3][PF_6]_2$ (33 mg, 5 mol%), 3-phenyl-5-methyl-1*H*-pyrazole (**2.43a**, 158 mg, 1 mmol), $Cu(OAc)_2.H_2O$ (500 mg, 2.5 mmol), methyl acrylate (**a**, 189 mg, 2.2 mmol) and DCE (10 ml). The product was purified by column chromatography eluting with 5 % ethyl acetate in hexane to give **3.16aa** as a brown solid (280 mg, 86%, 0.86 mmol). **3.16aa** is also formed by isomerisation of **3.17aa**.

Reaction of 2.43c with methyl acrylate (a)

Following the general procedure, a Schlenk flask was loaded with $[Cp^*Rh(MeCN)_3][PF_6]_2$ (33 mg, 5 mol%), 3,5-diphenyl-1*H*-pyrazole (**2.43c**, 220 mg, 1 mmol), $Cu(OAc)_2.H_2O$ (500 mg, 2.5 mmol), methyl acrylate (**a**, 103 mg, 1.2 mmol) and DCE (10 ml). The products were purified by column chromatography eluting with 30% ethyl acetate in petroleum ether (40-60 °C) to give **3.14ca** as pale yellow oil (107 mg, 35%, 0.35 mmol), **3.17ca** as yellow oil (impure) and **3.15ca** as a yellow solid (impure).

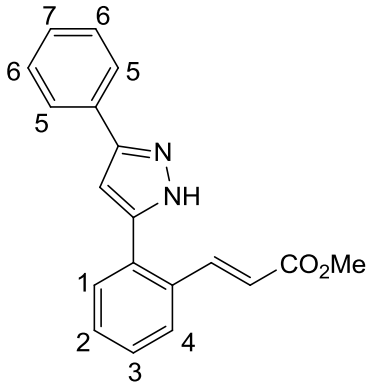

3.14ca: ^{1}H NMR (400 MHz, $CDCl_3$): δ 3.75 (s, 3H, CO_2*Me*), 6.43 (d, *J* = 16.0 Hz, 1H, *H*C=CH(CO_2Me)), 6.70 (s, 1H, *Pz-H*), 7.33-7.37 (m, 3H, H^2 + H^3 + H^7), 7.42 (td, *J* = 2.0, 7.0 Hz, 2H, H^6), 7.60 (dd, *J* = 1.2, 7.0 Hz, 1H, H^1), 7.67 (dd, *J* = 2.0, 7.4 Hz, 1H, H^4), 7.70 (d, *J* = 7.0 Hz, 2H, H^5), 8.11 (d, *J* = 15.7 Hz, 1H, =C*H*(CO_2Me)), ^{13}C {^{1}H} NMR (100 MHz, $CDCl_3$): δ 50.5 (CO_2*Me*), 102.8 (*C*-H (Pz)), 118.4 (H*C*=CH(CO_2Me)), 124.5 (C^5), 126.0 (C^4), 127.1, 127.2, 127.4, 127.7 (Ar), 127.7 (C^6), 128.5 (Ar), 128.8 (Ar), 131.1, 131.9, 142.5 (=C*H*(CO_2Me)), 166.1 (*C*O_2Me). ESIMS: *m/z* 305 $[M+H]^+$, 274 $[M\text{-}OMe]^+$. HRMS (ES): Calcd for $C_{19}H_{17}N_2O_2$ $[M+H]^+$ 305.1290, found 305.1283. Difficult to assign aryl carbon signals due to peaks being very close together.

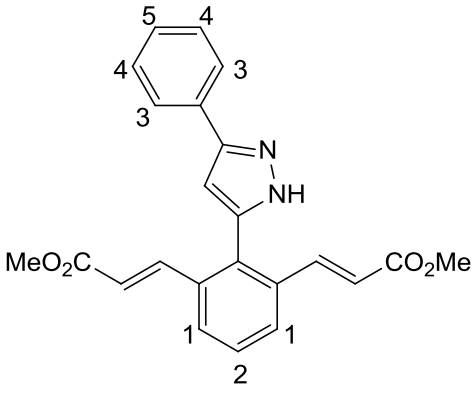

3.17ca: This product was purified by preparative TLC eluting from 30 % ethyl acetate in petroleum ether (40-60 °C) to give **3.17ca** as yellow oil (80 mg, 15%, 0.15 mmol). ^{1}H NMR (400 MHz, $CDCl_3$): δ 3.71 (s, 6H, CO_2*Me*), 6.37 (d, *J* = 16.0 Hz, 2H, *H*C=CH(CO_2Me)), 6.53 (br s, 1H, *Pz-H*), 7.32-7.43 (m, 4H, H^2 + H^4 + H^5), 7.54 (d, *J* = 7.0 Hz, 2H, H^3), 7.62 (dd, *J* = 1.2, 7.4 Hz, 2H, H^1), 8.06 (d, *J* = 16.0 Hz, 2H, =C*H*(CO_2Me)), 10.27 (br s, 1H, N*H*), ^{13}C {^{1}H} NMR (100 MHz, $CDCl_3$): δ 50.6 (*Me*), 118.4, 118.6 (H*C*=CH(CO_2Me)), 124.6 (C^1), 126.2, 127.2, 127.5, 127.6 (C^4), 127.8, 128.7, 128.9 (C^3), 132.0, 142.6, 166.2 (*C*O_2Me). Pyrazole CH not observed in normal ^{13}C spectrum but shows a correlation in

the HMQC spectrum at δ 107.6. HRMS (ES): Calcd for $C_{23}H_{21}N_2O_4$ $[M+H]^+$ 389.1501, found 389.1494.

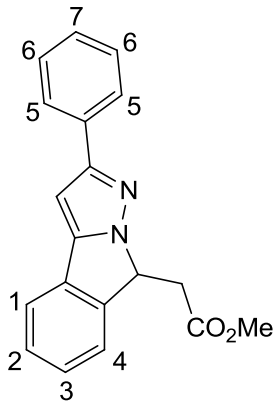

3.15ca: This product was obtained by preparative TLC eluting from 30 % ethyl acetate in petroleum ether (40-60 °C) to give **3.15ca** as a pale yellow solid (80 mg, 4%, 0.04 mmol). ^{1}H NMR (400 MHz, $CDCl_3$): δ 2.76 (dd, *J* = 8.6, 16.4 Hz, 1H, C*H*$_2$), 3.29 (dd, *J* = 5.1, 16.4 Hz, 1H, C*H*$_2$), 3.71 (s, 3H, CO_2*Me*), 5.55 (dd, *J* = 5.1, 8.6 Hz, 1H, CH_2C*H*), 6.60 (s, 1H, *Pz-H*), 7.22-7.27 (m, 2H, H^3 + H^7), 7.32-7.37 (m, 3H, H^2 + H^6), 7.41 (d, *J* = 7.4 Hz, 1H, H^4), 7.52 (d, *J* = 7.4 Hz, 1H, H^1), 7.77 (dd, *J* = 1.6, 7.4 Hz, 2H, H^5), ^{13}C {^{1}H} NMR (100 MHz, $CDCl_3$): δ 37.4 (*C*H_2), 50.7 (*Me*), 57.8 (CH_2*C*H), 92.3 (*C*-H (Pz)), 119.1 (C^1), 122.1 (C^4), 124.2 (C^5), 126.2 (C^3/C^7), 126.3 (C^3/C^7), 127.2 (C^6), 127.3 (C^2), 128.9, 132.6, 142.7, 144.8, 154.9, 169.9 (*C*=O). HRMS (ES): Calcd for $C_{19}H_{17}N_2O_2$ $[M+H]^+$ 305.1290, found 305.1280. The product was recrystallised from dichloromethane/hexane to give **3.15ca** as clear needles. **3.15ca** is also formed from a cyclisation reaction by adding tBuOK (1 eq.) to **3.14ca**.

Reaction of 2.43d with methyl acrylate (a)

Following the general procedure, a Schlenk flask was loaded with $[Cp^*Rh(MeCN)_3][PF_6]_2$ (16 mg, 5 mol%), 3-phenyl-5-(trifluoromethyl)-1H-pyrazole (**2.43d**, 212 mg, 1.0 mmol), $Cu(OAc)_2.H_2O$ (500 mg, 2.5 mmol), methyl acrylate (**a**, 103 mg, 1.2 mmol) and DCE (10 ml). The crude ^{1}H NMR spectrum showed the presence of two main products in an 8:1 ratio. The products were purified by column chromatography eluting from 100% dichloromethane to 10% ethyl acetate in dichloromethane to give **3.14da** as yellow oil (215 mg, 73%, 0.73 mmol) and **3.14da′** as a white solid (34 mg, 11%, 0.11 mmol).

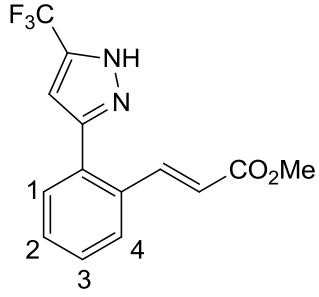

3.14da: ^{1}H NMR (400 MHz, $CDCl_3$): δ 3.75 (s, 3H, CO_2*Me*), 6.42 (d, *J* = 16.0 Hz, 1H, *H*C=CH(CO_2Me)), 6.64 (s, 1H, *Pz-H*), 7.47-7.49 (m, 3H, H^1 + H^2 + H^3), 7.69 (m, 1H, H^4), 7.81 (d, *J* = 16.0 Hz, 1H, =C*H*(CO_2Me)), 11.52 (br s, 1H, N*H*), ^{13}C {^{1}H} NMR (125 MHz, $CDCl_3$): δ 52.0 (CO_2*Me*), 105.1 (*C*-H (Pz)), 121.0 (H*C*=CH(CO_2Me)), 121.2 (q, *J* = 270.6

Hz, *C*F_3), 127.5 (*C*^{4}), 128.8, 129.8 (*C*^{2} + *C*^{3}), 130.3 (*C*^{1}), 133.2 (2C), 142.0 (=*C*H(CO_2Me)), 167.1 (*C*=O), ^{19}F {^{1}H} NMR (376 MHz, $CDCl_3$): δ -62.0 (C*F*$_3$). ESIMS: *m/z* 297 $[M+H]^+$. HRMS (ES): Calcd for $C_{14}H_{12}N_2F_3O_2$ $[M+H]^+$ 297.0851, found 297.0858. Could not assign *C*-CF_3 carbon atom.

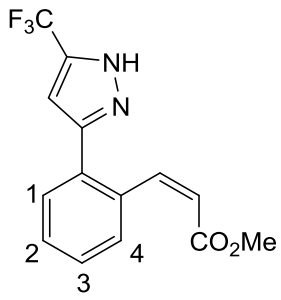

3.14da′: ^{1}H NMR (400 MHz, $CDCl_3$): δ 3.82 (s, 3H, CO_2*Me*), 5.26 (d, *J* = 14.1 Hz, 1H, *H*C=CH(CO_2Me)), 6.71 (d, *J* = 14.1 Hz, 1H, =C*H*(CO_2Me)), 6.92 (s, 1H, *Pz-H*), 7.31-7.35 (m, 2H, *H*^{3} + *H*^{4}), 7.42 (td, *J* = 2.0, 7.8, 8.2 Hz, 1H, *H*^{2}), 7.51 (br d, *J* = 7.4 Hz, 1H, *H*^{1}), ^{13}C {^{1}H} NMR (125 MHz, CD_2Cl_2): δ 52.3 (CO_2*Me*), 82.8 (H*C*=CH(CO_2Me)), 99.5 (=*C*H(CO_2Me)), 103.1 (*C*-H (Pz)), 121.7 (q, *J* = 263.6 Hz, *C*F_3), 128.2 (*C*^{1}), 128.4 (*C*^{3}/*C*^{4}), 129.1 (*C*^{3}/*C*^{4}), 129.8 (*C*^{2}), 131.3, 133.2, 144.3 (q, *J* = 35.8 Hz, *C*-CF_3), 151.4, 168.1 (*C*=O), ^{19}F {^{1}H} NMR (376 MHz, $CDCl_3$): δ -59.8 (C*F*$_3$). ESIMS: *m/z* 295 $[M-H]^-$. HRMS (ES): Calcd for $C_{14}H_{12}N_2F_3O_2$ $[M+H]^+$ 297.0851, found 297.0851.

Reaction of 2.43a with styrene (b)

Following the general procedure, a Schlenk flask was loaded with $[Cp^*Rh(MeCN)_3][PF_6]_2$ (33 mg, 5 mol%), 3-phenyl-5-methyl-1*H*-pyrazole (**2.43a**, 158 mg, 1 mmol), $Cu(OAc)_2.H_2O$ (500 mg, 2.5 mmol), styrene (**b**, 125 mg, 1.2 mmol) and DCE (10 ml). The products were purified by column chromatography eluting from 50% ethyl acetate in hexane to give **3.14ab** as yellow oil (157 mg, 60%, 0.60 mmol) and **3.17ab** as pale yellow oil (trace).

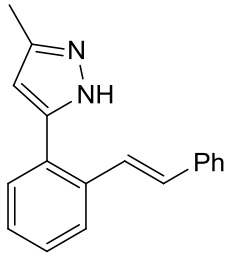

3.14ab: ^{1}H NMR (400 MHz, $CDCl_3$): δ 2.35 (s, 3H, *Me* (Pz)), 6.23 (br s, 1H, *Pz-H*), 7.06 (d, 1H, *J* = 16.0 Hz, C=C*H*), 7.32-7.40 (m, 6H, *Ar-H*), 7.44-7.51 (m, 3H, 2 x *Ar-H* + C=C*H*), 7.70 (dd, *J* = 7.4, 8.6 Hz, 1H, *Ar-H*), 10.05 (br s, 1H, N*H*), ^{13}C {^{1}H} NMR (125 MHz, $CDCl_3$): δ 11.9 (*Me* (Pz)), 100.6 (*C*-H (Pz)), 126.1, 126.7 (Ar), 127.6, 127.7 (Ar), 128.2, 128.3, 128.7 (Ar), 129.1, 129.5, 130.0 (C=*C*H), 131.7, 135.7, 136.0, 136.8, 137.6. ESIMS: *m/z* 261 $[M+H]^+$. HRMS (ES): Calcd for $C_{18}H_{17}N_2$ $[M+H]^+$ 261.1392, found 261.1391. Difficult to assign aryl carbon signals due to peaks being very close together.

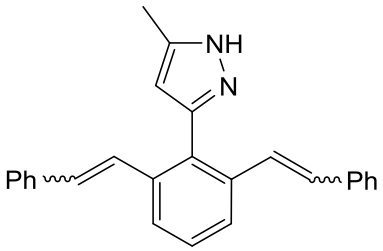

3.17ab: ESIMS: *m/z* 363 $[M+H]^+$. HRMS (ES): Calcd for $C_{26}H_{23}N_2$ $[M+H]^+$ 363.1861, found 363.1850.

Reaction of 2.43c with styrene (b)

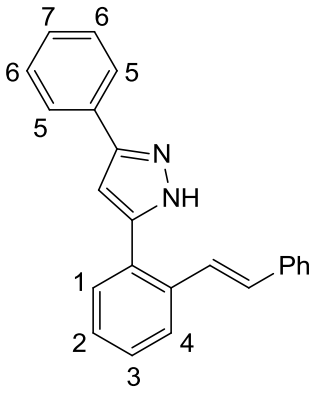

Following the general procedure, a Schlenk flask was loaded with $[Cp^*Rh(MeCN)_3][PF_6]_2$ (33 mg, 5 mol%), 3,5-diphenyl-1*H*-pyrazole (**2.43c**, 220 mg, 1 mmol), $Cu(OAc)_2.H_2O$ (500 mg, 2.5 mmol), styrene (**b**, 125 mg, 1.2 mmol) and DCE (10 ml). The product was purified by column chromatography eluting from 100% dichloromethane and 30% ethyl acetate in hexane to give **3.14cb** as a pale yellow solid (287 mg, 89%, 0.89 mmol). ^{1}H NMR (400 MHz, $CDCl_3$): δ 6.68 (br s, 1H, *Pz-H*), 7.03 (d, *J* = 16.0 Hz, 1H, C=C*H*), 7.18 (m, 1H, *Ar-H*), 7.24-7.31 (m, 5H, H^2 + H^3 + C=C*H*, *Ar-H*), 7.34-7.40 (m, 5H, *Ar-H*), 7.45 (br d, *J* = 7.4 Hz, 1H, H^1), 7.66 (d, *J* = 7.4 Hz, 1H, H^4), 7.71 (br d, *J* = 7.8 Hz, 2H, H^5), 10.40 (br s, 1H, N*H*), ^{13}C {^{1}H} NMR (125 MHz, $CDCl_3$): δ 103.7 (*C*-H (Pz)), 125.7 (C^5), 126.6 (Ar), 126.7 (C^4), 126.9, 127.8 (Ar), 127.9 (Ar), 128.1, 128.2 (Ar), 128.5, 128.8, 128.9 (2C, Ar), 129.0 (2C, Ar), 129.4 (C^1), 131.0 (C=*C*H), 136.1, 137.2. ESIMS: *m/z* 323 $[M+H]^+$. HRMS (ES): Calcd for $C_{23}H_{19}N_2$ $[M+H]^+$ 323.1548, found 323.1545.

Reaction of 2.43a with methyl vinyl ketone (c) (1.2 equiv.)

Following the general procedure, a Schlenk flask was loaded with $[Cp^*Rh(MeCN)_3][PF_6]_2$ (33 mg, 5 mol%), 3-phenyl-5-methyl-1*H*-pyrazole (**2.43a**, 158 mg, 1 mmol), $Cu(OAc)_2.H_2O$ (500 mg, 2.5 mmol), methyl vinyl ketone (**c**, 84 mg, 1.2 mmol) and DCE (10 ml). The crude ^{1}H NMR spectrum showed the presence of two products in a 4:1 ratio. The products were purified by column chromatography eluting from 100% dichloromethane to give **3.15ac** as yellow oil (158 mg, 70%, 0.70 mmol) and **3.18ac** as yellow oil (18 mg, 8%, 0.08 mmol).

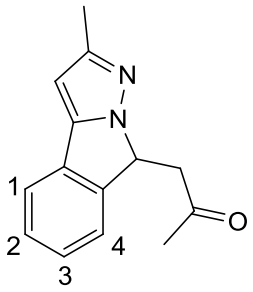

3.15ac: ^{1}H NMR (400 MHz, $CDCl_3$): δ 2.22 (s, 3H, CO*Me*), 2.36 (s, 3H, *Me* (Pz)), 2.86 (dd, *J* = 8.6, 18.0 Hz, 1H, C*H*$_2$), 3.47 (dd, *J* = 3.9, 18.0 Hz, 1H, C*H*$_2$), 5.55 (dd, *J* = 3.9, 8.6 Hz, 1H, CH_2C*H*), 6.14 (s, 1H, *Pz-H*), 7.27 (t, *J* = 7.4 Hz, 1H, *H*^{3}), 7.37 (t, *J* = 7.4 Hz, 1H, *H*^{2}), 7.44 (d, *J* = 7.4 Hz, 1H, *H*^{4}), 7.52 (d, *J* = 7.4 Hz, 1H, *H*^{1}), ^{13}C {^{1}H} NMR (100 MHz, $CDCl_3$): δ 14.4 (*Me*), 30.4 (CO*Me*), 47.9 (*C*H_2), 58.2 (CH_2*C*H), 96.2 (*C*-H (Pz)), 120.3 (*C*^{1}), 123.9, 127.3 (*C*^{4}), 128.5 (*C*^{3}), 129.5, 130.4 (*C*^{2}), 144.9, 153.4, 205.3 (*C*=O). ESIMS: *m/z* 227 $[M+H]^+$. HRMS (ES): Calcd for $C_{14}H_{15}N_2O$ $[M+H]^+$ 227.1184, found 227.1185.

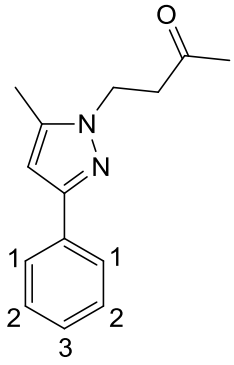

3.18ac: ^{1}H NMR (400 MHz, $CDCl_3$): δ 2.13 (s, 3H, CO*Me*), 2.30 (s, 3H, *Me* (Pz)), 3.06 (t, *J* = 6.7 Hz, 2H, C*H*$_2$(C=O)), 4.24 (t, *J* = 6.7 Hz, 2H, NC*H*$_2$), 6.25 (s, 1H, *Pz-H*), 7.24 (tt, *J* = 1.2, 7.4 Hz, 1H, *H*^{3}), 7.34 (td, *J* = 1.2, 7.4 Hz, 2H, *H*^{2}), 7.73 (dd, *J* = 1.2, 7.4 Hz, 2H, *H*^{1}), ^{13}C {^{1}H} NMR (100 MHz, $CDCl_3$): δ 11.1 (*Me*), 30.3 (CO*Me*), 43.0 (*C*H_2), 43.1 (*C*H_2), 102.5 (*C*-H (Pz)), 125.4 (*C*^{1}), 127.4 (*C*^{3}), 128.5 (*C*^{2}), 133.8, 139.8, 150.4, 206.3 (*C*=O). ESIMS: *m/z* 229 $[M+H]^+$. HRMS (ES): Calcd for $C_{14}H_{17}N_2O$ $[M+H]^+$ 229.1341, found 229.1337.

Reaction of 2.43a with methyl vinyl ketone (c) (2.2 equiv.)

Following the general procedure, a Schlenk flask was loaded with $[Cp^*Rh(MeCN)_3][PF_6]_2$ (33 mg, 5 mol%), 3-phenyl-5-methyl-1*H*-pyrazole (**2.43a**, 158 mg, 1 mmol), $Cu(OAc)_2.H_2O$ (500 mg, 2.5 mmol), methyl vinyl ketone (**c**, 154 mg, 2.2 mmol) and DCE (10 ml). The crude ^{1}H NMR spectrum showed the presence of two products in a 1.4:1 ratio. The products were purified by column chromatography eluting with 50 % ethyl acetate in petroleum ether (40-60 °C) to give **3.19ac** as yellow oil (137 mg, 46%, 0.46 mmol) and **3.15ac** as yellow oil (90 mg, 40%, 0.40 mmol).

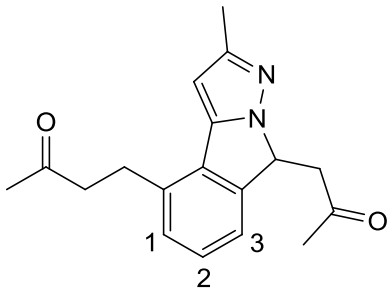

3.19ac: ^{1}H NMR (400 MHz, $CDCl_3$): δ 2.16 (s, 3H, CO*Me*), 2.21 (s, 3H, CO*Me*), 2.36 (s, 3H, *Me(Pz)*), 2.81 (t, *J* = 7.4, 7.8 Hz, 2H, C*H*$_2$), 2.87 (dd, *J* = 8.6, 17.6 Hz, 1H, C*H*$_2$CH), 3.09 (t, *J* = 7.0, 8.2 Hz, 2H, C*H*$_2$), 3.45 (dd, *J* = 4.3, 17.6 Hz, 1H, C*H*$_2$CH), 5.56 (dd, *J* = 4.3, 8.6 Hz, 1H, CH_2C*H*), 6.12 (s, 1H, *Pz-H*),

7.18-7.23 (m, 2H, H^1 + H^2), 7.30 (dd, J = 2.0, 7.0 Hz, 1H, H^3), ^{13}C {^{1}H} NMR (125 MHz, $CDCl_3$): δ 14.4 (*Me(Pz)*), 27.2 (CH_2), 30.1 (CO*Me*), 30.5 (CO*Me*), 43.5 (CH_2), 48.0 (CH_2CH), 58.2 (CH_2CH), 97.8 (*C*-H (Pz)), 121.7 (C^3), 127.7 (C^1/C^2), 128.7 (C^1/C^2), 129.2, 134.1, 144.8, 145.1, 153.5, 205.3 (*C*=O), 207.4 (*C*=O). ESIMS: *m/z* 297 $[M+H]^+$. HRMS (ES): Calcd for $C_{18}H_{21}N_2O_2$ $[M+H]^+$ 297.1603, found 297.1597.

Reaction of 2.43c with methyl vinyl ketone (c)

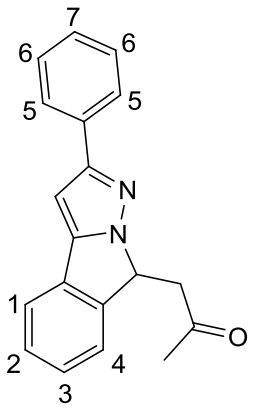

Following the general procedure, a Schlenk flask was loaded with $[Cp^*Rh(MeCN)_3][PF_6]_2$ (33 mg, 5 mol%), 3,5-diphenyl-1*H*-pyrazole (**2.43c**, 220 mg, 1 mmol), $Cu(OAc)_2.H_2O$ (500 mg, 2.5 mmol), methyl vinyl ketone (**c**, 84 mg, 1.2 mmol) and DCE (10 ml). The product was purified by column chromatography eluting from 1% ethyl acetate in dichloromethane to give **3.15cc** as a white solid (266 mg, 92%, 0.92 mmol). ^{1}H NMR (400 MHz, $CDCl_3$): δ 2.16 (s, 3H, CO*Me*), 2.83 (dd, J = 9.0, 18.0 Hz, 1H, CH_2), 3.46 (dd, J = 3.9. 18.0 Hz, 1H, CH_2), 5.59 (dd, J = 3.9, 9.0 Hz, 1H, CH_2CH), 6.58 (s, 1H, *Pz-H*), 7.21-7.25 (m, 2H, H^3 + H^7), 7.31-7.35 (m, 3H, H^2 + H^6), 7.40 (dd, J = 0.8, 7.8 Hz, 1H, H^4), 7.50 (d, J = 7.4 Hz, 1H, H^1), 7.76 (dd, J = 1.6, 8.6 Hz, 2H, H^5), ^{13}C {^{1}H} NMR (100 MHz, $CDCl_3$): δ 29.5 (*Me*), 47.0 (CH_2), 57.7 (CH_2CH), 92.7 (*C*-H (Pz)), 119.4 (C^1), 123.0 (C^4), 124.5 (C^5), 126.6 (C^3/C^7), 126.7 (C^3/C^7), 127.6 (C^2), 127.6 (C^6), 129.1, 133.0, 143.7, 145.2, 155.2, 204.3 (*C*=O). HRMS (ES): Calcd for $C_{19}H_{17}N_2O$ $[M+H]^+$ 289.1341, found 289.1336.

Reaction of 2.43a with crotonaldehyde (d)

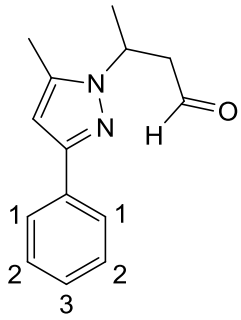

Following the general procedure, a Schlenk flask was loaded with $[Cp^*Rh(MeCN)_3][PF_6]_2$ (33 mg, 5 mol%), 3-phenyl-5-methyl-1*H*-pyrazole (**2.43a**, 220 mg, 1 mmol), $Cu(OAc)_2.H_2O$ (500 mg, 2.5 mmol), crotonaldehyde (**d**, 84 mg, 1.2 mmol) and DCE (10 ml). The product was purified by column chromatography eluting from 10% ethyl acetate in dichloromethane to give **3.24ad** as yellow oil (122 mg, 54%, 0.54 mmol). ^{1}H NMR (400 MHz, $CDCl_3$): δ 1.42 (d, J = 7.8 Hz, 3H, CH(*Me*)), 2.29 (s, 3H, *Me*), 2.83 (dd, J = 5.1. 16.8 Hz, 1H, CH_2), 3.38 (dd, J = 8.2, 16.8 Hz, 1H, CH_2), 4.74 (m, 1H, (Me)C*H*CH_2), 6.19 (s, 1H, *Pz-H*),

7.18 (tt, *J* = 2.0, 7.4 Hz, 1H, H^3), 7.28 (tt, *J* = 1.6, 7.0 Hz, 2H, H^2), 7.69 (dd, *J* = 1.6, 8.2 Hz, 2H, H^1), 9.69 (s, 1H, (C=O)*H*), ^{13}C {^1H} NMR (100 MHz, $CDCl_3$): δ 10.0 (CH(*Me*)), 20.4 (*Me*), 47.2 (CH_2*C*H), 48.6 (*C*H_2), 101.3 (*C*-H (Pz)), 124.5 (C^1), 126.3 (C^3), 127.5 (C^2), 132.9, 138.0, 149.2, 198.9 (*C*=O). HRMS (ES): Calcd for $C_{14}H_{17}N_2O$ $[M+H]^+$ 229.1341, found 229.1342.

Bibliography

1. V. Ritleng, J. P. Sutter, M. Pfeffer and C. Sirlin, *Chem. Commun.,* 2000, 129.
2. V. Ritleng, M. Pfeffer and C. Sirlin, *Organometallics,* 2003, **22**, 347.
3. L. Li, Y. Jiao, W. W. Brennessel and W. D. Jones, *Organometallics,* 2010, **29**, 4593.
4. D. Mc Cartney and P. J. Guiry, *Chem. Soc. Rev.,* 2011, **40**, 5122.
5. N. Umeda, K. Hirano, T. Satoh and M. Miura, *J. Org. Chem.,* 2009, **74**, 7094.
6. Y. Hashimoto, T. Ueyama, T. Fukutani, K. Hirano, T. Satoh and M. Miura, *Chem. Lett.,* 2011, **40**, 1165.
7. T. Gong, B. Xiao, Z. Liu, J. Wan, J. Xu, D. Luo, Y. Fu and L. Liu, *Org. Lett.,* 2011, **13**, 3235.
8. C. Feng and T. Loh, *Chem. Commun.*, 2011, **47**, 10458.
9. F. W. Patureau, T. Besset and F. Glorius, *Angew. Chem. Int. Ed.,* 2011, **50**, 1064.
10. Q. Zhang, H. Yu, Y. Li, L. Liu, Y. Huang and Y. Fu, *Dalton Trans.*, 2013, **42**, 4175.
11. K. Ueura, T. Satoh and M. Miura, *Org. Lett.,* 2007, **9**, 1407.
12. K. Ueura, T. Satoh and M. Miura, *J. Org. Chem.*, 2007, **72**, 5362.
13. S. Mochida, K. Hirano, T. Satoh and M. Miura, *J. Org. Chem.,* 2009, **74**, 6295.
14. F. Wang, G. Song and X. Li, *Org. Lett.,* 2010, **12**, 5430.
15. X. Li, X. Gong, M. Zhao, G. Song, J. Deng and X. Li, *Org. Lett.,* 2011, **13**, 5808.
16. X. Wang, X. Li, J. Xiao, Y. Jiang and X. Li, *Synlett,* 2012, 1649.
17. C. Zhu and J. R. Falck, *Tetrahedron,* 2012, **68**, 9192.
18. X. Wei, F. Wang, G. Song, Z. Du and X. Li, *Org. Biomol. Chem.,* 2012, **10**, 5521.
19. J. Zhang and T. Loh, *Chem. Commun.,* 2012, **48**, 11232.
20. N. Guimond, S. I. Gorelsky and K. Fagnou, *J. Am. Chem. Soc.,* 2011, **133**, 6449.
21. B. Ye and N. Cramer, *Science*, 2012, **338**, 504.
22. H. Wang and F. Glorius, *Angew. Chem. Int. Ed.,* 2012, **51**, 7318.
23. L. Xu, Q. Zhu, G. Huang, B. Cheng and Y. Xia, *J. Org. Chem.,* 2012, **77**, 3017.
24. M. P. Sibi and K. Itoh, *J. Am. Chem. Soc.,* 2007, **129**, 8064.
25. Q. Lin, D. Meloni, Y. Pan, M. Xia, J. Rodgers, S. Shepard, M. Li, L. Galya, B. Metcalf, T. Yue, P. Liu and J. Zhou, *Org. Lett.,* 2009, **11**, 1999.
26. A. Uhe, M. Hölscher and W. Leitner, *Chem. Eur. J.*, 2010, **16**, 9203.
27. X. Li and M. Zhao, *J. Org. Chem.,* 2011, **76**, 8530.

Chapter Four

Further Oxidative Coupling Reactions of Selected Substrates

4 Chapter Four

4.1 Introduction

Coupling reactions of *C*-phenylpyrazoles with alkynes and alkenes via AMLA C-H activation were explored in **Chapter Two** and **Chapter Three**. This chapter will deal with coupling reactions of other directing groups including imidazole, imidazoline, pyrazolidinone, hydrazine, carboxylic acid and oxime with alkynes via AMLA C-H activation, including a discussion on the different factors affecting product selectivity.

4.2 Results and Discussion

The same general reaction conditions applied to catalysis with *C*-phenylpyrazoles were used to explore the reaction scope with other directing groups. The results are discussed based on the directing group used.

4.2.1 Phenylimidazole

Results are first discussed for reactions of 2-phenylimidazole (**4.1**) with symmetrical alkynes followed by reactions with unsymmetrical alkynes and finally with DMAD (**e**), an alkyne bearing electron-withdrawing groups. Reaction of **4.1** with 4-octyne (**a**) led to a mixture of products in a 3:1 ratio of which the major was purified by column chromatography. The ^{1}H NMR spectrum for the major component shows signals for six protons in the aromatic region due to **4.1** (**Scheme 4.1**), suggesting that one C-H has been functionalised. There are signals in the alkyl region for two propyl groups suggesting that one equivalent of 4-octyne (**a**) has reacted with **4.1**. The signals for the phenyl protons in the aromatic region are complex multiplets which appear as two 1H multiplets at δ 7.84 and δ 8.69 and one 2H multiplet at δ 7.57-7.59. The COSY NMR spectrum shows correlations from both 1H multiplets to the 2H multiplet. Furthermore, the TOCSY NMR spectrum shows correlations between all three phenyl peaks in the aryl region, meaning that they are all part of the same ring system. The two imidazole protons appear as two mutually coupled doublets at δ 7.56 and 7.59. Both CH_2 signals of one of the propyl chains show an NOE to the 1H multiplet at δ 7.84, whereas all the signals of the other propyl chain show an NOE to the 1H imidazole doublet at δ 7.56. This allows assignment of which propyl is next to the phenyl and which is next to the

imidazole. The ^{13}C NMR spectrum shows 17 signals as expected. The ESIMS shows ions at *m/z* 253 due to $[M+H]^+$ and HRMS (ESI) is correct for the product, **4.2a** (**Scheme 4.1**). Hence the directing group has undergone deprotonation and C-N reductive elimination as for *C*-phenyl pyrazole. Stoichiometric cyclometallation of **4.1** with $[Cp^*IrCl_2]_2$ has been reported by the groups of Davies[1] and Ikariya[2] however the NH proton was retained in these cases. This may be different as these were stoichiometric rather than catalytic reactions and also because Ir was the metal used rather than Rh.

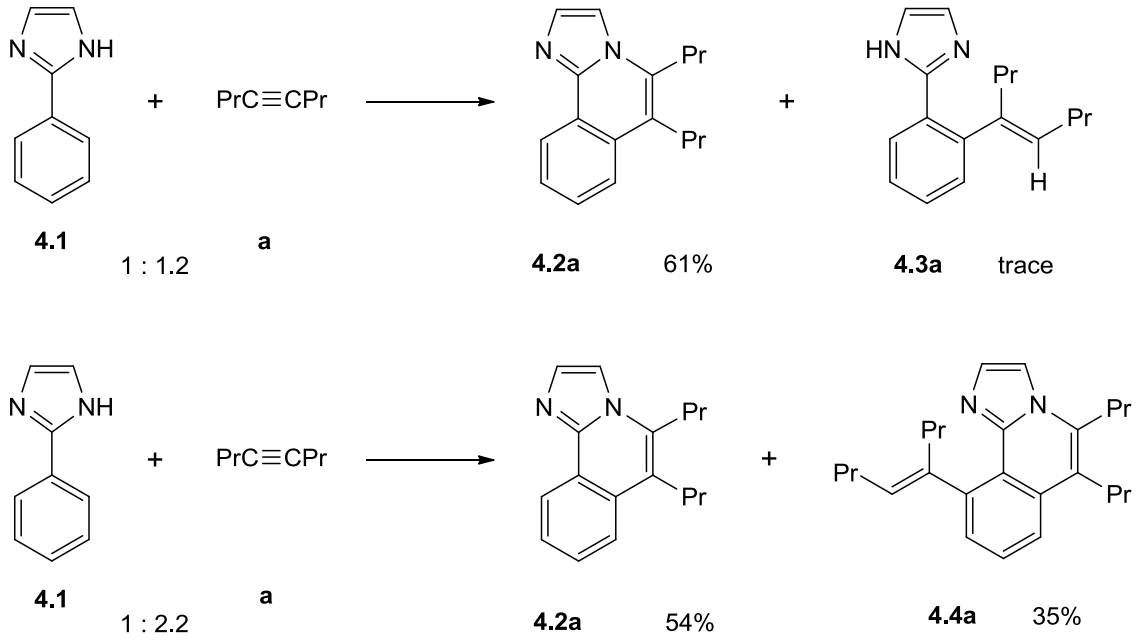

Reaction conditions: 5 mol% $[Cp^*Rh(MeCN)_3][PF_6]_2$, $Cu(OAc)_2.H_2O$ (2.5 eq.), DCE, 83 °C, 16 h

Scheme 4.1: C-H functionalisation of **4.1** with 4-octyne, (**a**) (1.2 or 2.2 equiv.).

Attempts to purify the minor component unfortunately failed and it was contaminated with **4.2a**. The ^1H NMR spectrum for the minor component shows a 1H triplet at δ 5.65 (J = 7.4 Hz) suggesting a vinylic product. There are signals for six protons in the aromatic region and a broad singlet at δ 9.81 is assigned as an NH group. There are two sets of signals in the alkyl region for two different propyl groups. Of the CH_2CH_2Me protons, one appears as a 2H triplet at δ 2.08 and the other as an apparent quartet at δ 2.24 as it is next to the vinyl CH as well as next to a CH_2. The ESIMS shows ions at *m/z* 255 due to $[M+H]^+$. Based on these data, the structure of the minor product is proposed to be the vinylic compound **4.3a** (**Scheme 4.1**).

As naphthalenes have sometimes been formed by incorporation of two equivalents of alkyne the reaction of **4.1** with 2.2 equivalents of 4-octyne (**a**) was carried out (**Scheme 4.3**). This reaction led to a mixture of products in a roughly 1:1 ratio which were purified by column chromatography. **Scheme 4.1** shows that one of these products was **4.2a**.

The ^{1}H NMR spectrum for the second product shows signals for two mutually coupled doublets for the imidazole protons and three phenyl protons, suggesting that two C-H's have been functionalised. There are four sets of signals in the alkyl region corresponding to four propyl groups, suggesting that two equivalents of 4-octyne (**a**) have reacted with **4.1**. A 1H triplet at δ 5.62 couples to a CH_2 of a propyl at ca. δ 2.5 and shows an NOE to a phenyl proton at δ 7.39, hence the triplet is assigned to a vinyl proton. The COSY NMR spectrum allows identification of the two other phenyl protons and the NOESY spectrum shows a correlation between one of these and another CH_2 group. The ^{13}C APT NMR spectrum shows the presence of eight CH_2 groups and ten peaks for CH and CH_3 carbons. The ESIMS shows an ion at *m/z* 363 due to $[M+H]^+$ and HRMS (ESI) agrees with the formulation of the product as **4.4a** (**Scheme 4.1**). The formation of **4.4a** can be explained by the fact that with imidazole, the first formed product still has another directing group atom. This can undergo C-H activation *meta* to the original site rather than *ortho* which would form a naphthalene. Following C-H activation migratory insertion is followed by protonation to give a vinyl rather than C-N reductive elimination which would generate a cationic heterocycle.

Attempts to grow crystals of **4.2a** from dichloromethane/hexane failed as the compound decomposed in solution and crystallised to give **4.5a** (**Fig. 4.1**). The ^{1}H NMR spectrum for **4.5a** is similar to that of **4.2a** with signals for four protons in the aromatic region but the doublets for the imidazole protons have been lost and instead there are two mutually coupled 1H doublets, a broad one at δ 9.08 and another at δ 9.67 which show a cross peak in the COSY spectrum. The ^{13}C APT NMR spectrum shows 16 signals including four negative peaks for CH_2 carbons and a peak at δ 164.1 which is assigned to a C=O. The product could not be unambiguously identified from this data but fortunately an X-ray crystal structure was obtained which showed the product to be **4.5a**. The ESIMS shows an ion at *m/z* 257 due to $[M+H]^+$ and the HRMS (ESI) is in agreement with this formula. The crystal structure shows the isoquinoline fragment found in **4.2a** but with a

formamido substituent in place of the fused imidazole ring. The original alkyne bond C(2)—C(3) is now a double bond (C=C = 1.38(3) Å). The mechanism of formation of this product is currently unknown.

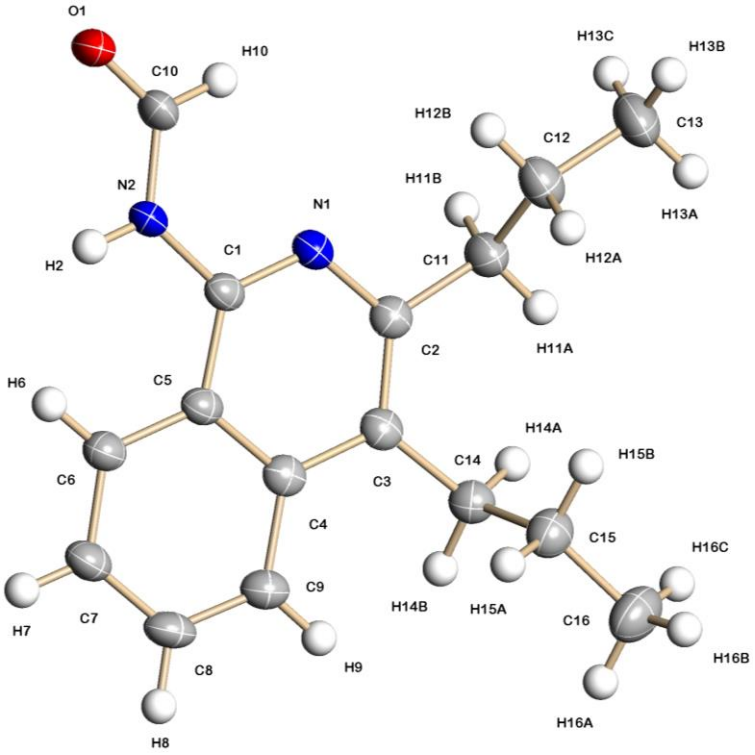

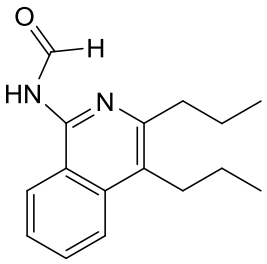

4.5a

N(1)-C(2)	1.349(7)	C(1)-C(5)	1.459(8)
C(2)-C(3)	1.405(8)	C(1)-N(2)	1.410(6)
C(3)-C(4)	1.408(7)	N(2)-C(10)	1.339(6)
C(1)-N(1)-C(2)	119.6(5)	N(1)-C(1)-N(2)	118.1(5)
C(2)-C(3)-C(4)	117.2(6)	C(1)-N(2)-C(10)	122.7(5)

Fig. 4.1: Decomposition product **4.5a** and its crystal structure with selected bond distances (Å) and angles (^{o}).

The vinylic minor product **4.3a** is formed when protonation occurs instead of C, N reductive elimination in the catalytic reaction. To investigate whether **4.3a** is formed only from within the catalytic cycle or whether it can be formed independently from **4.2a**, a reaction was carried out whereby pure **4.2a** was reacted with trifluoroacetic acid (**Scheme 4.2**). This reaction did not produce vinylic product **4.3a** and instead protonation of **4.2a** occurred to give the salt **4.2a′**. The ^{1}H NMR spectrum shows signals for the four phenyl protons, the two imidazole protons and two sets of signals in the alkyl region for the two propyl groups. All the signals are consistent for the structure of

4.2a but have different chemical shifts and some have different and there are similar NOEs. The ESIMS shows an ion at *m/z* 253 due to $[M+H]^+$. Suitable crystals of **4.2a′** were grown and the crystal structure of the cationic unit is shown in **Fig. 4.2** with selected bond distances (Å) and angles (^{o}).

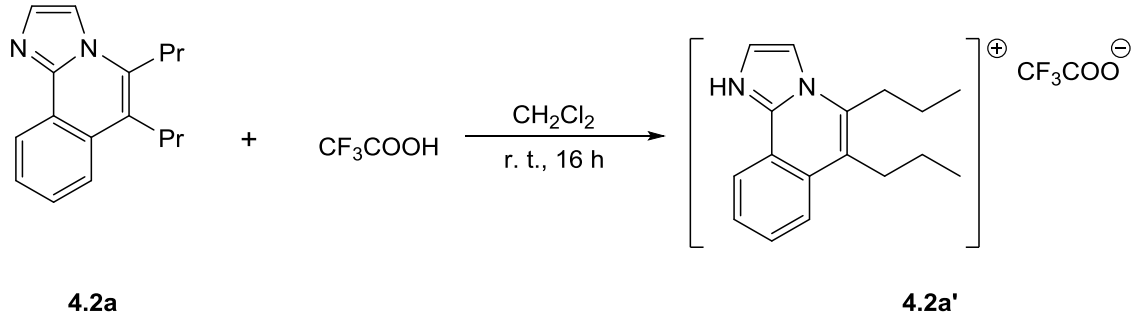

Scheme 4.2: Reaction of **4.2a** with trifluoroacetic acid.

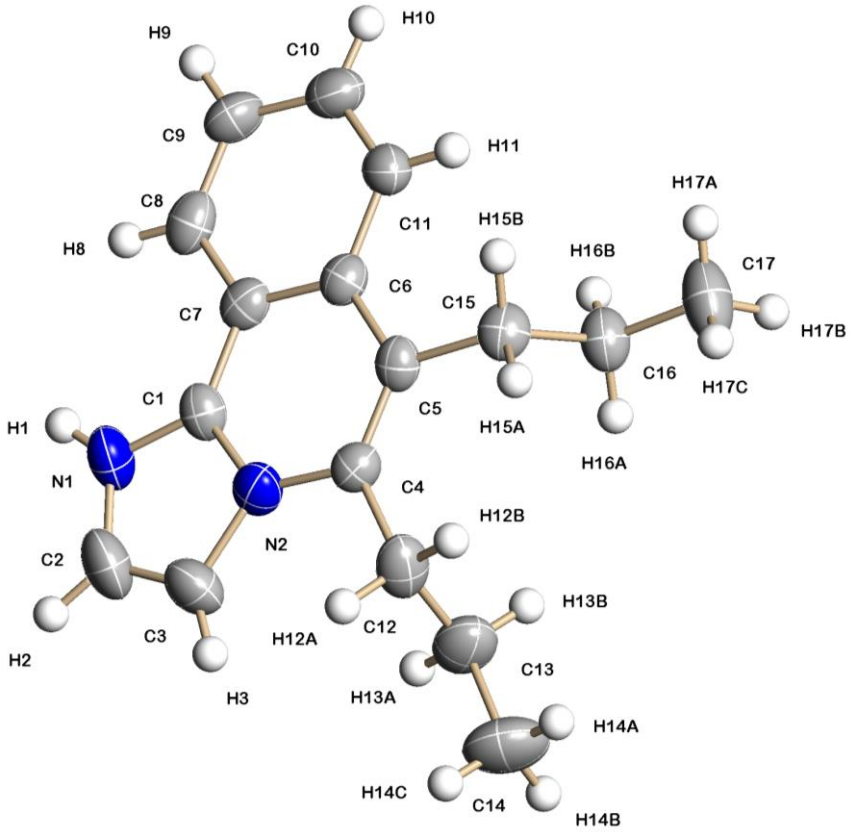

N(2)-C(4)	1.403(7)	C(4)-C(5)	1.348(7)
C(1)-C(7)	1.410(8)	C(5)-C(6)	1.456(7)
C(1)-N(2)-C(4)	123.4(4)	C(5)-C(6)-C(7)	120.7(5)
C(1)-C(7)-C(6)	115.8(5)	N(2)-C(4)-C(5)	117.7(5)

Fig. 4.2: Crystal structure of the cationic unit of **4.2a′**.

Reaction of **4.1** with diphenylacetylene (**b**) led to a mixture of products which were purified by column chromatography. For the major component the ESIMS shows an ion at *m/z* 321 corresponding to addition of one equivalent of diphenylacetylene (**b**) to **4.1**. In the ^{1}H NMR spectrum the aryl protons from diphenylacetylene and the two imidazole protons are difficult to fully assign due to overlapping signals but the aryl protons from the phenyl of the starting substrate are easily distinguishable and are able to be assigned with the help of COSY and NOESY NMR spectra. The COSY NMR spectrum shows correlations from a 1H triplet at δ 7.47 to a 1H doublet at δ 7.39 and the NOESY NMR spectrum shows an NOE from the latter doublet to a 2H doublet of doublets at δ 7.20. Therefore, the 1H doublet at δ 7.39 is assigned as H^6, the triplet to H^5 and the 2H doublet of doublets to H^7. The rest of the phenyl protons from **4.1** can then be assigned from their COSY correlations and signal multiplicities. The HRMS (ESI) is correct for the product, **4.2b** (**Scheme 4.3**). This product has also been reported by the group of Miura[3] and the data are in good agreement with the reported data. It has also been characterised by X-ray diffraction, see below.

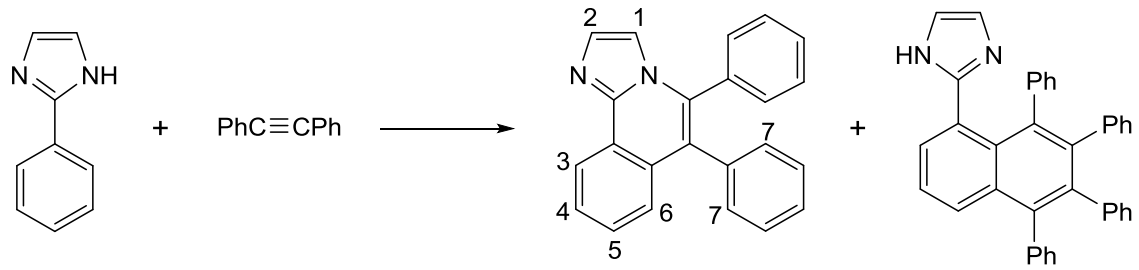

Reaction conditions: 5 mol% $[Cp^*Rh(MeCN)_3][PF_6]_2$, $Cu(OAc)_2.H_2O$ (2.5 eq.), DCE, 83 °C, 16 h

Scheme 4.3: C-H functionalisation of **4.1** with **b** (1.2 equiv.) with numbering for key NMR signals.

A crystal structure for **4.2b** was obtained (**Fig. 4.3**). The structure clearly shows that one equivalent of diphenylacetylene (**b**) has reacted with **4.1**. The original alkyne bond C(10)—C(11) is now a double bond (C=C = 1.35(4) Å) and the bond joining the phenyl to the imidazole is 1.43(4) Å.

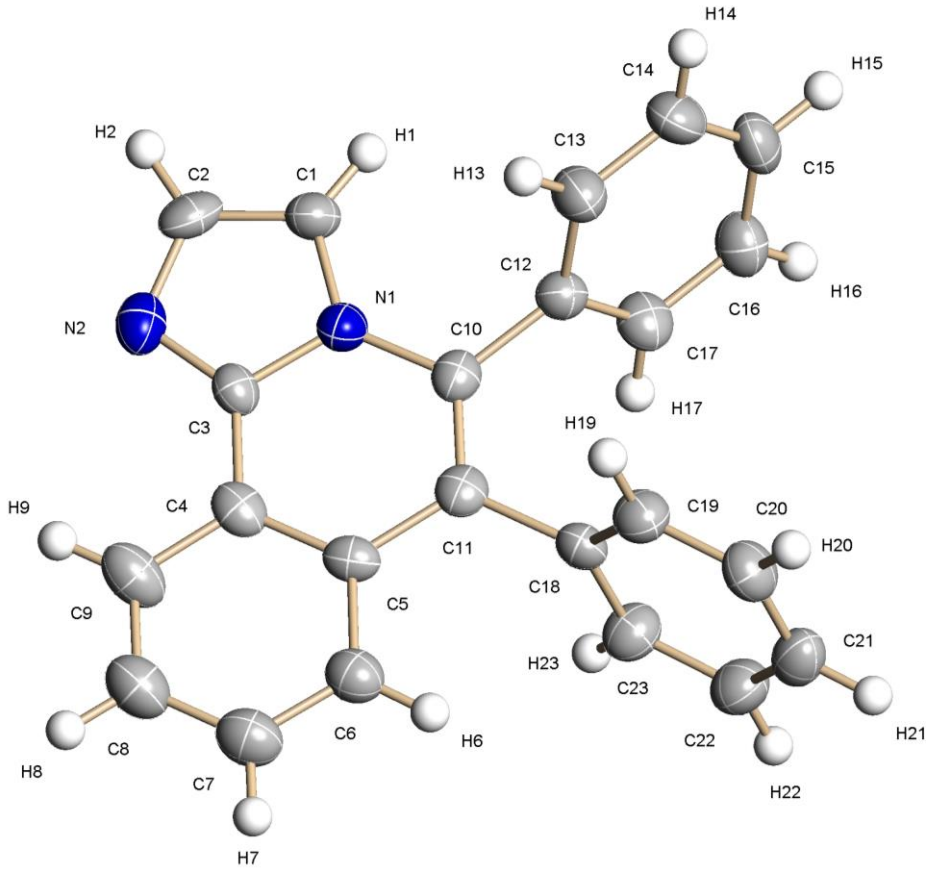

N(1)-C(10)	1.408(4)	C(4)-C(5)	1.392(4)
N(1)-C(3)	1.375(4)	C(5)-C(11)	1.450(4)
C(3)-C(4)	1.428(4)	C(10)-C(11)	1.353(4)
C(3)-N(1)-C(10)	123.7(3)	C(4)-C(5)-C(11)	120.9(3)
N(1)-C(3)-C(4)	118.8(3)	N(1)-C(10)-C(11)	118.1(3)

Fig. 4.3: Crystal structure of **4.2b** with selected bond distances (Å) and angles (^{o}).

The ^{1}H NMR spectrum for the minor component shows signals for two imidazole protons observed as a 2H singlet at δ 6.82. The ESIMS shows an ion at *m/z* 499 assigned to $[M+H]^{+}$ and the HRMS (ESI) is correct for the naphthalene product, **4.6b** (**Scheme 4.3**), ruling out a divinyl as the product which would have a mass two units higher. There is no 1H singlet visible in the vinyl region of the ^{1}H NMR spectrum so this rules out a cyclic monovinyl product such as **4.4a**. The ^{1}H NMR integration is consistent with 23 protons in the aromatic region as expected for incorporation of two molecules of alkyne. The ^{13}C DEPT NMR spectrum shows 16 C-H signals as expected for **4.6b**. This product was not observed by Miura *et al.*. The result of the reaction of **4.1**

with diphenylacetylene (**b**) is therefore different to the reaction with 4-octyne (**a**) which gives an *N*-heterocycle (**4.2a**) and a monovinyl (**4.3a**) as products.

Reactions of 2-phenylimidazole (**4.1**) with unsymmetrical alkynes were investigated next. Results are illustrated in **Scheme 4.4** for reactions of 2-phenylimidazole (**4.1**) with 1.2 equivalents of unsymmetrical alkynes. Reaction of **4.1** with 1-phenyl-1-propyne (**c**) led to a mixture of three products. Column chromatography gave an impure sample of the major product as a mixture of regioisomers, and a pure sample of a minor product.

The ^{1}H NMR spectrum for the major component shows signals consistent with the expected product **4.2c**. There are multiplets corresponding to four protons of the disubstituted aryl and five protons of a phenyl with a 3H singlet for a methyl group at δ 2.32 which shows an NOE to one of the aryl doublet of doublets and to a phenyl multiplet. There are additional minor signals in the aromatic region and a second singlet at δ 2.00 which could be assigned to the methyl of the opposite regioisomer (**4.2c′**). The ESIMS shows an ion at *m/z* 259 due to $[M+H]^{+}$ and the HRMS (ESI) is correct for the product, **4.2c** (**Scheme 4.4**). Unfortunately attempts to purify the products further failed.

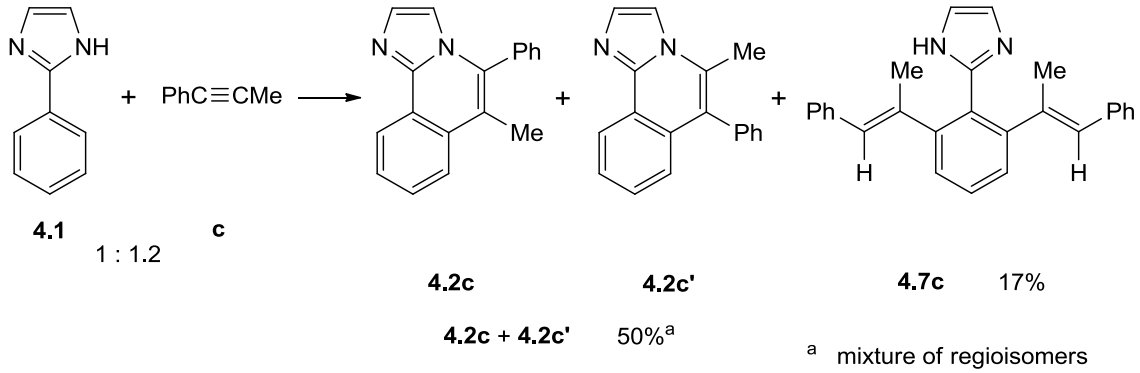

Reaction conditions: 5 mol% $[Cp^{*}Rh(MeCN)_3][PF_6]_2$, $Cu(OAc)_2.H_2O$ (2.5 eq.), DCE, 83 °C, 16 h

Scheme 4.4: C-H functionalisation of **4.1** with unsymmetrical alkyne **c** (1.2 equiv.).

The ^{1}H NMR spectrum for the minor component shows signals for 15 protons in the aromatic region, suggesting that two C-H's have been functionalised and that two equivalents of 1-phenyl-1-propyne (**c**) have reacted with **4.1**. The two imidazole protons are inequivalent and appear as singlets at δ 7.03 and δ 7.16. There is a 1H broad singlet at δ 9.02, indicating an NH proton. There are also two 3H methyl singlets both at δ 1.80 for the two methyl groups and a 2H singlet at δ 6.46 for two vinyl protons.

Tautomerisation is probably slow on the NMR timescale which means that the molecule is not symmetrical. This is consistent with the imidazole protons and the two methyl groups being different. The vinyl protons should be different as well but are further from the asymmetry so are too close to differentiate. The ESIMS shows ions at *m/z* 377 due to $[M+H]^+$ and HRMS (ESI) is correct for the product, **4.7c** (**Scheme 4.4**).

Finally, an alkyne bearing electron-withdrawing groups was tested. Reaction of **4.1** with DMAD (**e**) led to a mixture of products which after column chromatography led to isolation of the major product. The ^{1}H NMR spectrum for this product shows signals for five phenyl protons suggesting that there has been no C-H functionalisation. There are two mutually coupled doublets at δ 6.91 and δ 7.15 due to the imidazole protons, and a singlet at δ 6.93 which may be a vinyl proton. There are two 3H singlets at δ 3.56 and δ 3.57 for two CO_2Me groups, suggesting that one equivalent of DMAD (**e**) has reacted with **4.1**. The COSY NMR spectrum shows correlations between the vinyl proton at δ 6.93 and one of the CO_2Me signals, showing there is some long-range coupling between the two. The ^{13}C NMR spectrum shows 12 signals, including the vinyl CH at δ 126.3. The C=O carbon atoms are visible as the two most downfield peaks at δ 162.8 and δ 163.0. The ESIMS shows an ion at *m/z* 287 due to $[M+H]^+$ and the HRMS (ESI) is correct for the Michael addition product, **4.8e** (**Scheme 4.5**). This result is consistent with those obtained for DMAD reactions with *C*-phenylpyrazoles (see **Chapter Two**).

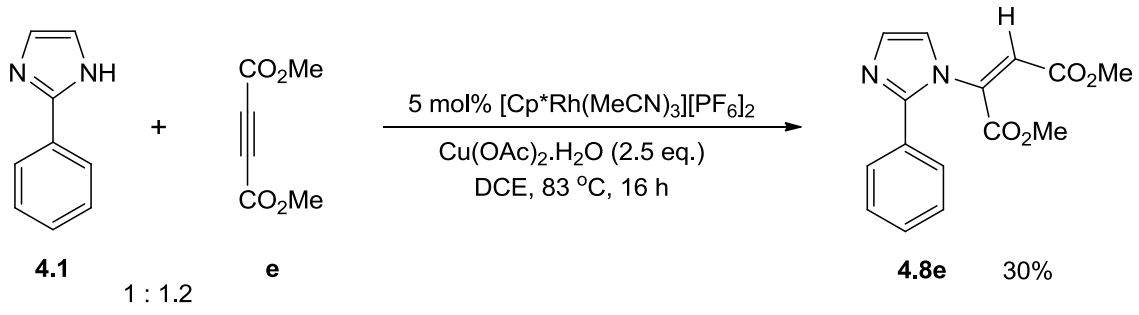

Scheme 4.5: C-H functionalisation of **4.1** with **e** (1.2 equiv.).

In conclusion, 2-phenylimidazole (**4.1**) successfully reacts with both symmetrical and unsymmetrical alkynes in Cp*Rh-catalysed oxidative coupling reactions. Deprotonation of the imidazole NH occurs to give N-heterocyclic products as the major products in most cases. Reactions of 2-phenylimidazole (**4.1**) are somewhat less selective than the equivalent reactions carried out with *C*-phenylpyrazoles. Whereas *C*-phenylpyrazoles give purely six-membered *N*-heterocyclic products from C, N reductive elimination, 2-phenylimidazole in addition gives vinyls and naphthalenes as minor products. This suggests that protonation to give vinylic minor products and double C-H activation to give naphthalene or divinyl minor products are competing pathways with C, N reductive elimination. It can be presumed that all these pathways have similar energy barriers in reactions with phenylimidazoles. Reactions of *C*-phenylpyrazoles with alkynes did not lead to any products incorporating two equivalents of alkyne (see **Chapter Two**). With 2-phenylimidazole (**4.1**), the first formed product still has another directing group atom which can undergo C-H activation. The reaction with DMAD is consistent with the results obtained with *C*-phenylpyrazole reactions in that an aza-Michael addition occurs in preference to C-H functionalisation.

4.2.2 Phenylimidazoline

2-Phenylimidazoline (**4.9**) was the next substrate tested. **Scheme 4.6** illustrates the results for reactions of 2-phenylimidazoline (**4.9**) with symmetrical alkynes. Reaction of **4.9** with 4-octyne (**a**) led to a mixture of products in a 2:1 ratio which were purified by column chromatography. Analysis of the NMR and mass spectrometry data shows that dehydrogenation of the imidazoline had occurred to give **4.2a** as the major product.

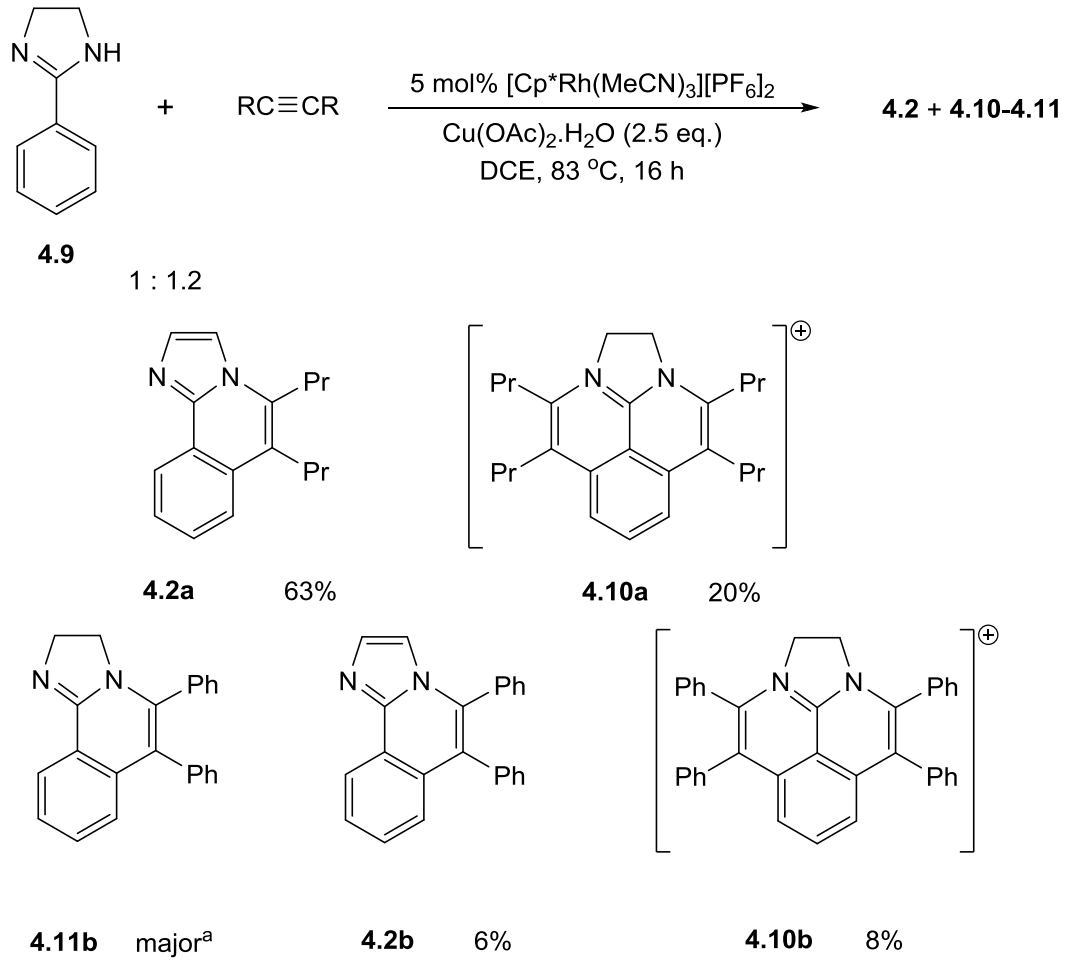

Scheme 4.6: C-H functionalisation of **4.9** with symmetrical alkynes (1.2 equiv.).

The ^{1}H NMR spectrum for the minor component shows a 4H singlet at δ 4.69 due to the imidazoline protons, a 2H doublet at δ 7.33 and a 1H triplet at δ 7.83 for the phenyl protons. These signals suggest that two C-H bonds have been functionalised to give a symmetrical product. There are two sets of signals in the alkyl region corresponding to four propyl groups suggesting that two equivalents of 4-octyne (**a**) have reacted with

4.9. Both CH_2 signals from one set of propyl peaks show NOEs to the 2H aryl doublet, whereas both CH_2 signals of the other propyl chain show NOEs to the 4H imidazoline singlet. The ^{13}C APT NMR spectrum shows five CH_2 environments and four for the CH_3 and CH carbons. The ESIMS shows an ion at *m/z* 363 due to $[M]^+$ and the HRMS (ESI) is correct for the cationic product, **4.10a** (**Scheme 4.6**). This cannot be a naphthalene product as there would then be three different aryl protons and the propyl chains would be inequivalent as well. Recently, substrates such as *N*-phenylpyrazole and phenylpyridine have been shown to react with diphenylacetylene (**b**) to give cationic products (**Fig 4.4**).[4]

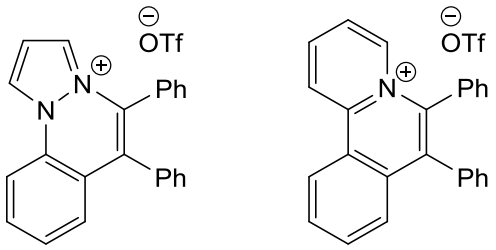

Fig 4.4: Cationic products obtained with *N*-phenylpyrazole and phenylpyridine.[4]

Reaction of **4.9** with diphenylacetylene (**b**) led to a mixture of products in a roughly 3:3:1 crude ratio which was purified by column chromatography. Analysis of the NMR and mass spectrometry data shows that dehydrogenation of the imidazoline had occurred to give **4.2b** as the minor product. One of the major products was isolated impure and was found to be contaminated with **4.2b**. The ^1H NMR spectrum for this major product shows two 2H triplets at δ 3.79 (*J* = 9.8 Hz) and at δ 3.98 (*J* = 9.8 Hz) for the imidazoline protons. The ESIMS and FAB MS both show an ion at *m/z* 323 due to $[M+H]^+$ which is consistent with the product being, **4.11b** (**Scheme 4.6**). The ^1H NMR integration is consistent with 14 protons in the aromatic region as expected for incorporation of one equivalent of diphenylacetylene. Fortunately a crystal of this was obtained from $CDCl_3$ and the crystal structure was determined (**Fig. 4.5**). The structure shows the imidazoline ring and the product is **4.11b**. The original alkyne bond C(10)—C(11) is now a double bond (C=C = 1.36(3) Å) and the bond joining the phenyl to the imidazoline is 1.45(3) Å in length.

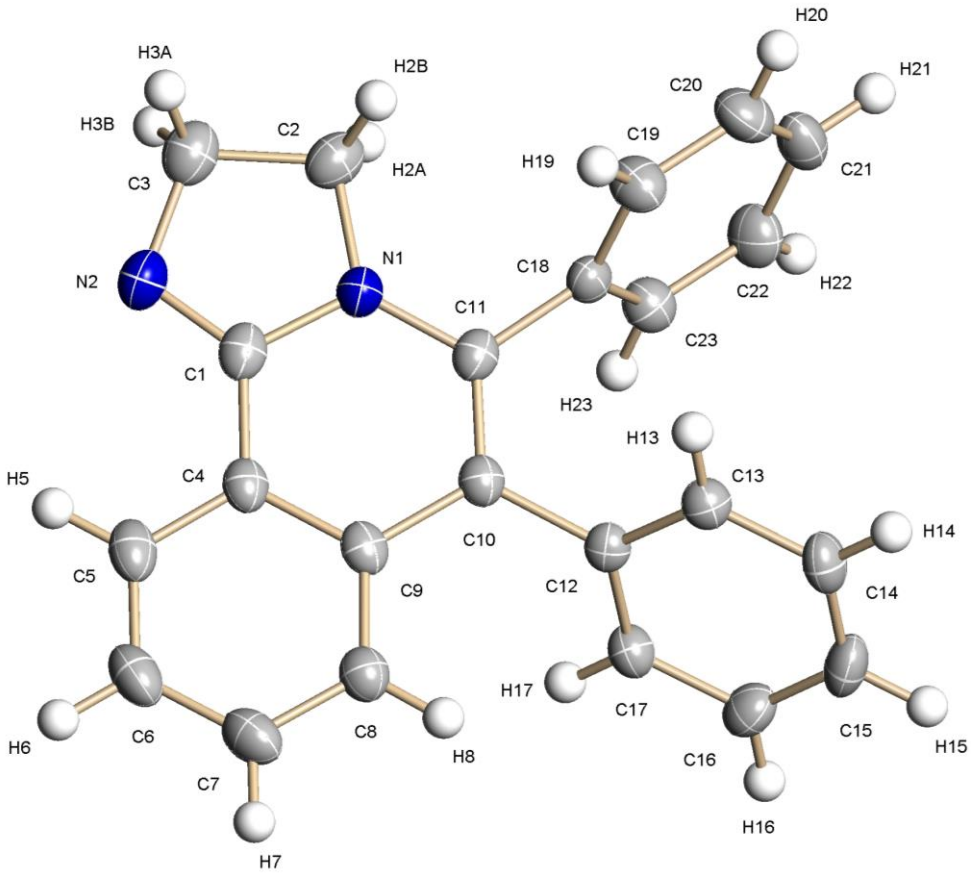

N(1)-C(1)	1.389(2)	C(4)-C(9)	1.408(3)
N(1)-C(11)	1.379(2)	C(9)-C(10)	1.458(3)
C(1)-C(4)	1.451(3)	C(10)-C(11)	1.361(3)
C(1)-N(1)-C(11)	123.9(18)	C(4)-C(9)-C(10)	119.8(2)
N(1)-C(11)-C(10)	120.1(19)	C(9)-C(10)-C(11)	119.5(19)

Fig. 4.5: Crystal structure of **4.11b** with selected bond distances (Å) and angles (^{o}).

The ^{1}H NMR spectrum for the third product shows signals for more than 20 protons in the aromatic region suggesting two equivalents of diphenylacetylene may have been incorporated. There is a 2H doublet at δ 7.07 (J = 7.8 Hz) and a 1H triplet at δ 7.66 (J = 7.8 Hz) which are assigned to the phenyl protons from **4.9**, and the imidazoline protons appear as a 4H singlet at δ 4.45, these are consistent with two C-H bonds having been functionalised to give a symmetrical product rather than a naphthalene product. The ^{13}C APT NMR spectrum also shows just one CH_2 environment. The ESIMS shows an ion at *m/z* 499 which corresponds to $[M]^+$ for the cationic product, **4.10b** (**Scheme 4.6**) and the HRMS (ESI) shows an ion at *m/z* 499.2173 which confirms this formula.

In conclusion, 2-phenylimidazoline (**4.9**) successfully reacts with symmetrical alkynes in Cp*Rh-catalysed oxidative coupling reactions. The substrate reacts as an anionic directing group whereby deprotonation of the imidazoline NH occurs which makes formation of N-heterocyclic products favourable by C, N reductive elimination. Dehydrogenation of the imidazoline ring is possible which leads to some of the same products as formed in reactions of 2-phenylimidazole (**4.1**) with alkynes. Formation of symmetrical cationic products (**4.10**) incorporating two equivalents of alkyne is also observed. This suggests that phenylimidazolines can react with two equivalents of alkyne to form stable cationic species. This is in contrast to reactions of 2-phenylimidazole which have been shown to react with two equivalents of alkyne to give naphthalenes (**4.6b**) or cyclic monovinyl (**4.4a**) compounds but not any cationic products analogous to **4.10** (as shown above in **Section 4.2.1**). This is likely due to the nitrogen atom on the imidazoline being more basic than the analogous one on imidazole and therefore alkylation of it by C, N reductive elimination to form cationic species **4.10** is easier. In the reaction with 2-phenylimidazole, protonation occurs instead to give a vinyl.

4.2.3 Phenylpyrazolidinone

1-Phenyl-3-pyrazolidinone (**4.12**) was tested in Cp*Rh-catalysed oxidative coupling reactions with alkynes. **Scheme 4.7** shows the results of the reaction of **4.12** with 4-octyne (**a**) which led to a mixture of products in a 4:1 ratio which were purified by column chromatography.

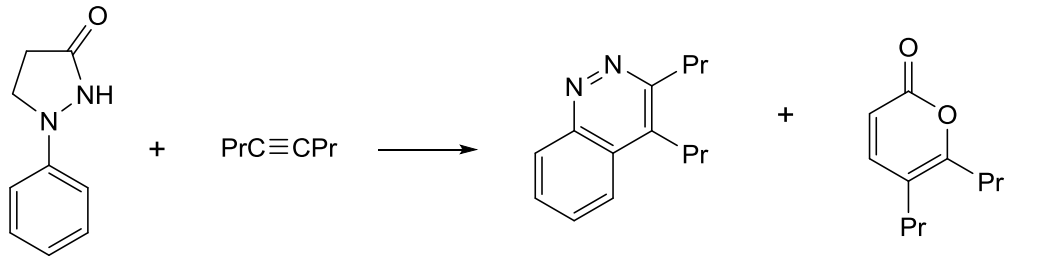

4.12 1 : 1.2 **a** **4.13a** 64% **4.14a** 17%

Reaction conditions: 5 mol% $[Cp^*Rh(MeCN)_3][PF_6]_2$, $Cu(OAc)_2.H_2O$ (2.5 eq.), DCE, 83 ^oC, 16 h

Scheme 4.7: C-H functionalisation of **4.12** with 4-octyne (**a**) (1.2 equiv.).

The ^{1}H NMR spectrum for the major component shows four multiplets in the aromatic region and two sets of signals for propyl groups, suggesting that one equivalent of 4-octyne (**a**) has reacted with **4.12**. However, there is no evidence for the C_2H_4 group of the pyrazolidinone ring. The ESIMS shows an ion at *m/z* 215 which is consistent with $[M+H]^+$ and HRMS (ESI) agrees with the formula for the cinnoline product, **4.13a** (**Scheme 4.7**). The assignment was proved further by independent synthesis of the same product (see phenylhydrazine below).

The ^{1}H NMR spectrum for the minor component was rather unexpected and shows no aromatic signals. There are two mutually coupled 1H doublets at δ 6.14 and δ 7.17 (J = 9.4 Hz) and two sets of signals in the alkyl region for two inequivalent propyl groups. All the signals from one set of propyl peaks show NOEs to the 1H doublet at δ 7.17. In total, there are only signals for 16 protons and the ^{13}C NMR spectrum only shows 11 signals. The ESIMS shows an ion at *m/z* 181 which corresponds to $[M+H]^+$ for the pyrone product, **4.14a** (**Scheme 4.7**) and the HRMS (ESI) agrees with this formulation. Hence, this product seems to have been formed from the oxidative coupling reaction of the fragment that breaks away from **4.12**. Pyrones similar to this product have been reported by Miura *et al.* from the Cp*Rh-catalysed reactions of acrylic acids with alkynes, however only the analogous compound formed with diphenylacetylene was reported.[5]

Similar cinnolines have been reported by Zhu and Yamane in their study of Pd-catalysed reactions of 2-iodophenyltriazenes with alkynes via an oxidative addition/reductive elimination mechanism.[6] The group of Huang was inspired by this to attempt the Cp*Rh-catalysed oxidative coupling reaction of triazenyl arenes with alkynes in order to synthesise cinnolines. However, the triazene substituent acted as a removable directing group and indoles were formed instead.[7, 8]

In 2013, You *et al.* reported the synthesis of various cinnolines, including **4.13a,** and cinnolinium salts, via Cp*Rh-catalysed oxidative coupling reactions of azobenzenes (**Scheme 4.8**).[9] In this formation of cinnolines the *t*-butyl that is presumably lost as isobutene in the reductive elimination step is similar to the reactions of aryl aldimines with alkynes to give isoquinolines reported by the group of Fagnou, (see **Chapter Two**, **Section 2.5**).[10] Related cinnolinium salts have also been reported in 2013 by Cheng *et al.* also from Cp*Rh-catalysed oxidative coupling reactions of azobenzenes.[11]

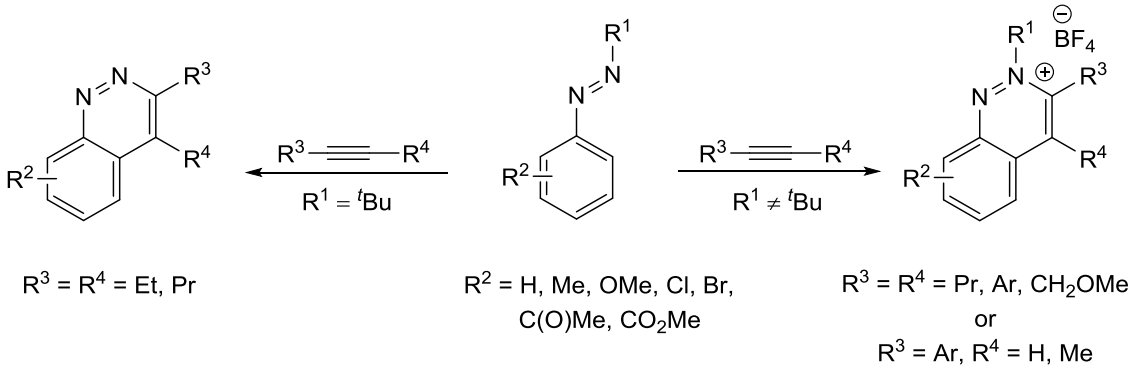

Scheme 4.8: Synthesis of cinnolines and cinnolinium salts, via Cp*Rh-catalysed oxidative coupling reactions of azobenzenes.[9]

The reaction of **4.12** with DMAD (**e**) was also tested and led to a mixture of products of which the major was purified by column chromatography. The ^{1}H NMR spectrum of the product shows two 3H singlets at δ 3.72 and at δ 3.90 for CO_2Me groups. There are signals for five aromatic protons in the range δ 7.27-7.60 which are in a 1:1 ratio with the signals from DMAD, suggesting that one equivalent of DMAD has reacted with **4.12** but that no C-H functionalisation has occurred. Additionally, there are two mutually coupled 1H doublets at δ 6.15 and δ 7.85 (J = 2.7 Hz). There is a singlet at δ 5.96, suggesting a vinyl proton which shows an NOE to one of the CO_2Me signals. The 1H doublet at δ 7.85 shows an NOE to the phenyl proton at δ 7.60. The ^{13}C NMR spectrum shows 13 peaks. The ESIMS shows an ion at *m/z* 303 due to $[M+H]^+$ and HRMS (ESI) is correct for the Michael addition product, **4.15e** or **4.15e′** (**Scheme 4.9**). Differentiating between the two isomers proved difficult so which isomer formed remains unknown. Here, it can be seen that dehydrogenation of the pyrazolidinone ring has occurred during the reaction. This was also the case for the pyrone product (**4.14a**) discussed earlier.

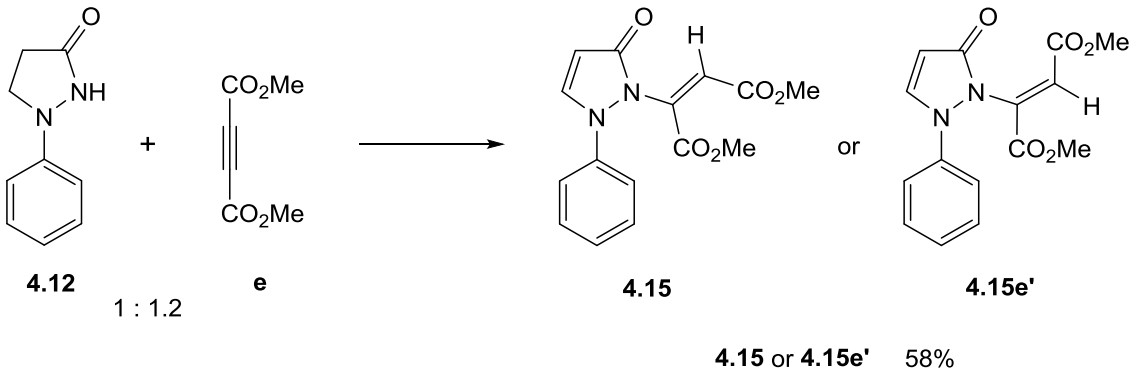

Reaction conditions: 5 mol% $[Cp^*Rh(MeCN)_3][PF_6]_2$, $Cu(OAc)_2.H_2O$ (2.5 eq.), DCE, 83 °C, 16 h

Scheme 4.9: C-H functionalisation of **4.12** with DMAD (**e**) (1.2 equiv.).

A blank reaction was carried out where **4.12** was reacted with DMAD (**e**) in the absence of Rh and Cu (**Scheme 4.10**). The reaction gave a mixture of products of which two were purified by column chromatography. The ^{1}H NMR spectrum of the first product shows no singlets for the CO_2Me groups and signals for five aromatic protons, suggesting that no reaction with DMAD has occurred nor any C-H functionalisation. There are two mutually coupled 1H doublets at δ 5.91 and δ 7.67 (*J* = *ca* 2.5 Hz). There is a broad singlet at δ 11.62, suggesting an NH proton. The ESIMS shows an ion at *m/z* 161 due to $[M+H]^+$ and is correct for the product, **4.16** (**Scheme 4.10**). This is the dehydrogenated analogue of **4.12** and is a known compound.[12] This shows that dehydrogenation of the pyrazolidinone ring can readily occur when heated in solution and therefore this may occur under the standard catalytic conditions. Indeed the formation of **4.15e** and **4.15e′** as well as the pyrone product (**4.14a**) must involve dehydrogenation of the CH_2-CH_2 bond.

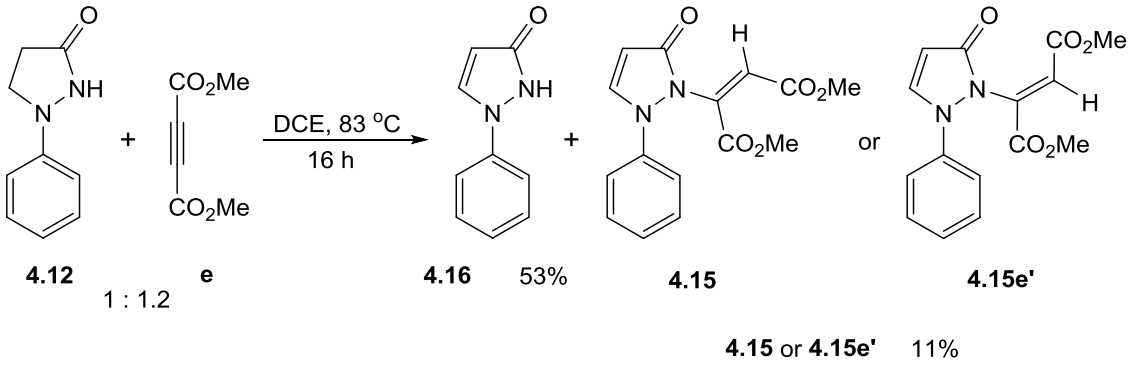

Scheme 4.10: Blank reaction of **4.12** with DMAD (**e**).

The ^{1}H and ^{13}C NMR spectra of the second product are very similar to those of **4.15e** except with slightly different chemical shifts for the signals, indicating an isomer of **4.15e**. The ^{1}H NMR spectrum of the product shows two 3H singlets at δ 3.65 and at δ 3.88 for CO_2Me groups. There are signals for five aromatic protons in the range δ 7.25-7.45 which are in a 1:1 ratio with the signals from DMAD, suggesting that one equivalent of DMAD has reacted with **4.12** but no C-H functionalisation has occurred. Again there are two mutually coupled 1H doublets at δ 5.69 and δ 7.62 (J = 3.9 Hz) typical of the dehydrogenated pyrazolidinone ring. There is a singlet at δ 5.52, indicating a vinyl proton and the ^{13}C NMR spectrum shows 13 peaks. The ESIMS shows an ion at *m/z* 303 due to $[M+H]^+$ and HRMS (ESI) is correct for the Michael addition product, **4.15e** or **4.15e′** (**Scheme 4.10**). Differentiating between the two isomers is difficult but the isomer formed was different to the one observed in the reaction in presence of Rh/Cu (**Scheme 4.9**). Again, dehydrogenation of the pyrazolidinone ring has occurred during the reaction, as found with **4.15** and the pyrone product (**4.14a**).

Following on from this blank reaction, product **4.16** was tested as a substrate in a reaction with DMAD (**Scheme 4.11**). As expected, it reacted in an aza-Michael reaction to give **4.15e** or **4.15e′** in 34% yield. The isomer formed was the same as the one formed in the reaction of **4.12** with DMAD in the presence of Rh/Cu (**Scheme 4.9**).

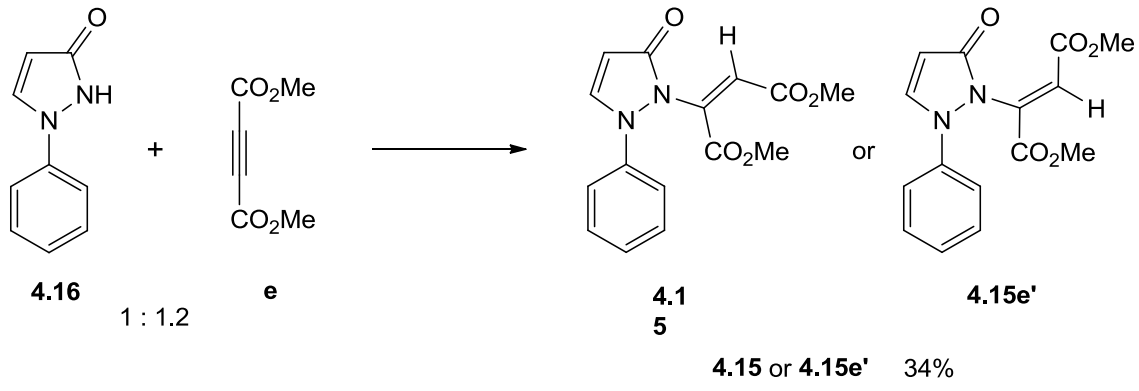

Scheme 4.11: C-H functionalisation of **4.12** with DMAD (**e**) (1.2 equiv.).

In conclusion, the results show that 1-phenyl-3-pyrazolidinone (**4.12**) successfully reacts with 4-octyne (**a**) in Cp*Rh-catalysed oxidative coupling reactions. This substrate

is quite reactive in that the pyrazolidinone ring is susceptible to ring cleavage which leads to the formation of a cinnoline (**4.13a**) and a pyrone (**4.14a**) in the reaction with 4-octyne (**a**). The substrate reacts in an aza-Michael addition reaction with DMAD which is consistent with the reactivity observed with *C*-phenylpyrazoles and 2-phenylimidazole (**4.1**). Mechanistic studies show that dehydrogenation of the pyrazolidinone ring readily occurs when **4.12** is reacted with DMAD without Rh and Cu being present. This suggests the dehydrogenation likely occurs under the standard reaction conditions.

4.2.4 Phenylhydrazine

As discussed in the previous section, 1-phenyl-3-pyrazolidinone (**4.12**) reacted with 4-octyne (**a**) to give a cinnoline (**4.13a**) as the major product. In principle, cinnolines may be formed from oxidative coupling reactions of phenylhydrazine with alkynes; therefore phenylhydrazine (**4.17**) was the next substrate tested. **Scheme 4.12** shows the results of the reaction of **4.17** with 4-octyne (**a**). As anticipated, phenylhydrazine reacted with 4-octyne to give the cinnoline **4.13a**. No reaction occurred when **4.17** was reacted with diphenylacetylene (**b**) or (4-nitrophenyl)but-3-yn-1-ol (**d**) and only the starting materials were recovered. This suggests that phenylhydrazine may only react with dialkyl alkynes. This is consistent with the results reported by You *et al.* in their study with azobenzenes where *N*-(*t*-Butyl)-2-phenyldiazene was shown to only form cinnolines with dialkyl alkynes ($R^1 = {}^t$Bu, **Scheme 4.8**).[9]

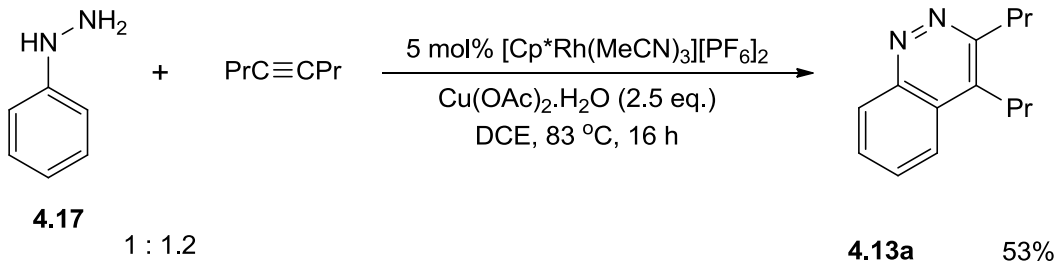

Scheme 4.12: C-H functionalisation of phenylhydrazine with 4-octyne (**a**).

4.2.5 Benzoic Acid

Miura *et al.* reported Cp*Rh-catalysed reactions of benzoic acids with alkynes bearing electron-donating groups.[13, 14] Diethylacetylene dicarboxylate (DEAD) was the only alkyne with electron-withdrawing groups reported in the study but the reaction was carried out using an Ir/Ag catalyst system. The reaction was not reported for a Rh/Cu system. The reaction of benzoic acid (**4.18**) with DMAD (**e**) was therefore tested using the cationic Cp*Rh/Cu system. Surprisingly, benzoic acid reacted with DMAD in an oxidative coupling reaction to give the isochromene **4.19e** (**Scheme 4.13**).

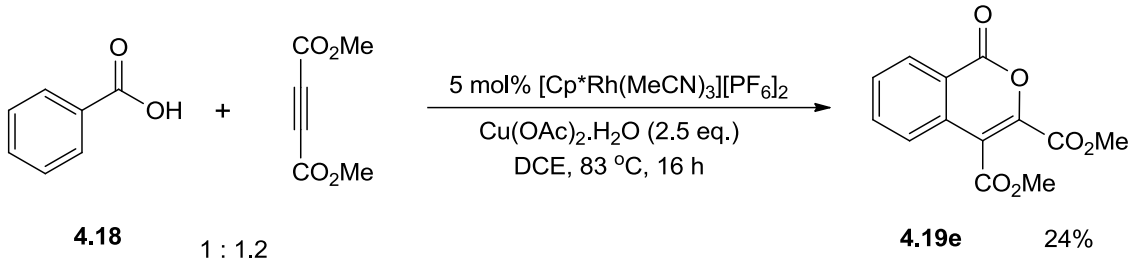

Scheme 4.13: C-H functionalisation of benzoic acid with DMAD (**e**).

The ^{1}H NMR spectrum of the product shows four multiplets for aromatic protons suggesting that one C-H bond has been functionalised. There are two 3H singlets at δ 3.90 and at δ 3.95 for the CO_2Me groups suggesting that one equivalent of DMAD has reacted with **4.18**. Complete assignment of the four phenyl protons is not possible because there are no NOEs visible in the NOESY NMR spectrum between any of these and the CO_2Me groups. The ^{13}C NMR spectrum shows 13 peaks as expected. The ESIMS shows an ion at *m/z* 263 due to $[M+H]^+$ and HRMS (ESI) is correct for the product, **4.19e** (**Scheme 4.13**).

The product was crystallised and the X-ray structure was determined. There are two unique molecules in the unit cell and one is shown in **Fig. 4.6**. The structure clearly shows that one equivalent of DMAD (**e**) has reacted with **4.18** to give an isochromene. The original alkyne bond C(4)—C(5) is now a double bond (average C=C = 1.41(8) Å) and the bond joining the phenyl to the C=O is 1.455(7) Å (average bond length).

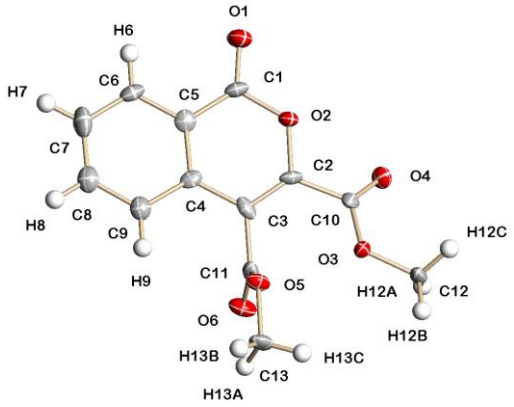

C(1)-O(2)	1.374(7)	C(3)-C(4)	1.443(8)
C(1)-C(5)	1.450(7)	C(2)-C(3)	1.329(7)
C(4)-C(5)	1.401(8)	C(2)-O(2)	1.389(5)
C(1)-O(2)-C(2)	121.4(4)	C(2)-C(3)-C(4)	118.3(6)
O(2)-C(2)-C(3)	123.0(5)	C(3)-C(4)-C(5)	120.3(5)

Fig. 4.6: Crystal structure of one molecule of **4.19e** with selected average bond distances (Å) and angles (^{o}).

This result is in contrast to the reactions of *C*-phenylpyrazoles and 2-phenylimidazole with DMAD in which an aza-Michael addition occurs to give vinylic products. This is possibly because Pz^- is a better nucleophile than CO_2^-.

4.2.6 (*E*)-Benzaldehyde Oxime

(*E*)-Benzaldehyde oxime (**4.20**) is a substrate that might be deprotonated at a remote site, hence this was tested in Cp*Rh-catalysed oxidative coupling reactions. Similar ketoximes and ketoxime esters have been reported to successfully undergo Cp*Rh-catalysed oxidative coupling with alkynes.[15-18] These reactions gave only isoquinolines or their derivatives as products. So far no reactions of aldoximes have been reported.

Scheme 4.14 shows the results of the reaction of **4.20** with 4-octyne (**a**). This reaction led to a mixture of three products which were difficult to purify by column chromatography which resulted in low isolated yields. The ^{1}H NMR spectrum of the major product shows signals for four aromatic protons, a 1H singlet at δ 9.08 and two sets of signals in the alkyl region for two different propyl groups, suggesting that one equivalent of 4-octyne has reacted with **4.20**. The ESIMS shows an ion at *m/z* 213 due to $[M+H]^+$ and is correct for the isoquinoline product, **4.21a** (**Scheme 4.14**). The data

are all consistent with that reported previously by Fagnou *et al.* from reactions of ^{t}BuN-aryl aldimines with alkynes (see **Chapter Two**, **Section 2.5**).[10]

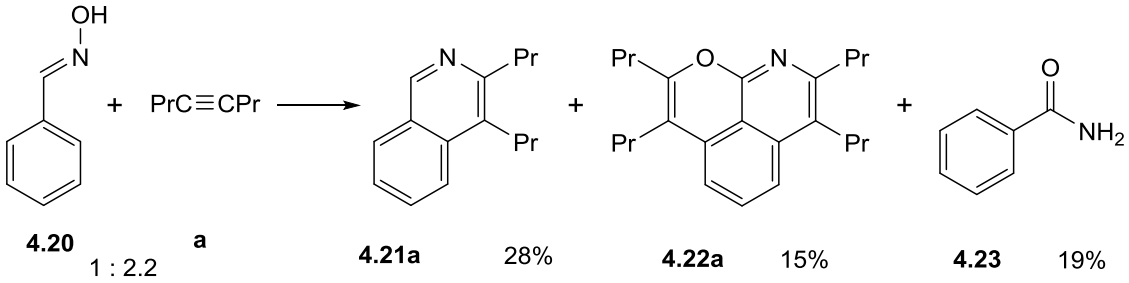

Reaction conditions: 5 mol% $[Cp^*Rh(MeCN)_3][PF_6]_2$, $Cu(OAc)_2.H_2O$ (2.5 eq.) DCE, 83 ^{o}C, 16 h

Scheme 4.14: C-H functionalisation of **4.19** with 4-octyne (**a**).

The ^{1}H NMR spectrum of one of the minor products shows two 1H doublets and one 1H doublet of doublets for three inequivalent aromatic protons suggesting that two C-H bonds have been functionalised to give an unsymmetrical product. The alkyl region shows signals for over 25 protons, suggesting that two equivalents of 4-octyne have reacted with **4.20**. Each of the aromatic 1H doublets shows NOEs to CH_2 signals of different propyl groups in the alkyl region. The ^{13}C APT NMR spectrum confirms the presence of four propyl groups. IR spectroscopy shows a peak at 1648 cm^{-1}, supporting the presence of a C=O bond of an amide but there is no accompanying N-H stretch. The ESIMS shows an ion at *m/z* 338 due to $[M+H]^+$ and HRMS (ESI) is correct for the pyranoisoquinoline, **4.22a** (**Scheme 4.14**). This cannot be a naphthalene product as in that case only one of the aromatic 1H doublets would show NOEs to the propyl signals.

The ^{1}H NMR spectrum of the second minor product signals for five aromatic protons suggesting that no C-H bonds have been functionalised. Also, there are no peaks in the alkyl region suggesting there has been no reaction with 4-octyne. IR spectroscopy shows a peak at 1655 cm^{-1} for an amide C=O bond and another at 3363 cm^{-1} for an amide N-H bond. The ESIMS shows an ion at *m/z* 122 due to $[M+H]^+$ which is correct for this component being benzamide, **4.23** (**Scheme 4.14**). The NMR and IR data is in good agreement with literature data.[19] It is possible that the oxime (**4.20**) could have undergone Beckmann rearrangement to form **4.23**. Indeed Rh^{I} has been shown to catalyse the conversion of aldoximes to amides so this is another possibility.[20]

As benzamide (**4.23**) was isolated from the reaction of (*E*)-Benzaldehyde oxime (**4.20**) with 4-octyne (**a**), it was also tested as a substrate. **Scheme 4.15** shows the results of the reaction with 2.2 equivalents of 4-octyne (**a**). The pyranoisoquinoline (**4.22a**) was isolated in 52% yield along with 30% of unreacted benzamide (**4.23**). This provides further evidence that tautomerisation of benzamide to benzimic acid (**4.24**) is likely during the reaction which leads to the formation of **4.22a**. It also shows that benzamide reacts to give yet another type of product as well as isoquinolones, benzoisoquinolones, naphthalenes and quinolinones illustrated in **Chapter Two**, **Section 2.5**.

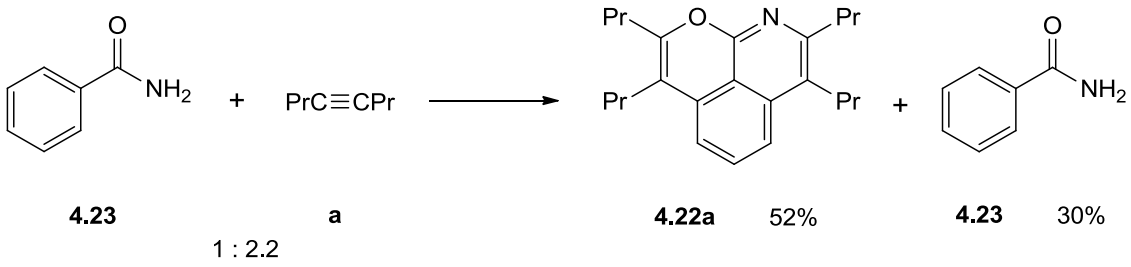

Reaction conditions: 5 mol% $[Cp^*Rh(MeCN)_3][PF_6]_2$, $Cu(OAc)_2.H_2O$ (2.5 eq.), DCE, 83 °C, 16 h

Scheme 4.15: C-H functionalisation of benzamide (**4.23**) with 4-octyne (**a**).

The formation of benzamide (**4.23**) in the reaction can help explain the formation of **4.22a**. Thus, tautomerisation of benzamide to benzimic acid (**4.24**) then Cp*Rh-catalysed oxidative coupling with two equivalents of 4-octyne (**a**) would give **4.22a** (**Scheme 4.16**). Moreover, formation of a naphthalene product from **4.23** is unlikely since primary benzamides usually react as anionic directing groups to give an isoquinolone. This has been reported by Li *et al.* for the reaction of benzamide (**4.23**) with 4-octyne.[21] A second C-H activation at the carbon *meta* to the amide functionality seems unlikely as C-N reductive elimination is likely to be favoured. The formation of **4.22a** differs from the result reported by Li *et al.* who reported formation of an isoquinolone from this reaction. This may be due to the fact that they used the neutral $[Cp^*RhCl_2]_2$ catalyst rather than the cationic Rh catalyst and also because they carried out their reaction with one equivalent of alkyne.

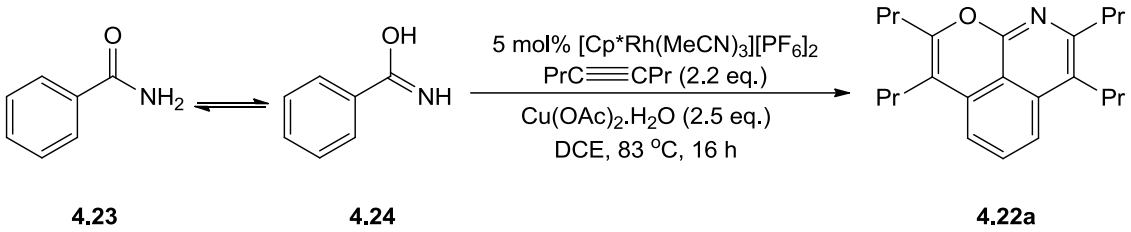

4.23 **4.24** **4.22a**

Scheme 4.16: Tautomerisation of **4.23** to **4.24** and subsequent C-H functionalisation with 4-octyne (2.2 equiv.).

To investigate the difference in this result and that obtained by Li *et al.*, the same reaction was carried out with just one equivalent of 4-octyne (**a**), neutral $[Cp^*RhCl_2]_2$ catalyst and AgOAc. Surprisingly, this still gave **4.22a** in 46% yield along with unreacted benzamide. The only difference in this reaction was the use of AgOAc instead of Ag_2CO_3 which suggests that the presence of acetate may be a factor in determining product selectivity. To probe this possibility, the reaction was repeated with silver oxide (**Scheme 4.17**). This led to formation of the isoquinolone product observed by Li *et al.* (**4.25a**) which was subsequently transformed to **4.22a** in a reaction with 1.2 equivalents of 4-octyne using the same standard conditions from this thesis. These results show that **4.25a** is a viable intermediate in the reactions that go straight to **4.22a**, i.e. formation of the N-heterocycle can occur first followed by formation of the O-heterocycle. This confirms that the presence of acetate controls product selectivity. It is possible that without the use of acetate, the C-H activation may go via a different mechanism, maybe involving transmetallation with silver.

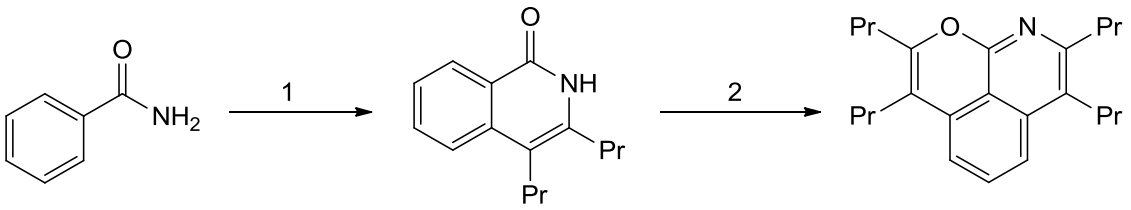

4.23 **4.25a** 19% **4.22a** 75%

Reaction conditions:

1. 4 mol% $[Cp^*RhCl_2]_2$, 4-octyne (1.2 eq.), Ag_2O (1.5 eq.), MeCN, 115 °C, 16 h
2. 5 mol% $[Cp^*Rh(MeCN)_3][PF_6]_2$, 4-octyne (1.2 eq.), $Cu(OAc)_2.H_2O$ (2.5 eq.), DCE, 83 °C, 16 h

Scheme 4.17: Formation of **4.25** leading to formation of **4.23**.

In conclusion, (*E*)-Benzaldehyde oxime (**4.20**) has been shown to react with 2.2 equivalents of 4-octyne (**a**) to give a mixture of products including an isoquinoline and a pyranoisoquinoline. Pure benzamide was also isolated which is likely formed from **4.20** via Beckmann rearrangement and which possibly leads to the pyranoisoquinoline product after tautomerising to benzimic acid. No isoquinoline N-oxide product was observed from the reaction of **4.20** with 4-octyne (**a**). The reported ketoximes give more selective results than **4.20** in that only isoquinoline products are obtained.[15-18] This could be due to the substituent on the C=N carbon hindering any isomerism of the oxime. Indeed, the Beckmann rearrangement requires the substituent to be hydrogen.

4.3 Conclusions

This chapter dealt with Cp*Rh-catalysed oxidative coupling reactions of selected substrates with alkynes. Reactions of *C*-phenylpyrazoles with alkynes were discussed extensively in **Chapter Two** and this chapter has shown that the same type of catalysis can be applied to various other substrates. In the majority of cases, the substrates reacted as anionic directing groups whereby deprotonation of Y-H (Y = N, O) occurred which led to heterocyclic products being formed as C-Y reductive elimination was favourable. These substrates include 2-phenylimidazole (**4.1**) which was found to be less selective than *C*-phenylpyrazoles. It reacted with one equivalent of alkyne to give *N*-heterocycles (**4.2**) as major products but naphthalenes (**4.6b**) and vinyls (**4.3a** and **4.4a**) were also formed as minor products. 2-phenylimidazoline (**4.9**) reacted with alkynes and also underwent dehydrogenation of the imidazoline ring to give the same products found with 2-phenylimidazole. In addition, symmetric cationic heterocycles (**4.10**) incorporating two equivalents of alkyne were also formed as minor products. 1-phenyl-3-pyrazolidinone (**4.12**) was found to be a very reactive substrate where, in the reaction with 4-octyne (**a**), cleavage of the pyrazolidinone ring occurred to give a cinnoline (**4.13a**) and a pyrone (**4.14a**). It reacted with DMAD to give aza-Michael addition products (**4.15e** and **4.15e′**) where dehydrogenation of the pyrazolidinone ring was evident. Phenylhydrazine (**4.17**) reacted with 4-octyne (**a**) to give a cinnoline (**4.13a**) but failed to react with diaryl and aryl-alkyl alkynes. Benzoic acid (**4.18**) was shown to successfully carry out oxidative coupling with DMAD. (*E*)-Benzaldehyde oxime gave rise to isoquinoline (**4.21a**) and pyranoisoquinoline (**4.22a**) products and also gave benzamide (**4.23**) by a Beckmann rearrangement. Benzamide was independently reacted with 4-octyne to give the pyranoisoquinoline (**4.22a**). The

isoquinolone **4.25a** was formed by the reaction of benzamide with 1.2 equivalents of 4-octyne (**a**) and was subsequently transformed to **4.22a**, showing that formation of the N-heterocycle can occur first followed by formation of the O-heterocycle

4.4 Experimental

See Experimental section of **Chapter Two** for general information. In addition, infrared spectra were recorded in the solid state with Universal ATR sampling accessories on a Perkin Elmer Spectrum One FTIR instrument. The reagents 2-phenylimidazole, 2-phenylimidazoline, 1-phenyl-3-pyrazolidinone, phenylhydrazine and benzoic acid were purchased from Aldrich Chemical Co. and used without further purification. (*E*)-Benzaldehyde oxime was prepared using literature procedures.[20]

General procedure for catalysis reactions

$[Cp^*Rh(MeCN)_3][PF_6]_2$ (33 mg, 5 mol%), the appropriate directing ligand (1.0 eq.), $Cu(OAc)_2.H_2O$ (2.5 eq.), appropriate alkyne (1.2 eq.) and DCE (10 ml) were added to a Schlenk flask. The Schlenk flask was sealed with a screw-cap and then transferred to a preheated oil bath and stirred at 83 °C for 16 hours. The reaction mixture was cooled to room temperature with continuous stirring and diluted with Et_2O (10 ml).The mixture was transferred to separating funnel and ammonium hydroxide solution (10 ml, 2 M) was added. The aqueous layer was extracted with Et_2O (3 x 10 ml) and the organic layers were combined and dried over $MgSO_4$. The drying agent was removed by filtration and solvent was removed under reduced pressure.

Reaction of 4.1 with 4-octyne (a) (1.2 equiv.)

Following the general procedure, a Schlenk flask was loaded with $[Cp^*Rh(MeCN)_3][PF_6]_2$ (33 mg, 5 mol%), 2-phenylimidazole (4.1, 144 mg, 1.0 mmol), $Cu(OAc)_2.H_2O$ (500 mg, 2.5 mmol), 4-octyne (a, 132 mg, 1.2 mmol) and DCE (10 ml). The crude ^1H NMR spectrum showed the presence of two products in a 3:1 ratio. Column chromatography was carried out, eluting with 40% ethyl acetate in petroleum ether (40-60 °C) to give **4.2a** as a brown solid (153 mg, 61%, 0.61 mmol) and **4.3a** as impure brown oil.

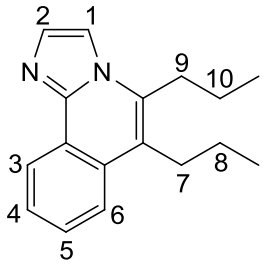

4.2a: ^{1}H NMR (400 MHz, $CDCl_3$): δ 1.10 (t, *J* = 5.9 Hz, 3H, CH_2CH_2*Me*), 1.12 (t, *J* = 5.9 Hz, 3H, CH_2CH_2*Me*), 1.65-1.73 (m, 2H, H^8), 1.75-1.83 (m, 2H, H^{10}), 2.91-2.95 (m, 2H, H^7), 2.98-3.02 (m, 2H, H^9), 7.56 (d, *J* = 1.2 Hz, 1H, H^1), 7.57-7.59 (m, 2H, H^4, H^5), 7.59 (d, *J* = 1.2 Hz, 1H, H^2), 7.84 (m, 1H, H^6), 8.69 (m, 1H, H^3), ^{13}C {^{1}H} NMR (125 MHz, $CDCl_3$): δ 14.3 (CH_2CH_2*Me*), 14.5 (CH_2CH_2*Me*), 20.6 (C^{10}), 23.8 (C^8), 29.71 (C^7), 31.4 (C^9), 111.9 (C^1), 119.9, 123.1, 123.6 (C^3/C^6), 123.7 (C^3/C^6), 126.8 (C^4/C^5), 128.0 (C^4/C^5), 129.6, 130.6, 131.0 (C^2), 132.6, 142.9 (N-*C*-N). ESIMS: *m/z* 253 $[M+H]^+$. HRMS (ESI): Calcd for $C_{17}H_{21}N_2$ $[M+H]^+$ 253.1705, found 253.1715.

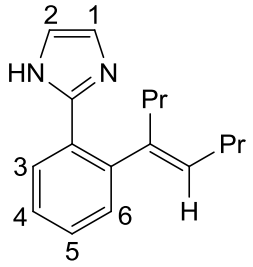

4.3a: This was obtained in a mixture with **4.2a**. ^{1}H NMR (400 MHz, $CDCl_3$): δ 0.78 (t, *J* = 7.4 Hz, 3H, CH_2CH_2*Me*), 0.83-0.91 (m, 2H, CH_2C*H*$_2$Me), 1.02 (t, *J* = 7.4 Hz, 3H, CH_2CH_2*Me*), 1.53 (sex, *J* = 7.4 Hz, 2H, CH_2C*H*$_2$Me), 2.08 (t, *J* = 7.8 Hz, 2H, C*H*$_2$$CH_2$Me), 2.24 (td, *J* = 7.4 Hz, 2H, C*H*$_2$C(H)=C), 5.65 (t, *J* = 7.4 Hz, 1H, PrC(*H*)=C), 7.10-7.12 (m, 3H, H^1, H^2, H^3/H^6), 7.29 (td, *J* = 1.6, 7.4 Hz, 1H, H^4/H^5), 7.35 (td, *J* = 1.2, 7.4 Hz, 1H, H^4/H^5), 8.06 (dd, *J* = 1.2, 7.4 Hz, 1H, H^3/H^6), 9.81 (br s, 1H, N*H*). ESIMS: *m/z* 255 $[M+H]^+$.

Reaction of 4.1 with 4-octyne (a) (2.2 equiv.)

Following the general procedure, a Schlenk flask was loaded with $[Cp^*Rh(MeCN)_3][PF_6]_2$ (33 mg, 5 mol%), 2-phenylimidazole (4.1, 144 mg, 1.0 mmol), $Cu(OAc)_2.H_2O$ (500 mg, 2.5 mmol), 4-octyne (**a**, 242 mg, 2.2 mmol) and DCE (10 ml). The crude ^{1}H NMR spectrum showed the presence of two products in a 1:1 ratio. The products were purified by column chromatography eluting with 5% ethyl acetate in dichloromethane to give **4.4a** as yellow oil (127 mg, 35%, 0.35 mmol) and **4.2a** as a brown solid (137 mg, 54%, 0.54 mmol).

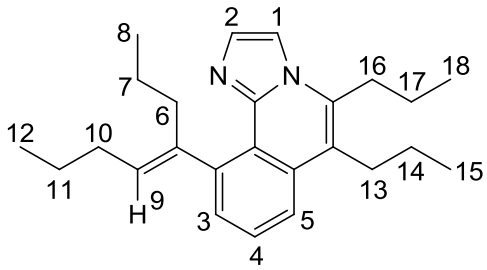

4.4a: ^{1}H NMR (400 MHz, $CDCl_3$): δ 0.86 (t, *J* = 7.4 Hz, 3H, H^8), 1.03 (t, *J* = 7.0 Hz, 3H, H^{12}), 1.14 (t, *J* = 7.4 Hz, 3H, H^{15}/H^{18}), 1.16 (t, *J* = 7.4 Hz, 3H, H^{15}/H^{18}), 1.26-1.36 (br m, 2H, H^7), 1.48-1.60 (br m, 2H, H^{11}), 1.73 (sex, *J* = 7.4 Hz, 2H, H^{14}), 1.80 (sex, *J* = 7.4 Hz, 2H, H^{17}), 2.26-2.50 (br m, 3H, H^6 + H^{10}), 2.87-2.95 (br m, 1H, H^6), 2.98-3.02 (m, 2H, H^{13}), 3.09 (t, *J* = 7.8 Hz, 2H, H^{16}), 5.62 (t, *J* = 7.4 Hz, 1H, H^9), 7.39 (dd, *J* = 1.2, 7.4 Hz, 1H, H^3), 7.69 (dd, *J* = 7.4, 8.2 Hz, 1H, H^4), 7.78 (d, *J* = 2.0 Hz, 1H, H^1), 7.90 (dd, *J* = 1.2, 8.2 Hz, 1H, H^5), 7.96 (br d, *J* = 1.2 Hz, 1H, H^2), ^{13}C {^{1}H} NMR (100 MHz, $CDCl_3$): δ 14.0 (C^8/C^{12}), 14.1 (C^8/C^{12}), 14.2 (C^{15}/C^{18}), 14.5 (C^{15}/C^{18}), 20.6 (C^{17}), 21.6 (C^7), 22.8 (C^{11}), 23.7 (C^{14}), 30.2 (C^{10} + C^{13}), 31.1 (C^{16}), 33.8 (C^6), 112.7 (C^1), 122.9 (C^5), 129.5 (C^4), 130.6 (C^3), 131.6 (C^9), 132.8, 142.7. ESIMS: *m/z* 363 $[M+H]^+$. HRMS (ESI): Calcd for $C_{25}H_{35}N_2$ $[M+H]^+$ 363.2800, found 363.2788. ^{13}C NMR spectrum does not show C^2.

Decomposition of 4.2a

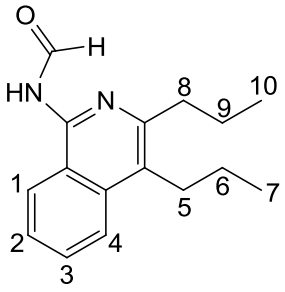

Recrystallisation of **4.2a** using dichloromethane/hexane gave the decomposition product **4.5a** as white crystals (57 mg, 22%, 0.22 mmol). ^{1}H NMR (400 MHz, $CDCl_3$): δ 1.02 (t, *J* = 7.4 Hz, 3H, H^{10}), 1.09 (t, *J* = 7.0 Hz, 3H, H^7), 1.66 (sex, *J* = 7.0 Hz, 2H, H^6), 1.81 (sex, *J* = 7.4 Hz, 3H, H^9), 2.85 (t, *J* = 7.4 Hz, 2H, H^8), 2.97 (t, *J* = 7.8 Hz, 1H, H^5), 7.56 (t, *J* = 7.4 Hz, 1H, H^2/H^3), 7.70 (t, *J* = 7.4 Hz, 1H, H^2/H^3), 7.95-7.98 (m, 2H, H^1 + H^4), 9.08 (br d, *J* = 8.2 Hz, 1H, N*H*), 9.67 (d, *J* = 9.8 Hz, 1H, C(O)*H*), ^{13}C {^{1}H} NMR (100 MHz, $CDCl_3$): δ 14.2 (C^{10}), 14.5 (C^7), 22.9 (C^9), 24.0 (C^6), 29.6 (C^5), 36.7 (C^8), 117.2, 121.9 (C^1/C^4), 123.9 (C^1/C^4), 125.3, 126.0 (C^2/C^3), 130.2 (C^2/C^3), 137.2, 145.3, 150.7, 164.1 (*C*=O). ESIMS: *m/z* 257 $[M+H]^+$. HRMS (ESI): Calcd for $C_{16}H_{21}N_2O$ $[M+H]^+$ 257.1654, found 257.1651.

Protonation of 4.2a

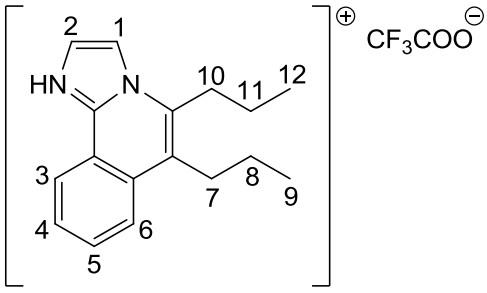

A round-bottomed flask was loaded with **4.2a** (64 mg, 0.25 mmol) which was dissolved in the minimum amount of dichloromethane. Trifluoroacetic acid (2 drops) was added and the mixture was stirred overnight. Solvent was removed under reduced pressure to give **4.2a′** as a white solid (74 mg, 80%, 0.20 mmol). Recrystallisation using dichloromethane/hexane gave the **4.2a′** as white crystals. ^{1}H NMR (400 MHz, $CDCl_3$): δ 1.16 (t, *J* = 7.4 Hz, 3H, H^9), 1.18 (t, *J* = 7.4 Hz, 3H, H^{12}), 1.74 (sex, *J* = 7.4 Hz, 2H, H^8), 1.81 (sex, *J* = 7.4 Hz, 3H, H^{11}), 3.03-3.07 (m, 2H, H^7), 3.12 (t, *J* = 7.8 Hz, 1H, H^{10}), 7.73 (d, *J* = 2.0 Hz, 1H, H^1), 7.85 (td, *J* = 1.2, 8.2 Hz, 1H, H^4), 7.90 (td, *J* = 1.2, 8.2 Hz, 1H, H^5), 8.01 (d, *J* = 2.0 Hz, 1H, H^2), 8.04 (d, *J* = 8.2 Hz, 1H, H^6), 8.84 (dd, *J* = 1.2, 8.2 Hz, 1H, H^3), ^{13}C {^{1}H} NMR (100 MHz, $CDCl_3$): δ 14.0 (C^9/C^{12}), 14.4 (C^9/C^{12}), 20.8 (C^{11}), 23.8 (C^8), 29.8 (C^7/C^{10}), 30.7 (C^7/C^{10}), 113.2 (C^1), 116.7, 122.1 (C^2), 124.5 (C^6), 124.9 (C^3), 125.8, 129.5 (C^4), 131.6, 132.3, 132.5 (C^5), 138.5, 161.0 (q, *J* = 35.2 Hz, CF_3COO). ESIMS: *m/z* 253 $[M]^+$.

Reaction of 4.1 with diphenylacetylene (b)

Following the general procedure, a Schlenk flask was loaded with $[Cp^*Rh(MeCN)_3][PF_6]_2$ (22 mg, 5 mol%), 2-phenylimidazole (**4.1**, 144 mg, 1.0 mmol), $Cu(OAc)_2.H_2O$ (500 mg, 2.5 mmol), diphenylacetylene (**b**, 214 mg, 1.2 mmol) and DCE (10 ml). The products were purified by column chromatography, eluting from 100% dichloromethane to 50% ethyl acetate in petroleum ether (40-60 °C) to give **4.2b** as a white solid (280 mg, 88%, 0.88 mmol) and **4.6b** as a white solid (39 mg, 8%, 0.08 mmol). Recrystallisation using dichloromethane/hexane gave **4.2b** as white needles.

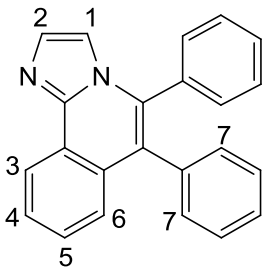

4.2b: ^{1}H NMR (400 MHz, $CDCl_3$): δ 7.20 (dd, *J* = 1.6, 7.8 Hz, 3H, H^7 + H^1/H^2), 7.25-7.33 (m, 8H, H^1/H^2 + *Ar-H*), 7.39 (d, *J* = 8.2 Hz, 1H, H^6), 7.47 (t, *J* = 1.6, 8.2 Hz, 1H, H^5), 7.51 (td, *J* = 1.6 Hz, 1H, H^1/H^2), 7.64 (td, *J* = 1.2, 8.2 Hz, 1H, H^4), 8.76 (d, *J* = 8.2 Hz, 1H, H^3). ^{13}C {^{1}H} NMR (100 MHz, $CDCl_3$): δ 113.9 (C^1/C^2), 123.1 (C^3), 124.5, 126.5 (C^6), 127.3 (Ar), 127.8 (C^4), 128.1 (C^5 + Ar), 128.4,

128.6 (C^1/C^2), 128.9 (Ar), 129.3, 130.2 (Ar), 130.6, 130.8, 131.4 (C^7), 133.4, 133.5, 135.9 (C-*N*-C). ESIMS: *m/z* 321 $[M+H]^+$. HRMS (ESI): Calcd for $C_{23}H_{17}N_2$ $[M+H]^+$ 321.1392, found 321.1388.

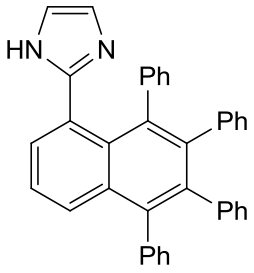

4.6b: ^{1}H NMR (500 MHz, $CDCl_3$): δ 6.82 (s, 2H, *Imidazole*), 7.09-7.12 (m, 4H, *Ar-H*), 7.18-7.35 (m, 5H, *Ar-H*), 7.37 (d, *J* = 7.7 Hz, 2H, *Ar-H*), 7.41 (dd, *J* = 1.2, 8.2 Hz, 2H, *Ar-H*), 7.45-7.50 (m, 4H, *Ar-H*), 7.57 (dd, *J* = 1.2, 7.7 Hz, 4H, *Ar-H*), 7.66 (dd, *J* = 1.2, 7.7 Hz, 2H, *Ar-H*). ^{13}C {^{1}H} NMR (125 MHz, $CDCl_3$): δ 113.4 (*C*-H (Im)), 124.6, 126.0 (Ar), 126.5 (Ar), 126.7 (Ar), 126.7 (Ar), 127.2 (Ar), 127.4 (Ar), 127.9 (Ar), 128.1 (Ar), 128.6 (Ar), 128.7 (Ar), 129.6 (Ar), 130.2 (Ar), 130.7 (Ar), 130.9 (Ar), 131.0 (Ar), 131.6 (Ar), 133.9, 136.7, 138.3, 140.5, 141.5, 144.0 (N-*C*-N). ESIMS: *m/z* 499 $[M+H]^+$. HRMS (ESI): Calcd for $C_{37}H_{27}N_2$ $[M+H]^+$ 499.2174, found 499.2177.

Reaction of 4.1 with 1-phenyl-1-propyne (c)

Following the general procedure, a Schlenk flask was loaded with $[Cp^*Rh(MeCN)_3][PF_6]_2$ (33 mg, 5 mol%), 2-phenylimidazole (**4.1**, 144 mg, 1.0 mmol), $Cu(OAc)_2.H_2O$ (500 mg, 2.5 mmol), 1-phenyl-1-propyne (**c**, 139 mg, 1.2 mmol) and DCE (10 ml). The crude ^{1}H NMR spectrum showed the presence of a mixture of products. The products were purified by column chromatography, eluting with 30% ethyl acetate in petroleum ether (40-60 °C) to give **4.2c** and **4.2c′** as a mixture of regioisomers as a brown powder.(128 mg, 50%, 0.50 mmol) and **4.7c** as a brown powder (64 mg, 17%, 0.17 mmol). Attempts to separate **4.2c** from **4.2c′** by preparative TLC failed.

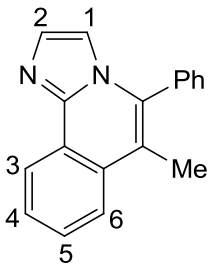

4.2c: This was found in a mixture with its regioisomer **4.2c′**. ^{1}H NMR (400 MHz, $CDCl_3$): δ 2.32 (s, 3H, *Me*), 6.99 (s, 1H, H^1/H^2), 7.41-7.43 (m, 3H, *Ar-H* + H^1/H^2), 7.54-7.58 (m, 3H, *Ar-H*), 7.62-7.65 (m, 2H, H^4 + H^5), 7.88 (dd, *J* = 2.3, 7.0 Hz, 1H, H^6), 8.71 (dd, *J* = 2.3, 6.7 Hz, 1H, H^3), ^{13}C {^{1}H} NMR (125 MHz, $CDCl_3$): δ 14.9 (*Me*), 113.8 (C^1/C^2), 116.8, 123.3, 123.5 (C^3), 124.1 (C^6), 127.8

(C^4/C^5), 128.2 (C^4/C^5), 129.4 (Ar), 129.4 (Ar), 129.9 (Ar), 130.2 (C^1/C^2), 130.5, 132.7, 134.0, 142.7 (N-*C*-N). ESIMS: *m/z* 259 $[M+H]^+$. HRMS (ESI): Calcd for $C_{18}H_{15}N_2$ $[M+H]^+$ 259.1235, found 259.1236.

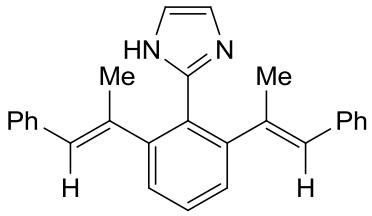

4.7c: ^{1}H NMR (400 MHz, $CDCl_3$): δ 1.80 (s, 3H, *Me*), 1.80 (s, 3H, *Me*), 6.46 (s, 2H, C=C*H*), 7.03 (s, 1H, *Imidazole-H*), 7.16 (s, 1H, *Imidazole-H*), 7.21 (t, *J* = 7.2 Hz, 2H, *Ar-H*), 7.24-7.26 (m, 5H, *Ar-H*), 7.33 (t, *J* = 7.7 Hz, 6H, *Ar-H*), 7.41 (dd, *J* = 7.2, 8.6 Hz, 1H, *Ar-H*), 9.02 (br s, 1H, N*H*), ^{13}C {^{1}H} NMR (100 MHz, $CDCl_3$): δ 18.5 (2C, *Me*), 125.7 (Ar), 126.9 (Ar), 127.4 (Ar), 128.2 (Ar), 129.0 (C=*C*H), 129.8 (Ar), 137.1 (Ar), 138.7 (Ar), 146.0 (N-*C*-N). ESIMS: *m/z* 377 $[M+H]^+$. HRMS (ESI): Calcd for $C_{27}H_{25}N_2$ $[M+H]^+$ 377.2018, found 377.2012.

Reaction of 4.1 with DMAD (e)

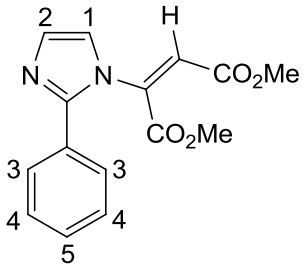

Following the general procedure, a Schlenk flask was loaded with $[Cp^*Rh(MeCN)_3][PF_6]_2$ (33 mg, 5 mol%), 2-phenylimidazole (**4.1**, 144 mg, 1.0 mmol), $Cu(OAc)_2.H_2O$ (500 mg, 2.5 mmol), DMAD (**e**, 170 mg, 1.2 mmol) and DCE (10 ml). The product was purified by column chromatography, eluting with 50% ethyl acetate in petroleum ether (40-60 °C) to give **4.8e** as brown oil (206 mg, 73%, 0.73 mmol). ^{1}H NMR (400 MHz, $CDCl_3$): δ 3.56 (s, 3H, CO_2*Me*), 3.57 (s, 3H, CO_2*Me*), 6.91 (d, *J* = 1.2 Hz, 1H, H^1), 6.93 (s, 1H, C=C*H*), 7.15 (d, *J* = 1.6 Hz, 1H, H^2), 7.29-7.33 (m, 3H, H^4 + H^5), 7.45-7.48 (m, 2H, H^3), ^{13}C {^{1}H} NMR (125 MHz, $CDCl_3$): δ 52.5 (CO_2*Me*), 53.4 (CO_2*Me*), 122.3 (C^1), 126.3 (C=*C*H), 128.0 (C^3), 128.5 (C^4 + C^5), 129.0 (C^2), 129.3, 130.2, 136.8, 162.8 (*C*=O), 163.0 (*C*=O). ESIMS: *m/z* 287 $[M+H]^+$. HRMS (ESI): Calcd for $C_{15}H_{15}N_2O_4$ $[M+H]^+$ 287.1032, found 287.1032.

Reaction of 4.9 with 4-octyne (a)

Following the general procedure, a Schlenk flask was loaded with $[Cp^*Rh(MeCN)_3][PF_6]_2$ (33 mg, 5 mol%), 2-phenylimidazoline (**4.9**, 146 mg, 1.0 mmol), $Cu(OAc)_2.H_2O$ (500 mg, 2.5 mmol), 4-octyne (**a**, 132 mg, 1.2 mmol) and DCE (10 ml). The crude ^{1}H NMR spectrum showed the presence of two products in a 2:1 ratio. The products were purified by column chromatography eluting with 5% ethyl

acetate in dichloromethane to give **4.10a** as a yellow powder (72 mg, 20%, 0.20 mmol) and **4.2a** as a white powder (159 mg, 63%, 0.63 mmol).

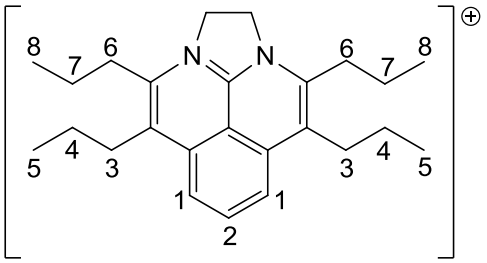

4.10a: ^{1}H NMR (400 MHz, CD_2Cl_2): δ 0.99 (t, *J* = 7.4 Hz, 6H, H^5), 1.04 (t, *J* = 7.4 Hz, 6H, H^8), 1.52 (sex, *J* = 7.4 Hz, 4H, H^4), 1.61 (sex, *J* = 7.4 Hz, 4H, H^7), 2.58-2.64 (m, 4H, H^3 + H^6), 4.69 (s, 4H, *Imidazoline-H*), 7.33 (d, *J* = 7.8 Hz, 2H, H^1), 7.83 (t, *J* = 8.2 Hz, 1H, H^2), ^{13}C {^{1}H} NMR (100 MHz, $CDCl_3$): δ 14.2 (C^5/C^8), 14.3 (C^5/C^8), 22.3 (C^4), 22.8 (C^7), 29.6 (C^3/C^6), 31.0 (C^3/C^6), 48.3 (*C*-H (Im)), 118.1 (C^1), 121.3, 137.1 (C^2), 137.9, 139.1. ESIMS: *m/z* 363 $[M]^+$. HRMS (ESI): Calcd for $C_{25}H_{35}N_2$ $[M]^+$ 363.1705, found 363.1715.

Reaction of 4.9 with diphenylacetylene (b)

Following the general procedure, a Schlenk flask was loaded with $[Cp^*Rh(MeCN)_3][PF_6]_2$ (33 mg, 5 mol%), 2-phenylimidazoline (**4.9**, 146 mg, 1.0 mmol), $Cu(OAc)_2.H_2O$ (500 mg, 2.5 mmol), diphenylacetylene (**b**, 214 mg, 1.2 mmol) and DCE (10 ml). The crude ^{1}H NMR spectrum showed the presence of three products in a roughly 3:3:1 ratio. The products were purified by column chromatography eluting with 50% ethyl acetate in petroleum ether (40-60 °C) to give **4.2b** as a brown powder (19 mg, 6%, 0.06 mmol), **4.10b** as a yellow powder (41 mg, 8%, 0.08 mmol) and **4.11b** as an impure orange solid (115 mg, 36%, 0.36 mmol).

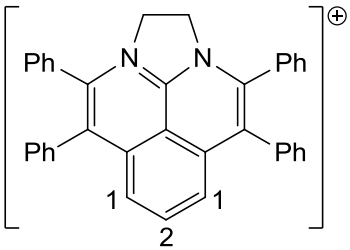

4.10b: ^{1}H NMR (400 MHz, CD_2Cl_2): δ 4.45 (s, 4H, *Imidazoline-H*), 7.07 (d, *J* = 7.8 Hz, 2H, H^1), 7.15 (dd, *J* = 1.6, 7.8 Hz, 4H, *Ar-H*), 7.25-7.34 (m, 16H, *Ar-H*), 7.66 (t, *J* = 7.8 Hz, 1H, H^2), ^{13}C {^{1}H} NMR (100 MHz, $CDCl_3$): δ 49.2 (*C*-H (Im)), 120.8 (C^1), 125.0, 128.1 (Ar), 128.9 (Ar), 129.8 (Ar), 130.6 (Ar), 130.8, 133.7, 136.8 (C^2), 138.0, 139.0. ESIMS: *m/z* 499 $[M]^+$. HRMS (ESI): Calcd for $C_{37}H_{27}N_2$ $[M]^+$ 499.2174, found 499.2173.

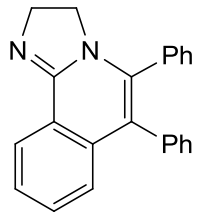

4.11b: This was obtained in a mixture with **4.2b**. ^{1}H NMR (400 MHz, $CDCl_3$): δ 3.79 (t, *J* = 9.8 Hz, 2H, *Imidazoline-H*), 3.98 (t, *J* = 9.8 Hz, 2H, *Imidazoline-H*), 7.05-7.40 (m, 13H, *Ar-H*), 8.33 (d, *J* = 7.4 Hz, 1H, *Ar-H*), ESIMS: *m/z* 323 $[M+H]^+$. FAB MS: *m/z* 323 $[M+H]^+$. Recrystallisation using of **4.11b** occurred in $CDCl_3$ to give an orange block.

Reaction of 4.12 with 4-octyne (a)

Following the general procedure, a Schlenk flask was loaded with $[Cp^*Rh(MeCN)_3][PF_6]_2$ (33 mg, 5 mol%), 1-phenyl-3-pyrazolidinone (**4.12**, 162 mg, 1.0 mmol), $Cu(OAc)_2.H_2O$ (500 mg, 2.5 mmol), 4-octyne (**a**, 132 mg, 1.2 mmol) and DCE (10 ml). The crude ^{1}H NMR spectrum showed the presence of three products in a 4:1 ratio. The products were purified by column chromatography eluting from 20% ethyl acetate in petroleum ether (40-60 °C) to 10% ethyl acetate in dichloromethane to give **4.13a** as brown oil (137 mg, 64%, 0.64 mmol) and **4.14a** as yellow oil (31 mg, 17%, 0.17 mmol).

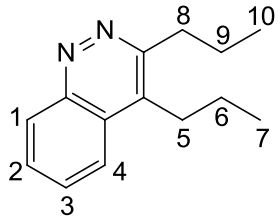

4.13a: ^{1}H NMR (400 MHz, $CDCl_3$): δ 1.08 (t, *J* = 7.4 Hz, 3H, H^{10}), 1.11 (t, *J* = 7.4 Hz, 3H, H^{7}), 1.66-1.76 (m, 2H, H^{6}), 1.88-1.97 (m, 2H, H^{9}), 3.02-3.06 (m, 2H, H^{5}), 3.20-3.24 (m, 2H, H^{8}), 7.67-7.75 (m, 2H, H^{2} + H^{3}), 7.97-8.00 (m, 1H, H^{4}), 8.46-8.48 (m, 1H, H^{1}), ^{13}C {^{1}H} NMR (100 MHz, $CDCl_3$): δ 14.3 (C^{7}/C^{10}), 14.6 (C^{7}/C^{10}), 23.7 (C^{6}), 24.0 (C^{9}), 29.0 (C^{5}), 35.4 (C^{8}), 122.8 (C^{4}), 125.8, 128.8 (C^{2}/C^{3}), 130.4 (C^{1}), 130.6 (C^{2}/C^{3}), 132.4, 149.0, 155.8. ESIMS: *m/z* 215 $[M+H]^+$. HRMS (ESI): Calcd for $C_{14}H_{19}N_2$ $[M+H]^+$ 215.1548, found 215.1552.

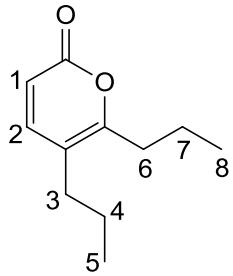

4.14a: ^{1}H NMR (400 MHz, $CDCl_3$): δ 0.95 (t, *J* = 7.4 Hz, 3H, H^{5}), 0.98 (t, *J* = 7.4 Hz, 3H, H^{8}), 1.51 (sex, *J* = 7.4 Hz, 2H, H^{4}), 1.70 (sex, *J* = 7.4 Hz, 2H, H^{7}), 2.28 (t, *J* = 7.4 Hz, 2H, H^{3}), 2.48 (t, *J* = 7.4 Hz, 2H, H^{6}), 6.14 (d, *J* = 9.4 Hz, 1H, H^{1}), 7.17 (d, *J* = 9.4 Hz, 1H, H^{2}), ^{13}C {^{1}H} NMR (100 MHz, $CDCl_3$): δ 13.6 (C^{5}/C^{8}), 13.7 (C^{5}/C^{8}), 21.0 (C^{7}), 23.3 (C^{4}), 31.2 (C^{3}), 32.6 (C^{6}), 113.4 (C^{1}), 115.1, 147.0 (C^{2}), 161.8, 163.0. ESIMS: *m/z* 181 $[M+H]^+$. FAB MS: *m/z*: 180 $[M]^+$, 151 $[M-2Me]^+$, 137 $[M-2Me-CH_2]^+$, 123 $[M-2Me-2CH_2]^+$, 109 $[M-2Me-3CH_2]^+$, 95 $[M-2Me-4CH_2]^+$. HRMS (ESI): Calcd for $C_{11}H_{17}O_2$ $[M+H]^+$ 181.1229, found 181.1235.

Reaction of 4.12 with DMAD (e)

Following the general procedure, a Schlenk flask was loaded with $[Cp^*Rh(MeCN)_3][PF_6]_2$ (33 mg, 5 mol%), 1-phenyl-3-pyrazolidinone (**4.12**, 162 mg, 1.0 mmol), $Cu(OAc)_2.H_2O$ (500 mg, 2.5 mmol), DMAD (**e**, 170 mg, 1.2 mmol) and DCE (10 ml). The product was purified by column chromatography eluting from 50% ethyl acetate in hexane to give either **4.15e** or **4.15e′** as yellow oil (164 mg, 58%, 0.58 mmol). Deducing the exact structure of the product proved difficult. It is likely to be one of the isomers shown below and its data is given as **Dataset A**.

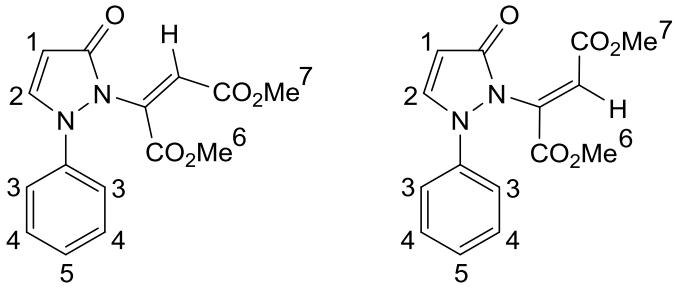

Dataset A: 4.15e or **4.15e′**: ^{1}H NMR (400 MHz, $CDCl_3$): δ 3.72 (s, 3H, H^7), 3.90 (s, 3H, H^6), 5.96 (s, 1H, C=C*H*), 6.15 (d, *J* = 2.7 Hz, 1H, H^1), 7.27 (t, *J* = 7.8 Hz, 1H, H^5), 7.43 (t, *J* = 7.8 Hz, 2H, H^4), 7.60 (dd, *J* = 1.2, 7.8 Hz, 2H, H^3), 7.85 (d, *J* = 2.7 Hz, 1H, H^2), ^{13}C {^{1}H} NMR (100 MHz, $CDCl_3$): δ 51.9 (C^7), 53.0 (C^6), 97.0 (C^1), 102.7 (C=*C*H), 118.5 (C^3), 126.6 (C^5), 128.3 (C^2), 129.5 (C^4), 139.5, 156.8, 158.8, 162.8, 165.6. ESIMS: *m/z* 303 $[M+H]^+$. HRMS (ESI): Calcd for $C_{15}H_{15}N_2O_5$ $[M+H]^+$ 303.0981, found 303.0973.

Dataset B: 4.15e or **4.15e′**: ^{1}H NMR (400 MHz, $CDCl_3$): δ 3.65 (s, 3H, CO_2*Me*), 3.88 (s, 3H, CO_2*Me*), 5.52 (s, 1H, C=C*H*), 5.69 (d, *J* = 3.9 Hz, 1H, H^1), 7.25 (dd, *J* = 1.2, 7.4 Hz, 2H, H^3), 7.31 (t, *J* = 7.4 Hz, 1H, H^5), 7.45 (t, *J* = 7.8 Hz, 2H, H^4), 7.62 (d, *J* = 3.9 Hz, 1H, H^2), ^{13}C {^{1}H} NMR (100 MHz, $CDCl_3$): δ 52.0 (CO_2*Me*), 53.2 (CO_2*Me*), 100.3 (C^1), 109.9 (C=*C*H), 121.1 (C^3), 127.7 (C^5), 130.3 (C^4), 137.5, 139.3, 150.8 (C^2), 162.5, 164.6, 166.2. ESIMS: *m/z* 303 $[M+H]^+$. EIMS: *m/z* 302 $[M]^+$, 271 $[M-2Me-H]^+$. FABMS: *m/z* 303 $[M+H]^+$. HRMS (ESI): Calcd for $C_{15}H_{15}N_2O_5$ $[M+H]^+$ 303.0981, found 303.0977.

Blank reaction of 4.12 with DMAD (e)

Following the general procedure, a Schlenk flask was loaded with 1-phenyl-3-pyrazolidinone (**4.12**, 162 mg, 1.0 mmol), DMAD (**e**, 170 mg, 1.2 mmol) and DCE (10 ml). After 16 hours the ^{1}H NMR spectrum of the crude reaction mixture showed the presence of a mixture of products. The products were purified by column chromatography eluting from 50% dichloromethane in petroleum ether (40-60 °C) to 50% ethyl acetate in petroleum ether (40-60 °C) to give **4.16** as a white powder (84 mg, 53%, 0.53 mmol) and **4.15e** or **4.15e′** as yellow oil (32 mg, 11%, 0.11 mmol). Differentiating between **4.15e** and **4.15e′** proved difficult. The product obtained from this reaction was different to the one obtained from the reaction of **4.12** with DMAD **(e)** in the presence of Rh/Cu. Its data are given above as **Dataset B**.

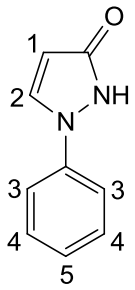

4.16: ^{1}H NMR (400 MHz, $CDCl_3$): δ 5.91 (d, *J* = 2.3 Hz, 1H, *H*^{1}), 7.26 (tt, *J* = 1.2, 7.0, 8.2 Hz, 1H, *H*^{5}), 7.43-7.48 (m, 2H, *H*^{4}), 7.52 (dd, *J* = 1.2, 8.6 Hz, 2H, *H*^{3}), 7.67 (d, *J* = 2.7 Hz, 1H, *H*^{2}), 11.62 (br s, 1H, N*H*). ESIMS: *m/z* 161 $[M+H]^{+}$.

Reaction of 4.16 with DMAD (e)

Following the general procedure, a Schlenk flask was loaded with $[Cp^*Rh(MeCN)_3][PF_6]_2$ (17 mg, 5 mol%), 1-phenyl-1,2-dihydro-3*H*-pyrazol-3-one (**4.16**, 84 mg, 0.53 mmol), $Cu(OAc)_2.H_2O$ (263 mg, 1.33 mmol), DMAD (**e**, 89 mg, 0.63 mmol) and DCE (7 ml). The product was purified by column chromatography eluting from 30% ethyl acetate in petroleum ether (40-60 °C) to give **4.15e** or **4.15e′** as yellow oil (54 mg, 34%, 0.18 mmol). The product obtained from this reaction is the same as the one obtained from the reaction of **4.12** with DMAD **(e)** in the presence of Rh/Cu and its data matches **Dataset A**.

Reaction of 4.17 with 4-octyne (a)

Following the general procedure, a Schlenk flask was loaded with $[Cp^*Rh(MeCN)_3][PF_6]_2$ (33 mg, 5 mol%), phenylhydrazine (**4.17**, 108 mg, 1.0 mmol), $Cu(OAc)_2.H_2O$ (500 mg, 2.5 mmol), 4-octyne (**a**, 132 mg, 1.2 mmol) and DCE (10 ml).

The product was purified by column chromatography eluting with 10% ethyl acetate in dichloromethane to give **4.13a** as yellow oil (114 mg, 53%, 0.53 mmol).

Reaction of 4.18 with DMAD (e)

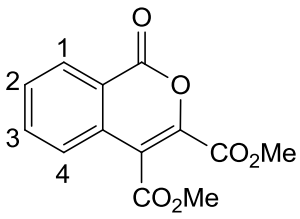

Following the general procedure, a Schlenk flask was loaded with [Cp*Rh(MeCN)$_3$][PF$_6$]$_2$ (33 mg, 5 mol%), benzoic acid (**4.18**, 122 mg, 1.0 mmol), Cu(OAc)$_2$.H$_2$O (500 mg, 2.5 mmol), DMAD (**e**, 170 mg, 1.2 mmol) and DCE (10 ml). The product was purified by column chromatography eluting with 10% ethyl acetate in dichloromethane to give **4.19e** as a white powder (62 mg, 24%, 0.24 mmol). The product was recrystallised from dichloromethane and hexane to give **4.19e** as clear needles. ^{1}H NMR (400 MHz, CDCl$_3$): δ 3.90 (s, 3H, CO$_2$*Me*), 3.95 (s, 3H, CO$_2$*Me*), 7.47 (dd, *J* = 2.0, 7.8 Hz, 1H, *H*^{1}/*H*^{4}), 7.63 (td, *J* = 1.2, 7.8 Hz, 1H, *H*^{2}/*H*^{3}), 7.77 (td, *J* = 1.2, 7.4 Hz, 1H, *H*^{2}/*H*^{3}), 8.31 (dd, *J* = 1.2, 7.4 Hz, 1H, *H*^{1}/*H*^{4}), ^{13}C {^{1}H} NMR (100 MHz, CDCl$_3$): δ 52.2 (CO$_2$*Me*), 52.4 (CO$_2$*Me*), 118.0, 120.9, 124.5 (*C*^{1}/*C*^{4}), 129.3 (*C*^{1}/*C*^{4}), 130.2 (*C*^{2}/*C*^{3}), 131.7, 134.6 (*C*^{2}/*C*^{3}), 139.9, 158.2, 159.2, 164.0. ESIMS: *m/z* 263 [M+H]$^+$. HRMS (ESI): Calcd for C$_{13}$H$_{11}$O$_6$ [M+H]$^+$ 263.0556, found 263.0551.

Reaction of 4.20 with 4-octyne (a) (2.2 equiv.)

Following the general procedure, a Schlenk flask was loaded with [Cp*Rh(MeCN)$_3$][PF$_6$]$_2$ (33 mg, 5 mol%), (*E*)-benzaldehyde oxime (**4.20**, 130 mg, 1.0 mmol), Cu(OAc)$_2$.H$_2$O (500 mg, 2.5 mmol), 4-octyne (**a**, 242 mg, 2.2 mmol) and DCE (10 ml). The products were purified by column chromatography eluting with 50% dichloromethane in hexane to 100% dichloromethane to give **4.21a** as dark yellow oil (65 mg, 28%, 0.28 mmol), **4.22a** as a yellow powder (50 mg, 15%, 0.15 mmol) and **4.23** as a white powder (25 mg, 19%, 0.19 mmol).

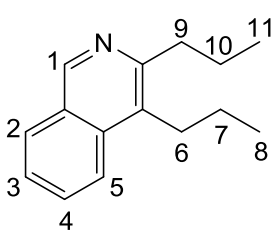

4.21a: ^{1}H NMR (400 MHz, CDCl$_3$): δ 1.05 (3H, t, *J* = 7.5 Hz, *H*^{8}/*H*^{11}), 1.10 (3H, t, *J* = 7.5 Hz, *H*^{8}/*H*^{11}), 1.64-1.74 (2H, m, CH$_2$C*H*$_2$Me), 1.77-1.87 (2H, m, CH$_2$C*H*$_2$Me), 2.92-3.05 (4H, m, 2 x C*H*$_2$CH$_2$Me), 7.48-7.53 (1H, m, *H*^{3}/*H*^{4}), 7.63-7.70 (1H, m, *H*^{3}/*H*^{4}), 7.91 (1H, dd, *J* = 8.1 Hz, *H*^{2}/*H*^{5}), 7.97 (1H, dd, *J* = 8.5 Hz, 0.5 Hz, *H*^{2}/*H*^{5}), 9.08 (1H, s, N=C*H*). IR (cm^{-1}): 1622 (C=N). ESIMS: *m/z* 214 [M+H]$^+$. This data is in agreement with that found in the literature.[10]

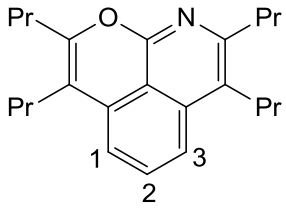

4.22a: ^{1}H NMR (400 MHz, $CDCl_3$): δ 0.99-1.07 (12H, m, $CH_2CH_2CH_3$), 1.54-1.63 (4H, m, $CH_2CH_2CH_3$), 1.71-1.82 (4H, m, $CH_2CH_2CH_3$), 2.45-2.54 (4H, m, $CH_2CH_2CH_3$), 2.75-2.82 (4H, m, $CH_2CH_2CH_3$), 6.96 (1H, d, J = 7.5 Hz, H^1/H^3), 7.41 (1H, d, J = 8.0 Hz, H^1/H^3), 7.55 (1H, dd, J = 7.5, 8.0 Hz, H^2). ^{13}C {^{1}H} NMR (100 MHz, $CDCl_3$): δ 14.2 (*Me*), 14.3 (*Me*), 14.3 (*Me*), 14.4 (*Me*), 21.3 (CH_2CH_2Me), 21.5 (CH_2CH_2Me), 23.0 (CH_2CH_2Me), 23.6 (CH_2CH_2Me), 28.4 (CH_2CH_2Me), 29.6 (CH_2CH_2Me), 32.7 (CH_2CH_2Me), 37.0 (CH_2CH_2Me), 112.3, 113.6 (C^1/C^3), 115.6, 118.0 (C^1/C^3), 121.9, 131.8 (C^2), 133.6, 138.5, 151.8, 153.5, 157.3. IR (cm^{-1}): 1648 (C=N). ESIMS: *m/z* 338 $[M+H]^+$. HRMS (ESI): Calcd for $C_{23}H_{32}NO$ $[M+H]^+$ 338.2484, found 338.2486.

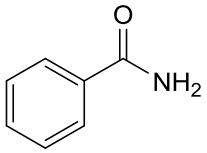

4.23: ^{1}H NMR (400 MHz, $CDCl_3$): δ 7.87–7.78 (m, 2H), 7.56–7.47 (m, 1H), 7.42 (dt, J = 8.3, 6.7, 1.4 Hz, 2H), 6.45 (br s, 2H, NH_2). IR (cm^{-1}): 1655 (C=N), 3363 (N-H). ESIMS: *m/z* 122 $[M+H]^+$. This data is in agreement with that found in the literature.[19]

Reaction of 4.23 with 4-octyne (a) (2.2 equiv.)

Following the general procedure, a Schlenk flask was loaded with $[Cp^*Rh(MeCN)_3][PF_6]_2$ (33 mg, 5 mol%), benzamide (**4.23**, 121 mg, 1.0 mmol), $Cu(OAc)_2.H_2O$ (500 mg, 2.5 mmol), 4-octyne (**a**, 242 mg, 2.2 mmol) and DCE (10 ml). The crude ^{1}H NMR spectrum showed the presence of two products in a 2:1 ratio. The products were purified by column chromatography eluting from 100% dichloromethane to give **4.22a** as a yellow powder (50 mg, 52%, 0.52 mmol) and **4.23** as a white powder (25 mg, 30%, 0.30 mmol).

Reaction of 4.23 with 4-octyne (a) (1.2 equiv.)

Following the general procedure, a Schlenk flask was loaded with $[Cp^*RhCl_2]_2$ (25 mg, 4 mol%), benzamide (**4.23**, 29 mg, 0.237 mmol), AgOAc (119 mg, 0.711 mmol), 4-octyne (**a**, 33 mg, 0.30 mmol), 1, 3, 5-trimethoxybenzene (8 mg, 0.050 mmol, 20 mol%) and MeCN (5 ml). The crude ^{1}H NMR spectrum showed the presence of **4.22a** (37 mg, 46%, 0.109 mmol) and unreacted **4.23**.

Reaction of 4.23 with 4-octyne (a) (1.2 equiv.)

Following the general procedure, a Schlenk flask was loaded with $[Cp^*RhCl_2]_2$ (25 mg, 4 mol%), benzamide (**4.23**, 121 mg, 1.0 mmol), Ag_2O (348 mg, 1.5 mmol), 4-octyne (**a**, 132 mg, 1.2 mmol) and MeCN (5 ml). The crude ^1H NMR spectrum showed the presence of two products (**4.23** and **4.25a**). Purification by column chromatography eluting from 20% ethyl acetate in hexane gave **4.25a** as a white powder (43 mg, 19%, 0.19 mmol).

Reaction of 4.25a with 4-octyne (a) (1.2 equiv.)

Following the general procedure, a Schlenk flask was loaded with $[Cp^*Rh(MeCN)_3][PF_6]_2$ (6 mg, 5 mol%), **4.25a** (43 mg, 0.19 mmol), $Cu(OAc)_2.H_2O$ (100 mg, 0.5 mmol), 4-octyne (**a**, 132 mg, 1.2 mmol), 1, 3, 5-trimethoxybenzene (8 mg, 0.05 mmol, 27 mol%) and DCE (5 ml). The crude ^1H NMR spectrum showed the presence of **4.22a** (47 mg, 75%, 0.14 mmol).

Bibliography

1. Y. Boutadla, D. L. Davies, R. C. Jones and K. Singh, *Chem. Eur. J.*, 2011, **17**, 3438.
2. Y. Kashiwame, S. Kuwata and T. Ikariya, *Chem. Eur. J.*, 2010, **16**, 766.
3. N. Umeda, H. Tsurugi, T. Satoh and M. Miura, *Angew. Chem. Int. Ed.*, 2008, **47**, 4019.
4. G. Zhang, L. Yang, Y. Wang, Y. Xie and H. Huang, *J. Am. Chem. Soc.*, 2013, **135**, 8850.
5. S. Mochida, K. Hirano, T. Satoh and M. Miura, *J. Org. Chem.*, 2009, **74**, 6295.
6. C. Zhu and M. Yamane, *Tetrahedron*, 2011, **67**, 4933.
7. C. Wang, H. Sun, Y. Fang and Y. Huang, *Angew. Chem. Int. Ed.*, 2013, **52**, 5795.
8. C. Wang and Y. Huang, *Synlett*, 2013, **24**, 145.
9. D. Zhao, Q. Wu, X. Huang, F. Song, T. Lv and J. You, *Chem. Eur. J.*, 2013, **19**, 6239.
10. N. Guimond and K. Fagnou, *J. Am. Chem. Soc.*, 2009, **131**, 12050.
11. K. Muralirajan and C. Cheng, *Chem. Eur. J.*, 2013, **19**, 6198.
12. S. Guillou and Y. L. Janin, *Chem. Eur. J.*, 2010, **16**, 4669.
13. K. Ueura, T. Satoh and M. Miura, *Org. Lett.*, 2007, **9**, 1407.
14. K. Ueura, T. Satoh and M. Miura, *J. Org. Chem.*, 2007, **72**, 5362.
15. T. K. Hyster and T. Rovis, *Chem. Commun.*, 2011, **47**, 11846.
16. J. M. Neely and T. Rovis, *J. Am. Chem. Soc.*, 2013, **135**, 66.
17. P. C. Too, T. Noji, Y. J. Lim, X. Li and S. Chiba, *Synlett*, 2011, 2789.
18. P. C. Too, Y. Wang and S. Chiba, *Org. Lett.*, 2010, **12**, 5688.
19. C. Tao, F. Liu, Y. Zhu, W. Liu and Z. Cao, *Org. Biomol. Chem.*, 2013, **11**, 3349.
20. S. Park, Y. Choi, H. Han, S. H. Yang and S. B. Chang, *Chem. Commun.*, 2003, 1936.
21. G. Song, D. Chen, C. Pan, R. H. Crabtree and X. Li, *J. Org. Chem.*, 2010, **75**, 7487.

Chapter Five

Overall Conclusions

5 Chapter Five

This thesis described investigations into Cp*Rh- and (*p*-Cy)Ru-catalysed C-H functionalisation reactions of various substrates with alkynes and alkenes for the formation of several heterocycles and carbocycles. Mechanistic studies and DFT calculations were also presented where relevant.

5.1 Conclusions from Chapter One

An overview of the different approaches to C-H activation and their applications in catalysis was given in **Chapter One**. The origins and details of the various mechanisms were described. Distinguishing between mechanisms can sometimes be difficult and it was shown that computation can help shed light in determining the mechanism of C-H activation. On the other hand computational studies can illustrate fine distinctions between processes which may not be able to be distinguished easily, if at all, experimentally. AMLA C-H activation was introduced and shown to be related to both CMD and IES, all being electrophilic types of activation using an intramolecular base. Different types of KIE experiment were also illustrated. It was concluded that only **Type A** experiments provide conclusive evidence on whether C-H activation is rate-limiting. However, the absence of a KIE from a **Type B** or **Type C** experiment can be used to show C-H activation is not rate-limiting.

An overview of direct arylations using AMLA C-H activation was provided. Overall, intra- and intermolecular Pd-catalysed AMLA/CMD direct arylation reactions can be carried out efficiently under various conditions with several substrates. There are many examples where oxidative addition of the C-X bond is the first step followed by AMLA C-H activation. There are fewer examples of reactions with non-halogenated substrates where an external oxidant is needed for catalyst turnover. Intermolecular direct arylation reactions with Ru have been reported but only for reactions using halogenated substrates. Direct alkylations are also possible with Pd and Ru. Direct arylation using Cp^*Rh^{III}-catalysed AMLA C-H activation has only been reported for reactions that use external oxidant. This is probably due to the difficulty in forming Rh(V) intermediates. There are not many reported examples of direct arylation with Ir possibly due to strong iridium-carbon bonds that form which are quite stable and make catalysis difficult.

5.2 Conclusions from Chapter Two

Chapter Two described the Cp*Rh- and (*p*-Cy)Ru-catalysed formation of a range of heterocycles (**2.45**-**2.48**, **Fig. 5.1**) from the coupling of *C*-phenylpyrazoles or *C*-thiophenylpyrazoles with aryl and alkyl alkynes. The reactions incorporate AMLA C-H activation in the catalytic cycle. The *C*-phenylpyrazoles react as anionic directing groups where N-H deprotonation occurs, making C-N reductive elimination favourable and therefore leading to the formation of heterocycles. In the rhodium catalysis, $[Cp^*Rh(MeCN)_3][PF_6]_2$ is shown to be a more effective catalyst precursor than $[Cp^*RhCl_2]_2$ with efficient catalysis achieved at 83 ^oC, while catalysis with $[(p\text{-}Cy)RuCl_2]_2$ requires higher temperatures. The reactions can be carried out for both metals using catalytic rather than stoichiometric copper as the reoxidant, however for Rh, this leads to **2.46aa** (**Fig. 5.1**) as a minor product in the reaction with 4-octyne. Analogous products (**2.48**) are seen in reactions with the alkyne, 1-phenyl-1-propyne. Both **2.46aa** and **2.48** are basically isomers of **2.45** by just a hydrogen shift.

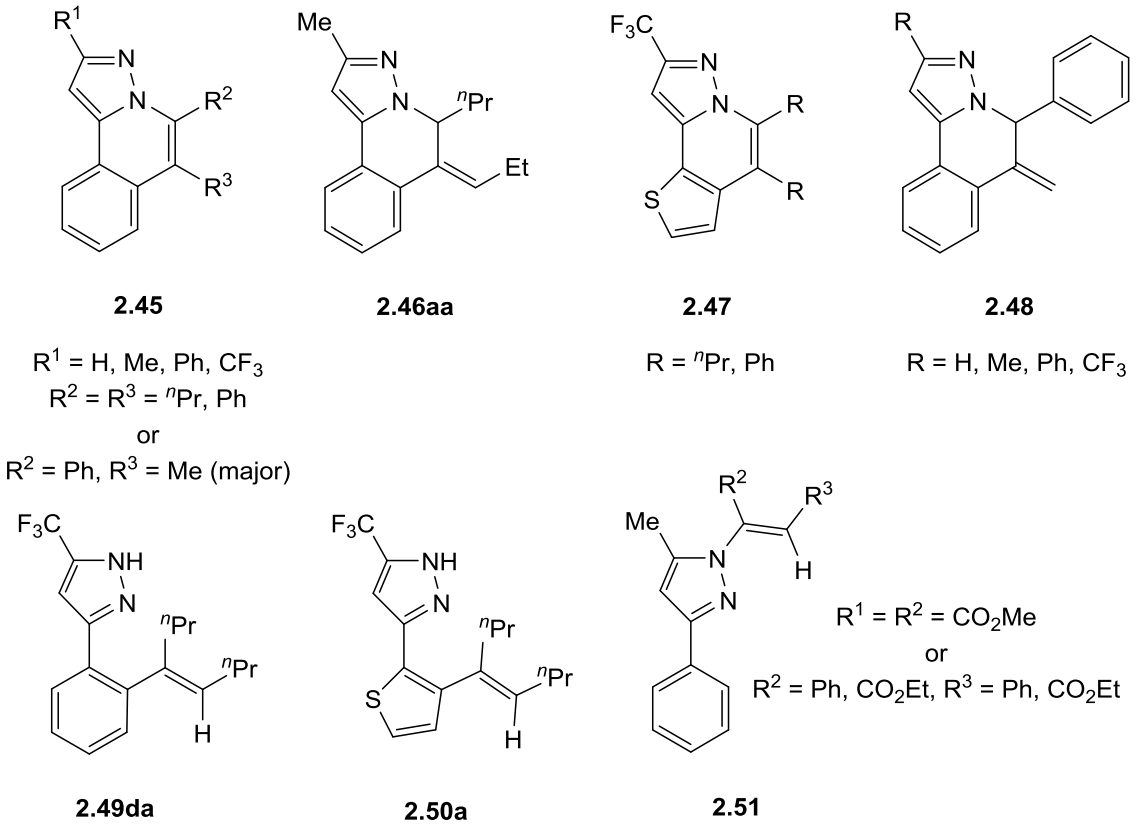

Fig. 5.1: Examples of different products obtained with *C*-phenylpyrazoles and alkynes.

Vinyl phenylpyrazoles (**2.49da** and **2.50a**, **Fig. 5.1**) are obtained as minor products in reactions with pyrazoles containing an electron-withdrawing substituent. Also, reactions with alkynes that contain electron-withdrawing groups lead to the formation of maleates or acrylates as products (**2.51**, **Fig. 5.1**) due to a Michael reaction taking place. Deuteration and competition experiments on the rhodium catalysis show that C-H activation is reversible and rate limiting, but that the subsequent reaction with alkynes can be competitive with this process. For ruthenium, C-H bond activation is much less reversible and in the presence of alkyne is essentially irreversible. Alkyne competition reactions show there is very little preference between dialkyl and diaryl alkynes.

DFT calculations on Rh and Ru catalysis indicate a mechanism involving sequential N-H and AMLA C-H bond activation, HOAc/alkyne exchange, migratory insertion and C-N reductive coupling. A higher overall barrier to catalysis is computed for Ru, in which the rate-limiting process also corresponds to C-H activation. This is consistent with the harsher reaction conditions used experimentally. The DFT calculations correctly reproduce the close competition between C-H bond activation and alkyne migratory insertion seen in the Rh system, as well as identifying C-H bond activation as being rate limiting for Ru. The calculations show that the observed deuterium isotope effects (Rh: k_H/k_D = 2.7 ± 0.5; Ru: 1.1 ± 0.2) can both be consistent with rate-limiting C-H activation due to the two-step (acetate dissociation and C-H bond cleavage) nature of the AMLA mechanism.

5.3 Conclusions from Chapter Three

The results presented in **Chapter Three** illustrated that alkenes can react with *C*-phenylpyrazoles to give products incorporating one or two equivalents of alkene depending on the substrate and excess of alkene used (**Fig. 5.2**). Reactions with methyl acrylate are not selective and give mixtures of both *cis* (**3.14′**) and *trans* (**3.14**) isomers of monovinyl products, cyclised products (**3.15** and **3.16aa**) (likely formed via chelation-assisted vinylation followed by aza-Michael addition) and divinyl products (**3.17**) which readily cyclise via aza-Michael addition. Using $[Cp^*Cp^*Rh(MeCN)_3][PF_6]_2$ even less reactive alkenes such as styrene react to give mono (**3.14**) or divinyl (**3.17**) products depending on the substituent on the pyrazole. Good Michael acceptors such as methyl vinyl ketone react to give cyclised products (**3.15** and **3.19ac**) likely formed via chelation-assisted vinylation followed by Michael

addition. In this case direct Michael reaction before C-H activation can also compete to give *N*-alkylated pyrazoles (**3.18**) if the reaction is carried out with only 1.2 equivalents of alkene. In the case of crotonaldehyde, the simple non-catalysed Michael addition is favoured. Some of the vinylic products were successfully cyclised by the addition of base, depending on the substituent on the pyrazole.

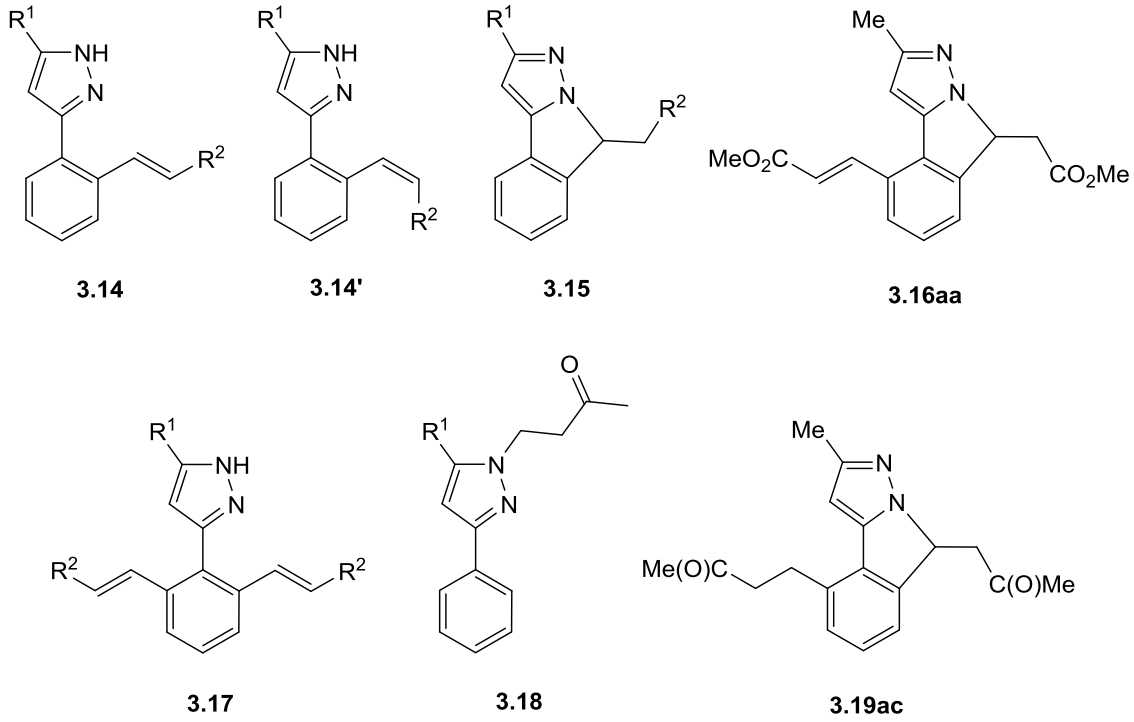

Fig. 5.2: Examples of different products obtained with *C*-phenylpyrazoles and alkenes.

Apart from the direct Michael addition products, the products observed from the reactions of *C*-phenylpyrazoles with alkenes result from regioselective insertion of the alkene in the catalytic cycle where the carbon atom with a substituent ends up next to the metal. DFT calculations support the non-observation of six-membered *N*-heterocyclic products and show that migratory insertion is regioselective for the carbon with the substituent to end up next to the metal, also in support of the observed experimental results. Finally the calculations support the formation of the *cis* monovinyl product (**3.14′**) being favoured with methyl acrylate and the *trans* monovinyl product (**3.14**) being favoured with styrene.

5.4 Conclusions from Chapter Four

Chapter Four included Cp*Rh-catalysed oxidative coupling reactions of other substrates with alkynes. In the majority of cases, the substrates reacted as anionic directing groups where deprotonation of Y-H (Y = N, O) occurred leading to heterocyclic products being formed as C-Y reductive elimination was favourable. The substrates included 2-phenylimidazole (**4.1**) which was found to be less selective than *C*-phenylpyrazoles as it reacted with one equivalent of alkyne to give *N*-heterocycles (**4.2**) as major products but naphthalenes (**4.6b**) and vinyls (**4.3a** and **4.4a**) were formed as minor products. *C*-phenylpyrazoles mostly gave *N*-heterocycles when tested with the same alkynes. 2-Phenylimidazoline (**4.9**) reacted with alkynes and also underwent dehydrogenation of the imidazoline ring to give the same products found with 2-phenylimidazole. In addition, symmetric cationic heterocycles (**4.10**) incorporating two equivalents of alkyne were formed as minor products. 1-Phenyl-3-pyrazolidinone (**4.12**) is a very reactive substrate where, in the reaction with 4-octyne, cleavage of the pyrazolidinone ring occurred to give a cinnoline (**4.13a**) and a pyrone (**4.14a**). It reacted with DMAD to give aza-Michael addition products (**4.15e** and **4.15e′**) where dehydrogenation of the pyrazolidinone ring was evident. Phenylhydrazine (**4.17**) reacted with 4-octyne to give a cinnoline (**4.13a**) but failed to react with diaryl and aryl-alkyl alkynes. Benzoic acid (**4.18**) successfully carried out oxidative coupling with DMAD. (*E*)-Benzaldehyde oxime gave isoquinoline (**4.21a**) and pyranoisoquinoline (**4.22a**) products and also gave benzamide (**4.23**) by a Beckmann rearrangement. Benzamide was independently reacted with 4-octyne to give the pyranoisoquinoline (**4.22a**).

Overall, *C*-phenylpyrazoles react with alkynes to give *N*-heterocycles as products in the majority of cases. N-H deprotonation occurs, favouring C-N reductive elimination which leads to the heterocycle products. This is in contrast to previous work with *N*-phenylpyrazoles which form naphthalenes since no N-H deprotonation is possible. *C*-phenylpyrazoles react with alkenes to give mainly mono- or divinyl products that can cyclise via aza-Michael addition if the alkene is a good Michael acceptor. Most of the directing groups discussed in **Chapter Four** react as anionic directing groups where deprotonation of Y-H (Y = N, O) occurs, leading to heterocycles. This work has shown that anionic directing groups can be formed by deprotonation at a remote site i.e. not at the coordinating atom. The ease of this deprotonation affects the products formed.

Appendix: Crystal Structures

X-Ray Crystallography

All X-ray crystallography was performed by Mr. Kuldip Singh. Data were collected on a Bruker Apex 2000 CCD diffractometer using graphite monochromated Mo-K_α radiation, λ = 0.7107 Å. The data were corrected for Lorentz and polarisation effects and empirical absorption corrections were applied. The structure was solved by direct methods and with structure refinement on F^2 employed in SHELXTL version 6.10. Hydrogen atoms were included in calculated positions (C—H = 0.93 – 1.00 Å, O—H = 0.84 Å) riding on the bonded atom with isotropic displacement parameters set to $1.5U_{eq}$ (O) for hydroxyl H atoms, $1.5U_{eq}$ (C) for methyl hydrogen atoms and $1.2U_{eq}$ (C) for all other H atoms. All non-hydrogen atoms were refined with anisotropic displacement parameters without positional restraints. Disordered solvent was removed with the Squeeze option in PLATON. Crystal data for the X-ray structures discussed in the main part of this thesis are given below, followed by X-ray structures not discussed in the main part of this thesis also with their crystal data.

2.45ac, $C_{19}H_{19}N_2O_{1.5}$, M = 299.36, Tetragonal, a = 22.783(3) Å, b = 22.783(3) Å, c = 5.7864(11) Å, α = β = γ = 90°, V = 3003.5(8) $Å^3$, T = 150(2) K, space group I-4, Z = 8, 10897 reflections measured, 2623 independent reflections (Rint = 0.0682). The final R1 values were 0.0597 (I > 2σ(I)), 0.0699 (all data). The final wR(F2) values were 0.1485 (I > 2σ(I)), 0.1522 (all data). GOF = 1.103.

2.51ae, $C_{16}H_{16}N_2O_4$, M = 300.31, Triclinic, a = 7.1573(14) Å, b = 8.3737(16) Å, c = 12.495(2) Å, α = 84.317(4)°, β = 84.086(4)°, γ = 88.851(4)°, V = 741.2(2) $Å^3$, T = 150(2) K, space group P-1, Z = 2, 5398 reflections measured, 2581 independent reflections (Rint = 0.0589). The final R1 values were 0.0551 (I > 2σ(I)) 0.0917 (all data). The final wR(F2) values were 0.1072 (I > 2σ(I)), 0.1205 (all data). GOF = 0.890.

2.52ae, $C_{28}H_{28}Cl_6N_4O_4$, M = 697.24, Triclinic, a = 6.003(4) Å, b = 8.169(5) Å, c = 16.746(10) Å, α = 78.131(10)°, β = 84.778(11)°, γ = 80.720(10)°, V = 791.7(8) $Å^3$, T = 150(2) K, space group P-1, Z = 1, 5733 reflections measured, 2762 independent reflections (Rint = 0.0675). The final R1 values were 0.0702 (I > 2σ(I)) 0.1061 (all data). The final wR(F2) values were 0.1585 (I > 2σ(I)), 0.1761 (all data). GOF = 0.986.

2.52ae′, $C_{28}H_{28}N_4O_4$, M = 458.51, Monoclinic, a = 8.4905(16) Å, b = 24.302(5) Å, c = 11.460(2) Å, α = 90°, β = 91.615(5)°, γ = 90°, V = 2363.8(8) $Å^3$, T = 150(2) K, space group P2(1)/n, Z = 4, 17113 reflections measured, 4163 independent reflections (Rint = 0.1561). The final R1 values were 0.0675 (I > 2σ(I)) 0.1304 (all data). The final wR(F2) values were 0.1357 (I > 2σ(I)), 0.1605 (all data). GOF = 0.857.

4.2a′, $C_{22}H_{28}F_3N_2O_2$, M = 409.46, Monoclinic, a = 20.971(9) Å, b = 13.314(6) Å, c = 14.392(6) Å, α = 90°, β = 98.790(9)°, γ = 90°, V = 1644.7(9) $Å^3$, T = 150(2) K, space group C2/c, Z = 8, 14152 reflections measured, 3497 independent reflections (Rint = 0.1236). The final R1 values were 0.1121 (I > 2σ(I)) 0.1727 (all data). The final wR(F2) values were 0.3518 (I > 2σ(I)), 0.3780 (all data). GOF = 1.113.

4.2b, $C_{23}H_{16}N_2$, M = 320.38, Monoclinic, a = 13.334(4) Å, b = 8.606(3) Å, c = 14.332(5) Å, α = 90°, β = 90.092(7)°, γ = 90°, V = 1644.7(9) $Å^3$, T = 150(2) K, space group P2(1)/n, Z = 4, 10641 reflections measured, 2891 independent reflections (Rint = 0.1966). The final R1 values were 0.0715 (I > 2σ(I)) 0.1559 (all data). The final wR(F2) values were 0.11154 (I > 2σ(I)), 0.1405 (all data). GOF = 0.936.

4.5a, $C_{16}H_{20}N_2O$, M = 256.34, Monoclinic, a = 33.87(2) Å, b = 4.565(3) Å, c = 18.123(13) Å, α = 90°, β = 100.078(12)°, γ = 90°, V = 2744(3) $Å^3$, T = 150(2) K, space group C2/c, Z = 8, 9131 reflections measured, 2431 independent reflections (Rint = 0.0930). The final R1 values were 0.0565 (I > 2σ(I)) 0.0939 (all data). The final wR(F2) values were 0.1243 (I > 2σ(I)), 0.1389 (all data). GOF = 0.972.

4.11b, $C_{23}H_{18}N_2$, M = 322.39, Monoclinic, a = 7.8383(15) Å, b = 10.556(2) Å, c = 20.066(4) Å, α = 90°, β = 94.047(4)°, γ = 90°, V = 1656.2(6) $Å^3$, T = 150(2) K, space group P2(1)/n, Z = 4, 11469 reflections measured, 2911 independent reflections (Rint = 0.1066). The final R1 values were 0.0517 (I > 2σ(I)) 0.0926 (all data). The final wR(F2) values were 0.0929 (I > 2σ(I)), 0.1043 (all data). GOF = 0.914.

Crystal structure of **2.45da** with selected bond distances (Å) and angles (°). Hydrogen atoms have been omitted for clarity.

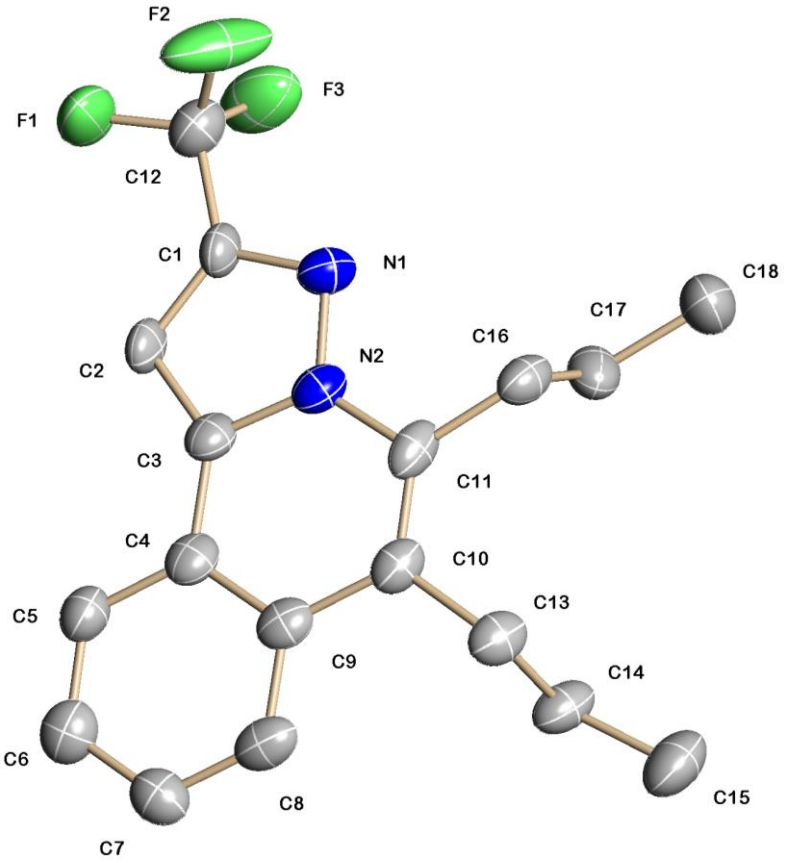

N(2)-C(11)	1.394(6)	C(4)-C(9)	1.408(7)
C(3)-N(2)	1.382(6)	C(9)-C(10)	1.468(7)
C(3)-C(4)	1.433(6)	C(10)-C(11)	1.366(7)
C(3)-N(2)-C(11)	125.5(5)	C(4)-C(9)-C(10)	120.6(5)
N(2)-C(11)-C(10)	117.6(5)	C(9)-C(10)-C(11)	120.0(5)

2.45da, $C_{18}H_{19}F_3N_2$, M = 320.35, Triclinic, a = 16.927(16) Å, b = 4.693(5) Å, c = 21.28(2) Å, α = 90°, β = 110.54(2)°, γ = 90°, V = 1583(3) $Å^3$, T = 150(2) K, space group P2(1)/n, Z = 4, 10780 reflections measured, 2788 independent reflections (Rint = 0.2392). The final R1 values were 0.0722 (I > 2σ(I)) 0.2318 (all data). The final wR(F2) values were 0.1216 (I > 2σ(I)), 0.1655 (all data). GOF = 0.782.

Crystal structure of **2.45ab** with selected bond distances (Å) and angles (°). Hydrogen atoms have been omitted for clarity.

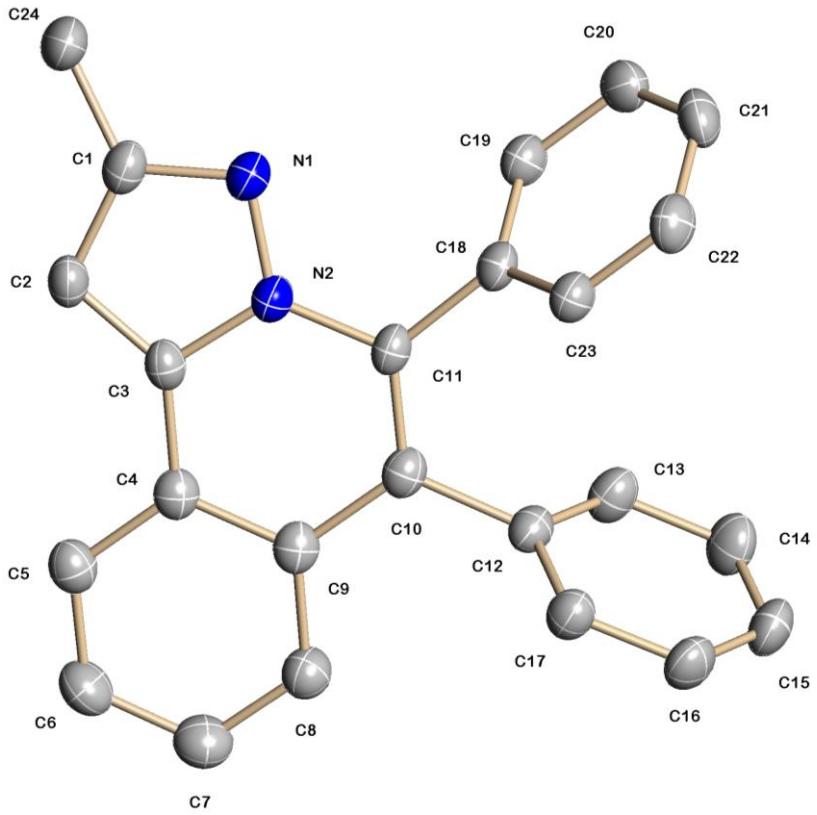

N(2)-C(11)	1.394(2)	C(4)-C(9)	1.413(2)
C(3)-N(2)	1.377(2)	C(9)-C(10)	1.453(2)
C(3)-C(4)	1.437(2)	C(10)-C(11)	1.369(2)
C(3)-N(2)-C(11)	124.5(15)	C(4)-C(9)-C(10)	119.8(16)
N(2)-C(11)-C(10)	118.1(16)	C(9)-C(10)-C(11)	120.6(16)

2.45ab, $C_{24}H_{18}N_2$, M = 334.40, Triclinic, a = 9.496(2) Å, b = 9.512(2) Å, c = 10.728(3) Å, α = 67.992(4)°, β = 76.867(4)°, γ = 76.341(4)°, V = 862.6(4) $Å^3$, T = 150(2) K, space group P-1, Z = 2, 6267 reflections measured, 3005 independent reflections (Rint = 0.0471). The final R1 values were 0.0566 (I > 2σ(I)) 0.0689 (all data). The final wR(F2) values were 0.1492 (I > 2σ(I)), 0.1586 (all data). GOF = 1.038.

Crystal structure of **2.45cb** with selected bond distances (Å) and angles (°). Hydrogen atoms have been omitted for clarity.

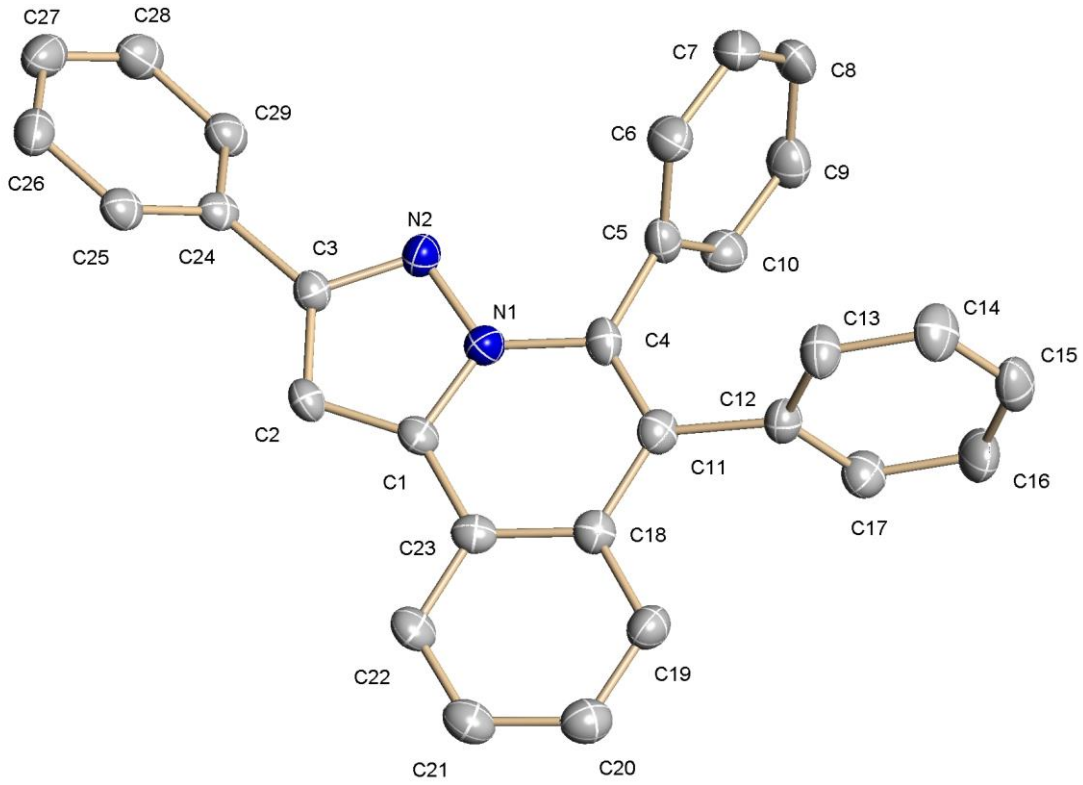

N(1)-C(1)	1.379(3)	C(11)-C(18)	1.450(4)
C(4)-N(1)	1.397(3)	C(18)-C(23)	1.413(4)
C(4)-C(11)	1.358(4)	C(1)-C(23)	1.429(4)
C(1)-N(1)-C(4)	124.5(3)	C(4)-C(11)-C(18)	120.9(3)
N(1)-C(4)-C(11)	117.8(3)	C(11)-C(18)-C(23)	122.1(3)

2.45cb, $C_{29}H_{20}N_2$, M = 396.47, Monoclinic, a = 10.207(2) Å, b = 24.109(5) Å, c = 8.1070(18) Å, α = 90°, β = 92.987(5)°, γ = 90°, V = 1992.3(7) $Å^3$, T = 150(2) K, space group P2(1)/c, Z = 4, 14376 reflections measured, 3506 independent reflections (Rint = 0.1561). The final R1 values were 0.0629 (I > 2σ(I)) 0.1360 (all data). The final wR(F2) values were 0.1030 (I > 2σ(I)), 0.1229 (all data). GOF = 0.874.

Crystal structure of **2.45db** with selected bond distances (Å) and angles (°). Hydrogen atoms and a molecule of CH_3CN have been omitted for clarity.

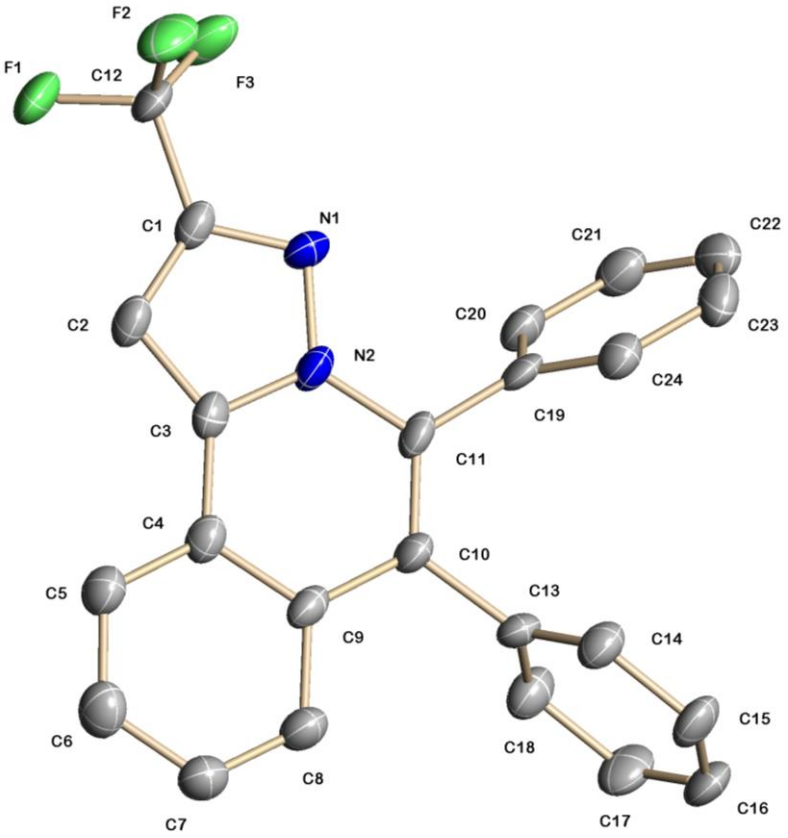

N(2)-C(3)	1.370(4)	C(3)-C(4)	1.437(5)
C(11)-N(2)	1.406(4)	C(4)-C(9)	1.409(4)
C(10)-C(11)	1.366(4)	C(9)-C(10)	1.444(4)
C(3)-N(2)-C(11)	124.2(3)	C(4)-C(9)-C(10)	120.6(3)
N(2)-C(11)-C(10)	117.3(3)	C(9)-C(10)-C(11)	121.2(3)

2.45db, $C_{24}H_{15}F_3N_2 \bullet C_2H_3N$, M = 429.43, Triclinic, a = 9.5265(15) Å, b = 9.5816(15) Å, c = 12.880(2) Å, α = 70.575(3)°, β = 70.337(4)°, γ = 84.964(3)°, V = 1043.7(3) $Å^3$, T = 150(2) K, space group P-1, Z = 2, 7678 reflections measured, 3671 independent reflections (Rint = 0.0990). The final R1 values were 0.0723 (I > 2σ(I)) 0.1219 (all data). The final wR(F2) values were 0.1530 (I > 2σ(I)), 0.1780 (all data). GOF = 0.896.

Structures of the two unique molecules in the cell of **2.45cc** with selected average bond distances (Å) and angles (°). Hydrogen atoms have been omitted for clarity.

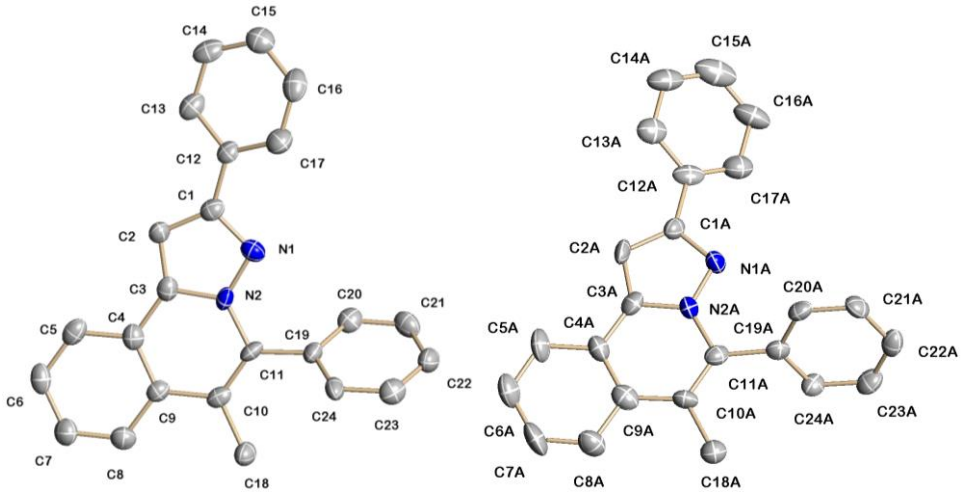

N(2)-C(3)	1.391(6)	C(3)-C(4)	1.431(7)
C(11)-N(2)	1.405(6)	C(4)-C(9)	1.408(7)
C(10)-C(11)	1.359(6)	C(9)-C(10)	1.467(6)
C(3)-N(2)-C(11)	125.0(5)	C(4)-C(9)-C(10)	119.4(5)
N(2)-C(11)-C(10)	118.0(5)	C(9)-C(10)-C(11)	120.6(5)

2.45cc, $C_{24}H_{18}N_2$, M = 334.40, Monoclinic, a = 20.554(6) Å, b = 5.9346(18) Å, c = 28.478(8) Å, α = 90°, β = 96.651(6)°, γ = 90°, V = 3450.4(18) $Å^3$, T = 150(2) K, space group P2(1)/n, Z = 8, 6049 reflections measured, 6049 independent reflections (Rint = 0.0000). The final R1 values were 0.0703 (I > 2σ(I)) 0.2368 (all data). The final wR(F2) values were 0.0841 (I > 2σ(I)), 0.1209 (all data). GOF = 0.771.

Structures of the two unique molecules in the cell of **2.45dc**.

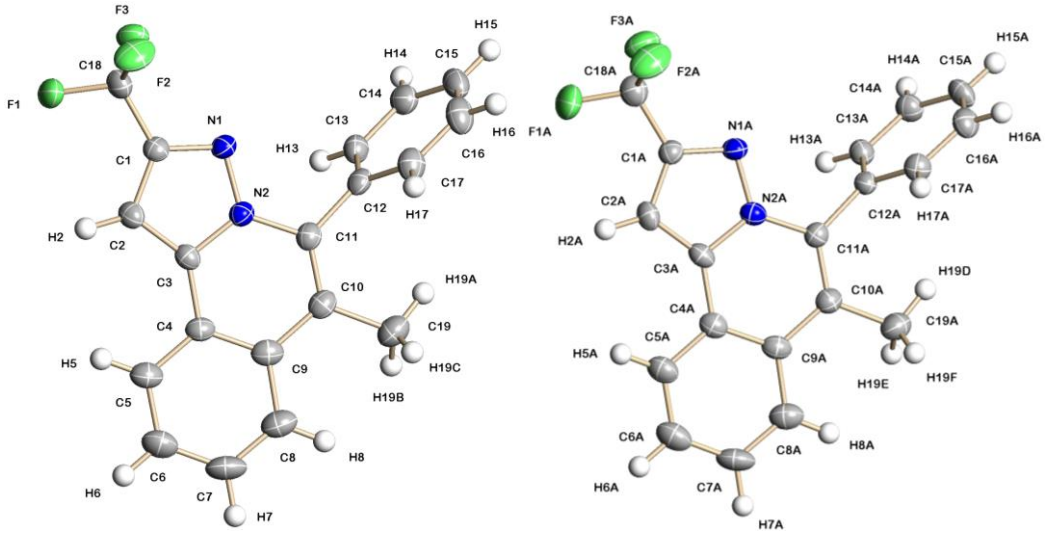

2.45dc, $C_{19}H_{13}F_3N_2$, M = 326.31, Monoclinic, a = 10.826(4) Å, b = 16.541(7) Å, c = 17.451(7) Å, α = 90°, β = 96.945(9)°, γ = 90°, V = 3102(2) $Å^3$, T = 150(2) K, space group P2(1)/n, Z = 8, 22238 reflections measured, 5462 independent reflections (Rint = 0.1020). The final R1 values were 0.0511 (I > 2σ(I)) 0.0991 (all data). The final wR(F2) values were 0.0896 (I > 2σ(I)), 0.1027 (all data). GOF = 0.877. Selected average bond distances (Å) and angles (°) given in **Chapter Two**, **Section 2.9**.

Crystal structure of **2.45ad** with selected bond distances (Å) and angles (°). Hydrogen atoms have been omitted for clarity.

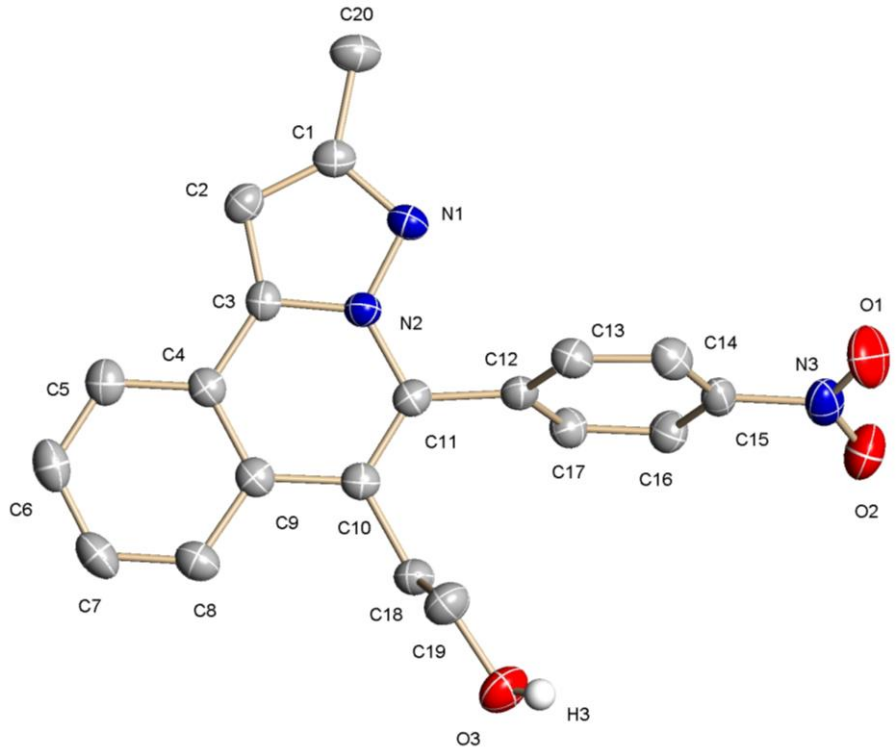

N(2)-C(3)	1.370(2)	C(3)-C(4)	1.434(2)
C(11)-N(2)	1.391(2)	C(4)-C(9)	1.406(3)
C(10)-C(11)	1.356(3)	C(9)-C(10)	1.457(3)
C(3)-N(2)-C(11)	124.1(15)	C(4)-C(9)-C(10)	119.8(16)
N(2)-C(11)-C(10)	119.3(16)	C(9)-C(10)-C(11)	119.7(16)
N(2)-C(11)-C(12)	116.4(15)	C(10)-C(18)-C(19)	114.0(15)

2.45ad, $C_{20}H_{17}N_3O_3$, M = 347.37, Monoclinic, a = 8.0425(16) Å, b = 13.939(3) Å, c = 14.737(3) Å, α = 90°, β = 92.875(3)°, γ = 90°, V = 1650.0(6) $Å^3$, T = 150(2) K, space group P2(1)/n, Z = 4, 12539 reflections measured, 3234 independent reflections (Rint = 0.0460). The final R1 values were 0.0522 (I > 2σ(I)) 0.0703 (all data). The final wR(F2) values were 0.1263 (I > 2σ(I)), 0.1347 (all data). GOF = 1.039.

Crystal structure of **2.45bd** with selected bond distances (Å) and angles (°).

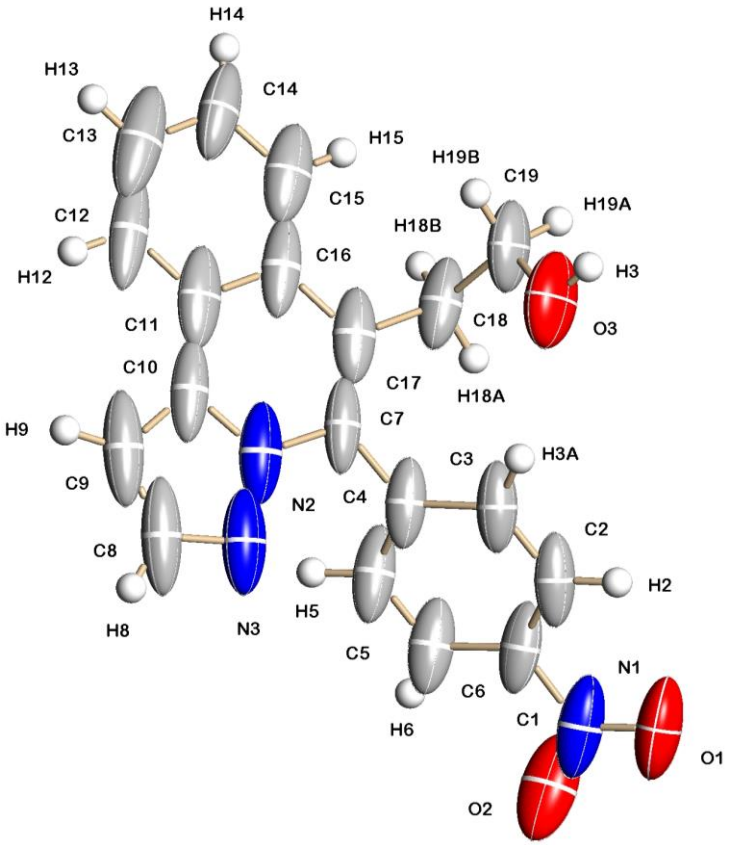

N(2)-C(7)	1.407(8)	C(11)-C(16)	1.422(9)
C(10)-N(2)	1.398(8)	C(16)-C(17)	1.467(9)
C(10)-C(11)	1.398(10)	C(7)-C(17)	1.349(8)
C(7)-N(2)-C(10)	122.7(8)	C(16)-C(17)-C(18)	118.3(7)
N(2)-C(7)-C(17)	118.9(7)	N(2)-C(7)-C(4)	114.5(7)

2.45bd, $C_{19}H_{15}N_3O_3$, M = 333.34, Monoclinic, a = 9.8265(17) Å, b = 10.3009(18) Å, c = 17.832(3) Å, α = 90°, β = 121.425(8)°, γ = 90°, V = 1540.2(5) Å^3, T = 150(2) K, space group P2(1)/c, Z = 4, 10904 reflections measured, 2710 independent reflections (Rint = 0.0954). The final R1 values were 0.0869 (I > 2σ(I)) 0.1798 (all data). The final wR(F2) values were 0.2071 (I > 2σ(I)), 0.2500 (all data). GOF = 1.054.

Structures of the two unique molecules in the cell of **2.47a** with selected average bond distances (Å) and angles (°). Hydrogen atoms have been omitted for clarity.

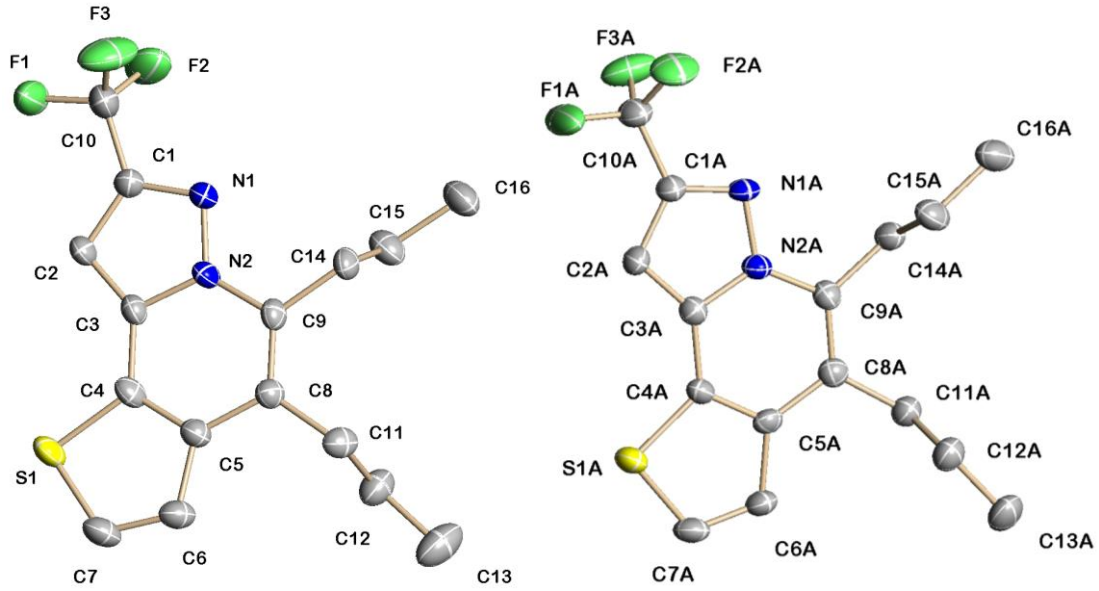

N(2)-C(3)	1.382(4)	C(5)-C(8)	1.442(5)
C(9)-N(2)	1.395(4)	C(4)-C(5)	1.376(5)
C(8)-C(9)	1.366(5)	C(3)-C(4)	1.425(5)
C(3)-N(2)-C(9)	125.1(3)	C(5)-C(8)-C(9)	118.6(3)
N(2)-C(9)-C(8)	118.8(3)	C(4)-S(1)-C(7)	90.7(18)

2.47a, $C_{16}H_{17}F_3N_2S$, M = 326.38, Triclinic, a = 8.548(2) Å, b = 9.543(2) Å, c = 19.894(5) Å, α = 88.270(5)°, β = 81.218(6)°, γ = 82.774(5)°, V = 1591.0(7) $Å^3$, T = 150(2) K, space group P-1, Z = 4, 11669 reflections measured, 5558 independent reflections (Rint = 0.0973). The final R1 values were 0.0645 (I > 2σ(I)) 0.1188 (all data). The final wR(F2) values were 0.1217 (I > 2σ(I)), 0.1436 (all data). GOF = 0.896.

Crystal structure of **2.49dd** with selected bond distances (Å) and angles (°).

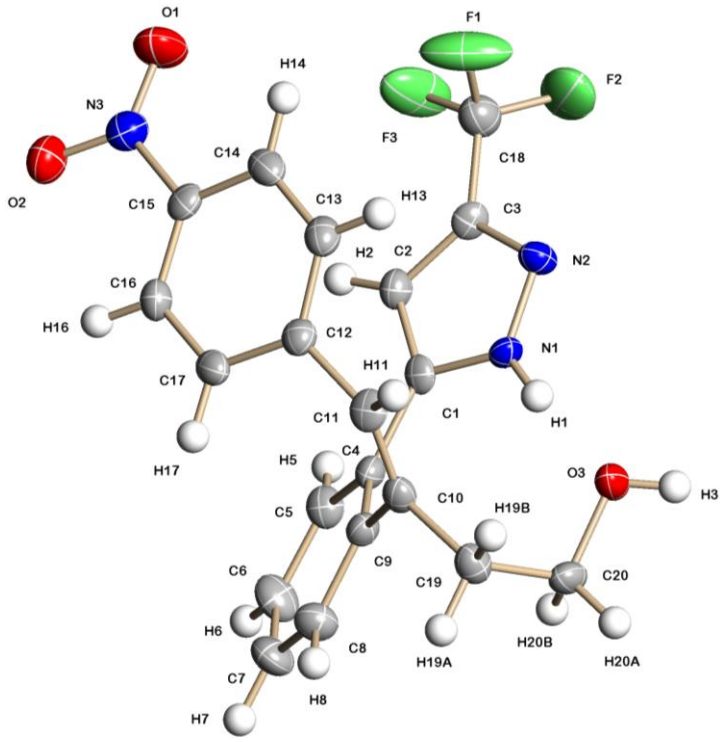

C(9)-C(10)	1.493(5)	C(1)-C(4)	1.458(5)
C(10)-C(11)	1.311(5)	O(3)-C(20)	1.415(4)
C(4)-C(9)-C(10)	123.8(3)	C(19)-C(20)-O(3)	108.1(3)
C(10)-C(19)-C(20)	112.9(3)	C(10)-C(11)-C(12)	126.2(4)

2.49dd, $C_{20}H_{16}F_3N_3O_3$, M = 403.36, Triclinic, a = 7.050(2) Å, b = 10.490(3) Å, c = 13.386(4) Å, α = 98.273(6)°, β = 103.262(6)°, γ = 108.653(6)°, V = 887.2(5) $Å^3$, T = 150(2) K, space group P-1, Z = 2, 6516 reflections measured, 3122 independent reflections (Rint = 0.0788). The final R1 values were 0.0672 (I > 2σ(I)) 0.1290 (all data). The final wR(F2) values were 0.1335 (I > 2σ(I)), 0.1559 (all data). GOF = 0.917.

Structures of the two unique molecules in the cell of **3.15ca**. Hydrogen atoms have been omitted for clarity.

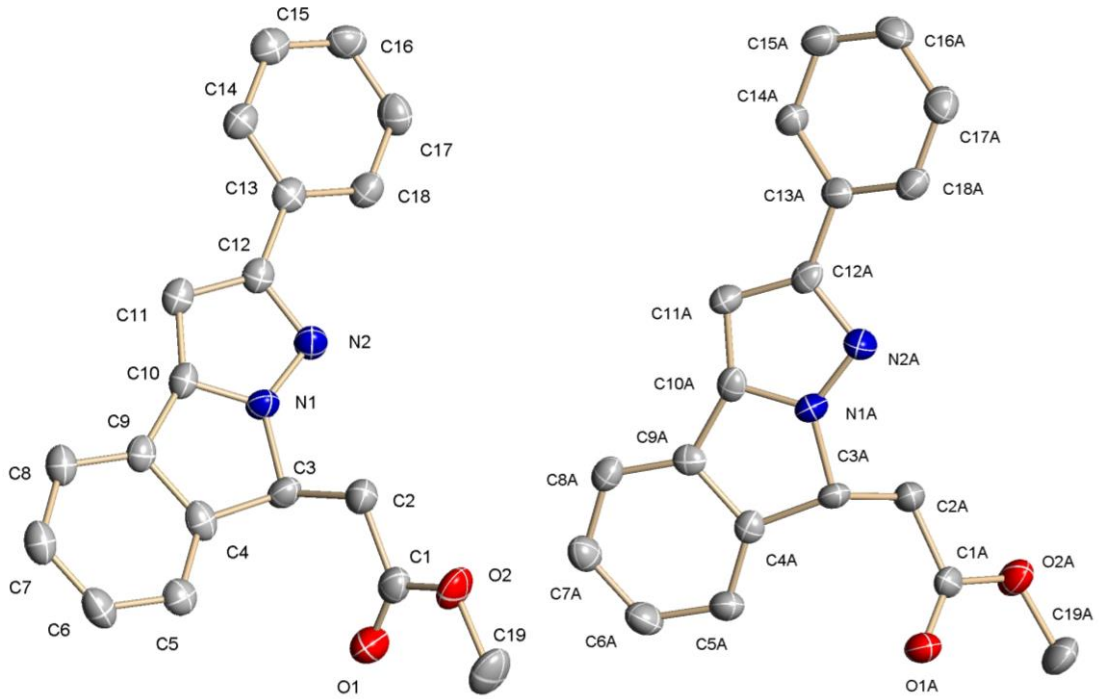

3.15ca, $C_{19}H_{16}N_2O_2$, M = 304.34, Triclinic, a = 9.9460(18) Å, b = 13.007(2) Å, c = 13.248(2) Å, α = 114.451(4)°, β = 98.994(4)°, γ = 95.003(4)°, V = 1518.9(5) $Å^3$, T = 150(2) K, space group P-1, Z = 4, 8088 reflections measured, 5068 independent reflections (Rint = 0.0595). The final R1 values were 0.0689 ($I > 2\sigma(I)$) 0.1175 (all data). The final wR(F2) values were 0.1461 ($I > 2\sigma(I)$), 0.1707 (all data). GOF = 0.932. Selected average bond distances (Å) and angles (^{o}) are given in **Chapter Three**, **Section 3.2**.

Structures of the two unique molecules in the unit cell of **4.19e**.

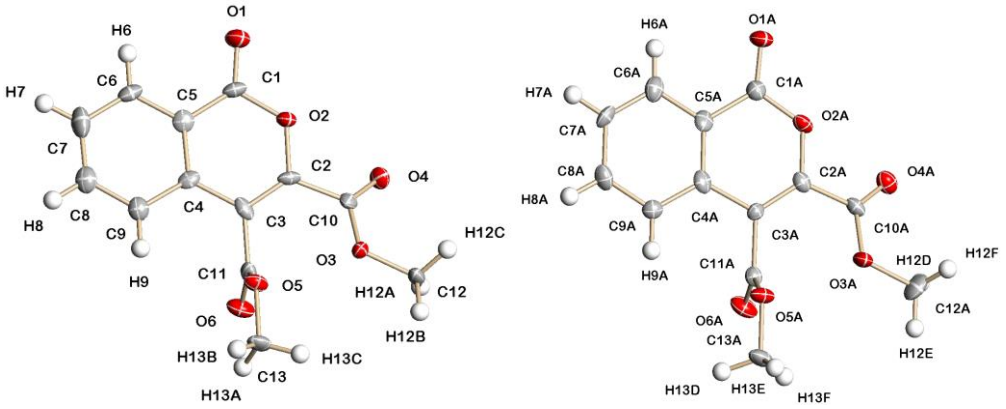

4.19e, $C_{13}H_{10}O_6$, M = 262.21, Orthorhombic, a = 7.9686(17) Å, b = 8.3194(18) Å, c = 34.932(8) Å, α = 90°, β = 90°, γ = 90°, V = 2315.8(9) $Å^3$, T = 150(2) K, space group Pca2(1), Z = 8, 14030 reflections measured, 2073 independent reflections (Rint = 0.0837). The final R1 values were 0.0609 ($I > 2\sigma(I)$) 0.0688 (all data). The final wR(F2) values were 0.1426 ($I > 2\sigma(I)$), 0.1486 (all data). GOF = 1.041. Selected average bond distances (Å) and angles (^{o}) are given in **Chapter Four**, **Section 4.2.5**.

Appendix: Chapter Two Mechanistic Experiments

Initial Rates Experiments with Rh

Reaction vials equipped with a stirrer bar were loaded with 5-methyl-3-phenyl-1H-pyrazole (**2.43a**, 52 mg, 0.33 mmol), 4-octyne (**a**, various amounts, see table below), $Cu(OAc)_2.H_2O$ (165 mg, 0.83 mmol, 2.5 eq.), 1,3,5-trimethoxybenzene (3.0 mg, 0.017 mmol, 5 mol%) as internal standard and DCE (reaction made up to 5 ml volume). The vials were sealed with a screw cap and transferred to a preheated heating block at 50 °C to stir for 5 min. $[Cp^*Rh(MeCN)_3][PF_6]_2$ (11 mg, 0.017 mmol, 5 mol%) was added and timing was started. Each of these reactions was repeated to calculate the average rate. At the end of a time interval (see table below), a vial was removed and placed in an ice bath to stop the reaction. The mixture from each vial was diluted with diethyl ether (10 ml) and 2M ammonium solution (10 ml) was added. The blue aqueous layer was extracted with diethyl ether (3 x 10 ml) and the combined organic layers were dried over $MgSO_4$.The solvent was removed on the rotary evaporator. The ^1H NMR spectra were recorded and yield was found by integrating the CH_2 2H peak of the product. After data analysis (see below) the order was found to be 0.07 ± 0.1.

A similar procedure was used with $[(p\text{-Cy})RuCl_2]_2$ as catalyst except the reactions were carried out a smaller scale in *t*-amyl alcohol at 100 °C. The amounts used were, 5-methyl-3-phenyl-1H-pyrazole (**2.43a**, 32 mg, 0.20 mmol), 4-octyne (**a**, 0.3-2.4 equiv.), $Cu(OAc)_2.H_2O$ (100 mg, 0.50 mmol, 2.5 equiv.), 1,3,5-trimethoxybenzene (1.7 mg, 0.010 mmol, 5 mol%) as internal standard and *t*-amyl alcohol (reaction made up to 5 ml volume). The vials were sealed with a screw cap and transferred to a preheated heating block at 100 °C to stir for 5 min. $[(p\text{-Cy})RuCl_2]_2$ (6.1 mg, 0.01 mmol, 5 mol%) was added and timing was started. The reactions were worked up as for Rh above.

2a/eq.	**2a/mol**	**2a/µl**	**2a/mol dm^{-3}**	**Time/s**	**Average Yield/%**	**Rate/mol dm^{-3} s^{-1}**
0.3	0.00010	14.6	0.020	900	4.08	0.0000030
0.6	0.00020	29.2	0.040	600	3.23	0.0000036
1.2	0.00039	58.4	0.078	1200	6.18	0.0000034
1.8	0.00059	86.3	0.118	720	4.16	0.0000038
2.4	0.00079	115.5	0.158	540	2.98	0.0000036

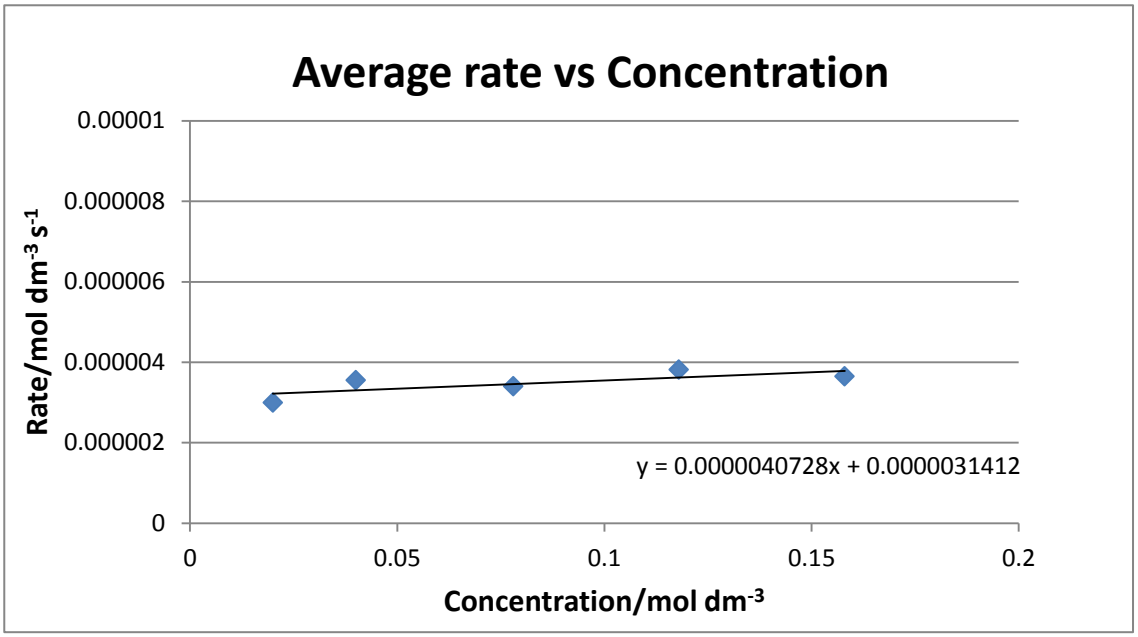

KIE Experiment with Rh

The same general procedure as above was followed using 5-methyl-3-phenyl-1H-pyrazole (**2.43a**, 52 mg, 0.33 mmol) and **d^3-2.43a** (53 mg, 0.33 mmol) with 4-octyne (**a**, 44 mg, 0.39 mmol, 1.2 eq.) $Cu(OAc)_2.H_2O$ (165 mg, 0.83 mmol, 2.5 eq.) and the catalyst (5 mol % $[Cp^*Rh(MeCN)_3][PF_6]_2$), 1,3,5-trimethoxybenzene (3.0 mg, 0.017 mmol, 5 mol%) as internal standard and DCE (reaction made up to 5 ml volume). Each reaction was done twice. The ^{1}H NMR spectra were recorded and yield was found by integrating the CH_2 2H peak of the product. After calculating rates for each reaction the kinetic isotope effects were calculated as $k_H/k_D = 2.7 \pm 0.5$ for Rh.

KIE Experiment with Ru

The general procedure for the initial rates experiment was followed using 5-methyl-3-phenyl-1H-pyrazole (**2.43a**, 32 mg, 0.20 mmol) and **d^3-2.43a** (32 mg, 0.20 mmol) with 4-octyne (**a**, 26 mg, 0.24 mmol, 1.2 eq.), $Cu(OAc)_2.H_2O$ (100 mg, 0.50 mmol, 2.5 eq.), 1,3,5-trimethoxybenzene (1.7 mg, 0.01 mmol, 5 mol%) and DCE (reaction made up to 3 ml volume). The vials were sealed with a screw cap and transferred to a preheated heating block at 83 °C to stir for 5 min. $[RuCl_2(p\text{-cymene})]_2$ (6.1 mg, 0.01 mmol, 5 mol%) was added and timing was started. All reactions were left on for 60 min. Each reaction had a repeat reaction within the same heating block in order to calculate averages. The ^{1}H NMR spectra were recorded and yield was found by integrating the CH_2 2H peak of the product. This led to a $k_H/k_D = 1.1 \pm 0.2$.

Appendix: Conferences and Symposia Attended

Internal Seminars

10th Oct 2012	Dr Richard Bayliss, University of Leicester
31st Oct 2012	Dr Ross Denton, University of Nottingham
14th Nov 2012	Prof. Jonathan Clayden, University of Manchester
28th Nov 2012	Prof. Tim Bugg, University of Warwick
16th Jan 2013	Dr John Slattery, University of York
23rd Jan 2013	Prof. Sabine Flitsch, University of Manchester
6th Feb 2013	Prof. Nicholas Tomkinson, University of Strathclyde
13th Feb 2013	Dr Miles Congreve, Head of Chemistry, Heptares Therapeutics
20th Feb 2013	Dr Richard Layfield, University of Manchester
27th Feb 2013	Prof. Michael Greaney, University of Manchester
6th Mar 2013	Dr Andrew J Wilson, University of Leeds

Internal Symposia

University of Leicester Department of Chemistry Postgraduate Research Symposia:

2009: Attended

2010, 2011, 2012: *Poster presented: "Atom-Efficient Ambiphilic C-H Functionalisation Routes to Heterocycles"*

2013: *Oral presentation given: "Atom-Efficient Ambiphilic C-H Activation Routes to Heterocycles"*

External Symposia/Conferences

RSC Award Winners Symposium 2011, Loughborough University

RSC East Midlands Organic Section Meetings 2011, 2012, 2013:

Poster presented: "Atom-Efficient Ambiphilic C-H Functionalisation Routes to Heterocycles"

RSC Dalton Division Meeting 2012, University of Warwick:

Poster presented: "Atom-Efficient Ambiphilic C-H Functionalisation Routes to Heterocycles"

XXV International Conference on Organometallic Chemistry (ICOMC) 2012, Lisbon, Portugal:

Poster presented: "Atom-Efficient Ambiphilic C-H Functionalisation Routes to Heterocycles"

RSC Heterocycle Division Meeting 2013, Astex Pharmaceuticals, Cambridge Science Park, Cambridge:

Oral presentation given: "Atom-Efficient Ambiphilic C-H Functionalisation Routes to Heterocycles"